The Role of BMP8A in Breast Cancer and its Involvement in Bone Metastasis

By

Laijian Sui

Cardiff China Medical Research Collaborative

School of Medicine, Cardiff University

Cardiff

May 2022

Supervisors: Lin Ye, Wen G. Jiang

Thesis submitted to Cardiff University for the degree of Doctor of Medicine

Acknowledgements

I would like to express my sincere appreciation to my supervisor Dr Lin Ye for his consistent support and scrupulous guidance throughout my two-year MD study. With his expertise, I overcame many difficulties and avoided many detours during the study, which also fostered me an even greater interest in the scientific research.

I would especially like to offer my heartfelt thanks and great respect to Professor Wen G. Jiang for his kindness, encouragement and help in the past two years.

I am also grateful to my co-supervisor, Dr Andrew Sanders, he is always supportive and helpful throughout my MD study, as well as the thanks for Dr Jane, who did help me a lot in modifying my thesis. Meanwhile, I would like to thank all the staff members and PhD students in CCMRC including Dr Tracey A Martin, Mrs Fiona Ruge, Ziqian Fang, Amy, Yali Xu, Jimmy Zeng, Yiming Yang, Hanson Gao who have been really friendly and helpful all the time.

My study began in the midst of the COVID19 pandemic and national lockdown. The lengthy lockdown ran almost the entire period of my study and had in many ways affected my research. However, supported by the meticulous management skill of the COVID officers of CCMRC, the School of Medicine and the University, I was able to limit the disruption of my experimental work to minimum. I wish to express my sincere gratitude to my host laboratories and supervisory team for guide me and help me through this difficult period of time.

I would like to show my special appreciation for my home institute, Yantai Yuhuangding Hospital, which has supported me and allowed me to fulfil my dream as a clinician scientist by funding me for the doctoral study at Cardiff University.

Finally, I would like to dedicate this work to my parents, my wife and my daughter. Unfaltering support and encouragement from the warm family gave me the endless motivation to overcome all the difficulties and frustrations to complete my research.

Full papers

1. L Sui, L Ye, AJ Sanders, Y Yang, C Hao, R Hargest, and WG Jiang. 2021. Expression of Death Associated Proteins DAP1 and DAP3 in Human Pancreatic Cancer, Anticancer Res, 2021, 41: 2357-62.

2. L Sui, AJ Sanders, WG Jiang and L Ye. Deregulated molecules and pathways in the predisposition and dissemination of breast cancer cells to bone. Computational and Structural Biotechnology Journal. 2022 in press.

Abstracts and conference presentations

1. Sui, L J, A Sanders, W G Jiang, and L Ye. Aberrant expression of BMP8A and the BMPRs involves in the progression of breast cancer, British Journal of Surgery, 108. Surgical Research Society Annual meeting, 24th March 2021. British Journal of Surgery, Volume 108, Issue Supplement_5, July 2021, znab282.034, https://doi.org/10.1093/bjs/znab282.034

2. Sui, Laijian, Lin Ye, Chunyi Hao, Yuxin Cui, Ke Ji, Jiafu Ji, and Wen G Jiang. The Expression and Clinical Significance of MLN64 in Human Pancreatic Cancer. British Society of Gastroenterology Annual Meeting, 8th -12th November 2021. Gut, 2021, 70(Suppl4):A145.2-A146. DOI: 10.1136/gutjnl-2021-BSG.270

3. Sui, Laijian, Jianyuan Zeng, Lin Ye, Andrew J Sanders, Huishan Zhao, Aihua Jiang, Jinkui Zhu, Xicheng Song, Rachel Hargest, and Wen G Jiang. DAP3 and the DAP3 Binding Cell Death Enhancer-1 (DELE1) in human colorectal cancer, Gut, 70: A163-A63. British Society of Gastroenterology Annual Meeting, 8th - 12th November 2021. Gut, 2021, 70(Suppl4):A163.1-A163. DOI: 10.1136/gutjnl-2021-BSG.303

Summary

Emerging evidence showed a putative oncogenic role played by bone morphogenetic protein 8A (BMP8A) in breast cancer. The present study aims to dissect the role played by BMP8A in breast cancer. Initial analyses showed that BMP8A was increased in the tissues of primary breast cancer at both mRNA and protein levels. The elevated expression was associated with poorer survival of patients with luminal B tumours but tends to be a feasible marker for overall survival of patients with HER2 positive tumours suggesting a subtype specific involvement. BMP8A promoted invasion of luminal B cancer cells by upregulating MMPs and promoting EMT in which both Smad dependent and independent signalling are involved. Similarly, BMP8A also enhanced the invasiveness of HER2 positive breast cancer cells by promoting MMPs and EMT. However, BMP8A exhibited both inhibitory and promotive effects on proliferation of HCC1419 and SKBR3 cells, respectively. These altered cell behaviours may be coordinated by BMP8A through orchestrated signalling comprising Smad1/5/8, MAPK (ERK) and AKT pathways in HER2 positive tumours. Increased cell invasion together with upregulated MMPs and EMT by BMP8A were also seen in TNBC (triple negative breast cancer) cells, in which elevated expression of EGFR and activation of Smad3 were observed. There was positive correlation between BMP8A and osteoblastic/osteolytic markers revealed in primary tumours of breast cancer. Together with the observed activation of RANKL/P38 signalling in the BMP8A overexpression MDA-MB-231 cells, it collectively suggests that BMP8A may be actively involved in the bone metastasis of breast cancer. In conclusion, BMP8A is upregulated in breast cancer which presents subtype specific correlation with patients' survival. It promotes invasion of breast cancer through a promotion of MMPs and EMT in which both Smad dependent and independent signalling are involved. Further study will shed light on its therapeutic potential in the personalised disease management of different subtype breast cancer.

Contents

List of figures

Chapter 1

Chapter 2

Chapter 3

Chapter 6

Chapter 7

Chapter 8

List of tables

Chapter 1

Chapter 2

Chapter 3

Chapter 4

Abbreviations

5-FU	Fluorouracil
ABS	Antibiotics
ActR	Actin Related Protein
ACVR	Activin A receptor
AKT	Protein kinase B
APS	Ammonium Persulfate
BAG2	BAG Cochaperone 2
BAMBI	BMP and Activin Membrane Binding Inhibitor
BC	Breast cancer
BECN1	Beclin 1
BGCAN	Betaglycan
BISC	BMP-induced signal complex
BME	Bone matrix extract
BMP	Bone morphogenetic protein
BMPR	Bone morphogenetic protein receptor
BSP	Bone sialoprotein
BSS	Balanced salt solution
CAF	Cancer-associated fibroblasts
CALD1	Caldesmon 1
CaSR	Calcium-sensing receptor
CAV1	Caveolin 1
CAVIN1	Caveolae Associated Protein 1
Cbfα1	Core binding factor α1
CBR1	Carbonyl Reductase 1
CCDC86	Coiled-Coil Domain Containing 86
CDH	Cadherin
CHL2	Chordin like 2
CM	Conditional medium
CSCs	Cancer stem-like cells
CTSK	Cathepsin K
CXCL12	Chemokine ligand 12
CXCR4	Chemokine receptor 4
DCIS	Ductal cell carcinoma *in situ*
DDX27	DEAD-Box Helicase 27
DEPC	Diethyl pyrocarbonate
DKK1	Dickkopf-1
DMFS	Distant metastasis free survival
DMSO	Dimethyl sulfoxide
DTC	Disseminating tumour cell
DTT	Dithiothreito
DTX	Docetaxel
ECM	Extracellular matrix

EDTA	Ethylenediaminetetraacetic Acid
EGFR	Epidermal growth factor receptor
EMT	Epithelial mesenchymal transition
ENG	Endoglin
ER	Oestrogen receptor
ERBB	v-erb-b2 erythroblastic leukaemia viral oncogene homolog
ERK	Extracellular signal-regulated kinase
FACS	Fluorescence-activated cell sorting
FERMT3	FERM Domain Containing Kindlin 3
FGF	Fibroblast growth factor
FLNC	Filamin C
FOXA1	Fork head-box A1
FST	Follistatin
GATA3	Trans-Acting T-Cell-Specific Transcription Factor GATA-3
GDF	Growth differentiation factor
GREM	GREMLIN
GSDME	Gasdermin E
GSTP1	Glutathione S-Transferase Pi 1
H4K16	Histone H4 at lysine 16
HA	Hydroxyapatite nanocrystals
HER2	Human epidermal growth factor receptor 2
hES	Human embryonic stem
HGF	Hepatocyte growth factor
HGF	Hepatocyte growth factor
HIF	Hypoxia Inducible Factor
HLA-A	Major Histocompatibility Complex, Class I, A
HSC	hematopoietic stem cell
HSC	hematopoietic stem cells
ICC	Immunocytochemical staining
ID1	Inhibitor Of DNA Binding 1
IFI16	Interferon Gamma Inducible Protein 16
IHC	Immunohistochemical staining
IL	Interleukin
JNK	Jun N-terminal kinase
LB	Lysis buffer
LGALS1	Lectin, Galactoside-Binding, Soluble, 1
MAPK	Mitogen-activated protein kinase
M-CFS	Macrophage colony stimulating factor
MMP	Metalloprotease
MSCs	Mesenchymal stem cells
MSK1	Mitogen and stress-activated kinase 1
MSN	Moesin
MT1E	Metallothionein 1E
NAA15	N-Alpha-Acetyltransferase 15

NDRG1	N-myc downstream-regulated gene1
NOG	Noggin
NR2F1	Nuclear Receptor Subfamily 2 Group F Member 1
NRG4	Neuregulin-4
NTX	N-telopeptide of type I collagens
OP2	Osteogenic protein 2
OPG	Osteoprotegerin
OPN	Osteopontin
OS	Overall survival
PBS	Phosphate buffered solution
PCR	Polymerase chain reaction
PDGF	Platelet-derived growth factor
PEI	Polyetherimide
PMSF	Phenylmethylsulfonylfluoride
PPS	Post-progression survival
PR	Progesterone receptor
PTEN	Phosphatase and Tensin Homolog
PTH	Parathyroid hormone
PTHrP	Parathyroid hormone-related peptide
PYGL	Glycogen Phosphorylase L
RANKL	Receptor activators for Nuclear factor-κB ligand
RFS	Relapse free survival
RGM	Repulsive guidance molecule
RIPA	Radioimmunoprecipitation assay
RNF11	Ubiquitin ligase ring finger protein 11
RNF34	Ring Finger Protein 34
RT	Reverse transcription
RTK	Receptor tyrosine kinase
RUNX2	Runt-related transcription factor 2
SDS-PAGE	Sodium dodecyl sulfate- poly acrylamide gel electrophoresis
SEC16A	SEC16 Homolog A, Endoplasmic Reticulum Export Factor
SETD2	SET Domain Containing 2
siRNA	Small interfering RNA
SMAD	Sons of mothers against decapentaplegic
SMARCA4	SWI/SNF Related, Matrix Associated, Actin Dependent Regulator of Chromatin, Subfamily A, Member 4
Smurf	Smad ubiquitination regulator
SNX29	Sorting Nexin 29
SPARC	Secreted protein acidic and cysteine rich
SRE	Skeletal related event
TBE	Tris-Boric Acid EDTA
TCGA	The Cancer Genome Atlas
TGF	Transforming growth factor

TMA	Tissue microarray
TNBC	Triple-negative breast cancer
TNF	Tumour necrosis factor
TNS3	Tensin 3
TRIM24	Tripartite Motif Containing 24
TRIM3	Tripartite Motif Containing 3
TSG	Twisted gastrulation
TSP1	Thrombospondin 1
TUT4	Terminal Uridylyl Transferase 4
uPA	Urokinase plasminogen activator
V-ATPase	Vacuolar H^+-ATPase
VEGF	Vascular endothelial growth factor
VEGFR	Vascular endothelial growth factor receptor
XIAP	X-linked apoptotic protein
ZEB1	Zinc finger E-box-binding homeobox 1
ZNF100	Zinc Finger Protein 100

Chapter 1

Introduction

1.1 Breast cancer

Breast cancer is the leading malignant tumour in females that seriously threatens women's health. In recent years, the number of patients suffering from this disease has been increasing year by year and in 2020, it has surpassed lung cancer for the first time and becoming the most frequently diagnosed cancer globally in the entire population, males and females combined (Sung et al., 2021)

1.1.1 Aetiology and risk factors

The breast is composed of skin, fibrous tissue, breast glands and adipose tissue. Breast cancer is a common malignant tumour that occurs in the epithelial tissue of the breast (Aronson et al., 2000). Breast cancer seriously threatens women's health, 99% of breast cancers occur in women, while men account for only 1% (Rojas and Stuckey, 2016).

Breast cancer *in situ* is not fatal, however, due to the fact that breast cancer cells lose the characteristics of normal cells, the fibrous connections between cells are loose and prone to detach. The detached cancer cells can spread throughout the body within the blood or lymph circulation, forming metastases and endangering life. Breast cancer has become a common tumour threatening women's physical and mental health worldwide (Akram et al., 2017).

The global morbidity of breast cancer has been rising since the late 1970s. Although the mortality has decreased by 35% since the early 1970s owing to the progress in early diagnosis and advanced therapy, it is estimated that 10% to 12.5% of females may be attacked by this disease during their lifetime and the incidence is estimated to increase by 2% in the United Kingdom by 2035 (Smittenaar et al., 2016).

The aetiology and risk factors of breast cancer are not yet fully understood. Studies have found that there is a certain regularity in the incidence of breast cancer. Women with high risk factors for breast cancer are more likely to develop breast cancer. The so-called high-risk factors refer to various risk factors related to the onset of breast cancer, and the risk factors that most breast cancer patients have are called high-risk factors of breast cancer. Studies have shown that the age-specific incidence of breast cancer in women is relatively low in the age group of 0-24 years old. It gradually rises after the age of 25, reaches a peak among the 50-54 year-old group, and gradually

decreases after the age of 55 (Clavel-Chapelon and Gerber, 2002). Family history of breast cancer is another risk factor for breast cancer. The so-called family history refers to breast cancer cases in first-degree relatives (mother, daughter, sister). In recent years, it has been discovered that compact breast glands have become a risk factor for breast cancer (Brewer et al., 2017). Risk factors for breast cancer include early menarche (<12 years old), late menopause (>55 years old); unmarried, no childbearing, late childbearing, no breastfeeding; not timely diagnosis and treatment of benign breast diseases; hospital biopsy (biopsy) confirmed to have breast atypical hyperplasia; breast received high-dose radiation, long-term use of exogenous oestrogen, postmenopausal obesity, long-term excessive drinking (well-reviewed by (Rojas and Stuckey, 2016)). Proven breast cancer susceptibility genes include BRCA-1, BRCA-2, as well as p53 and PTEN (Paul and Paul, 2014). Breast cancers related to these gene mutations are called hereditary breast cancers, accounting for 5% to 10% of all breast cancers.

1.1.2 Classification of Breast cancer

According to the size and type of tumour, the degree of invasion in breast cancer tissue and whether the tumour has local or distant metastasis, breast cancer is classified into five stages from 0 to 4 (Heim et al., 1997).

Stage 0: Breast cancer cells are confined to the border of the breast where the cancer occurs, and there is no infiltration of surrounding tissues. Ductal cell carcinoma *in situ* (DCIS) is a typical stage 0 (Bednarek et al., 1997).

Stage I: Microscopic infiltration may occur at this stage. Stage I is divided into two categories: IA and IB. The tumours of category IA grow to 2 cm without lymph node metastasis. If a small amount of cancer cells larger than 0.2 mm are detected in the lymph nodes, the tumour belong to stage IB (Segal et al., 2001).

Stage II also includes two categories, IIA and IIB. Stage IIA tumours have metastasis to axillary lymph nodes or sentinel lymph nodes, but no tumours are found in the breast or tumours are less than 5 cm in diameter. Stage IIB tumours are larger than 5 cm in diameter and have no axillary lymph node metastasis (Moran et al., 2014).

Stage III is divided into three sub-categories, IIIA, IIIB and IIIC. Stage IIIA tumours have metastases in 4-9 axillary lymph nodes or sentinel lymph nodes, but no tumours are found in the breast. Breast cancer that causes breast skin swelling or ulcers

and spreads to 9 axillary lymph nodes or sentinel lymph nodes is classified as stage IIIB regardless of the size of the primary lesion. Inflammatory breast cancer manifests as red, swollen, and warm breast skin and also belongs to stage IIIB. Breast cancer that has spread to as many as 10 or more axillary lymph nodes, with involvement of the lymph nodes above and below the clavicle belongs to stage IIIC (Jacquillat et al., 1990).

Stage IV is an advanced and metastatic stage of cancer. Breast cancer has metastasised to distant organs such as lung, bone, liver and brain (Neuman et al., 2010).

Definition of Primary Tumour (T) – Clinical and Pathological

T Category	**T Criteria**
TX	Primary tumour cannot be assessed
T0	No evidence of primary tumour
Tis (DCIS)*	Ductal carcinoma *in situ*
Tis (Paget)	Paget disease of the nipple NOT associated with invasive carcinoma and/or carcinoma *in situ* (DCIS) in the underlying breast parenchyma. Carcinomas in the breast parenchyma associated with Paget disease are categorized based on the size and characteristics of the parenchymal disease, although the presence of Paget disease should still be noted.
T1	Tumour ≤20 mm in greatest dimension
T1mi	Tumour ≤1 mm in greatest dimension
T1a	Tumour >1 mm but ≤5 mm in greatest dimension (round any measurement >1.0–1.9 mm to 2 mm).
T1b	Tumour >5 mm but ≤10 mm in greatest dimension
T1c	Tumour >10 mm but ≤20 mm in greatest dimension
T2	Tumour >20 mm but ≤50 mm in greatest dimension
T3	Tumour >50 mm in greatest dimension
T4	Tumour of any size with direct extension to the chest wall and/or to the skin (ulceration or macroscopic nodules); invasion of the dermis alone does not qualify as T4
T4a	Extension to the chest wall; invasion or adherence to pectoralis muscle in the absence of invasion of chest wall structures does not qualify as T4
T4b	Ulceration and/or ipsilateral macroscopic satellite nodules and/or edema (including peaud'orange) of the skin that does not meet the criteria for inflammatory carcinoma
T4c	Both T4a and T4b are present
T4d	Inflammatory carcinoma (see section "Rules for Classification")

*Note: Lobular carcinoma in situ (LCIS) is a benign entity and is removed from TNM staging in the AJCC Cancer Staging Manual, 8th Edition.

Definition of regional Lymph nodes pathological (pN)

pN Category	pN Criteria
pNX	Regional lymph nodes cannot be assessed (e.g., not removed for pathological study or previously removed)
pN0	No regional lymph node metastasis identified or ITCs only
pN0(i+)	ITCs only (malignant cell clusters no larger than 0.2 mm) in regional lymph node(s)
pN0(mol+)	Positive molecular findings by reverse transcriptase polymerase chain reaction (RT-PCR); no ITCs detected
pN1	Micrometastases; or metastases in 1–3 axillary lymph nodes; and/or clinically negative internal mammary nodes with micrometastases or macrometastases by sentinel lymph node biopsy
pN1mi	Micrometastases (approximately 200 cells, larger than 0.2 mm, but none larger than 2.0 mm)
pN1a	Metastases in 1–3 axillary lymph nodes, at least one metastasis larger than 2.0 mm
pN1b	Metastases in ipsilateral internal mammary sentinel nodes, excluding ITCs
pN1c	pN1a and pN1b combined
pN2	Metastases in 4–9 axillary lymph nodes; or positive ipsilateral internal mammary lymph nodes by imaging in the absence of axillary lymph node metastases
pN2a	Metastases in 4–9 axillary lymph nodes (at least one tumour deposit larger than 2.0 mm)
pN2b	Metastases in clinically detected internal mammary lymph nodes with or without microscopic confirmation; with pathologically negative axillary nodes
pN3	Metastases in 10 or more axillary lymph nodes;
	or in infraclavicular (Level III axillary) lymph nodes;
	or positive ipsilateral internal mammary lymph nodes by imaging in the presence of one or more positive Level I, II axillary lymph nodes;
	or in more than three axillary lymph nodes and micrometastases or macrometastases by sentinel lymph node biopsy in clinically negative ipsilateral internal mammary lymph nodes;
	or in ipsilateral supraclavicular lymph nodes
pN3a	Metastases in 10 or more axillary lymph nodes (at least one tumour deposit larger than 2.0 mm);
	or metastases to the infraclavicular (Level III axillary lymph) nodes
pN3b	pN1a or pN2a in the presence of cN2b (positive internal mammary nodes by imaging);
	or pN2a in the presence of pN1b
pN3c	Metastases in ipsilateral supraclavicular lymph nodes

Note: (sn) and (f) suffixes should be added to the N category to denote confirmation of metastasis by sentinel node biopsy or FNA/core needle biopsy respectively, with no further resection of nodes.

Definition of Distant Metastasis (M)

M Category	M Criteria
M0	No clinical or radiographic evidence of distant metastases*
cM0(i+)	No clinical or radiographic evidence of distant metastases in the presence of tumour cells or deposits no larger than 0.2 mm detected microscopically or by molecular techniques in circulating blood, bone marrow, or other nonregional nodal tissue in a patient without symptoms or signs of metastases
cM1	Distant metastases detected by clinical and radiographic means
pM1	Any histologically proven metastases in distant organs; or if in non-regional nodes, metastases greater than 0.2 mm

*Note that imaging studies are not required to assign the cM0 category

The TNM staging of breast cancer is cited from the 8th version of AJCC (American Joint committee on Cancer)(Chavez-MacGregor et al., 2017)

Subtypes of breast cancer

It has been found that clinical characters, response to treatment, and prognosis present significant difference in patients with the same histological classification and pathological stage. Research on molecular classification of breast cancer plays an essential role in guiding clinical treatment and predicting prognosis. The subtypes of breast cancer were firstly mentioned by Perou and his co-workers in Stanford University in the United State in 2000 (Perou et al., 2000), including: luminal subtype, basal-like subtype, human epidermal growth factor receptor 2 (HER-2) over-expression type and normal breast-like subtype. In 2003, Sorlie et al. divided the luminal type into A type and B type/C type (Sorlie et al., 2003). Since then, many researchers have performed other molecular classifications of breast cancer, but the classification method most widely used is the one proposed by Perou and Sorlie.

The clinical significance of subtypes of breast cancer

Luminal A subtype: Luminal A is the most common molecular subtype with incidence rates of 40% to 50% of breast cancers, which is characterized by being

positive for oestrogen receptor (ER) or progesterone receptor (PR), negative for human epidermal growth factor receptor 2 (HER-2), and having low expression of Ki67 in immunohistochemical detection (Voduc et al., 2010). In addition to expressing hormone receptors and glandular epithelial cytokeratin CK8/18, luminal A subclass also expresses Fork head-box A1 (FOXA1) with a high expression to 84% (Badve et al., 2007). The expression of FOXA1 gene is positively correlated with the prognosis. The prognosis of luminal A subtype is the best in breast cancer. It occurs mostly in early stage and has a lower risk of recurrence. In terms of treatment, luminal A subtype is sensitive to endocrine therapy, with an effective rate of up to 40%, and the ER level is positively correlated with the sensitivity of endocrine therapy.

HER-2 (+) subtype: This subtype is characterised by overexpression of HER-2, and negative for both ER and PR. HER-2 (+) subtype contains around 15% of breast cancer patients which often indicates a poor prognosis. Most are advanced cases, prone to axillary lymph node metastasis (Tsang and Tse, 2020). HER-2 (+) breast cancer is characterised by ERBB2 amplicon and an upregulation of TRAP100 (Thyroid Hormone Receptor-Associated Protein Complex 100), GRB7 (Growth Factor Receptor Bound Protein 7) and other genes that are located on same locus of chromosome 17, whilst RRM2 (Ribonucleotide Reductase Regulatory Subunit M2) and SHPRH (SNF2 Histone Linker PHD RING Helicase) are down-regulated (Birnbaum et al., 2004, Provenzano et al., 2018). Due to ER and PR negativity, endocrine therapy is largely ineffective. In terms of postoperative adjuvant chemotherapy, they are more sensitive to anthracycline-containing chemotherapy and have a dose-effect relationship (Harbeck et al., 2017).

Luminal B subtype: In this subtype either ER or PR are positive, and HER-2 is also positive, being more common in elderly patients. Tumours of this subtype are also sensitive to endocrine therapy. However, owing to the elevated overexpression of HER-2 and alternative resources of hormone in elderly, it is less effective for tamoxifen than luminal A, and has a better response to aromatase inhibitors (Ellis et al., 2001). As HER-2 is positive, some patients can be treated with molecular targeted therapy.

Basal-like subtype: Study of this subtype has attracted more attention in recent years. Immunohistochemical tests for ER, PR, and HER-2 are all negative, but basal-like subtype is not equivalent to triple-negative breast cancer. Studies have shown that

5% to 45% of basal-like breast cancer patients are positive for ER (Rakha et al., 2007b), 14% of them are HER-2 positive (Rouzier et al., 2005), and triple-negative breast cancers accounts for 80% to 90% of basal-like breast cancer (Rakha et al., 2007a). The diagnostic criteria proposed by Nielsen et al. are ER, HER-2 negative, at least one positive among CK5/6, CK14 and CK17, with or without EGFR expression (Nielsen et al., 2004). CK5/6 is widely considered to be the most specific indicator for the diagnosis of basal-like breast cancer. The age of onset for basal-like subtype is between 47 and 55 years old, which is lower than that of other subtypes. Basal-like subtype is characterised by myoepithelial cells originating from the outer layer of breast ductal epithelium, expressing basal cell cytokeratin (such as CK5/6, CK14, etc.) and vimentin. 85% of patients present p53 gene mutations, and 60% of patients express EGFR (Savage et al., 2008). Basal-like subtype is prone to distant metastases and the prognosis is the worst in breast cancers (Harbeck and Gnant, 2017). Endocrine and anti-HER-2 molecular targeted therapy is ineffective against this subtype of breast cancer. Chemotherapy is currently the only systemic treatment approach.

In addition, there is another subtype in luminal breast cancer, named luminal C type, which is positive for ER, PR and HER-2, which is also called triple-positive breast cancer. At present, there are few related reports, because the hormone receptor and HER-2 are both positive, and endocrine and anti-HER-2 molecular targeted therapy can be accepted, but the prognosis is still very poor and is prone to axillary lymph node metastasis (Van Calster et al., 2009).

1.1.3 Metastasis of breast cancer

Breast cancer metastasis is a multi-step complex process which originates from the local infiltration to the surrounding tissues by the primary breast cancer cells. The tumour cells detach from the primary tumour, infiltrate the surrounding tissues and penetrate into the blood or lymph vessels (Hunter et al., 2008, Talmadge and Fidler, 2010). Then they spread to distant organs through the blood or lymphatic circulation. Before settling down in the distant sites, disseminated breast cancer cells undergo cell cycle arrest and adhere to the capillary bed in the target organ. Once the number of the cell reach a certain amount, adapted cells grow rapidly and subsequently recruit new vasculature (Hunter KW et al.2008). Meanwhile, tumour cells must escape immune surveillance and apoptosis signals (Hunter KW et al.2008). After conquering these

barriers, the tumour cells will achieve successful colonisation (Talmadge and Fidler, 2010).

1.1.3.1 Invasion

Invasion of breast cancer cells into surrounding tissues arises from alterations of intercellular adhesion and the adhesion between cells and the extracellular matrix (ECM). The role of the cadherin family is prominent in this process (Li and Feng, 2011). E-Cadherin is vital in mediating cell-to-cell adhesion, and the downregulation of E-Cadherin leads to attenuated intracellular adhesion of breast cancer cells, leading to the detachment of cancer cells from the primary lesion (Wendt et al., 2011). Therefore, downregulated E-cadherin is closely correlated with advanced invasion and poor prognosis of breast cancer (Gould Rothberg and Bracken, 2006). N-Cadherin was closely associated with epithelial-mesenchymal transition (EMT) in breast cancer cells and proved to be another vital factor for tumour invasion (Kotb et al., 2011). High expression of N-cadherin increases the adhesion of tumour cells to stromal cells which facilitates tumour cells to colonise the matrix (Cavallaro and Christofori, 2004). EMT induces the production of proteases involved in ECM degradation to enhance the tumour invasion (Bonnomet et al., 2010). ECM degradation enhances tissue penetration, which is also an essential step in tumour invasion. The degradation of ECM is mainly accomplished by metalloprotease (MMP) and urokinase plasminogen activator (uPA) (Dano et al., 2005). In breast cancer patients, uPA levels are closely related to the risk of distant metastasis (Barajas-Castaneda et al., 2016). Inhibition of uPA by small interfering RNA (siRNA) can inhibit tumour invasion, and the expression of matrix metalloproteinases is suppressed simultaneously (Huang et al., 2010). MMP-mediated degradation of ECM proteins is a prerequisite for breast cancer cell infiltration (Kelly et al., 1998). Integrins are transmembrane receptors of ECM, which regulate tumour motility by modulating the activity of ECM degrading enzymes (Li and Feng, 2011).

Increased expression of heparan sulphate proteoglycans (such as Glypican-1 and syndecan-1) has been observed in the advanced stages of breast cancer (Matsuda et al., 2001). Heparan sulphate proteoglycan is the proteoglycan in ECM or cell surface, which helps to maintain the integrity of ECM and mediate the interaction between cell matrix adhesion and growth factor receptor (Arvatz et al., 2011). Heparinase (a type of β-glucosidase) can promote ECM degradation by decomposing heparan sulphate

proteoglycans (Gotte and Yip, 2006). Tumour cells can synthesize heparinase to degrade heparan sulphate to increase tumour cell invasiveness. Studies have confirmed that overexpression of heparinase in MCF7 cell-lines *in vitro* and *in vivo* promote cell proliferation and matrix invasion (Cohen et al., 2006).

1.1.3.2 Migration and vitality

The migration of tumour cells can be accomplished individually or in a coordinated manner. Moderately and highly differentiated breast lobular carcinoma cells prefer to coordinate migration whilst poorly differentiated tumours are inclined to undergo single cell migration due to the abnormal structure and function of intercellular adhesion proteins (McSherry et al., 2007). The co-migration of tumour cells requires a firm intracellular connection in case of being scattered. As a result, they usually aggregate as emboli after invasion in blood vessels (Fidler, 1973). EMT is a key process in the mesenchymal movement of a single migrating cell. During EMT, tumour cells lose their epithelial phenotype (E-cadherin expression) and express mesenchymal markers, such as N-cadherin, SNAI1, SLUG (SNAI2), TWIST, vimentin, fibronectin (Ye et al., 2011a). Breast tumour cells that undergo EMT are more aggressive. They can remodel their shapes to move through the degraded ECM with the least resistance (Mego et al., 2010). The transcriptional repressors of E-cadherin include E-box-binding homeobox 1 (ZEB1), zinc finger E-box-binding homeobox 2 (ZEB2), twist related protein (Twist), zinc Finger proteins, Snail and Slug, etc., which initiate EMT through TGF-β, Wnt, and phosphatidylinositol 3'kinase serine/threonine kinase (PI3K/AKT) pathway and indicate poor prognosis of breast cancer (Scully et al., 2012).

Tumour stromal cells promote tumour cell migration. Most stromal cells in breast cancer are fibroblasts, commonly referred to as cancer-associated fibroblasts (CAF). Conditioned medium collected from CAF can promote breast cancer cell motility and invasion *in vitro* (Mego et al., 2010).

1.1.3.3 Tumour microenvironment

The tumour microenvironment is composed of fibroblasts, immune cells, blood vessels and ECM (Kalluri and Zeisberg, 2006, Folkman and Kalluri, 2004) and exerts crucial effect in tumour metastasis. The microenvironment of metastatic lesions is essential for the proliferation of disseminating tumour cells (DTCs)(Psaila et al., 2006). The interaction of breast cancer cells with the tumour microenvironment makes *in situ*

breast cancer progress to invasive cancer (Coghlin and Murray, 2010). Macrophages in the tumour environment can interact with breast cancer cells and endothelial cells to form a niche to facilitate tumour colonisation, proliferation, and escape from immune surveillance (Gao and Mittal, 2009). In breast cancer bone metastasis, the interaction between tumour cells and matrix components will impact the proliferation of tumour cells, therefore, successful colonisation of breast cancer in bone depends largely on the bone microenvironment (Parker and Sukumar, 2003). Tumour cells themselves may affect the microenvironment of the secondary site before metastasis, establishing a "pre-metastasis niche" (Psaila et al., 2006). Vascular endothelial growth factor receptor 1 (VEGFR-1)-positive clusters of hematopoietic progenitor cells are observed in the pre-metastatic lymph nodes of breast cancer patients before the tumour cells spread to the distant site (Psaila et al., 2006).

Chemokines are involved in the colonisation of tumour cells to target organs. Chemokine receptor 4 (CXCR4) is highly expressed by breast cancer tissues, and its ligand, chemokine ligand 12 (CXCL12), is mainly in the lymph nodes. Organs with high CXCL12 expression are associated with some sites of metastatic breast cancer (Muller et al., 2001). The interaction of CXCR4-CXCL12 promotes the migration of breast cancer cells to the common site of breast cancer metastasis (Muller et al., 2001).

Another important aspect of metastasis is neovascularisation, which provides nutrition and oxygen for metastases (de Castro Junior et al., 2006). Tumours grow faster than normal tissues and this easily leads to hypoxia in the lesions. The feedback of hypoxia stimulates tumour cells to produce more pro-angiogenic factors to promote the synthesis of blood vessels. For example, hypoxia-inducible factor-1 (HIF-1) triggers the production of an angiogenic protein vascular endothelial growth factor (VEGF) (de Castro Junior et al., 2006, Pugh and Ratcliffe, 2003). Through binding with specific VEGFRs, VEGF can enhance the proliferation of vascular endothelial cells and increased the permeability of micro-vessels to induce neovascularisation (Dvorak, 2002). Tumour vasculature is different from the normal vessel both in structure and function. Abnormal blood vessels do not provide sufficient oxygen for the tumour, leading to a vicious cycle of tumour hypoxia (Jain, 2005). In breast cancer, the expression of VEGF indicates a poor prognosis and the tumour is prone to metastasis (Mareel et al., 2009).

1.1.3.4 Breast cancer and bone metastasis

1.1.3.4.1 Molecular mechanism of bone metastasis

Bone metastasis is one of the most serious complications, which often occurs in the advanced stage of solid tumours such as lung, breast, prostate, colorectal, thyroid, gynaecologic, and melanoma (Fornetti et al., 2018). The morbidity of bone metastasis is about 70% in aggressive breast cancer (Hernandez et al., 2018). As the advanced phase of breast cancer, bone metastasis is incurable and often leads to a debilitating disease with many other skeletal related events (SREs) including pathological fracture caused by osteolysis, dysfunction of the limb and bone marrow aplasia (Coleman, 2006). Bone metastasis not only minimises the life quality but also decreases the overall survival of the patients. Mortality in patients with bone metastases was significantly higher, especially for bone metastasis complicated by SREs (Sathiakumar et al., 2012).

Bone remodelling and the bone metastasis of breast cancer

Normal bone metabolism is the process within dynamic balance of bone remodelling which is well orchestrated by osteoblasts, osteoclasts and osteocytes. Bone remodelling can regulate calcium homeostasis, repair bone damage to resist stress and maintain skeletal system function. Bone remodelling is a process in which osteoclasts and osteoblasts coordinate with each other. First, osteoclasts destroy the existing unhealthy bone, this process is called bone resorption, then the osteoblasts absorb matrix and minerals to rebuild bone, namely, reconstruction (Parfitt, 2002). Recent studies showed that osteocytes were the main producer of cytokine receptor activators for Nuclear factor-κB ligand (RANKL), which was the main promoter for bone remodelling (Xiong and O'Brien, 2012). RANKL is crucial in modulating the differentiation and activity of osteoclasts. In remodelling of cancellous bone , RANKL is mainly secreted by osteocytes, whilst hypertrophic chondrocytes are the main secretor of RANKL in the formation of endochondral bone (Xiong and O'Brien, 2012). Studies revealed that the bone cells and hypertrophic chondrocytes in the bone matrix could response to the signal of bone resorption and adjust the maturation and activity of osteoclasts (Xiong and O'Brien, 2012). Hormones, cytokines and growth factors influence the proliferation of osteoclasts and osteoblast progenitor cells by modulating the expression of RANKL in osteocytes. Parathyroid hormone (PTH) induced the generation of osteoclast by stimulating RANKL secretion in bone cells (Fu et al., 2006).

When osteocytes underwent apoptosis, increased production of RANKL could promote bone absorption (Tatsumi et al., 2007). Sex steroids inhibited maturation of osteoclasts, and reduced secretion of sex hormone enhanced the activity of osteoclasts, which may lead to apoptosis of bone cells to promote bone resorption (Xiong and O'Brien, 2012). In normal bone metabolism, these key components maintain a normal dynamic balance. Once the balance is destroyed, it may lead to osteolytic lesions, presenting lower bone density or osteoblastic lesions, with excessive bone deposition. After menopause, due to the rapid decline in oestrogen levels, osteoclasts are active and bone loss is accelerated. After breast cancer patients received chemotherapy or hormone adjuvant therapy, the risk of low bone density and osteoporosis has been found to be increased (Van Poznak and Sauter, 2005). When breast cancer cells spread to the bones, they will gradually adapt to the bone microenvironment, destroy the normal bone homeostasis, then, start a vicious cycle of bone metastasis under various mechanisms.

The process of bone metastasis of breast cancer is a multi-steps cascade which contains four main steps: "(1) invasion, proliferation and dissociation of cancer cells from the primary lesion, (2) intravasation, migration in the circulation (3) extravasation of cancer cells (4) colonisation in the bone, disseminated tumour cells settle down in the bone niche, where normally hosts hematopoietic stem cells (HSCs), survival under dormancy, reactivation and ultimate outgrowth" (Roodman, 2004, Yoneda and Hiraga, 2005).

1.1.3.4.1.2 Predilection to metastasis to the bone

Although it is lacking in understanding, characteristics of bone environment and properties of breast cancer cells certainly bear traits at levels of tissues, cells and genes for the predisposition of bone metastasis from breast cancer. The inorganic phase of bone is mainly composed of the mineral hydroxyapatite nanocrystals (HA). High HA induced the secretion of pro-osteoclastic interleukin-8 (IL-8) by MDA-MB-231 cells to facilitate bone colonisation (Pathi et al., 2010). The extracellular bone matrix is enriched with type-I collagen, osteopontin (OPN), and bone sialoprotein (BSP). Elevated expression of OPN and BSP can facilitate tumour cell adhesion to collagen and increase metastatic propensity to bone (Kruger et al., 2014, Pecheur et al., 2002). The skeletal microenvironment is known to be a highly hypoxic environment and the pressure of oxygen (pO2) in mouse bone marrow is significantly lower than other

tissues or organs (Ferrer et al., 2020). Hypoxia is known to be involved in various steps of bone metastasis, including the premetastatic niches, dormancy and osteolytic vicious cycles (Hiraga et al., 2007, Cox et al., 2015). Bone marrow hypoxia can promote the expression of HIF-1 (Spencer et al., 2014), which subsequently induce the secretion of C-X-C motif chemokine 12 (CXCL12) (Devignes et al., 2018). Upon binding with Ca^{2+} and chemokine receptor 4 (CXCR-4), CXCL12 activate multiple signalling pathways such as PI3K/Akt, ERK/MAPK pathway to facilitate the colonisation of disseminated tumour cells in bone tissue (Wang et al., 2016). Hypoxia could also enhance the activity of osteoclasts and suppress the differentiation of osteoblasts (Hiraga et al., 2007). The bone environment contains a lot of alkaline minerals (hydroxyapatite) and the buffer system to maintain a normal pH value. In the early stage of bone metastasis, due to the hypoxia and excess secretion of H+ both inside and outside of the cell membrane, caused by a high glycolysis status in the tumour cells, the bone microenvironment is maintained in a state of acidosis. Among this process, vacuolar H^+-ATPase (V-ATPase) performed actively for bone microenvironment acidosis, which was expressed in both tumour cells and osteoclasts (Avnet et al., 2017). Acidosis significantly enhanced the activity of osteoclasts with elevated secretion of cytokines, leading to bone loss, such as activated T-cell nuclear factor 1 in activated osteoclasts (Yuan et al., 2016). Acidosis could also inhibit the biological functions of osteoblasts, leading to impaired trabecular bone formation and promoted the expression of osteoclast RANKL (Arnett, 2010). In addition, the acidosis environment activated NF-κB signal transduction pathway in mesenchymal stromal cell can promote the secretion of inflammatory factors, chemokines and growth factors, such as IL-1, IL-6 and CXCL2, which can subsequently induce tumour-induced nociception and hyperalgesia to facilitate invasion and immune escape (Avnet et al., 2017).

Trabecular of cancellous bone is fenestrated which contains rich blood vessels with slow blood flow and is suitable for breast cancer cells to colonise after successfully spreading through blood circulation (Theriault and Theriault, 2012).

Various kinds of tumour cells including ovarian, gastric and colorectal cancers can be detected in the bone marrow (Juhl et al., 1994, Banys et al., 2009, Dardaei et al., 2011), which indicates that the bone metastasis of breast cancer at the initial stage is passive. However, only a few kinds of cancer cells including breast cancer cells can form overt metastatic bone lesions (Coleman, 2006), which indicates that passive

dissemination of breast tumour cells to the bone marrow is an early step in forming bone metastasis, but it is not the critical driving event of bone metastasis. Apart from the passive transportation，the properties of breast cancer cells are essential in bone metastasis. The bone environment is a reservoir for minerals, especially for calcium ions. Breast cancer cells highly express calcium-sensing receptor (CaSR), which could bind with Ca^{2+}, by identifying extracellular Ca^{2+}, and promotes breast tumour cell spread to the bone tissue with high Ca^{2+} concentration. *In vitro* studies have shown that extracellular Ca^{2+} combined with CaSR expressed by tumour cells activate AKT and MAPK pathways to enhance migration and proliferation of cancer cells, whilst application of CaSR antagonists to interfere with renal cancer in mice significantly reduced the incidence of bone metastasis (Frees et al., 2018).

RANK was highly expressed on the surface of breast cancer cells, while RANKL was overexpressed in bone tissues (Rose and Siegel, 2010, Jones et al., 2006). In addition, the chemokine receptor CXCR4 was highly expressed in breast cancer tissues, and its ligand CXCL12 was overexpressed in common metastatic sites of breast cancer including bone marrow (Muller et al., 2001). These findings may explain why bone is the preferential metastatic site for breast cancer cells. Mechanisms of bone metastasis in breast cancer were elucidated in Figure 1.1.

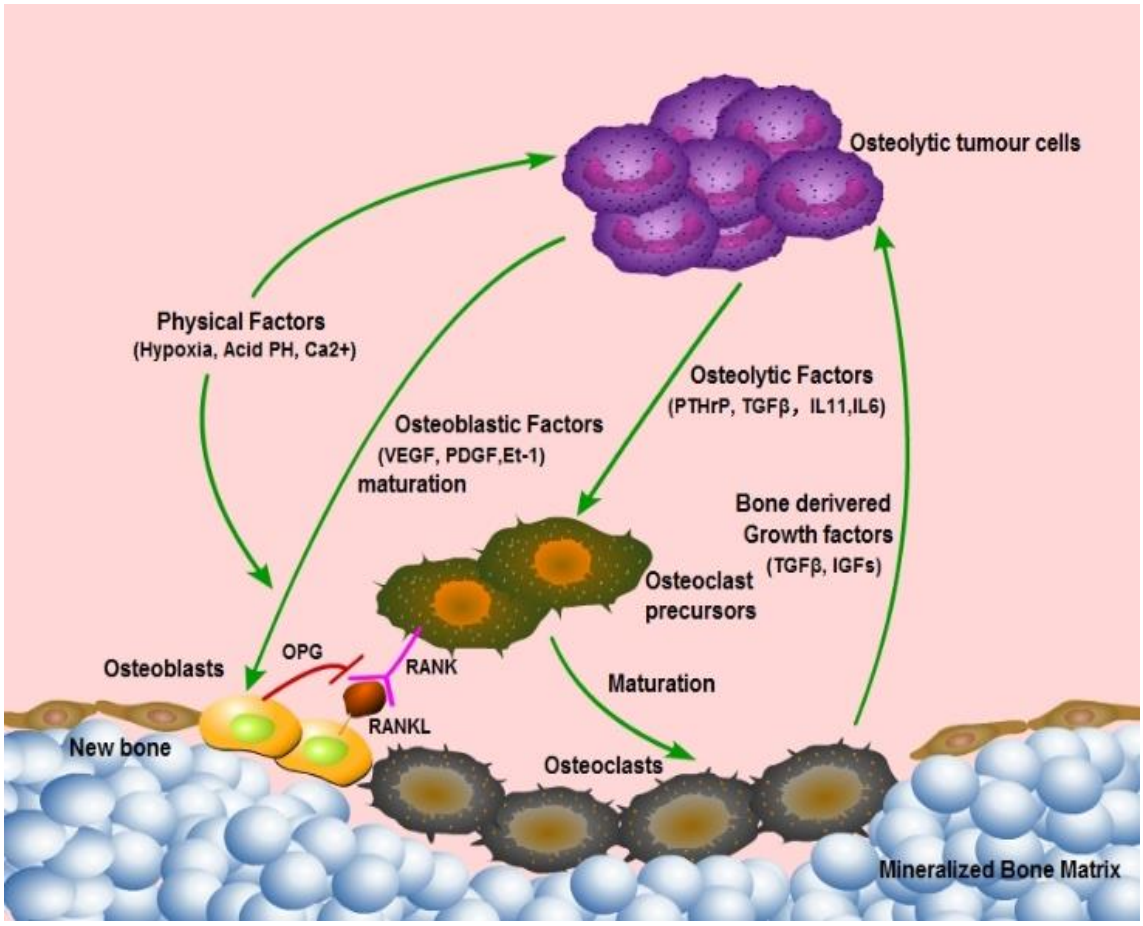

Figure 1.1 Mechanism of bone metastasis in breast cancer. Osteolytic factors such as PTHrP, TGFβ, IL11, IL6 etc. secreted from the tumour cells induce the maturation of osteoclast, leading to the bone destruction. Tumour cells also secrete osteoblastic factors including VEGF, PDGF etc. to promote the maturation of osteoblast to induce bone formation. RANKL produced by the osteoblast also contributes to the maturation of osteoclast to lyse the bone matrix. Released growth factors due to the bone destruction support the expansion of tumour cells in turn and aggravate the bone destruction. This process is named vicious cycle.

1.1.3.4.2 Biological character of bone metastasis in breast cancer

Bone metastasis is preferential in poorly-differential and ER-positive breast tumours (James et al., 2003). Notably, although the early incidence of bone metastasis in ER-negative cancers is higher, the frequency of bone recurrence is higher in ER-positive cancers, this phenomenon may be caused by effective endocrine therapy in ER-positive cases (Colleoni et al., 2000). Lymph circulation plays a vital role in the invasion of breast cancer and the lymph node status is very important in predicting the prognosis of breast cancers. Generally, the assessment of the incidence of bone metastasis in breast cancer includes the number of positive lymph nodes, the size of the tumour, and age of the patient. If the numbers of lymph nodes are more than 4, and the

size of the tumour is larger than 2cm and the patient is younger than 35 years, the patients are usually associated with higher risk of bone metastasis (Colleoni et al., 2000).

Dormancy:

After settling down in the bone, in order to evade host immunosurveillance and adapt to the bone environment, disseminated breast cancer cells remain in a quiescent state for a long period, characterised by arresting at G0/G1 phase without obvious proliferating features (Aguirre-Ghiso, 2007, Sosa et al., 2014). The duration of dormancy varies in different subtypes of breast cancer. In luminal A/B breast cancer subtypes, dormancy may experience a steady probability of metastatic relapse to bone up to 10 years, however in triple-negative breast cancer (TNBC) subtype, bone metastases are often developed within 5 years following after diagnosis (Kennecke et al., 2010).

Regulation of the dormancy

The local microenvironment of the primary tumour continues to affect the dormant state of bone metastases. Primary tumours often present a hypoxic state, and the subgroups of DTC produced by hypoxic state highly express the dormant gene program driven by NR2F1 (Nuclear Receptor Subfamily 2 Group F Member 1) and enter a dormant state in metastases (Fluegen et al., 2017). Bone marrow is the place where hematopoietic stem cells (HSC) are produced. Two stem cell compartments are present in the bone marrow, which are the perivascular niche and the endosteal niche. Endothelial cells and osteoblast lineage cells are resident in the perivascular niche and endosteal niche, respectively, to produce growth and apoptosis signal to maintain the HSC population (Crane et al., 2017). There are many cell chemokines in the bone microenvironment, including CXCL12, CXCR4 and E-selectin, which can attract metastatic breast cancer to colonize the perivascular niche, and where, the residual endothelial cells can secrete angiogenesis inhibitors such as thrombospondin 1 (TSP1) to promote the disseminated breast cancer cells into dormancy (Ghajar et al., 2013). The cooperation between the endosteal niche and the hematopoietic stem cell (HSC) niche can also provide a microenvironment that facilitates dormancy of breast cancer metastases and is feasible for the survival of metastatic cancer cells (Shiozawa et al., 2011, Price et al., 2016).

The dormancy of metastatic tumours in bone metastases is also impacted by the internal signal of the tumour. The p38 pathway plays a significant role in mediating the regulation of tumour dormancy signals (Gomis and Gawrzak, 2017). Bone morphogenetic proteins in the bone microenvironment up-regulate the expression of p38 and down-regulate the expression of ERK, thereby inducing metastatic tumour dormancy in the bones (Gomis and Gawrzak, 2017). TGFβ2 is more abundantly expressed in bone marrow than other tissues, which can induce tumour dormancy in bones (Sosa et al., 2014). Mitogen and stress-activated kinase 1 (MSK1), the downstream mediator of p38 MAPK signal, can effectively regulate the dormancy and progression of breast cancer in bone metastases (Gawrzak et al., 2018). Down-regulation of MSK1 changes the structure of chromatin, resulting in decreased expression of luminal differentiation genes (GATA3, FOXA1) and promoting the colonisation of bone-disseminated breast cancers. Genes regulated by MSK1 expression or p38 MAPK are associated with advanced metastasis in breast cancer patients (Gawrzak et al., 2018, Kim et al., 2012a). The orphan nuclear receptor NR2F1 is another mediator of p38 MAPK activation, which can drive a variety of cancer types, including breast cancer, into a pre-dormant state (Sosa et al., 2015). Recent clinical evidence shows that the expression of NR2F1 is associated with early recurrence of breast cancer, expression of NR2F1 is positively correlated with the recurrence of breast cancer (Borgen et al., 2018). Autophagy is another critical mechanism to increase the survival of breast cancer cells by inducing dormancy via Beclin 1 (BECN1)-independent pathway (Vera-Ramirez et al., 2018).

Outgrowth:

When metastatic cells are successfully accustomed to the bone microenvironment, the balance between cell proliferation and apoptosis of breast cancer cells will be interrupted and altered by a unique positive feedback cycle composed of tumour cells, osteoclasts, osteoblasts, and the bone matrix, named “the vicious cycle of bone metastasis” (Roodman 2004). Having undergone EMT, disseminated breast cancer cells in the bone can obtain a phenotype similar to the osteoblasts, which is named osteomimicry. The osteoblast-like phenotype is characterized by the significantly high expression of pro-osteoblastic genes (Tan et al., 2016).

After Osteomimicry transition, tumour cells can imitate the function of osteoblasts as the paracrine regulators of osteoclasts. Several cytokines such as nuclear factor-κB receptor activator (RANK), interleukin-1 (IL-1), IL-6, IL-11, macrophage inflammatory protein 1a (MIP1a), macrophage colony stimulating factor (M-CFS), parathyroid hormone-related peptide (PTHrP) are released by the osteo-mimicking tumour cells to accelerate the formation and activity of osteoclasts, eventually leading to the exacerbated bone erosion which cannot be balanced by bone formation (Weidle et al., 2016).

These osteo-mimicking breast cancer cells can also upregulate the expression of RANK ligand (RANKL) on the surface of osteoblasts (Roodman, 2004). RANKL can combine with RANK on the surface of the pre-existing osteoclasts to increase their activity (Chen et al., 2018). On the other hand, osteoblasts secrete osteoprotegerin (OPG), a decoy receptor sharing the same extracellular structure of RANK, which can competitively bind to RANKL and inhibit osteoclastic activity (Maroni et al., 2016). PTHrP, released by osteoblasts, acts as an important paracrine regulator for the vicious cycle. PTHrP can promote the expression of RANKL in osteoblasts to enhance the osteoclastogenesis induced by tumour cells (Ricarte et al., 2018). PTHrP can inhibit OPG activity and activate osteoclasts, which, in turn, leads to bone destruction (Ricarte et al., 2018). Metastatic breast cancer cells secrete this factor, thereby, leading to an aggravated bone destruction (Roodman, 2004). The destruction of bone structure provides space for disseminated breast cancer cells to be accommodated. The bone resorption also leads to the release of cytokines stored in the bone matrix, such as BMP, TGFβ, FGF and platelet-derived growth factor (PDGF). These factors can promote the proliferation of tumour cells and the production of PTHrP, leading to more bone destruction (Weidle et al., 2016).

Following osteolysis, large amounts of calcium within the matrix is released to the peripheral blood, which is responsible for hypercalcemia. Calcium-sensing receptors expressed on the surface of breast cancer cells can interact with calcium ions to promote tumour cell proliferation and survival (Maurizi and Rucci, 2018).

The Wnt signalling cascade is involved in enhancing osteoblast differentiation and suppressing osteoblast activity (Clevers, 2006). Dickkopf-1 (DKK-1) is highly expressed in breast cancer patients with bone metastasis, which can promote osteoblast

differentiation by inhibiting Wnt signalling (Voorzanger-Rousselot et al., 2007). Apart from DKK-1, breast cancer cells can also secrete other inhibitors for osteoblastic differentiation such as Noggin to enhance osteolysis (Clezardin, 2011).

Although breast cancer bone metastases are mainly characterised as osteolytic lesions, there are also osteogenic skeletal lesions in approximate 12-50% of breast cancer (Kozlow and Guise, 2005). In addition, bone destruction in osteolytic lesions can induce subsequent osteogenesis, leading to osteoblastic manifestation (Weidle et al., 2016), which explains the existence of mixed lesions in breast cancer bone metastases.

The molecular mechanism of osteoblastic lesions in breast cancer is less explored. Recent studies have shown that core binding factor α1 (Cbfα1), also known as Runx-2, is closely related to osteoblastic differentiation (Weidle et al., 2016). Runx-2 was proved to exert multiple roles essential for the metastatic process (Baniwal et al., 2010). N-telopeptide of type I collagens (NTX), a biomarker of bone resorption, is higher in osteoblastic disease. The ratio between urinary NTX and creatinine is routinely monitored as a measure for bone resorption currently (Coleman et al., 2005). Osteoblast cadherin (CDH11) was also proved as an important stromal interaction protein in osteoblastic metastasis in prostate cancer (Chu et al., 2008). Other cytokines that enhance the growth, differentiation and activity of osteoblasts include platelet-derived growth factor (PDGF) , fibroblast growth factor , TGF-β , bone morphogenetic protein (BMP) and Endothelin-1 (Tahara et al., 2019). Endothelin-1 can suppress the expression of DKK-1 gene in bone marrow stromal cells (Guise et al., 2003). When the inhibitory effect of Dkk-1 for Wnt signalling is blocked, more active osteoblasts will be produced, which is conducive to the development of osteoblastic lesions. Signalling pathways associated with the bone metastasis in breast cancer were summarised in Table 1.1.

Table 1.1 Signalling pathways associated with the bone metastasis in breast cancer

Cytokines	Role	Result
Parathyroid hormone related peptide (PTHrP)	promote the expression of RANKL in osteoblasts	Induce bone resorption by osteoclasts
Receptor activator of nuclear factor κB ligand (RANKL)	Binding with RANK receptor on osteoclast precursors	Facilitate osteoclast maturation and activation, leading to bone resorption
Osteoprotegerin (OPG)	a decoy RANK receptor	Blocks the interaction of RANK and RANKL, suppresses osteoclast maturation
Insulin-like growth factor 1 (IGF-1)	induces chemotaxis of tumour cells and guides migration	induces proliferation of metastatic tumour cells in bone
Transforming growth factor beta (TGF-β)	Promote the secretion of PTHrP and the apoptosis of osteoclast; blocks the apoptosis of osteoclasts	Accelerates the bone resorption inducing by osteoclast
Interleukin 6 (IL-6)	Promotes osteoclastogenesis and inhibits osteoblasts	Facilitates bone resorption, reduced bone formation
Interleukin 11 (IL-11)	Promotes the maturation of osteoclasts and inhibits osteoblasts	Facilitates bone resorption, reduced bone formation
Prostaglandin E2	Promotes the maturation and activity of osteoclasts via inducing RANKL expression	Facilitates bone resorption
Macrophage colony stimulating factor (M-CSF)	Promotes the maturation of osteoclasts and inhibits osteoblasts	promotes bone resorption
Tumour necrosis factor alpha (TNF-α)	Induces osteoclastogenesis and suppresses osteoblasts	promotes bone resorption
Integrins	Facilitates the colonisation of tumour cells in metastatic lesions	Accelerates the progression of tumour cells
Osteopontin (OPN)/bone sialoprotein (BSP)	Induces the proliferation of osteoblast	Promotes bone resorption

PTHRP (Fu et al., 2006), RANKL (Nagy and Penninger, 2015), OPG (Deligiorgi et al., 2020), IGF-1 (Rieunier et al., 2019), TGF-β (Juarez and Guise, 2011), IL-6 (Ara and Declerck, 2010), IL-11 (Maroni et al., 2021), Prostaglandin E2 (Ohshiba et al., 2003), M-CSF (Kim and Kim, 2016), TNF-α (Graham et al., 2010), OPN (Si et al., 2020).

1.1.4 Gaps and challenges in the current therapy and understanding of the disease

Following the advance in early diagnosis and novel treatments, the treatment of breast cancer has been transformed from the original surgical resection to a combination with optimised drug treatment and reduced levels of surgical removal. Meanwhile, the prognosis of breast cancer has vastly progress improved in recent years. Generally, current drug treatments for breast cancer contain local and systemic therapy, the optimised disease management can be tailored for different subtypes of the disease.

For luminal type breast cancer, ERα acts as the major oncogenic promoter, endocrine therapy including ERα-blockade, oestrogen synthesis inhibition, and selective ERα degradation is the primary choice. Follow-up study shows that breast cancer of luminal subtype presents the best prognosis and 5-year overall survival rate reaches approximately 90% (American Cancer Society. Breast cancer facts and figures 2019–2020). Despite the successfully treatment with endocrine therapy, arising therapeutic resistance often triggers the recurrence of breast cancer. Several mechanism, such as the alteration of ESR1 (Hanker et al., 2020) and its coregulators (Bertucci et al., 2019, Zheng et al., 2020), aberrant cell-cycle (Razavi et al., 2018, Finn et al., 2016, Chandarlapaty and Razavi, 2019) and/or dysregulated epigenetic factors (Xu et al., 2020, Morel et al., 2020) have been hypothesized for the endocrine resistance. However, no effective treatment could be applied to significantly improve endocrine resistance in breast cancer.

HER2 overexpression subtype comprises 15% to 20% of breast cancers. For HER2 positive breast cancer, ErbB2-neutralizing antibody, trastuzumab (Herceptin), is used as a target therapy combined with systemic chemotherapy. Following activation, HER2 exerts its influence and downstream signalling through heterodimerization with the co-receptors. HER2 signalling pathway cannot be distinguished from other RTKs such as EGFR, HER3 or HER4 pathways. Actually, one serious issue for the treatment of breast cancer is that the cellular event of the tumour is not caused by the mutation of a unique gene, it is the epigenomic alteration regulated by the crosstalk of various kinds of signalling pathways, that is the main reason for the complexity of cancer and treatment associated difficulties. Although the expression of the major oncogene Her2 could be intercepted, the subsequent elevated expression of ErbB3, ErbB3 mRNA transcription is inversely correlated with HER2 signalling(Garrett et al., 2011), could activate the

PI3K/Akt pathway, leading to the robust proliferation and invasion of breast cancer (Schoeberl et al., 2009). Another challenge for the anti-ErbB2 target therapy is the drug-induced cardiotoxicity (Vermeulen et al., 2016). Recent research suggested that this side effect could be avoided without disturbing the ligand-dependant Her2 signalling (De Keulenaer et al., 2010).

For the triple negative breast cancer, no effective targeted therapy is currently available, which means the patient can exclusively accept the systemic chemotherapy and the prognosis of this subtype is the worst. More effort should be paid to this subtype to reveal the core mechanism involved to help patients.

Recently, many novel targeted therapies have been exploited based on the research of signalling pathways, for example, the DKK1-neutralizing antibody to block Wnt signalling for bone metastases therapy (Chen et al., 2012b), bisphosphonates and denosumab to target the activity of osteoclasts (Steger and Bartsch, 2011) and Rapamycin, a specific inhibitor of mTOR for PI3K/Akt signalling pathway, to suppress the progression of breast cancer (Royce and Osman, 2015).

Another problem for the treatment of breast cancer is tumour recurrence after surgical resection and the conservative therapy, one reason accounting for relapse being disseminated cells in a dormant state (Zhang et al., 2013). Currently, such dormant cells are insensitive to existing treatment, however, research in BMP signalling pathways have revealed that BMP signalling impacted the self-renewal and regulated the transition of active and indolent cells (Buijs et al., 2012).

1.2 BMPs

1.2.1 Introduction of BMPs

Bone morphogenetic proteins (BMPs) are a branch of the transforming growth factor-beta (TGF-β) superfamily, which were purified in the late 1980s by Dr. Urist (Urist, 1965). To date, more than 20 BMPs have been identified. Members of Bone Morphogenetic Protein and Growth Differentiation Factors were summarised in Table 1.2. Initially, BMPs were found as vital modulators in bone homeostasis and turnover. For instance, BMPs can facilitate intramembranous and endochondral osteogenic and cartilage formation. BMPs actively participate in development and homeostasis of diverse tissues and organs including kidney, heart, prostate and breast. Moreover, they

also play a pivotal role in coordinating cellular functions and events including cellular differentiation, proliferation and apoptosis (Ye et al., 2011a). In recent years, BMPs have been implicated in many solid tumours, especially in hormone related tumours, such as breast cancer and prostate cancer (Ye et al., 2007b, Davis et al., 2016). Due to the preference of breast cancer to metastasise to bone and their implication in other hormone related cancers, BMPs may exert important role in breast cancer bone metastasis. Exploring their impact on the biological behaviour breast cancer will help us deepen our understanding of this disease and may provide novel target therapies to prevent and treat bone metastasis.

Table 1.2 Members of Bone Morphogenetic Protein and Growth Differentiation Factors (Identified in Humans)

Official Symbol	Alternative Name	Gene Location in homo sapiens	Year of identification
BMP2	BMP2A	20p12	1988
BMP3	BMP3A; KFS3	4p14-q21	1988
BMP4	ZYME; BMP2B; BMP2B1	14q22-q23	1988
BMP5	MGC34244	6p	1990
BMP6	VGR; VGR1	6p24-p23	1990
BMP7	OP-1	20	1990
BMP8A	OP-2	1p35-p32	1996
BMP8B	BMP8; Osteogenic Protein2	1p35-p32	1992
BMP10		2p13.3	1999
BMP15	GDF9B, ODG2	Xp11.2	1998
GDF1	CES1	19p12	1991
GDF2	BMP-9; BMP9; HHT5	10q11.22	1994
GDF3	MCOP7; KFS3; MCOPCB6; MCOP7	12p13.1	2000
GDF5	CDMP1; BMP14; Radotermin	20q11.2	1994
GDF6	BMP13; KFS1	8q22.1	1999
GDF7	BMP12	2p24-2p23	1998
GDF8	MSTN; MSLHP	2q32.1	1997
GDF9	POF14	5q23-5q33.1	1993
GDF10	BMP-3b	10q11.22	1995
GDF11	BMP-11	12q13.13	1998
GDF15	PLAB, MIC-1, PDF, MIC1, NAG-1, PTGFB	19p13.1-13.2	1997

Table 1.2 Derived from the literature published (Ye et al., 2007b). Based on literature published BMP2 (Wozney et al., 1988); BMP3 (Wozney et al., 1988); BMP4 (Wozney et al., 1988); BMP5 (Celeste et al., 1990); BMP6 (Celeste et al., 1990); BMP7 (Ozkaynak et al., 1990); BMP8A (Strausberg et al., 2002); BMP8B (Ozkaynak et al., 1992); BMP10 (Neuhaus et al., 1999); BMP15 (Dube et al., 1998); GDF1 (Lee, 1990); GDF2 (Celeste et al., 1994); GDF3 (McPherron and Lee, 1993); GDF5 (Hotten et al., 1994); GDF6 (Davidson et al., 1999); GDF7 (Lee et al., 1998); GDF8 (McPherron et al., 1997); GDF9 (McPherron and Lee, 1993);GDF10 (Cunningham et al., 1995); GDF11 (Gamer et al., 1999); GDF15 (Yokoyama-Kobayashi et al., 1997).

Structure of BMPs

BMPs consist of an amino-terminal (N-terminal) pro-region and a carboxy-terminal (C-terminal) ligand (Ozkaynak et al., 1990, Wozney et al., 1990). Once they are synthesised, cleavage by enzymes transforms the precursor proteins into ligands and pro-protein fragments. BMP ligands form both homodimers and heterodimers to fulfil their biological functions. Intriguingly, the heterodimers of BMP4/7, BMP2/6, BMP2/7 and BMP7/GDF7 are often more effective than their respective homodimers (Suzuki et al., 1997, Butler and Dodd, 2003).

1.2.2 BMP signalling pathways

1.2.2.1 Smads dependent pathway

In this canonical BMP signalling pathway, BMP ligands bind to a complex of serine-threonine kinase transmembrane receptors including type I receptors (BMPRIA, BMPRIB, ACVRI, ACVR1B, ACVR1C and ACVRLI) and type II receptors (BMPRII, ACVRIIA, and ACVRIIB), resulting in a phosphorylation of the type I receptors (Table 1.3). The activated receptor complex then recruits and phosphorylates the downstream transcription factor, Smad (Sons of mothers against decapentaplegic) 1, 5, and 8. Subsequently, phosphorylated Smads1/5/8 forms a heteromeric complex with Smad4 which acts as a shuttle to transport the Smad complex into the nucleus (Nickel and Mueller, 2019) (Fig. 1.1).

1.2.2.2 Smad independent pathway

BMP signalling transduction in cell events can also be achieved without the mediation by Smads, which are collectively referred to as non-canonical (Smad- independent) BMP signalling pathways. BMPs are involved in cytoskeletal dynamics regulation by activating Rho-like GTPases (Nickel and Mueller, 2019). BMPs modulate various cell events including differentiation and apoptosis through mitogen-activated protein kinase (MAPK) pathway. In non-canonical BMP signalling pathways, BMP ligands present higher affinity for type I receptors than type II receptors. BMP ligands preferentially bind to ALK3 or ALK6, then recruit BMPRII to form the hetero-oligomeric complexes

(BMP-induced signal complex (BISC)) (da Silva Madaleno et al., 2020). Depending on the ligands and receptors recruited, the Smad-independent pathway involves the transmission via a variety of other signal pathways, including the MAPK pathway, RAS pathway, PI3K/Akt pathway, Rho-GTPases pathway (Zabkiewicz et al., 2017). X-linked apoptotic protein (XIAP), p52ShcA and TRAF6 serve as a scaffold protein to bridge type I receptors and TGF-ß activation binding protein (TAB1/2/3) during intracellular signal transduction (Ye and Jiang, 2016). TAB1 acts as the activator of TGF-ß activation binding protein (TAK1), leading to the activation of downstream molecules in mitogen-activated protein kinase (MAPK) signalling pathways, such as p38, Jun N-terminal kinases (JNKs), NF-κB and Nemo-like kinases (NLK), to regulate the cellular biological events (Kimura et al., 2000, Malireddi et al., 2019) (Figure 1.2). Receptors and R-Smads involved in BMP signalling were summarised in Table 1.4.

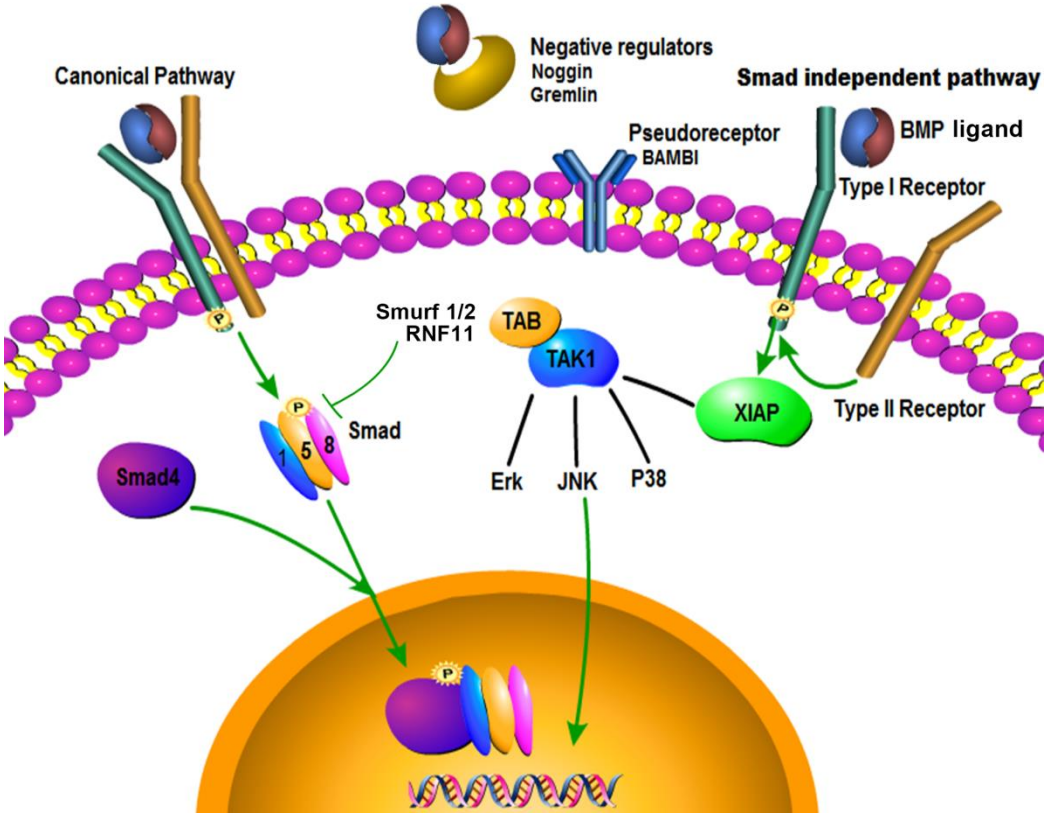

Figure 1.2 Signalling pathway of BMPs including Smad-dependent pathway and Smad-independent pathway. Pathway builder tools from www. proteinlounge.com was used to create the figure.

Table 1.3 Transmembrane serine/threonine kinase receptors

Type I receptor	Type II receptor
ACVRL1 (ALK-1, ACVRLK1, ALK1, SKR3)	TGFBR2 (TGFR-2, TGFbeta-RII)
ACVR1 (ALK2, ACTRI, ACVRLK2, FOP, SKR1)	TGFBR3
BMPR1A (ALK3, ACVRLK3, CD292)	***BMPR2*** (BMPR-II, BMPR3, BMR2, BRK-3, T-ALK)
ACVR1B (ALK4, ACTRIB, ACVRLK4, SKR2)	***ACVR2B*** (ActR-IIB)
TGFBR1 (ALK-5, ACVRLK4, SKR4, TGFR-1)	***ACVR2A*** (ACTRII, ACVR2)
BMPR1B (ALK-6, ALK6, CDw293)	AMHR2(MISR2)
ACVR1C (ALK7, ACVRLK7)	Punt
Thickveins	

Transmembrane serine/threonine kinase receptors updated from (Ye et al., 2011b). There are seven Type I and five Type II transmembrane serine/threonine kinase receptors identified in humans. Six Type I receptors and three Type II receptors that have been found to be involved in the signal transduction of BMPs, which are ***bold italic*** in the table. ACVRL1, activin A receptor type II-like 1; ACVR1, activin A receptor, type I; BMPR1A, bone morphogenetic protein receptor, type IA; ACVR1B, activin A receptor, type IB; TGFBR1, transforming growth factor, beta receptor I; BMPR1B, bone morphogenetic protein receptor, type IB; ACVR1C, activin A receptor, type IC; TGFBR2, transforming growth factor, beta receptor II; TGFBR3, transforming growth factor, beta receptor III; BMPR2, bone morphogenetic protein receptor, type II; ACVR2B, activin A receptor, type IIB; ACVR2A, activin A receptor, type IIA.

Table 1.4 Receptors and R-Smads involved in BMP signalling

Official Symbol	Type II receptor	Type I receptor	R-Smad
BMP2	BMPRII ActRIIA	ALK 3/6	Smad 1/5/8
BMP3	ActRIIA	ALK 4	Smad 2/3
BMP4	BMPRII ActRIIA	ALK 3/6	Smad 1/5/8
BMP5		ALK 3	Smad 1/8
BMP6	ActRIIA ActRIIB BMPRII	ALK 1/2/3/6	Smad 1/5
BMP7	BMPRII ActRIIA	ALK 2/3/6	Smad 1/5/8
BMP8A	ACVR2A BMPR2 ACVR2A ACVR2B TGFBR2	ALK3/6 ALK4/5	Smad1/5/8 Smad2/3
BMP8B			
BMP10	ActRIIB	ALK 3/6	Smad 1/5/8
BMP15	BMPRII	ALK 6	Smad 1/5/8
GDF1	ActRIIB	ALK 4	Smad 2/3
GDF2	ActRIIA ActRIIB BMPRII	ALK 1	Smad 1/5
GDF3			
GDF5	BMPRII ActRIIA	ALK 3/6	Smad 1/5/8
GDF6	BMPRII ActRIIA	ALK 3/6	

GDF7	BMPRII ActRIIA	ALK 3/6	
GDF8	ActRIIB	ALK4/5	Smad 2/3
GDF9	BMPRII	ALK5	Smad 2/3
GDF10			
GDF11	ActRIIA ActRIIB	ALK4	Smad 2/3
GDF15			Smad 2/3

Receptors and R-Smads involved in BMP signalling. Updated from literature published (Ye et al., 2011b). BMP2 (Koenig et al., 1994, Yamaji et al., 1994, Liu et al., 1995); BMP3 (Daluiski et al., 2001); BMP4 (Koenig et al., 1994, ten Dijke et al., 1994, Yamaji et al., 1994, Nohno et al., 1995, Rosenzweig et al., 1995, Aoki et al., 2001); BMP5 (Beck et al., 2001, Zuzarte-Luis et al., 2004); BMP6 (Ebisawa et al., 1999, Ahmed et al., 2001, Aoki et al., 2001); BMP7 (ten Dijke et al., 1994, Liu et al., 1995, Rosenzweig et al., 1995, Aoki et al., 2001); BMP8A (Wu et al., 2017, Wu et al., 2020) BMP10 (Mazerbourg et al., 2005); BMP15 (Moore et al., 2003); GDF1 (Cheng et al., 2003); GDF2 (Brown et al., 2005, Lopez-Coviella et al., 2006); GDF5 (Nishitoh et al., 1996, Aoki et al., 2001, Nakahara et al., 2003, Sammar et al., 2004, Chen et al., 2006); GDF6 (Mazerbourg and Hsueh, 2006); GDF7 (Mazerbourg et al., 2005); GDF8 (Rebbapragada et al., 2003); GDF9 (Mazerbourg and Hsueh, 2006); GDF11 (McPherron et al., 1999, Andersson et al., 2006); GDF15 (Xu et al., 2006).

1.2.3 Regulation of the BMP signalling pathway

The BMP signalling pathway is regulated by a variety of mechanisms through intervening in the binding between extracellular ligands and receptors (extracellular regulation), or in the process of intracellular signal relay (intracellular regulation) (Table 1.5).

Intracellular regulator of Smad signalling transduction

Intracellular BMP signal transduction is negatively modulated by inhibitory Smads (I-Smads), including Smad6 and Smad7, which is accomplished by down-regulating type I receptors on the cell surface, interfering with the interaction between R-Smads and type I receptors, or competing with Smad4 for the binding of R-Smads (Hata et al., 1998). Smad6 preferentially inhibits Smad signalling of BMP type I receptors ALK-3 and ALK-6 (Goto et al., 2007), while Smad7 inhibits Smad signalling

induced by both TGF-β and BMP receptors (Hanyu et al., 2001).

Smad ubiquitination regulator 1 (Smurf1) is the ligase of Smad 1/5/8 and other substrates. Smurf induces ubiquitination and proteasome degradation of type I receptor and interacts with I-Smads and other E3 ubiquitin ligases to induce down-regulation of the number of type I receptors on the surface of the cell. This results in inhibition of BMP signal transduction. Smurf2 can induce degradation of Smurf1. Reduced expression of Smurf1 inhibited tumour metastasis in the MDA-MB-231 cell line (Xie et al., 2013). Silencing of Smurf 2 in triple negative breast cancer cells elevated the expression of Smurf1, leading to enhanced tumour metastasis (Jin et al., 2009). Ubiquitin ligase ring finger protein 11 (RNF11) interacted with Smurf 1 and 2, Smad4 and other ubiquitin ligases to regulate the BMP signalling pathway, and highly expressed mRNA and protein have been found in breast carcinoma tissues (Azmi and Seth, 2005).

Extracellular regulation

Pseudo-receptor

BAMBI (BMP and Activin Membrane Binding Inhibitor) is a transmembrane protein with extracellular and transmembrane domains similar to type I receptors. However, upon binding with BMP ligands, BAMBI cannot trigger any further downstream signalling as it lacks the intracellular kinase (Onichtchouk et al., 1999). Interestingly, BAMBI is able to competitively bind to BMP ligands, eliciting BMP signalling transduction inside the cells.

Naturally occurring BMP antagonists

BMP antagonists competitively bind to the BMP receptors to impede their binding with BMP ligands (Walsh et al., 2010). To date, three families including Chordin, Noggin (NOG) and DAN families are established as the BMP antagonists, (Walsh et al., 2010). On the flip side, the expressions of BMP antagonists are also regulated by BMP ligands. Noggin expression in osteoblasts can be induced by BMP2, 4, and 6. Therefore, BMP can achieve self-regulation via upregulating its antagonist expression (Gazzerro et al., 1998). The activity of extracellular BMP signal antagonists are further regulated by extracellular matrix (ECM) components (Ben-Zvi et al., 2008).

Co- receptors of BMPs

The repulsive guidance molecule family, including RGMa. RGMb and RGMc, are co-receptors of BMP ligands. They can enhance BMP signal orientation (Gazzerro et al., 1998, Babitt et al., 2005, Ben-Zvi et al., 2008). RGMb, also known as DRAGON, can directly bind to BMP2 and BMP4 to enhance signalling transduction. This augment can be silenced by Noggin (Samad et al., 2005). cGMP receptor kinase I (cGKI) can phosphorylate BMPR-II, leading to the substitution of BMP receptor signal (Schwappacher et al., 2009). In breast cancer models, beta-glycan inhibits BMP-induced invasion and migration of breast cancer through binding with the BMP ligand. Beta-glycan (TGF-β receptor III) intercepted BMP signalling by binding to BMP 2, 4, 7 and GDF5 (Gatza et al., 2014). Thus, BMP signalling events are heterogeneous and complex, and the regulation of the signal transduction needs further study and clarification.

Table 1.5 Regulatory factors of BMP signalling

Location	Category	Official Symbol	Target
Extracellular	*Antagonist*	Noggin (NOG)	BMP2, 4, 6 and 7; GDF5 and GDF6
		Chordin (CHRD)	BMP4, 7
		Chordin like 2 (CHL2)	BMP2, 4, 5, 6, 7 and GDF5
		Follistatin (FST)	BMP6, 7, 11 and 15, GDF8 and 9
		Ventroptin	BMP4
		FLRG	BMP2
		Twisted gastrulation (Tsg)	BMP2, 4
		Gremlin1 (GREM1)	BMP2, 4 and 7
		DAN	BMP2, 4 and GDF5
		Cerberus	BMP2, 4
		PRDC	BMP2, 4
		SOSTDC1	BMP6 and 7
		Caronate	BMP2, 4 and 7
		CoCo (DAND5)	BMP4
		NOV (CCN3)	BMP2
	Enhancer	Kielin/Chordin like	BMP7
Membrane	*Pseudoreceptor*	BAMBI	BMP4
	Co-receptor	Dragon (RGMb)	BMP2, 4
		Betaglycan (BGCAN)	BMP2, 4, 7 and GDF5
		Hemojuvelin (RGMc)	BMP2,4
		RGMa (RGM)	BMP2, 4
		Endoglin (ENG)	BMP9, 10
Intracellular	*Inhibitory Smads*	Smad6 and 7	R-Smad, Co-Smad
	Smad binding protein	Ski	Smad 2, 3 and 4
		SKIL/SnoN	Smad 2, 4
		Tob	Smad 1, 5 and 8
		AMSH	Smad6
	Ubiquitination and degradation of Smad	Smurf1 and 2	Smad 1, 5, 6 and 7
		NEDD4-2	Smad 2
	Deubiquitination of Smad	UCH37	Smad7

Regulatory factors on BMP signalling updated from the literature published (Ye et al., 2007b). The regulation of BMP signalling can happen during the process of ligand binds to receptor, and the intracellular signal transduction. Dan, Cerberus, Gremlin, PRDC, Sclerostin, Caronate and DAND5 belong to DAN/Cerberus family. Based on literatures published: ***Noggin*** (Zhu et al., 2006, Pera et al.,

2004, Haudenschild et al., 2004, Chang and Hemmati-Brivanlou, 1999, Re'em-Kalma et al., 1995); ***Chordin*** (Dale et al., 1999, Piccolo et al., 1996, Sasal et al., 1995); Kielin/Chordin like(Lin et al., 2005); ***Chordin like 2, CHL2*** (Nakayama et al., 2004); ***Follistatin*** (Fainsod et al., 1997, Iemura et al., 1998, Otsuka et al., 2001, Balemans and Van Hul, 2002, Pierre et al., 2005); Sclerostin (Kusu et al., 2003); ***Ventroptin*** (Sakuta et al., 2001); ***FLRG*** (Tsuchida et al., 2000); ***Gremlin*** (Hsu et al., 1998, Merino et al., 1999); ***Twisted gastrulation*** (Ross et al., 2001, Chang et al., 2001); ***Dan*** (Hsu et al., 1998, Gerlach-Bank et al., 2004, Dionne et al., 2001); ***Cerberus*** (Piccolo et al., 1999); Protein related to DAN and Cerberus, ***PRDC*** (Sudo et al., 2004); Dan domain family member 5, ***DAND5*** (Marques et al., 2004); ***Caronate*** (Yokouchi et al., 1999); ***BAMBI***(Grotewold et al., 2001, Onichtchouk et al., 1999); ***Dragon*** (Samad et al., 2005); RGMa (Babitt et al., 2005); ***Ski*** (Luo et al., 1999); Ski like, ***SKIL/SnoN*** (Vignais, 2000, Stroschein et al., 1999);***Tob*** (Yoshida et al., 2000); SH3 domain of STAM, ***AMSH*** (Itoh et al., 2001); Smad ubiquitination regulatory factor, ***Smurf*** (Arora and Warrior, 2001, Murakami et al., 2003); Neural precursor cell expressed, developmentally down-regulated 4-2, ***NEDD4-2*** (Kuratomi et al., 2005); ubiquitin C-terminal hydrolase, ***UCH37*** (Wicks et al., 2005).

1.2.4 Effects of BMP signalling on tumourigenesis and dissemination of breast cancer

1.2.4.1 BMPs and *the growth of breast cancer cells*

BMP signalling is associated with the proliferation of a variety of tumour cell types. Aberrant BMP expression can make demonstrable alterations in cell-regulation factors, such as cyclinD1 and CDK-interacting protein p27. Increased expression of cyclinD1 and decreased expression of CDK-interacting protein p27 accelerate the cell cycle from the G0/G1 phases toward the S-phase (Besson et al., 2008, Garcia-Alvaro et al., 2015). Activated BMP signalling pathway also modulates expression of other key factors of mitotic checkpoint, including MAD2, TTK, BUB3 and Hec1, which can significantly reverse the mitotic arrest defect (Yan et al., 2012).

BMPs also promote tumour proliferation by co-acting with tumour stimulating factors. In the presence of conditioned media, derived from cancer-related fibroblasts *in vitro*, BMP2 enhanced the proliferation as well as multi-drug resistance of breast cancer cells (Tan et al., 2016). Co-acting with epidermal growth factor (EGF), fibroblast growth factor (FGF) and hepatocyte growth factor (HGF), BMP4 facilitated the proliferation of breast epithelial cells (Montesano et al., 2008).

1.2.4.2 BMP and Cancer Stem-like Cells

Cancer stem-like cells (CSCs) are referred to as a small proportion of tumour-initiating cells presenting properties of classic stem cells, which is depicted as immortal, possessing self-renewal capacity (Dalerba and Clarke, 2007, Liu et al., 2016a) and resistant to chemotherapies (Liu et al., 2016b). CSCs were first reported in acute myeloid leukaemia (Minami, 2015). CSCs have been isolated from a series of tumours such as prostate cancer (Jaworska et al., 2015), breast cancer (Bahena-Ocampo et al., 2016) liver cancer (Ochiya, 2016), and lung cancer (Pore et al., 2016). Through fluorescence-activated cell sorting (FACS), breast cancer stem-like cells (BCSC) are characterized as $CD44^{+}$, $CD24^{-/low}$, and ESA^{+} (epithelial specific antigen) (Al-Hajj et al., 2003). CSCs remain mainly in a dormant status in both the primary lesion and secondary lesion, which are not sensitive to chemotherapy (Yang et al., 2016, Martinez and Zhang, 2013). This indicates a small number of CSCs survive after chemotherapy, leading to drug resistance and high rate of recurrence.

CSCs emerge in the primary tumour by a process of EMT (Yoshida and Saya, 2016). BMPs are vital regulators in inducing EMT of mammary epithelial cells to $CD44^{+}$, $CD24^{-}$ cell phenotype (Mani et al., 2008). BMP signalling impacts the functional properties and involves in CSC-related tumour proliferation and progression (Baccelli and Trumpp, 2012). BMP-2 enhanced the invasiveness of cancer cells by inducing CSC proliferation through activation of STAT3 (Kim et al., 2015). Inversely, BMP-4 inhibited the differentiation and self-renew of CSCs, suppressing tumour proliferation and progression (Lombardo et al., 2011, Whissell et al., 2014). BMP-7 upregulated the expression of cell cycle inhibitor p21 and metastasis suppressor gene NDRG1 (N-Myc downstream-regulated gene1) to enhance CSC degradation (Kobayashi et al., 2011). BMP2/7 heterodimer could suppress the Smad signalling induced by TGF-β and decrease $ALDH^{hi}/CD44^{hi}$/ CD24–/low BCSCs pool to inhibit cancer invasiveness (Buijs et al., 2012).

BMP signalling can regulate stemness of cancer cells by interacting with other signalling pathways. For instance, high expression of Notch-1 can up-regulate SMAD3 expression to enhance the expression of EMT/stem-related molecules CD44 and Slug, leading to a more aggressive tumour (Czerwinska and Kaminska, 2015). BMP4 enhanced cancer stem-like cell properties of breast cancer cells via Notch signalling

(Choi et al., 2019).

1.2.4.3 BMP signalling and EMT

EMT is a process where tumour cells forfeit epithelial morphology and obtain a mesenchymal phenotype and is critical for indolent cells acquiring metastatic propensity (Gonzalez and Medici, 2014). Several characteristic biomarkers have been summarized for epithelial and mesenchymal cells. Epithelial markers include E-cadherin, Claudins, Occludins, Desmoplakin Cytokeratin 8/9/18 and Mucin-1. Mesenchymal markers contain Fibronectin, Vitronectin, FSP1, Vimentin, Smooth-muscle actin, FGFR2 IIIb and IIIc splice variants (Gonzalez and Medici, 2014). During EMT, the epithelial marker E-cadherin is down-regulated while the mesenchymal markers, N-cadherin, vimentin and SNAI2 are upregulated in breast cancer (Park et al., 2015).

BMP signalling exerts a pivotal role in modulating EMT through diverse intracellular messengers (Rothhammer et al., 2005, Kang et al., 2009). The cell signalling cascade is initiated from specific binding between the BMP receptor and the ligand on the cell surface, to form the homodimer/heterodimer (Itoh et al., 2000, Moustakas et al., 2001, Chen et al., 2004). This is followed by phosphorylation of BMPRI and recruitment of the downstream transcription factor SMAD1/5/8 to induce the expression of EMT encoding genes. R-SMADs could directly bind to the Snai1 promoter to form a complex and inhibit the gene encoding E-cadherin and occludin, key markers of EMT (Vincent et al., 2009). Smad-independent pathways (such as through PI3K and ILK) were able to activate Akt, thereby inhibiting the function of GSK-3β, which suppresses the nuclear translocation of Snai1 and β-catenin. SMAD6/7 prevented the binding and phosphorylation of SMAD1/5/8 through Smurf1 and Smurf2 to restrain SMAD signalling transduction (Arora and Warrior, 2001). In addition, Akt can also enhance the transcription of Snai1 via the activation of nuclear factor kB (NF-kB) to induce EMT (Julien et al., 2007).

BMP-2 expression was inversely associated with Rb expression. Downregulated expression of Rb would lead to ubiquitin-mediated degradation, which reduced the polyubiquitination of EMT factors and thus promote EMT and bone metastasis (Huang et al., 2017). BMP4 signalling was found to be involved in the EMT process in a number of solid tumours (Kestens et al., 2016). BMP4 could promote EMT

and tumour progression by suppressing the expression of E-cadherin and elevating the expression of N-cadherin and Snai2 (Park et al., 2015), resulting in an invasive phenotype of cancer cells (Serrao et al., 2018). Notably, BMP4 can also inhibit EMT through restraining the Notch signalling pathway, which augments EMT properties in epithelial cells of the mammary gland (Choi et al., 2019).

BMP7, a potent inhibitor of EMT, counteracted Smad-dependent BMP signalling and reversed EMT. BMP-7 upregulated expression of cytokeratin and suppressed vimentin, giving rise to an epithelial-like morphology in breast cancer cells (Buijs et al., 2007c). Similarly, BMP6 exerted an inhibitory effect on EMT, which restrained the metastasis of breast cancer cells by downregulating the expression of miR-21 and δEF1 (ZEB1) and restored the expression of E-cadherin (de Boeck et al., 2016). Lower expression of BMP6 in MCF7 cells enhanced the expression of mesenchymal proteins and silenced E-cadherin, rendering a more invasive phenotype of the cancer cells (Liu et al., 2014).

Interestingly, BMPs could suppress EMT induced by TGF-β signalling. BMP5 inhibited the up-regulation of Snail and fibronectin induced by TGFβ, and suppressed TGFβ-induced migration *in vitro* (Romagnoli et al., 2012). BMP7 also suppressed TGF-β-induced EMT, similar to that seen with BMP5 (Buijs et al., 2007b, Naber et al., 2012, Ying et al., 2015).

1.2.4.4 BMPs and angiogenesis

Tumour vascular angiogenesis (which is known as neovascularisation) is a crucial hallmark of cancer. The neovasculature provides essential nutrition and oxygen to maintain the robust metabolism of cancer cells. This process is essential when the size of tumour is more than 3mm in its diameter, when interspatial diffusion of nutrients is not adequate for the fast growth of tumour cells. Neovascularisation begins from the activated proliferation and migration of endothelial cells, leading to the construction of blood vessels by the migrated endothelial cells (Goumans et al., 2002). BMPs such as BMP2/4/6/7 and GDF5 were demonstrated as important promoters in tumour-associated angiogenesis (Ye et al., 2011a). BMPs induced activation of endothelial cells for blood vessel construction which was transduced via the ALK1/Smad1/5 or the ALK5/Smad2/3 pathway (Goumans et al., 2002). BMP2 could enhance the motility of

endothelial cells to promote micro-vessel tubule formation (Kim et al., 2012b). BMP-4 and BMP-7 could facilitate the migration of vascular smooth muscle cells to stimulate angiogenesis (Dorai et al., 2000, Morrell et al., 2001). Inversely, BMP9 and BMP10 restrained the proliferation and motility of endothelial cells via ALK1, leading to suppression of tumour angiogenesis (Mitchell et al., 2010, Hawinkels et al., 2016). BMP2 also induced angiogenesis by mobilizing endothelial cells through induction of non-canonical p38 and suppression of ERK1/2 signalling (Raida et al., 2005). BMP-9 and BMP-10 increased gene expression via the Notch signalling pathway in vascular endothelial cells, thereby coordinating postnatal vascular remodelling (Ricard et al., 2012).

1.2.4.5 BMPs and tumour apoptosis

Apoptosis is a programmed cell death that occurs in multicellular organisms which is fundamentally important in maintaining tissue homeostasis and genome integrity. Abnormal apoptosis is a prominent hallmark of tumour proliferation and progression (Kaczanowski, 2016). The BMP signalling pathway exerts a pivotal role in modulating the apoptosis of tumour cells. BMP could induce the apoptosis of myeloma cells via ALK (Scharpfenecker et al., 2007). BMPs could also modulate the transcription of apoptosis genes through the canonical signalling pathway. For instance，BMP9 enhanced the expression of prostate apoptosis response-4 (Par4), leading to the prostate cell apoptosis (Dai et al., 2004).

BMP regulated the expression of apoptosis mediator DRP-1 death kinase and ZIP kinase through type I receptors (Korchynskyi et al., 2003). After treatment with BMP4, cell viability was reduced and the expressions of related genes such as VEGF and Bcl2 were decreased (Buckley et al., 2004).

BMPs are also able to regulate cell apoptosis via the Smad independent pathways. BMP2 could promote the apoptosis of medulloblastoma cells by activating the p38 mitogen-activated protein kinase (MAPK) pathway (Hallahan et al., 2003). BMP10 could induce prostate cancer cell apoptosis by activating the MAPK pathway (Ye et al., 2009b). In addition, BMPs are involved in regulating the activity of other apoptosis-inducing genes. For example, GDF15 was found to be essential for the pro-

apoptotic activity of several apoptosis inducers including retinoid-related molecules (Ramoshebi and Ripamonti, 2000).

Different cells present diverse apoptotic responses to BMPs. In the same cell type, apoptosis responses varied among different phenotypes, hormone and growth factor status and survival conditions. BMP4 could restrain cell proliferation and induce apoptosis in IL-6-dependent myeloma cells (OH-2 and IH-1), but little effect was apparent on IL-6-independent cells (Lv et al., 2015). The regulation of BMP on apoptosis of cancer cells presented a biphasic effect depending on the survival status of cancer cells. For example, under a general culture condition, BMP2 induced the expression of apoptosis-related genes such as protein kinase R (PKR) and the activation of its substrate eIF2α to promote breast cancer cell (MCF-7) apoptosis (Woltje et al., 2015). Once the cells were deprived from serum, BMP2 facilitated MCF-7 cells to resist apoptosis induced by hypoxia by activating the MAPK pathway and ID-1 and inhibiting Caspase-3 (Dyer et al., 2014, Ricard et al., 2012). BMP6 could up-regulate the expression of miRNA-192 and inhibit the proliferation of breast cancer cells (MDA-MB-231). However, in the case of serum-free culture, BMP6 up-regulated survival through Smad-dependent pathways and activated p38 through Smad-independent pathways, thereby protecting these cancer cells from stress-induced apoptosis (Yoshimatsu et al., 2013).

Studies have shown that regulating BMP signal transduction could adjust cell apoptosis. In MDA-MB-231 cell lines, the elevated expression of Neogenin (BMP co-receptor) could inhibit BMP-2 induced Smad1/5/8 phosphorylation to accelerate cell apoptosis (Zhang et al., 2015). Knocking down the repellent guide molecule RGMB (BMP's co-receptor) in MDA-MB-231 cells could reduce Caspase 3 expression, leading to promoted cell proliferation and migration (Li et al., 2012).

1.2.4.6 BMPs and dissemination of breast cancer

BMP regulates the dissemination of breast cancer through a variety of mechanisms. BMP signalling alters the expression and activity of matrix metalloproteinases (MMP), contributing to tumour invasion and metastatic spread. BMP2 has been shown to up-regulate the expression of MMP11 (Huang et al., 2017), whilst BMP4 was found to stimulate the expression or increase the activity of MMP1,

MMP2 and MMP9. MMP inhibitors Batimastat or BMP antagonists Chrd11, Noggin and Gremlin can reverse this invasive phenotype induced by BMPs (Ampuja et al., 2013, Cyr-Depauw et al., 2016). In addition, BMP6 can inhibit the p38/AP-1 pathway through the canonical pathway, thereby down-regulating MMP1 and MMP9 (Wang et al., 2011a, Hu et al., 2016). Importantly, stromal cells in the microenvironment of tumours participate in the BMP-mediated regulation of MMP and other cytokines. For example, BMP4 intervention induced the secretion of MMP2, MMP3 and other tumour-promoting cytokines, such as IL6, from breast fibroblasts, promoting the tumour progression (Owens et al., 2013). On the contrary, elevated expression of BMP9 in tumour cells inhibited the production of MMP2, IL6, SDF1 (PI3K/AKT signal inducer) and MCP1 of bone marrow mesenchymal stem cells, thereby inhibiting tumour invasion when they were co-cultured (Wang et al., 2015).

BMPs also modulate the motility of breast cancer cells. BMP2 enhanced the motility of breast cancer cells through tenascin-W in the surrounding stroma. Tenascin-W belongs to a family of extracellular matrix glycoproteins, which is highly expressed in the stroma around breast carcinoma lesions. Tenascin-W interacts with α8 integrin on the cell surface. Breast cancer with high α8 integrin could readily infiltrate tenascin-W-coated filters. This α8 integrin-tenascin-W mediated aggressiveness is augmented by BMP2 through p38 MAPK and JNK pathways (Scherberich et al., 2005).

1.2.4.7 BMPs and Dormancy

Research from the clinical findings reveals that breast cancer is prone to relapse many years after the resection of primary lesions (Retsky and Demicheli, 2014). The reason for the recurrence is hypothesized to be through dormant cancer cells at the primary site or in metastatic lesion. For the cellular dormancy, cancer cells remain in a quiescent state, however for tumour mass, dormancy meant the balance between the proliferation and apoptosis. Dormant cancer cells present indolent metabolism, which could facilitate resistance to chemotherapy (Endo and Inoue, 2019). The BMP signalling pathway plays a vital role in governing the dormancy of cancer cells. Although BMPs present dual roles in cancer progression, they are only implicated in the induction of dormancy (Bach et al., 2018). BMP4 and BMP7 could induce dormancy in mouse models of breast cancer (Gao et al., 2012). BMP7 bound to BMPR2

to activate p38, thereby elevating the expression of CDK inhibitors p18 and p21. P21 up-regulated the expression of the metastasis suppressor gene NDRG1 (N-Myc downstream regulation 1), which eventually lead to the G1 cell cycle arrest of tumour cells (Kobayashi et al., 2011, Sharma et al., 2016). Studies have shown that BMP4 induced dormancy of breast cancer cells by binding to BMPR1A and BMPR2 to activate the canonical SMAD1/5 signal and this induced response could be reversed by the extracellular BMP antagonist DAND5 and inhibitory SMAD6 (Gao et al., 2012). The high expression of NDRG1 in breast cancer cells was associated with lung metastatic recurrence, and the low expression of NDRG1 gene was associated with the metastatic recurrence of breast cancer cells in the bone (Gao et al., 2012), which indicated that NDRG1 might be involved in the escape of breast cancer lung metastasis cell dormancy, however NDRG1 was also observed to promote the dormancy of breast cancer cells in bone metastasis. It was reported that BMP7 also had similar effect on inhibiting the growth of prostate cancer cells in bone metastasis and inducing their dormancy (Kobayashi et al., 2011). Other studies had shown that over-expression of the transcription factor DeltaNp63a (an isoform of p53 family member p63) in dormant MCF-7 cells could up-regulate the expression of the target gene ID1 in the BMP pathway, leading to G0/G1 cell cycle arrest in breast cancer cells (Amin et al., 2016).

1.2.5 BMPs and clinical implications

1.2.5.1 BMPs and breast cancer relapse

As the advance in breast cancer therapy, especially the development of targeted therapy in recent years, the survival rate of women diagnosed with breast cancer has improved rapidly. However, the early relapse ratio in patient with basal-like subset is still high, for these triple-negative cases, well-targeted treatments are still being explored. For luminal A subtype, the oestrogen receptor is positive, although the risk of relapse is relatively low due to effective endocrine therapy, though the potential risk exits even for decades after diagnosis (Yamashita et al., 2016). Recurrence of breast cancer is often caused by cancer stem-like cells, which possess tumourigenesis potential and can remain in an inactive state to escape from chemotherapy, and then, once conditions permit, these quiescent or dormant cells can revive and proliferate, resulting in clinical symptoms manifesting at a later stage (Oskarsson et al., 2014). Similar in

many characteristics of tumour cells, stem cells possess the ability of proliferation through self-renew and are free from contact inhibition. BMPs could regulate stem cell via progenitor determination. In MCF10A mammary cells, BMP-2 induced the maturation of luminal progenitors, whereas BMP-4 exerted a diverse role, which directed these progenitors to reverse to an immature phenotype (Clement et al., 2017). BMPs promoted differentiation of human embryonic stem (hES) cells to the trophoblast lineage and this effect could be suppressed by Noggin (Varga and Wrana, 2005). In breast cancers, the impact of BMP signalling on stem cell proliferation remains unclear and contrasting results have been observed on experimental conditions. *In vitro*, the BMP2/7 heterodimer strongly inhibited the amount of breast cancer stem cells and the heterodimer reduced bone metastasis *in vivo* (Buijs et al., 2012). However, the similar inhibit effect for the proliferation and colony formation capacity of stem cells were found in primary murine breast cancer cells model with a BMPR inhibitor (Balboni et al., 2013).

BMP-4 signalling contributed to maintaining the stem cell phenotype and the silencing of BMP-4 resulted in loss of stem-features and self-renewal ability, via downregulation of Snail and Slug transcription factors (Garulli et al., 2014). However, contrasting results have also been reported, where BMP-4 inhibited the differentiation, apoptosis and impaired the self-renewal property of CSCs, which exerted a negative role on tumour proliferation and progression (Lombardo et al., 2011, Whissell et al., 2014). Such observations may have been caused by differential BMPs and receptor profiles in autocrine and paracrine signalling, resulting in the variety of effect on breast stem cell populations.

1.2.5.2 BMPs and bone metastasis

BMPs and the bone environment

Bone metastasis is a multi-step process which involves cancer cells to detach from the primary lesion, infiltrate into the blood circulation, transport to the bone marrow and undergo colonisation in the bone (Yoneda T et.al 2005). Since BMPs actively participate in regulating the formation and resorption of bone, many studies have focused on their potential role in bone metastasis (Weidle et al., 2016).

BMP signalling exerts fundamental effect in the osteogenic differentiation and homeostasis through regulating the balance of osteoblasts and osteoclasts (Figure 1.3). BMPs, such as BMP-2, BMP-4, BMP-7, have been proved to promote the differentiation of the mesenchymal stem cells (MSCs) into osteoblasts (Alarmo and Kallioniemi, 2010, Carreira et al., 2014). BMPs can impact the maturation and the activation of osteoclasts through the RANKL-OPG pathway (Yahiro et al., 2020). BMP signalling orchestrates the function of osteoclast and osteoblast via the secretion of BMP related transcription factor such as Wnts. Osteoclasts can modulate the osteogenesis formation through Smad1/5 signalling by regulating the differentiation of osteoblasts (Tasca et al., 2018). BMP signalling transduction is necessary in inducing the differentiation of bone marrow derived mesenchymal stem cells into mature osteoblasts. In osteolysis, caused by osteoclasts, BMPs in the bone matrix are released, which could regulate the expression of CX43/GJA1 through BMP signalling pathways to interact with osteoblast to adjust mineralization (Shi et al., 2016). Role of BMPs in the bone remodelling was summarised in Figure 1.3.

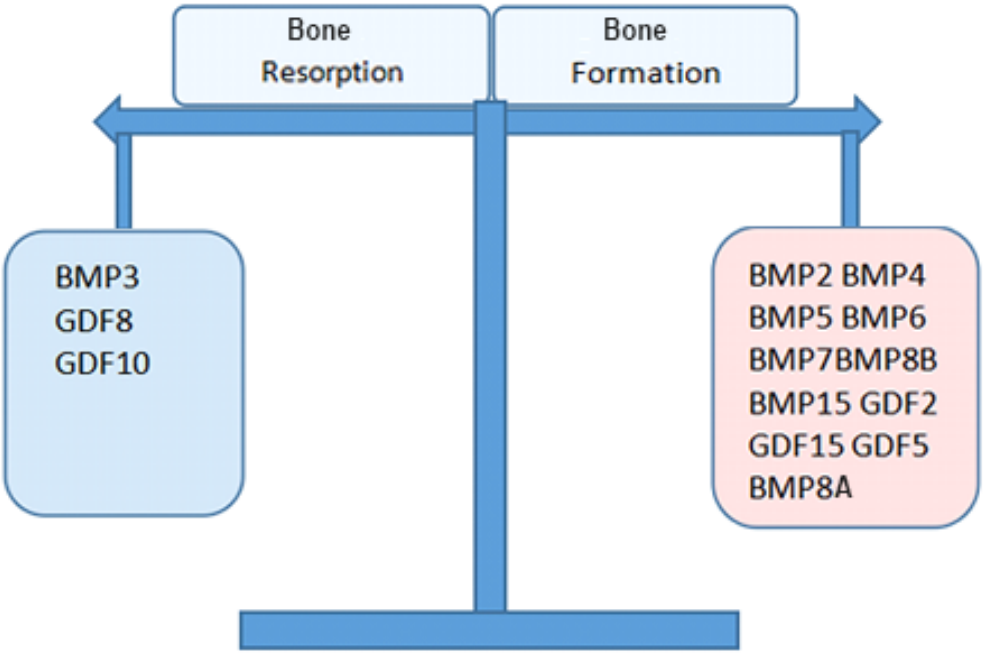

Figure 1.3 Role of BMPs in skeletal development and homeostasis.

Aberration of BMPs in bone metastasis

BMPs signalling pathways actively participate in breast cancer bone metastasis, and bone metastasis is attenuated through down-regulation of BMP receptors *in vivo* (Katsuno et al., 2008). According to research, BMP-7 could restrain the proliferation of disseminated tumour cells in bone microenvironment *in vivo* and primary tumours with low-expression of BMP-7 are inclined to bone metastasis (Buijs et al., 2007c). However, opposite results have also been reported in other studies and bone metastasis has also been found to be enhanced with high-expression of BMP-7 in primary tumours (Alarmo and Kallioniemi, 2010). In murine cell lines with enhanced bone tropism, expression of BMP-7, BMPR and the downstream transcription factors in the canonical pathway, phosphorylated Smad1/5/8, are upregulated. However, when BMP-7 is suppressed, the invasive features of 4T1E/M3 mammary cells are reduced (Sakai et al., 2012). BMP-9 could suppress both the proliferation of primary breast cancer cells *in vitro* and *in vivo*, and the growth of disseminated cells in bone by the downregulation of expression of connective tissue growth factor (CTGF) (Wang et al., 2011b, Ren et al., 2014b).

As metastatic tumour cells disseminate to the bone, interactions between the DTCs and the bone microenvironment constantly determine the survival of the disseminated cells. To accommodate and proliferate in the "foreign" bone microenvironment, disseminated tumour cells can acquire an ability to resemble the osteoblast phenotype via expressing bone matrix proteins, this progress is also called osteomimicry. A series of proteins are involved in this progress, including bone sialoprotein (BSP), osteopontin (OPN), osteoprotegerin (OPG) and osteoblast-specific cadherins (Ibrahim et al., 2000, Kapoor et al., 2008, Tan et al., 2016). In the study of Tan and coworkers (Tan et al., 2016), exposure to BMP-2 could upregulate the expression of bone-related genes (BRGs) and as a result the invasion of breast cancer cells were increased, which helped the tumour cells to hijack and survive in the bone. Whereas, application of Noggin, the BMPs antagonist, reversed these effects (Alarmo and Kallioniemi, 2010, Carreira et al., 2014, Tan et al., 2016).

Regulators of BMP signalling in bone metastasis

BMPs can regulate bone remodelling to affect breast cancer bone metastasis (Chi et al., 2019). For example, orthotropic implant with BMP-2 exhibits higher metastatic spread of breast cancer cells to bone *in vivo* (Moreau et al., 2007). Adding

their antagonists such as Noggin into breast cancer cells could reverse the osteoblastic behaviour of osteoprogenitor cells (Bunyaratavej et al., 2000). Aberrant expression of Noggin has high correlation with bone metastasis in breast cancer cell models and clinical cases (Tarragona et al., 2012). High expression of Noggin in breast cancer cells could accelerate the differentiation and maturity of osteoclasts *in vitro*, resulting in osteolytic influence in bone microenvironment (Mock et al., 2015). Down-regulation of GREM1 can reduce the metastasis of breast cancer, whereas high-expression of GREM1 is correlated with enhanced metastasis and poor prognosis in breast cancer patients (Neckmann et al., 2019). However, the role of BMP antagonists in orchestrating the osteoblastic and osteolytic activities in bone metastatic lesions still needs further research.

Oestrogen and ER can impact the transduction of BMP signalling and influence bone metastasis of breast cancer. Oestrogen can affect the activity of BMPs on osteogenic factors such as RANKL, OPG, ALP and osteocalcin to maintain bone turnover. Oestrogen deficiency can trigger BMP-2-induced imbalance between osteoclastogenesis and osteoblastogenesis, eventually leading to reduced bone mass and facilitating the secondary bone formation of breast tumours (Lee et al., 2018). ER-α is essential to activate BMP-4 and may contribute to alleviate osteoporosis and reduce the risk of breast cancer (van den Wijngaard et al., 2000). Oestradiol can promote BMP4 to induce more osteoblastic cytokines, such as Runx2 and osterix in osteoprogenitor cells. BMP-4 treatment can suppress the expression of ER-α, indicating BMPs can regulate osteoblast differentiation with a negative feedback (Matsumoto et al., 2013).

The biological activity of BMP-6 was enhanced with anti-oestrogen treatment and reduced with oestradiol treatment, indicating that ER modulates BMP-6 in bone, and ER-dependent pathways (such as BMPs) may influence bone colonisation in breast cancer, which is consistent with the previous observation that patients with ER positive breast tumours are more likely to develop skeletal metastases (Ong et al., 2004).

Role of BMP in bone metastasis

Osteomimicry

Disseminated breast cancer cells in the bone can obtain a similar phenotype to the osteoblasts, which contributes to the survival and proliferation of DTCs in the bone microenvironment. The osteoblast-like phenotype is obtained by ectopically expression of bone matrix proteins, such as bone sialoprotein (BSP) (Kovacheva et al., 2014), osteopontin (OPN) (Reufsteck et al., 2012), osteoprotegerin (OPG) (Kapoor et al., 2008) and secreted protein acidic and cysteine rich (SPARC)/osteonectin (ON) (Ribeiro et al., 2014), osteoblast-specific cadherins (e.g., cadherin 11 (CDH11) (Tamura et al., 2008) and transcription factors that regulate bone remodelling (e.g., runt-related transcription factor 2 (RUNX2) (Rucci and Teti, 2010). These proteins were found to be highly expressed in breast tumour cells and contributed to their colonisation in the bone site. BMPs were crucial osteogenic factors which exerted a vital effect in mediating the differentiation of osteoblasts and osteoclasts (Zhang et al., 2010), and it was also critical in osteomimicry transition. Different subtypes of BMPs including BMP2, 4, 6 and 7 were proved to be involved in the transition.

Silencing BMP2 and BMP4 in osteoblasts significantly restrained osteogenic activity, whereas BMP-7 could promote their ALP activity. BMP2 could induce the expression of RUNX2, which acted as the major mediator for osteomimicry transition for the epithelial tumour cells (Li et al., 2015).

1.3 Crosstalk of BMP signalling with other signalling pathways

BMPs exert pivotal roles in regulating the biological behaviour of tumours through crosstalk with various other signalling pathways. Among them, the ER signalling pathway, the epidermal growth factor receptor (EGFR) signalling pathway (Clement et al., 1999), PI3k/Akt signalling pathway (Zhang et al., 2016b), Wnt signalling pathway (Duchartre et al., 2016, Teo and Kahn, 2010), receptor tyrosine kinase (RTK)/MAPK pathway (Lehmann et al., 2000, Yue and Mulder, 2000) and hepatocyte growth factor (HGF)/Met signalling pathway (Zhen et al., 2018) are well-established. Interaction of BMP signalling with other signalling was summarized in Figure 1.4.

Generally, the interaction is accomplished by modulating the ligands, receptors, antagonists and downstream transcription factors, as well as the cytoplasmic effectors.

1.3.1 Regulation by ER signalling.

It is well established that oestrogens actively participate in the tumourigenesis and progression of breast cancer. Abnormal oestrogen levels are closely associated with the morbidity of breast cancer. The role of oestrogen is accomplished by the interaction between oestrogen and the oestrogen receptors (ER). ER has two major subtypes, ER-α (ESR1) and ER-ß (ESR2), which are important indicators for endocrine therapy and associated with the prognosis of breast carcinoma (Fuentes and Silveyra, 2019). The ER signalling pathway has been shown to regulate the BMP signalling pathway in breast cancer in recent research.

ER is capable of modulating the expression of BMP and BMPRs in breast cancer (Takahashi et al., 2008). Several BMPs and BMPRs are differentially expressed in different subtypes of breast cancer with different ER status. For instance, BMP-7 expression is influenced by ER status (Schwalbe et al., 2003). BMP2 expression was markedly higher in ER negative subtypes and expression of BMP2 was elevated when ER expression was silenced in the ER positive breast cancer (Al Saleh et al., 2011). ER also regulates the function of BMPs and BMPRs in breast cancer. Elevated expression of BMP6 contributed to immunological surveillance and prolonged the overall survival in ER-positive patients, however the survival time reduced in ER negative cases with high expression of BMP6 (Katsuta et al., 2019b).

High expression of BMPR-IB often leads to high tumour proliferation and a poor prognosis, whilst reduced expression of BMPR-IB often correlated with shorter overall survival in ER-negative patients (Bokobza et al., 2009).

ER status is also correlated with the BMPs promoter methylation. Research in tumour samples revealed the hyper methylation of the BMP-6 promoter in ER-negative cases. Triple negative breast cancer (TNBC) cell line exhibited the promoter methylation of BMP6, but a demethylation of the promoter was seen in the luminal A subtype breast cancer cell line (Zhang et al., 2007) .

BMPs have been demonstrated to reciprocally impact on ER signalling. Elevated expression of p21, a cell cyclin kinase inhibitor, induced by BMP2, could suppress the biological activity of cyclin D1-associated kinase induced by oestrogen, thereby, suppressing the proliferation of tumour cells (Ghosh-Choudhury et al., 2000).

1.3.2 Crosstalk between BMPs and EGFR signalling pathway

EGFR belongs to the ERBB family and, as an oncogenic molecule, is actively involved in the proliferation, differentiation and invasion of various tumours, i.e., lung cancer, gastric carcinoma and pancreatic cancer (Weng et al., 2015, Sigismund et al., 2018). Research revealed that EGFR signalling could regulate the expression of BMPs in breast cancer. In the MCF-7 cell line, a luminal A subtype cell type with high expression of EGFR, expression of BMP6 is elevated (Clement et al., 1999). Study in the drosophila embryo showed that BMP signal response was inversely modulated by EGFR signalling (Deignan et al., 2016).

EGFR signalling is also capable of modulating the function of the BMP pathway. Under the regulation of EGFR, BMP-7 reduced the progression of liver fibrosis (Wang et al., 2014). The same study also revealed that BMP-7 was able to reduce the expression and the phosphorylation of EGFR (Wang et al., 2014). The study of astrocytes *in vitro* highlighted that BMP signalling down-regulated the expression of EGFR significantly (Scholze et al., 2014).

1.3.3 Interaction between BMP and ErbB2 receptor signalling

The BMP signalling pathway has been shown to cooperate with that of the Her2 signalling pathway to promote cancer progression (Siegel and Massague, 2003). Highly expressed BMPs or BMPRs in the HER2 positive breast cancer murine model increased the mortality caused by metastases (Muraoka et al., 2003, Muraoka-Cook et al., 2006, Seton-Rogers et al., 2004). Following treatment with trastuzumab, a specific antibody of Her2, migration induced by BMP signalling was suppressed in Her2 (+) breast cancer cells (Ueda et al., 2004), which is indicative that the Her2 signal is essential for the transforming effect exerted by BMP signalling.

Alternatively, BMP proteins have been shown to reciprocally regulate the Her2 signal by activating the downstream receptor tyrosine kinases, such as Ras/MAPK (Mulder, 2000) and PI3K/Akt (Yi et al., 2005, Wilkes et al., 2005). Silencing of endogenous BMP signals significantly reduced the proliferation of Ras-transformed cancers (Ventura et al., 2004), indicating that Her2 signal induced tumour progression at least partly relies on the function of BMP signalling pathway. It has also been reported that BMP signals in Her2 (+) breast cancer induced the activation of PI3K. PI3K triggered the recruitment of actin and actinin to phosphorylated HER2 to form

the HER2/actin/actinin complex. The protein complex was correlated with the cytokines' role in cytoskeletal reformation such as Pak2, Rac1 and Vav2. BMP signals also facilitate the phosphorylation of TACE (Tumour Necrosis Factor, Alpha, Converting Enzyme) to promote the maturation of EGFR ligands. Activation of EGFR stimulates the Src-FAK pathway to form the complex with integrin and Her2 (Wang et al., 2009) and the further heterodimerisation with HER2 (Wang et al., 2009). Integrin/ EGFR/HER2 signalling is closely correlated with the invasion and morphology of cancer cells (Kass et al., 2007).

1.3.4 BMP and MAPK cascades

MAPK cascades, including ERK/MAPK, JNK/MAPK and p38/MAPK, are involved in various kinds of cellular events which cover proliferation, differentiation and cell death. Interaction of MAPK and BMP signalling pathways contributes to a more progressive phenotype in tumours and MAPK signalling cascade regulates BMP signalling mainly through BMP Smad-independent signalling transduction (Lehmann et al., 2000, Yue and Mulder, 2000). As the downstream transcription factor of the MAPK pathway, ERK was proved to promote the expression of Smad3 in smooth muscle tissues (Ross et al., 2007). Ras could inhibit the transduction of Smad3 signalling and in doing so block the Smad-independent signal translocation to the nucleus (Kretzschmar et al., 1999).

Influence of MAPK signalling on BMPs tends to depend on the linking region of Smad proteins. The loosely organized and highly flexible linker region of Smad proteins with enriched serine, threonine and proline residues enables the kinases to phosphorylate. JNK and ERK induced by the MAPK pathway could phosphorylate the endogenous Smad2/3. ERK could also phosphorylate the linker region of Smad3, Thr178, Ser207 and Ser203, to prevent the signal transduction to the nucleus (de Caestecker et al., 1998, Brown et al., 1999). However, contrasting results were also observed in a breast cancer cell line, namely phosphorylation by p38 MAPK on Ser203 and Ser 207, linker region of Smad3, augmented the role of BMP as a growth inhibitor (Kamaraju and Roberts, 2005). Collectively, these findings indicate that the regulation of MAPK signalling on BMPs are dependent on the kinase and the phosphorylation region.

MAPK signalling could modulate the canonical BMP signalling pathway. ERK exerted a powerful role on the phosphorylation of Smad1/5 on their linker region to block the trans-nuclear signalling of BMP (Guo and Wang, 2009). Subsequently, the activated EGFR signals for BMP from EGFR, FGF (fibroblast growth factor) and IGF (insulin-like growth factor) were inhibited (Eivers et al., 2008, Sapkota et al., 2007).

Ras was reported to promote the degradation of Smad4 in the ERK/MAPK pathway (Saha et al., 2001). Activated JNK/P38 MAPK was reported to associate with the mutation of Smad4 with poor stability (Saha et al., 2001). MAPK indirectly impacts other transcription factors involved in nuclear BMP signal transcription. Jun and activator protein 1, which are involved in regulation of BMP nuclear signal translocation, could be activated via the MAPK pathway (Jin et al., 2006, Thomas and Massague, 2005). Conversely, BMP signalling could modulate the signalling of the MAPK pathway and the BMP receptors regarded as the platforms to initiate the ERK/MAPK signalling pathways. Phosphorylation of BMPRII mediated by Src was correlated with the activation of the p38 MAPK signalling pathway (Galliher and Schiemann, 2007). Activation of ERK-MAPK could be achieved via the phosphorylation of Src by the intrinsic kinase of BMPRI (Lee et al., 2007).

Notably, the MAPK pathway also participates in the communication between HER2/Neu/ErbB2 signalling and BMP signalling pathways in breast cancer. Activated MAPK and PI3K/Akt pathways by HER2/Ras could antagonize the cell silencing signal from the BMP pathway and promote the pro-motility function as well (Ueda et al., 2004, Janda et al., 2002).

1.3.5 Crosstalk between AKT and BMP signalling pathways

AKT, also known as protein kinase B (PKB), has been indicated in regulation of cell metabolism and other cell functions. AKT facilitates cell proliferation and represses apoptosis induced by cytokines (Bellacosa et al., 2005, Zhao et al., 2015). Binding with multiple extracellular ligands triggers the phosphorylation of AKT, promoting the proliferation and inhibiting the apoptosis of tumour cells (Bellacosa et al., 2005). The AKT signalling pathway could facilitate the trans-nuclear signalling of β-catenin, which is the key mediator in the canonical Wnt signalling pathway and promoter of the EGFR signalling pathway. Crosstalk among AKT, Wnt and EGFR

signalling pathways further aggravates the malignant activities of tumour cells.

Recently, it has been reported that the BMP signalling pathway was capable of regulating the AKT pathway to adjust the biological behaviours of tumour cells through Smad-independent signal transduction (Kang et al., 2011, Zhang et al., 2016b). Modulating the expression and the activity of PTEN (Phosphatase and Tensin Homolog), the specific antagonist of AKT, is another way to regulate the PI3K/AKT pathway. Elevated expression of PTEN induced by BMP-2 was seen to promote apoptosis of pulmonary artery smooth muscle cells (Pi et al., 2012). However, there is also research showing that BMP-2 reduced the expression of PTEN in Smad-4-null colon cancer cells through the Ras/ERK pathway (Pi et al., 2012). BMP-7 increased the expression of PTEN and contributed to the suppression of AKT and reduction of renal fibrosis (Higgins et al., 2017).

Beside altering the expression of PTEN, the BMP/Smad pathway was also shown to enhance the biological activity of PTEN (He et al., 2004, Tian et al., 2005). Inhibition of BMP signalling on AKT could also be achieved through regulation of SH2 domain of proteins (Valderrama-Carvajal et al., 2002). In addition, activated PI3K/AKT signalling contributed to the shuttling of beta-catenin, which augmented the EGFR signal, leading to a vicious circle for tumour invasion (Lu et al., 2003, Ji et al., 2009).

1.3.6 BMP and Wnt pathway

The Wnt pathway is comprised of the canonical Wnt signalling pathway (Wnt/β-Catenin signalling) and non-canonical signalling pathway (Wnt/PCP and Wnt/Ca^{2+} signalling pathways) and is closely associated with the biological behaviour of tumour cells. The BMP pathway is reported to interact with the Wnt signalling pathway in various patterns.

BMP2 and BMP4 have been shown to modulate the Wnt pathway via alter the expression of Wnt proteins (Jin et al., 2006, Hoppler and Moon, 1998). Wnt signalling was also reported to act as a regulator for BMP ligands, co-receptors and antagonists in tumour cells (Guo and Wang, 2009).

As an important component of the protein complex in the Wnt signalling

pathway, GSK-3β could phosphorylate the linker point of Smad or degrade the Smad protein to regulate BMP signalling transduction (Luo, 2017, Millet et al., 2009). For instance, GSK-3β deconstructed Smad1/3 and subsequently downstream signalling transduction (Luo, 2017). Moreover, BMP signalling can also modulate Wnt signalling. As the downstream molecules in the BMP signalling pathway, Smurf is actively involved in the degeneration of the protein complex of the Wnt pathway (Kim and Jho, 2010). Co-acting with Smurf2, the Wnt/PCP pathway could promote the expression of Priklel-Rictor complex, a newly discovered complex with a powerful role in inducing dissemination of breast cancer and upregulating the activity of RhoA, thereby promoting the motility of cancer cells (Zhang et al., 2016a).

1.3.7 BMP and the HGF/Met pathway

Generally, hepatocyte growth factor (HGF) is secreted by fibroblasts, however the solid tumour can also generate HGF (Jiang et al., 2005). Aberrant HGF and its receptor c-Met are reported as tumour promoters, inducing proliferation, spread, angiogenesis and morphogenesis of tumours (Jiang et al., 2005). Cell functional studies, both *in vitro* and *in vivo*, presented that specific silencing the HGF/c-Met suppressed the mitogenesis and motility of cancer cells (Jiang et al., 2003, Jiang et al., 2005). HGF/Met was reported to co-act with BMP signalling. Interaction of BMP-7 and HGF could induce kidney fibrosis in mice model (Yunus et al., 2020). HGF was reported to modulate the expression of RGMB (repulsive guidance molecule B), the co-receptor of BMP, to exert pro-angiogenic effects (Sanders et al., 2014). Research in prostate cancer showed that regulated by HGF enhanced expression of BMP-7, BMPRIB and BMPR2 (Ye et al., 2007a, Ye et al., 2008). HGF was also reported to induce the skeletal formation and angiogenesis by increasing the expression of BMP-2 via the c-Met receptor/FAK/JNK/Runx2/P300 signalling pathways (Tsai et al., 2012, Zhen et al., 2018).

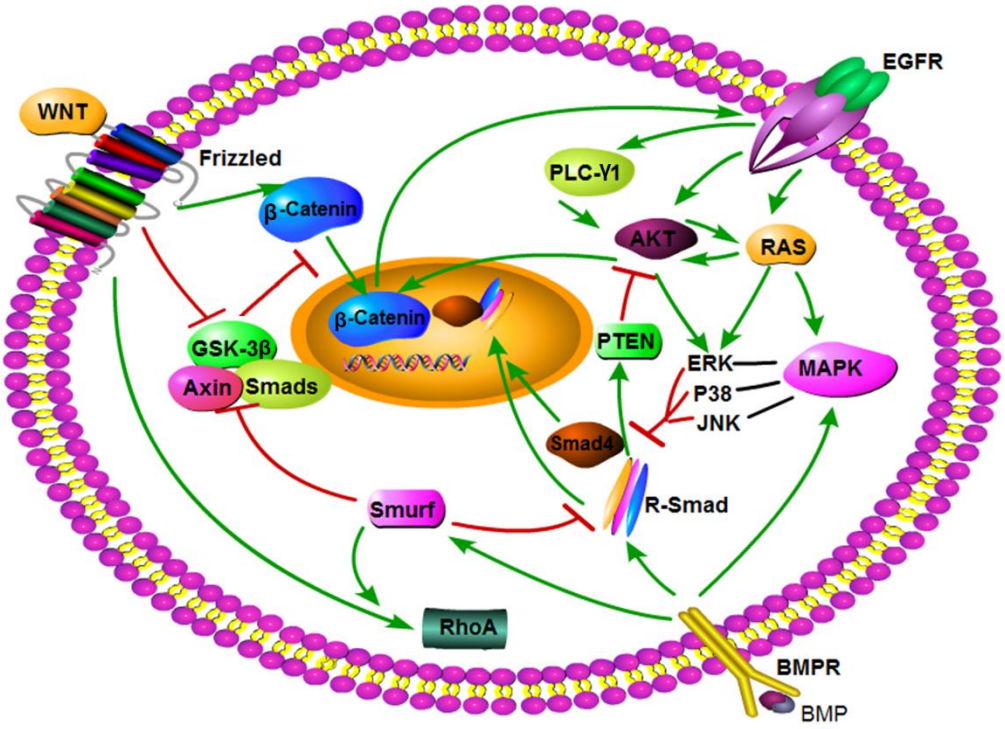

Figure 1.4 Interaction between BMPs and Wnt/EGFR/MAPK/AKT/RAS signalling. The figure was created applying pathway builder tools 2.0 from www. proteinlounge.com.

1.4 BMP8, its biological role in cancer

BMP8A, also known as osteogenic protein 2 (OP2), is a member of the BMP family. Mouse OP2 was firstly identified in 1992 (Ozkaynak et al., 1992). Human BMP8A is located at chromosome 1p34.3, whereas BMP8B is located at 1p34.2 which is 235kb away from BMP8A. BMP8A and BMP8B are highly conserved proteins that share 97% homology of their amino acid sequence, with only two different amino acids manifested in the mature domain at both N- and C-terminals shown by the protein blast alignment. The expression of BMP8A is enriched in thyroid (57.449 ± 40.258 RPKM) followed by endometrium (2.571 ± 1.197 RPKM). In an gene expression array assay of hepatocellular carcinoma, BMP8A expression was upregulated in tumours (n=17) compared with adjacent non-tumour liver tissues (Zekri et al., 2008). Hypermethylation of BMP8A was detected in rhabdomyosarcomas (Mahoney et al., 2012), whereas hypomethylation of BMP8A was found in oesophageal cancer (Singh et al., 2015). However, compared with other members of the BMP family, BMP8A and 8B are yet

to be investigated for their possible role in breast cancer.

BMP8B signalling protein participates in regulation of thermogenesis and energy expenditure. Silencing of BMP8B diminished thermogenesis, contributing to a diet related fatness (Whittle et al., 2012). Further research revealed that BMP8B interacted with NRG4 (Neuregulin-4) to modulate the neuro-vascular network in adipose tissue (Pellegrinelli et al., 2018). Recently, research has revealed that BMP8B was associated with regulating the progression of inflammation and cancers. In a study using a tissue microarray of 42 gastric tumour samples paired with adjacent normal controls, BMP8B was presented to be a possible tumour suppressive protein in gastric cancer (Wisnieski et al., 2017). Reduced expression of BMP8B regulated by histone H4 at lysine 16 (H4K16) correlated with poor prognosis in gastric cancer ($P<0.05$) (Wisnieski et al., 2017). In pancreatic cancer, the finding was in clear contrast to that in gastric cancer. Pancreatic cancer tissues had significantly higher expression of BMP8B than normal adjacent tissues ($P<0.01$). High expression of BMP8B suppressed the proliferation and promoted the apoptosis of pancreatic cancer while reduced expression of BMP8B accelerated the progression and growth of tumour cells (Cheng et al., 2014). Mutation in BMP8B may promote the metastasis of benign uterine leiomyoma to the pulmonary metastases. BMP8B has also been shown to interact with BMP4 in inducing the genesis of primordial germ cells in the mouse model (Soritsa et al., 2018).

Comparing with BMP8A, BMP8B is more preferentially expressed in various tissues, though the thyroid is still the organ with the top expression (7.377 ± 4.902 RPKM). In an gene expression array assay of hepatocellular carcinoma, BMP8A was upregulated in tumours ($n=17$) compared with adjacent non-tumour liver tissues (Zekri et al., 2008). Hypermethylation of BMP8A was detected in rhabdomyosarcomas (Mahoney et al., 2012), whereas hypomethylation of BMP8A was found in oesophageal cancer (Singh et al., 2015).

Due to the high sequence identity of BMP8A and BMP8B, they are hypothesized to share similar downstream transduction (Zhao and Hogan, 1996). Similar as the other secreted ligand of BMP family, BMP8 was capable of binding type I and type II receptors on the membrane, contributing to the recruitment and the activation of downstream transcription factors to complete the signal transduction.

Different from the other BMPs, BMP8 can induce activation of both BMP specific R-Smad1/5/8 and TGF-β specific R-Smad 2/3 signal pathways synchronously. The former pathway was mediated by receptor complexes formed by type I receptor（ALK3 or ALK6) and type II receptor (ACVR2A or BMPR2). Whilst SMAD2/3 signal pathway was activated through receptor complexes formed by type I receptor (ALK5 or ALK4) and type II receptor (ACVR2A, ACVR2B or TGFBR2) (Wu et al., 2017).

Differential expression of BMP8A in development stages was observed in the intermuscular bone formation in bream (Zhang et al., 2018). BMP8 is closely correlated with the feet and leg structures in pig models (Fan et al., 2009a). BMP8a was also predicted as an indicator of osteogenesis process in AS (Shahba et al., 2018). BMP8A was proved to induce the subsequent differentiation of spermatogonia through the Smad1/5/8 signal pathway, whilst the proliferation of germ cells was facilitated by the Smad2/3 signal pathway in mouse models (Wu et al., 2017).

BMP8A suppressed the ubiquitination of Nrf2, which modules the expression of Tripartite Motif Containing 24 (TRIM24), leading to the inhibition of apoptosis and drug resistance of renal cancer (Yu et al., 2020).

BMP8B signalling protein participates in regulation of thermogenesis and energy expenditure. BMP8B plays pivotal role in lipolysis induced by the adrenaline and noradrenaline in brown adipose tissue, which is accomplished by thermogenic factors, such as thyroid hormone (triiodothyronine, T3) through thyroid hormone receptor β1. Silence of BMP8B diminished thermogenesis contributing to a diet related fatness (Whittle et al., 2012). Further research revealed that BMP8B was capable of interacting with NRF4 to modulate the neuro-vascular network in adipose tissue (Pellegrinelli et al., 2018).

Recently, BMP8B has been implicated in the progression of inflammation and cancers (Mahli et al., 2019, Gomez de Cedron et al., 2019). BMP8B exerts pro-inflammatory effect in hepatic stellate cells (HSCs) which enhances the progression of steatohepatitis (Mahli et al., 2019, Vacca et al., 2020).

In a microarray test of 42 gastric tumour samples paired with adjacent normal controls, BMP8B presents to be an inhibitor of gastric cancer. Reduced expression of BMP8B, regulated by histone H4 at lysine 16 (H4K16), correlates with poor prognosis

in gastric cancer ($P<0.05$) (Wisnieski et al., 2017). Expression of BMP8B is higher in pancreatic cancer comparing with the normal adjacent tissues ($P<0.01$). Over-expression of BMP8B suppressed the proliferation and promoted the apoptosis of pancreatic cancer while reduced expression of BMP8B accelerated the progression and growth of tumour cells (Cheng et al., 2014). Mutation in BMP8B may promote the metastasis of benign uterine leiomyoma to pulmonary metastases. BMP8B signal was observed to interact with BMP4 to induce the genesis of primordial germ cells in the mouse model (Soritsa et al., 2018).

Analysis of BMPs in the TCGA breast cancer cohort demonstrated the higher expression of both BMP8A and BMP8B in breast cancers than adjacent normal controls, which was also correlated with poorer overall survival (Katsuta et al., 2019b). The study revealed the involvement of BMP8A/8B in the proliferation and progression of breast cancer, however, the result needs to be independently validated through the experiments. Research on exploring the molecular mechanism of BMP8 involved in breast cancer and bone metastasis is meaningful. Additionally, the corresponding cellular and molecular mechanism and the predicted signalling pathway of BMP8A/8B in breast cancer cells also represents important areas of scientific study to enhance our understanding of breast cancer progression and management.

1.5 Aims of the present study:

Biological behaviour of breast cancer is regulated by various signalling pathways. BMP signalling exerts a pivotal role in modulating the tumourigenesis, invasion and migration of breast cancer. According to previous research, expression of BMP8A and BMP8B are significantly increased in breast cancer tissue compared with the normal adjacent control. However, the mechanism of BMP8A and BMP8B signals involved in breast cancer, especially their role in subtypes of breast cancer is elusive. If the molecular mechanism of BMP8A and BMP8B in primary breast cancer and bone metastasis could be fully established, it will render the further understanding of the pathogenesis of breast cancer and shed light on targeted therapy of breast cancer in the future.

The aims of this study were:

1. To evaluate expression and clinical relevance of BMP8A and BMP8B in breast cancer. The study builds on the bioinformatical analysis of the aberrant expression of BMP8A and BMP8B in breast cancer and their clinical relevance on the TNM staging and the prognosis with epigenome databases. Involvement of BMP8A and BMP8B in the subtypes of breast cancer will further dissected by assessing their expression in the different subtype diseases and association with disease progression and prognosis.

2. To evaluate the influence of BMP8A on cellular functions of breast cancer cells. Lentiviral vectors carrying either coding sequence of human BMP8A will be employed to create breast cancer cell line models with BMP8A overexpression and knockdown, respectively. Impact of BMP8A on cellular functions will be determined, including proliferation, adhesion, migration and invasion. Molecular mechanisms intimately associated with the altered cellular functions will be assessed in the cell lines with BMP8A overexpression.

3. To explore the potential signal transduction of BMP8A in different subtype breast cancers. BMP8A induced Smad dependent and independent signal transduction will be examined in the breast cancer cell lines that represent different subtypes of the disease. Involvement of BMP receptors in the subtype specific signalling will be determined to elucidate corresponding implication in the subtype specific role of BMP8A.

4. To investigate the impact of BMP8A in the bone metastasis of breast cancer. *In vitro* co-culture models will be employed to evaluate the influence of BMP8A on proliferation, migration and invasion of breast cancer cells in exposure to *in vitro* bone environment.

Chapter 2

Material and methods

2.1 Cell lines

Eleven Breast cancer cell lines were chosen to provide coverage across all the subclasses, together with a bone cell line. Cell lines were purchased from the ATCC (American type culture collection, Boulevard Manassas, USA). The cell lines are summarised below, and additional details described in Table 2.1.

Luminal A subtype: MCF-7 and ZR-751

Luminal B subtype: MDA-MB-361 and BT-474

Her2(+) subtype: SKBR3 and HCC1419

TNBC subtype: MDA-MB-231, BT20, BT549, MDA-MB-436 and MDA-MB-468

Osteoblast cell line: hFOB1.19

Details of the cell characteristics are listed in the Table 2.1.

Table 2.1 Breast cancer cell lines

Cell line	Morphology	Origin	Features	Medium
MCF-7	Epithelial	Derived from pleural effusion of breast cancer	ER (+) PR (+)	DMEM-F12+10% fetal serum+Abx
ZR-75-1	Epithelial	Derived from ductal breast carcinoma.	ER (+)	RPMI 1640 + 2mM Glutamine + 1mM Sodium Pyruvate (NaP) + 10% Foetal Bovine Serum (FBS).
MDA-MB-361	Epithelial	mammary gland/breast; derived from metastatic site: brain	ER (+) Her2 (+)	RPMI 1640 + 2mM Glutamine + 1mM Sodium Pyruvate (NaP) + 10% Foetal Bovine Serum (FBS).
BT-474	Epithelial	ductal breast carcinoma	ER (+) PR (+) Her2 (+)	RPMI+10% fetal serum+Abx
SKBR3	Epithelial	mammary gland/breast; derived from metastatic site: pleural effusion	Her2 (+)	DMEM-F12+10% fetal serum+Abx
HCC1419	Epithelial	Mammary gland, ductal breast carcinoma	Her2 (+)	RPMI+10% fetal serum+Abx
MDA-MB-231	Epithelial	established from a pleural effusion of metastatic breast cancer.		DMEM-F12+10% fetal serum+Abx
BT-20	Epithelial	mammary gland/breast		DMEM-F12+10% fetal serum+Abx
BT-549	Epithelial	ductal breast carcinoma		RPMI 1640 + 2mM Glutamine + 1mM Sodium Pyruvate (NaP) + 10% Foetal Bovine Serum (FBS).
MDA-MB-436	pleomorphic with multinucleated component cells	mammary gland/breast; derived from metastatic site: pleural effusion		DMEM-F12+10% fetal serum+Abx
MDA-MB-468	epithelial	mammary gland/breast; derived from metastatic site: pleural effusion		DMEM-F12+10% fetal serum+Abx
hFOB1.19		osteoblast		Ham's F12 Medium with L-glutamine (without phenol red) +0.3mg/dl G418+10%fetal bovine serum

2.2 Primers

Primers used in the present study were designed using the Primerblast software and synthesised by Sigma Aldrich (Poole, Dorset, UK), which contained three different categories corresponding to different kinds of PCRs. Two adjacent exons were spanned within the paired primers and at least one intron is contained in the amplified genome sequence. Details for the primers are presented in Table 2.2.

Table 2.2 Primers for qPCR and conventional PCR

Gene	Primer Name	Primer Sequence (5'-3')
GAPDH	SGF1	TGCACCACCAACTGCTTAGC
	SGR1	GGCATGGACTGTGGTCATGAG
	F8	GGCTGCTTTTAACTCTGGTA
	R8	GACTGTGGTCATGAGTCCTT
BMP8A	SGF1	CTGGTTGCTGAAGCGTCACAAG
	SGR1	AGTGACCACGAAAGGCTGTTGG
	F8	GCCTCTATGTGGAGACTGAG
	R8	CACTCCCCCTCACAGTAATA
BMP8B	SGF1	CTGGTTGCTGAAGCGTCACAAG
	SGR1	AGTGACCACGAAAGGCTGTTGG
	F8	CAACAGGGAGTCTGACTTGT
	R8	CACTCCCCCTCACAGTAATA
E-cad	F22	CAGGAGCCAGACACATTTAT
	R22	TCTAAGGTGGTCACTTGGTC
Snail	F17	CACACTGGCGAGAAGC
	ZR17	***ACTGAACCTGACCGTACA***CTTCTTGACATCTGAGTGGG
Slug	F17	TGGACACACATACAGTGATT
	ZR17	***ACTGAACCTGACCGTACA***GATCTCTGGTTGTGGTATGA
CDH2	F17	CATTGATCCAAATGCTGGAC
	ZR17	***ACTGAACCTGACCGTACA***AAATCACCATTAAGCCGAGT
BACT	F8	GGACCTGACTGACTACCTCA
	ZR8	***ACTGAACCTGACCGTACA***AGCTTCTCCTTAATGTCACG

MMP1	SGF1	GGGAGATCATCGGGACAACTC
	SGR1	GGGCCTGGTTGAAAAGCAT
PDPL	F8	GAATCATCGTTGTGGTTATG
	ZR8	***ACTGAACCTGACCGTACA***CTTTCATTTGCCTATCACAT
MMP2	SGF1	TGATCTTGACCAGAATACCATCG
	SGR1	GGCTTGCGAGGGAAGAAGTT
MMP3	SGF1	TGGCATTCAGTCCCTCTATGG
	SGR1	AGGACAAAGCAGGATCACAGTT
MMP11	SGF1	CCTGCATCTGTCTGCCTTCT
	SFR1	GCTTTHHAGGATAGCAGTGC
MMP14	SGF1	TCGACGAAGAGACCAAGGAG
	SGR1	CGGTCATCATCGGGCAGCACAAA
CCND1	F1	AACAAACAGATCATCCGCAA
	ZR1	***ACTGAACCTGACCGTACA***AAATGAACTTCACATCTGTGGC
CCNE1	F1	GCAGGATCCAGATGAAGAAA
	ZR1	***ACTGAACCTGACCGTACA***ATTATTGTCCCAAGGCTGG
ID01	F11	AAAAGGATCCTAATAAGCCCC
	ZR11	***ACTGAACCTGACCGTACA***CAGTCTCCATCACGAAATGA
C-MYC	F1	TGCTCCATGAGGAGACAC
	ZR11	***ACTGAACCTGACCGTACA***TGATCCAGACTCTGACCTTT
ACVR1	F1	TGGTGTAACAGGAACATCAC
	R1	ATGTCTGAAGCAATGAAACC
	ZR1	***ACTGAACCTGACCGTACA***AACCTCCAAGTGGAAATTCT
BMPR1A	F1	GACCAGTCACAAAGTTCTGG
	R1	TTTTTGCTCTTTAGGTCTCG
	ZR1	***ACTGAACCTGACCGTACA***GACCATCTGAATCTGTTTGG
ACVR1B	F1	GATATACCAGACGGTCATGC
	R1	GGGCATAAATATCAGCACAT
	ZR1	***ACTGAACCTGACCGTACA***CGTGCTCATGATAGTCAGAA
ACVR2	F1	ACTTGTTCCAACTCAAGACC
	R1	ACTTTTGATGTCCCTGTGAG
	ZR1	***ACTGAACCTGACCGTACA***CTTTCCAGACACAACCAAAT
ACTR2B	F1	TCATGTGGACATCCATGAG

	R1	GTCGCTCTTCAGCAATACAT
	ZR1	***ACTGAACCTGACCGTACA***AGCCTTGATCTCCAGCAG
BMPR1B	F5	TGTAGTTTGCTCTTGGTCCT
	R5	CATTGATTTAGCGTCTAGGG
BMPR2	F5	GCACACCTTTGACTATAGGG
	R5	AGTAGGCAGAACATCAGGAA
	F1	TTTGGGAAAGAAACAAATCT
	ZR1	***ACTGAACCTGACCGTACA***TGCATAAGGACC

Note: The italic sequence, ***ACTGAACCTGACCGTACA*** in the respective primers is known as the Z-sequence was used in the respective primer pairs for quantitative PCR assays.

2.3 Primary and secondary antibodies used in the present research

Full details of both the primary and secondary antibodies used in the present study are summarised in Table 2.3 and 2.4.

Table 2.3 Primary antibodies

Name	Species	Molecular Weight(kDa)	Supplier	Product Code
Anti-BMP8A	Rabbit	43	Abcam	ab60290
Anti-GAPDH	Mouse	37	Santa Cruz Biotechnology Inc	sc-32233
Anti-Snail1	Mouse	29	Santa Cruz Biotechnology Inc	sc271977
Anti-Slug	Mouse	29.9	Santa Cruz Biotechnology Inc	sc166476
Anti-AKT1	Mouse	55.7	Santa Cruz Biotechnology Inc	sc5298
Anti-P-AKT-1	Mouse	55.7	Santa Cruz Biotechnology Inc	sc81433
Anti-Smad5	Goat	52.3	Santa Cruz Biotechnology Inc	sc26418
Anti-Smad 1	Mouse	52	Santa Cruz Biotechnology Inc	sc7963
Anti-Smad 8	Rabbit	46.4	Santa Cruz Biotechnology Inc	sc11393
Anti-JNK	Rabbit	46	Santa Cruz Biotechnology Inc	sc-571
Anti-P-JNK	Mouse	46	Santa Cruz Biotechnology Inc	sc6254
Anti-P38	Mouse	38	Santa Cruz Biotechnology Inc	sc7972
Anti-P-ERK	Mouse	44	Santa Cruz Biotechnology Inc	sc7383
Anti-ERK	Mouse	44	Santa Cruz Biotechnology Inc	sc514302
Anti-BMPR1A	Rabbit	60.2	Thermo Fisher	12702-1-AP
Anti-BMPR1B	Goat	56.9	Santa Cruz Biotechnology Inc	sc5679
Anti-BMPR2	Rabbit	115.2	Thermo Fisher	19087-1-AP
Anti-c-MYC	Mouse	48.8	Santa Cruz Biotechnology Inc	sc70465
Anti-Vimentin	Mouse	53.7	Santa Cruz Biotechnology Inc	sc66002
Anti-ACTR2	Mouse	44.8	Santa Cruz Biotechnology Inc	sc390971
Anti-P-Smad1/5/8	Rabbit	53	Sigma-Aldrich	ab3848-1
Anti-RANKL	Rabbit	35.5, 27.7, 30.5	Santa Cruz Biotechnology Inc	sc9073
Anti-KI67	Rabbit	35.9, 32	Abcam	ab15580
Anti-EGFR	Mouse	134.3	Santa Cruz Biotechnology Inc	sc71034
Anti-P-EGFR	Mouse	134.3	Santa Cruz Biotechnology Inc	sc377547
Anti-CDH11	Rabbit	88, 76.5	Abnova	M04
Anti-CD44	Mouse	81.5, 78, 80	Autogen Bioclear	Ad154

Anti-CD133	Rabbit	97.2, 96.3, 93.2	Biorbyt	Orb99118
Anti-CD34	Mouse	40.7	Santa Cruz Biotechnology Inc	sc19587
Anti-CTSK	Mouse	37	Santa Cruz Biotechnology Inc	sc48353
Anti-PTHrP	Rabbit	20.2	Santa Cruz Biotechnology Inc	sc20728
Anti-PCNA	Mouse	28.8	Santa Cruz Biotechnology Inc	sc25280
Anti-VEGF	Goat	27, 25, 24	Sigma-Aldrich	V6627
Anti-RANK	Rabbit	66, 56.4, 36.3	Santa Cruz Biotechnology Inc	sc9072
Anti-P-Smad2/3	Rabbit	48.1	Santa Cruz Biotechnology Inc	sc130218
Anti-P21	Mouse	21	Santa Cruz Biotechnology Inc	sc6246
Anti-P27	Mouse	27	Santa Cruz Biotechnology Inc	sc1641

Table 2.4 Second antibodies

Name	Species	Supplier	Product Code
Anti-mouse IgG peroxidase conjugate	Rabbit	Sigma-Aldrich	A-9044
Anti-rabbit IgG peroxidase conjugate	Goat	Sigma-Aldrich	A-9169
Anti-goat IgG peroxidase conjugate	Rabbit	Sigma-Aldrich	A-5420

2.4 Reagents and recipe

2.4.1 Reagents for DNA cloning

Ampicillin

Ampicillin sodium salt (Melford Laboratories Ltd, Suffolk, UK) was dissolved in sterile balanced salt solution (BSS) at a concentration of 100mg/ml and stored at 4℃ fridge for use.

Liquid Broth (LB)

10g of tryptone, 10g of sodium chloride NaCl), 5g of yeast extract and 1.5g of Tris/Tris HCl (Melford Laboratories Ltd, Suffolk, UK) were dissolved in 1L of distilled water. The solution was adjusted to pH 7.0 and was then sterilised by an autoclaving for 15 minutes and stored at room temperature for further use. Selective antibiotics were added if necessary.

LB agar

10g of tryptone, 5g of yeast extract, 15g of agar and 10g of NaCl were dissolved in 1L of distilled water, the pH was adjusted to 7.0, then the solution was autoclaved. Before use, the solution was melted in a microwave and left to cool before adding selective ampicillin (100μg/ml). The solution was poured into single vented 10cm^2 petri dishes (Bibby Sterilin Ltd, Staffs, UK), then left to cool before storing at room temperature for further use.

2.4.2 Solutions for molecular biology

Diethyl pyrocarbonate (DEPC) water

250ml of DEPC was dissolved in 4.75ml of distilled water. The mixture was autoclaved and stored at room temperature for further use.

Tris-Boric Acid EDTA (TBE) (5×)

40g of Tris-HCl (Melford Laboratories Ltd, Suffolk, UK), 275g of boric acid (Melford Laboratories Ltd, Suffolk, UK) and 46.5g of EDTA were dissolved in 10L of distilled water, NaOH was used to adjust the PH value to 8.3. The buffer was stored at room temperature. The concentrated TBE was diluted to 1x concentration using distilled water to prepare agarose gels and as electrophoresis buffer.

2.4.3 Solutions for protein research

10% Ammonium Persulfate (APS)

APS (1g) was dissolved in 10ml of distilled water and was then aliquoted and stored in a freezer at -20℃ for further use.

Lysis Buffer

50mM TRIS base (0.61g), 5mM EGTA (0.19g), 150mM NaCl (0.87g) and 1ml Triton X100 were dissolving in 100ml of distilled water. Protease inhibitors were added just before use.

Recipe for protease inhibitors:

Reagent contains phenylmethylsulfonyl fluoride (PMSF) (100μg/ml in isopropanol), aprotinin (10μg/ml), leupeptin (10μg/ml), sodium vanadate (5mM) and sodium fluoride (50mM) were prepared and stored in the freezer for further use.

Running buffer (10x) (for sodium dodecyl sulfate- poly acrylamide gel electrophoresis [SDS-PAGE])

Tris (303g), glycine (1.44kg) (Melford Laboratories Ltd, Suffolk, UK) and (SDS) (100g) (Melford Laboratories Ltd, Suffolk, UK) were dissolved in 10L of distilled water, before adjusting the pH value to 8.3. This solution was further diluted 1:10 using distilled water before use.

Transfer buffer

Tris (15.5g) and glycine (72g) were dissolved in 4L distilled water. Following this 1L of methanol (Fisher Scientific, Leicestershire, UK) was added into the mixture to a final volume of 5L in distilled water.

Tris Buffered Saline (TBS) (10x)

Tris (24.228g) and NaCl (80.06g) (Melford Laboratories Ltd, Suffolk, UK) were dissolved in 1L of distilled water. HCL was used to adjust the PH value to 7.4. The solution was stored at room temperature and diluted with distilled water to 1x as required.

2.4.4 Solutions for tissue culture

Antibiotics (ABS) (100×)

Streptomycin (5g), penicillin (3.3g) and amphotericin B (12.5mg) in DMSO were dissolved in 0.5L of BSS. The solution was filtered and divided into 5ml containers, which could be added directly to 500ml medium as required.

Phosphate-buffered saline (PBS)

NaCl(8g), KCl (0.2g), Na2HPO4(1.44g) and KH2PO4(0.24g) were added into 800ml of dH2O. The pH value was adjusted to 7.4. and the volume was made up to 1 Litre using dH2O. The solution was then autoclaved and aliquoted for further use.

Balanced Saline Solution (BSS)

NaCl (79.5g), KH_2PO_4 (2.1g), KCl (2g) and Na_2HPO_4 (11g) were dissolved in 10L of distilled water. NaOH (1M) was used to adjust the pH value to 7.4 for further use.

Ethylenediaminetetraacetic Acid (EDTA) (0.02%)

KCl (1g), Na_2HPO_4 (5.72g), KH_2PO_4(1g), NaCl (40g) and EDTA (1.4g) were dissolved in 5L of distilled water. The pH value of the mixture was adjusted to 7.4, then the solution was autoclaved and stored at room temperature for further use.

Trypsin (25mg/ml)

After dissolving 500mg of trypsin in 20ml 0.02% EDTA, the solution was filtered and aliquoted into 250µl containers and stored at -20℃ for further use.

An aliquot could be diluted in 10ml of 0.05M EDTA before using to detach cells.

2.5 Cell maintenance, culture and storage

2.5.1 Preparation of growth medium for maintenance of cells

MCF-7, SKBR3, BT20, BT549, MDA-MB-231, MDA-MB-436 and MDA-MB-468 cell lines were cultured in DMEM/Ham's F12 with L-glutamine medium (Sigma, Dorset, UK) supplemented with ABS (as described in section 2.5.4) and 10% Foetal Calf serum (FCS).

ZR-751, BT474, MDA-MB-361, HCC1419 cell lines were cultured in RPMI 1640 medium (Sigma, Dorset, UK) supplemented with ABS and 10% FCS.

HFOB cells were maintained in a base medium supplemented with 0.3 mg/ml G418 and foetal bovine serum to a final concentration of 10%. The base medium used was a 1:1 mixture of Ham's F12 Medium Dulbecco's Modified Eagle's Medium, with 2.5mM L-glutamine (without phenol red).

2.5.2 Cell Maintenance

Breast cancer cells were cultured in an incubator at 37℃, 5% CO_2 and 95% humidity, whilst hFOB 1.19 cells were maintained in the incubator at 34℃, 5% CO_2 and 95% humidity. Tissue culture was performed with autoclaved pipette tips inside a class II laminar flow cabinet and aseptic techniques was strictly abided to whilst performing tissue culture. Cells were maintained in the medium as described in section 2.5.1 and routinely passage once reaching 80-90% confluence.

2.5.3 Detachment of adherent cells

Cell passaging was undertaken once cells reached a certain confluence. The medium inside the flask was aspirated, the cells washed with sterile phosphate buffered solution

(PBS) to remove the remaining medium. Following these adherent cells were detached from the bottom of the flask through incubation with trypsin (0.01% trypsin: 0.02% EDTA in BSS buffer) for about 5 minutes at 37℃. Then 5ml of medium was added into the flask, detached cells were resuspended in the medium. The cell suspension was collected in a universal container (Greiner Bio-One Ltd, Gloucestershire, UK) and centrifuged at 1000rpm for 5 minutes. After removing the supernatant, the cell pellet was resuspended in 5ml of pre-warmed medium, followed by transferring 20% of the cell volumes into the tissue culture flask for sub-culturing.

2.5.4 Cell counting

A neubauer haemocytometer counting chamber (Mod-Fuchs Rosenthal, Hawksley, UK) was utilised in current study. Cell suspension was added into the chamber between the plate and cover slip to count and calculate the number of cells per millilitre. An inverted light microscope (Reichert, Austria) was used under 10 × 10 magnification in this process. Nine large squares (1mm × 1mm × 0.2mm) were included in the chamber, each large square was further divided into 16 small squares. Cells in four of the large squares were counted to acquire the cell numbers with the following equation: Cell number/ml = (summed number of cells counted in 4 large squares/4/2) × (1×10^4).

2.5.5 Storage of cell stocks in liquid nitrogen

Liquid nitrogen was used for a long-term storage of cells. Cells were first trypsinised from the flask using trypsin for 2-5 minutes at 37℃. Then, the detached cells were resuspended in medium. The cell suspension was further mixed with recommended percentage (generally 10%) of dimethyl sulfoxide (DMSO). Cell suspensions of 1ml was aliquoted into previously labelled (name of the cell line, the passage and the date) 1.8ml cryotubes (Greiner BioOne, Germany) and transferred into the storage box in a -80℃ freezer for overnight. Finally, the cryotube was transferred to liquid nitrogen tank the following day for a long-term storage.

2.5.6 Cell revival from liquid nitrogen

Frozen cells were removed from liquid nitrogen and revived when necessary. Before cell revival, to the medium was preheated in the incubator. Subsequently, frozen cells were defrosted immediately in warm water of approximately 37℃. The cell suspension was then transferred to a universal container with 5ml of prewarmed medium to dilute

the DMSO inside. The universal containers were then centrifuged at 1000rpm for 5 minutes to pellet the cells. Medium and supernatant, including cell debris, were removed following by a re-suspension of the cells in 5ml of medium. The re-suspended cells were transferred to a new T25 ($25cm^2$) tissue culture flask and incubated at 37℃ with 5% CO_2. Following 24 hr incubation, the cells were observed under the microscope to examine their viability. The medium was then changed to remove dead cells. The flask was placed to the incubator and followed by sub-culture techniques once cells reached appropriate confluence.

2.6 Synthesis of complementary DNA for use in PCR analysis

2.6.1 Total RNA isolation

The TRI Reagent protocol from Sigma-Aldrich was applied to isolated Ribonucleic acid (RNA). This process contained several steps, as follows:

Step 1: Homogenisation of cells. Cells were harvested from 6-well plates or flasks. Medium was removed from the cell container; PBS was used to wash the cells and then TRI Reagent (1ml per 5-10 × 105 cells) was added to lyse cells. A cell scraper was used in this step to harvest the cells if necessary. The cell lysate was transferred into a 1.8ml microfuge tube and incubated on ice for 5 minutes.

Step 2: Separation of RNA, DNA and protein. 0.2ml of chloroform (per 1ml of TRI Reagent) was added into the microfuge tube and the sample was strongly shaken for 15 seconds and subsequently incubated on the ice for 5 minutes. The homogenate was centrifuged at 12,000rpm for 15 minutes at 4℃ (Boeco, Wolf Laboratories, York, UK). Following this stage, phase separation was seen within the tubes.

Step 4: Precipitation and extraction of RNA. The supernatant which contained RNA (top layer/ aqueous phase) was carefully collected and transferred into a 1.8ml pre-labelled microfuge tube. Equal volumes (~500µl) of isopropanol were added into the tube and samples incubated for 10 minutes on ice before a centrifugation at12,000rpm for 10 minutes at 4℃. The supernatant was removed and ethanol (Fisher Scientific, Leicestershire, UK) with DEPC (3:1 ratio) was used to wash the RNA pellet. Following centrifugation at 7,500rpm for 5 minutes at 4℃, ethanol was removed and the RNA pellet was dried at 55℃ for less than 5 minutes in a drying heater (Techne Hybridiser

HB-1D, Wolf Laboratories, York, UK). The pellet was then dissolved in 30µl of DEPC water.

2.6.2 RNA quantification

Following RNA extraction, an Implen Nanophotometer (Munchen, Germany) was used to measure the concentration and purity of the single strand RNA in the sample, through measuring the ratio of absorbance of 260nm and 280nm in the RNA sample compared to a DEPC water blank control.

2.6.3 Reverse transcription of RNA

Following RNA extraction and quantification, 2000ng of RNA was reverse transcribed into complementary DNA (cDNA) utilizing the reverse transcription kit (Promega, Southampton, UK) according to the protocol below.

Step 1: Calculate the volume of the RNA sample and PCR water required. Two thousand ng of RNA was required in this process, PCR water was added into the RNA sample to reach a total volume of 10µl. Another 10µl of 2× RT mixture was added into the RNA sample in the thin-walled 200µl PCR reaction tube.

Step 2: PCR tubes were inserted placed in the T-Cy thermocycler (Creacon Technologies Ltd, Netherlands), and reaction was performed under the following parameters: 25℃ for 10 minutes, followed by 37℃ for 120 minutes and 85℃ for 5 minutes.

Step 3: Once the reverse transcription was completed, the cDNA samples were diluted in three times its volume of PCR water. Samples were stored at -20℃ for further use.

2.6.4 Polymerase chain reaction (PCR)

RT-PCR was performed using a GoTaq Green master mix (Promega, Madison, USA). A reaction was prepared as outlined in table 2.5.

Table 2.5 Reaction reagent formulated for conventional PCR

Component	Volume(µl)
2x GoTaq Green master mix	8
Forward primer (10pmol)	1
Reverse primer (10pmol)	1
Nuclease-free water	5
cDNA template	1
Total	16

PCR water was used to substitute the cDNA as the negative control to exclude possible false positive results caused by any contamination in the reagents and buffer. The reaction reagent was prepared in 200µl PCR reaction tubes or a 96 well plate (Bio-Rad Laboratories, Hemel Hampstead, UK). Following by mixing briefly, the samples were placed in a Simpliamo Thermocycler (Thermo Fisher Scientific, Waltham, MA USA), as the parameters below.

Initial denaturing period 94℃ for 5 minutes

Denaturing: 94℃ for 1 minute

Annealing: reaction specific temperature for 40-60 seconds

Extension: 72℃ for 40 seconds

Final extension period 72℃ for 10 minutes

The denaturing, annealing and extension steps were repeated for 30-36 cycles. Details for annealing temperatures and primer information are provided in the Table 2.2. Primer3 online software (https://primer3.ut.ee/) was used to validate the binding sites as well as the size of predicted product.

2.6.5 Agarose gel electrophoresis

RT-PCR products (DNA) were separated by stained agarose gel electrophoresis.

The gel was formulated by adding the proper amount of agarose (Melford Chemicals,

Suffolk, UK) in 1×TBE solution, then the reagent was heated in the microwave oven to dissolve the agarose completely. The concentration of the gel used was determined by the size of the PCR products; 0.8% for DNA fragments 1-10kb or 2% for DNA fragments less than 100bps, 1.5% agarose gel was preferred for PCR products at a range between 100bps and 1000bps. SYBR safe DNA gel stain (Invitrogen, Manchester, UK) was added into the agarose at a ratio of 1:10000 before setting.

The stained agarose was transferred to the electrophoresis cassette carefully to avoid any bubbles and a plastic comb was inserted into the gel to generate wells for loading samples. Once set, the gel was submerged in 1×TBE buffer, the comb removed and 8µl of a 1Kb DNA ladder (Cat No. M106R; GenScript USA Inc), or 10µl of sample were loaded per well. The samples were then subject to electrophoresis, using a power pack 123 (Gibco BRL, Life technologies Inc) at a constant voltage of ~100V for 30-50 minutes (dependent on predicted product size).

2.6.6 DNA visualization

Gels were visualised and photographed using a blue light illuminator in the Syngene U: Genius 3 closed system (Geneflow, Elmhurst, Lichfield Staffs).

2.6.7 Quantitative RT-PCR (QPCR)

QPCR is a sensitive technique which is capable of capturing the fluorescent signal produced by the PCR product to detect the accurate amount of PCR products in real time. A reaction was prepared as outlined in table 2.6. Amplifluor Uniprimer Universal system (Intergen Company, New York, USA) was utilized in present study to quantify transcript copy number. Different from the conventional PCR, the amplifluor probe of QPCR contains standard F primer and the ZR primer. The ZR primer contains a Z-sequence (ACTGAACCTGACCGTACA), which is integrated into the PCR products during the initial amplification and is $1/10^{th}$ the concentration of the forward primer and Uniprobe that were added to a QPCR reaction. After the initial amplification of a gene specifically with a pair of specifically designed primers, including the forward primer and reverse primer (ZR) containing Z sequence, the Uniprobe starts to work with the specific forward primer to continue the amplification using the PCR products from the initial amplification as templates instead of the gene itself which is detectable for the quantitative analysis.

Universal probe (Uniprobe, Millipore, Watford, UK) is the core component of the QPCR reaction, which is composed by a 3' region specific to the Z-sequence (ACTGAACCTGACCGTACA) and a 5' hairpin structure marked with a fluorophore (FAM). The hairpin is linked to an acceptor moiety (DABSYL) which shields the fluorescent signal, however, simultaneous with the initial amplification, Uniprobe incorporates with the Z sequence and works as the template for the DNA polymerisation. The hairpin is disentwined by DNA polymerase, fluorescent signal is unquenched. Detection of this fluorescence during qPCR cycles allows quantification of the amount of DNA that has been amplified.

The cDNA applied in qPCR was reversely transcript from the RNA extracted from the cells as described in previous section.

Table 2.6 Reaction mixture for QPCR

Component	Volume
2× FAST precision mix (Primerdesign)	5µl
Forward primer (10pmol/µl)	0.3µl
Reverse primer (1pmol/µl)	0.3µl
Amplifluor™ probe(10pmol/µl)	0.3µl
cDNA	1µl
PCR H_2O	3µl
Total volume per reaction	10µl

After each sample was loaded into a 96 well plate (Applied Biosystems™, Life Technologies Ltd, Paisley, UK) and covered with MicroAmp® Optical Adhesive film (ThermoFisher Scientific, Life Technologies Ltd, Paisley, UK), the plate was placed in an StepOne plus systems ((ThermoFisher Scientific, Life Technologies Ltd, Paisley, UK)) for amplification and quantification. Experimental conditions were listed below:

Step 1: Initial denaturing period - 94℃ for 5 minutes

Step 2: Denaturing step - 94℃for 10 seconds

Step 3: Annealing step - 55℃ for 15 seconds

Step 4: Extension step - 72℃ for 20 seconds

Steps 2 - 4 were repeated over 80 cycles. In this established method, approximately 20 cycles are required for the generation of Z-tagged products.

Fluorescent signal was captured in the annealing stage when the geometric increase of the signal was correlated with the exponential increase of product. The threshold level of amplified gene was also chosen in the log phase, comparing with the standard curve (plotting by the known copy number of a reference gene (PDPL) correlated with the degree of fluorescent signal), the copy number of the target gene was accurately calculated by the software according to the CT value of each reaction.

PCR water was used to substitute the cDNA to act as a negative control. House-keeping genes such as β-actin or GAPDH were applied to normalise the transcript copy number of the genes of interest in the samples.

2.7 SDS-polyacrylamide gel electrophoresis (SDS-PAGE) and Western blotting

2.7.1 Protein extraction and preparation of cellular lysates

Cells in the culture flask were harvested using a disposable cell scraper, followed by a centrifugation at 2,000rpm for 5minutes, cells were lysed in lysis buffer (80µl per 2million cells). The cell lysate was transferred to a 1.8ml microfuge tube and subject to continuous rotation on a Labinco rotating wheel (Wolf Laboratories, York, UK) for 1 hour at 4℃. Insoluble cell debris was discarded after another centrifugation at 13,000rpm for 15 minutes. Protein samples generated were then quantified and stored at -20℃ until required.

2.7.2 Protein quantification

Protein quantification was performed using a Bio-Rad DC protein assay kit (Hemel Hampstead, UK). The procedures were listed as follows.

- Bovine serum albumin (BSA) was diluted with lysis buffer in a series of concentrations from 0.005mg/ml to 10mg/ml on a 96-well-plate.
- Protein sample (5µl) was added into one well, followed by addition of 25µl of Reagent A containing 2% of Reagent S and 200µl of Reagent B sequentially. Blue color was developed after an incubation of 45 minutes at room temperature.

- Absorbance was determined at a wavelength of 620nm using an ELx800 plate reading spectrophotometer (Bio-Tek, Wolf Laboratories, York, UK). Concentration of the protein samples were calculated according to the standard curve.
- Protein samples for an experiment were standardised to a same concentration within a range of 2.0mg/ml to 3.0mg/ml with the lysis buffer. The protein samples were then mixed with equal volume of 2 × Lamelli sample buffer (Sigma-Aldrich, Poole, Dorset, UK) followed by a boiling at 100ºC for 5-10 minutes. The protein samples were stored at -20℃ for further use.

2.7.3 Sodium dodecyl sulphate polyacrylamide gel electrophoresis (SDS-PAGE)

SDS-PAGE was performed with an OmniPAGE VS10 vertical electrophoresis system (Wolf Laboratories, York, UK).

Prior to the preparation of an SDS-PAGE gel, two large rectangle and two notched glass plates were cleaned and dried. Proper assembly of the glass plates was checked using 0.1% SDS solution or pure ethanol to avoid any leakage.

The SDS-PAGE gel was then prepared according to the recipe (Table 2.7). The concentration of the gel was chosen subject to the predicted molecule weight of a target protein. For example, 8% gels were used for separation of proteins > 100kDa whilst a 10% gel was appropriate for a protein less 100kDa. Fifteen millilitres of resolving gels were required to make two pieces of gels and the TEMED (Sigma-Aldrich, Poole, Dorset, UK) was only added just before pouring into the cassette.

The well-mixed resolving gel solution was carefully added into the space between the plates until 1cm below the edge of notch. 0.1% SDS solution was used to cover the resolving gel to warrant a smooth top edge.

The SDS solution could be removed followed by a preparation of stacking gel (outlined in Table 2.8) after the resolving gel was set (about 30 minutes at room temperature). Then, a Teflon comb was put into the stacking gel prior to the stacking setting.

Table 2.7 Recipe for the Resolving Gels for Tris-glycine SDS-Ploya crylamide Gel Electrophoresis

Solution components		Component volumes (ml) per gel mold volume of							
		5ml	10ml	15ml	20ml	25ml	30ml	40ml	50ml
8%	H_2O	2.3	4.6	6.9	9.3	11.5	13.9	18.5	23.2
	30% acrylamides mix	1.3	2.7	4.0	5.3	6.7	8.0	10.7	13.3
	1.5 M Tris (pH8.8)	1.3	2.5	3.8	5.0	6.3	7.5	10.0	12.5
	10% SDS	0.05	0.1	0.15	0.2	0.25	0.3	0.4	0.5
	10% ammonium persulfate	0.05	0.1	0.15	0.2	0.25	0.3	0.4	0.5
	TEMED	0.003	0.006	0.009	0.012	0.015	0.018	0.024	0.03
10%	H_2O	1.9	4.0	5.9	7.9	9.9	11.9	15.9	19.8
	30% acrylamides mix	1.7	3.3	5.0	6.7	8.3	10.0	13.3	16.7
	1.5 M Tris (pH8.8)	1.3	2.5	3.8	5.0	6.3	7.5	10.0	12.5
	10% SDS	0.05	0.1	0.15	0.2	0.25	0.3	0.4	0.5
	10% ammonium persulfate	0.05	0.1	0.15	0.2	0.25	0.3	0.4	0.5
	TEMED	0.002	0.004	0.006	0.008	0.01	0.012	0.016	0.02

Table 2.8 Solutions for preparing 5% Stacking Gels for Tris-glycine SDS-Polyacrylamide Gel Electrophoresis

Solution components	Component volumes (ml) per gel mold volume of							
	1ml	2ml	3ml	4ml	5ml	6ml	8ml	10ml
H_2O	0.68	1.4	2.1	2.7	3.4	4.1	5.5	6.8
30% acrylamide mix	0.17	0.33	0.5	0.67	0.83	1.0	1.3	1.7
1.5 M Tris (pH8.8)	0.13	0.25	0.38	0.5	0.63	0.75	1.0	1.25
10% SDS	0.01	0.02	0.03	0.04	0.05	0.06	0.08	0.1
10% ammonium persulfate	0.01	0.02	0.03	0.04	0.05	0.06	0.08	0.1
TEMED	0.001	0.002	0.003	0.004	0.005	0.006	0.008	0.01

Once the stacking gels was set, the gel cassette was translocated into the electrophoresis tank, followed by pouring 1x running buffer into the tank, the comb was then gently

pulled out.

Protein molecular weight ladder (Santa Cruz Biotechnology, supplied by Insight Biotechnologies Inc, Surrey, England, UK) and the protein samples were loaded into the wells in the stacking gel orderly. The amount of the ladder and the protein samples were 10 µl and 10-14µl, respectively.

Electrophoresis was performed to separate the proteins, the parameter for the electrophoresis were 100 - 125V, 50mA and 50W, over a duration depending on the molecule weight of a protein and the concentration of the gel.

2.7.4 Western blotting

Electrical blotting

Once the target proteins were successfully separated according to the indication of the ladders, the western blotting process was performed to transfer them into a PVDF membrane. SD10 SemiDry Maxi System blotting unit (SemiDRY, Wolf Laboratories, York, UK) was applied in this procedure. Before the trans-membrane, the filter paper and the PVDF membrane were pre-soaked in 1x transfer buffer (Whatman International Ltd, Maidstone, UK) and methanol for 15 minutes. An order of the assembly for the electrical transferring from the positive electrode to the negative electrode was the filter paper, gel, PVDF membrane and filter paper (Figure 2.1). Every level was checked for close contact to avoid air bubbles becoming trapped inside. A roller was used to disperse any bubbles and the screw of the unit were tightened afterwards.

The parameters for electrode Electroblotting were 15-20V, 300-500mA, 8W for 30-60 minutes (depending on protein molecule weight).

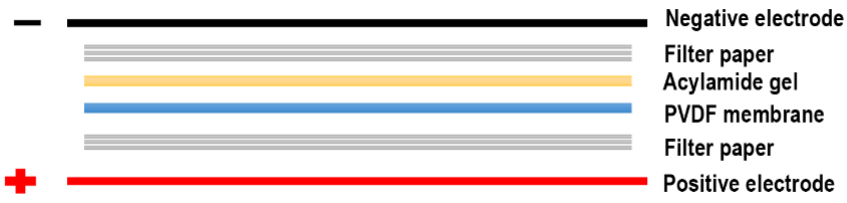

Figure 2.1 Alignment of the items for the trans-membrane.

Protein probing with antibodies

Three solutions were applied in the probing of proteins, the recipe of the solution was

depicted as follows:

Solution A: 10% skimmed milk powder in TBS with 0.1% Tween20

Solution B: 3% skimmed milk powder in TBS with 0.1% Tween 20

Solution C: 0.2% Tween 20 in TBS

Blocking procedure was carried out as the first step of protein probing for one hour using solution A, followed by a 10-minute wash in 5ml of solution B.

The membrane was then incubated with primary antibody, diluted in solution B, overnight at 4℃ followed by three washes using solution B, 15 minutes for the first wash and 5 minutes for the following two washes.

The membrane was then incubated with the second antibody, diluted in solution B, at room temperature for 1 hour. The membrane was washed three times, similar to previous washes after primary antibody.

Solution C was used to wash the membrane for 15 minutes and was repeated once, followed by two washes with TBS at 15 minutes per wash.

Dilution of each antibody used in the study was provided in the method session of corresponding results chapters.

Chemiluminescent detection of protein bands

EZ-ECL solution (Cat. No. 1921593, Biological industries, USA), a sensitive chemiluminescent substrate, was used to visualise the protein bands probed by the antibodies. In brief, 1ml of EZ-ECL solution A and 1ml of EZ-ECL solution B were mixture immediately before a 15-minute incubation with the membrane.

Protein bands were detected and documented using an imager (UVprochemi, UVITech Inc., Cambridge, UK). Image J software was used for a semi-quantification of the bands when required.

2.8 Immunohistochemical staining and immunocytochemical staining

2.8.1 Immunocytochemical staining

Pre-treatment of the cover slips

The cover slips were soaked in 75% ethanol for 30 minutes and subsequently in 100%

ethanol for dehydration. The cover slips were transferred into the six-well-plate, followed by a further sterilisation in the UV chamber for 15 minutes. Following this the slips were soaked in PBS for 10 minutes and treated with attachment factor (1ml attachment factor was added into each well) for 30 minutes. Cells were harvested with trypsin and seeded on the plate in 2ml medium per well and allowed to reach an appropriate confluence.

Fixation

The medium was aspirated and cells gently washed with PBS twice to remove the proteins in the culture medium. Following this, 1ml of 4% formalin was added into each well followed by a 10-minute incubation at room temperature.

Permeabilization

The formalin was removed and cells washed with PBS twice. 1ml of permeabilization buffer mixture (0.1% Triton in TBS buffer) was added into each well followed by an incubation at room temperature for 2-5 minutes.

Staining

The permeabilization buffer was aspirated and the cells washed twice with PBS (2ml per well). Following this horse serum was added for 20 minutes. (1 drop horse serum into 5ml PBS) to block before washing 4 times with PBS.

Next the cells were incubated with diluted primary antibody overnight at 4℃.

Subsequently, the slides were washed with PBS 4 times before incubating the slides with a secondary antibody for 30 minutes at room temperature (during this time the ABC complex (PK-6200, Vectastain Universal Elite ABX Kit, Vector laboratories, UK) was prepared at this time). Following incubation, the slides were washed with PBS for 4 times Before incubating with ABC complex for 30 minutes at room temperature and again washing with PBS for 4 times. Next the slides were incubated with DAB chromogen for 5 minutes in a dark area, washed with tap water for 2 minutes and counter stained with Mayer's HTX for 1 minute (1ml per well) before a final wash with tap water for 5 minutes.

Preparation of ABC complex and DAB Chromogen

ABC complex

8 drops of reagent A were added to 20ml of PBS, then 8 drops of Reagent B was added into and mixed immediately. The mixture was allowed to stand at room temperature for 30 minutes before use.

DAB Chromogen:

0.5ml DAB stock with 4.5 ml PBS were mixed, and 6ul H_2O_2 solution was added into the mixture.

2.8.2 Immunohistochemical staining

Labelling of the TMA slide with the information of antibody

The proper concentration of antibody as well as the reagent for antigen retrieval (for the antibody BMP8A (ab 60290, citrate is recommended according to the protocol) were labelled on the slides with pencil. Then the slide was placed in the rack.

De-waxing and re-hydration.

The slides were placed in an oven (less than 55 ºC for half an hour) and cooled on the desk to the room temperature. The slides were then treated for 5 minutes in each of the following solutions in order: 100% Xylene, 100% Xylene, 50% Xylene/50% Ethanol, 100% Ethanol, 100% Ethanol, 90% Ethanol, 70% Ethanol,50% Ethanol, Distilled Water and PBS buffer.

An antigen retrieving buffer (Citrate is suggested for BMP8A antibody (ab60290)) was made by adding 20ml reagent to 2000ml distilled water. The slide was soaked with the antigen retrieval buffer in a microwave oven for 20 minutes. The slide rack was shaken in the middle of the process to disperse bubbles produced.

The slide was the washed under tap water gently to cool down them before the slide was incubated with blocking buffer (10% horse serum in washing buffer) for 2 hours. Following this the slide was probed with the primary antibody (1:1000) in blocking buffer at 4 ℃ overnight. Prior to incubation with the biotinylated second antibody for half an hour, the slide was washed with washing buffer twice. The slide was then incubated with the premade ABC solution at room temperature for 30 minutes following the instructions previously described. The slide was then washed in the washing buffer for 3-5 minutes. The staining colour was developed by an incubation of the slide with DAB solution in the dark for 10 minutes followed by sufficient washing in running water.

Counterstaining of nuclei with Gill's Haematoxylin was achieved within 2 minutes, this process was monitored under the microscope, followed by a wash with tap water for 5 minutes.

The slide was then dehydrated in each of the following reagents for 5 minutes: 50% Ethanol, 70% Ethanol, 90% Ethanol, 100% Ethanol, 100% Ethanol, 50% Xylene/50% Ethanol, 100% Xylene and 100% Xylene.

The slide was mounted with DPX and a cover slip and air dried before photographing.

2.9 Tumour cell functional assays

2.9.1 Proliferation

Cells were harvested using trypsin solution and counted. Cells were seeded on 96-well plates with 2000-3000 cells per well in 200µl medium. The number of cells per well may vary for different cell lines subject to their proliferation speed and duration of the experiment. The cells were incubated at 37℃ with 5% CO_2 for 1, 3 and 5 days.

Medium was aspirated from the wells and 100µl of 4% Formalin was added into every well for 10 minutes to fix the cells inside. This was followed by staining with crystal violet for 10 minutes and gentle washing of the plate with tap water to remove the superfluous crystal violet. The plate was left to dry at room temperature for 24 hours. After adding 100µl of 10% acetic acid into the wells, the absorbance was investigated under the plate reading spectrophotometer (BIO-TEK, Elx800, UK) at the wavelength of 595nm.

The cell proliferation speed was calculated by the equation below:

Growth rate = (absorbance of the third day or the fifth day - absorbance of the first day)/absorbance of the first day ×100.

Each cell line was repeated for six wells in this experiment.

2.9.2 Adhesion assay

Matrigel (Corning Incorporated, Flintshire, UK), man-made basement membrane was applied to assess the adhesion ability of tumour cells using a modified procedure as previously reported (Jiang et al., 1995).

Precoat the Plate

Matrigel was defrosted on ice to avoid gel setting at room temperature. Serum-free medium was applied to dilute the gel to the concentration of 5µg per 100µl. One hundred microliters of Matrigel was added into the wells of the 96-well-plate, prior to transfer of the plate into the heater at 60℃ for 2 hours (this temperature promote setting of the Matrigel as well as the sterilization). Once the gel was set, sterilized distilled water was add into the well to rehydrate the gel for approximately 1 hour. Water inside the wells was aspirated before seeding the cells.

Seeding the cells

Cells were harvested from the flask with trypsin, quantified and used to prepare a suitable density (section 2.5.3 and 2.5.4). Cell suspension (200µl containing 30000 cells) was transferred into the wells and incubated for 40 minutes at 37℃ with 5% CO_2. Following incubation, the wells were washed gently with PBS to remove non-adherent cells. Then adherent cells were fixed in 4% Formalin for 10 minutes and stained with 0.5% crystal violet for 15 minutes subsequently. The plate was washed gently in tap water to remove the superfluous crystal violet. The plate was left to dry at room temperature for 24 hours. After adding 100µl of 10% acetic acid into each well, the absorbance was investigated under the plate reading spectrophotometer (BIO-TEK, Elx800, UK) at the wavelength of 595nm.

Six replicates were included for each cell line in each experiment.

2.9.3 *In vitro* migration assays

Cellular migration was assessed using one of two methods as described below according to the adherence and performance of the cell lines used in the study.

2.9.3.1 Cytodex-2 bead motility assay

After the cell counting procedure, cells (1×10^6) in 10ml of growth medium and 100µl of cytodex-2 beads (20mg/ml) were incubated at 37ºC and 5% CO_2 overnight to allow cells to adhere to the beads. The beads were then washed by the medium (5ml for two times) to remove non-adherent cells and resuspended in 1ml of growth medium. The mixture (well mixed cells, beads and medium) was aliquoted to a 96 well plate (100µl

each well) and incubated for 4 to 8 hours (depending on the cells) at 37ºC and 5% CO_2. After incubation, the medium was removed, and the wells were washed with 150µl PBS to remove remaining beads or nonadherent cells. Cells in the plate were fixed in 4% formaldehyde (100µl) for 10 minutes and then stained with 0.5% crystal violet for 10 minutes. The plate was washed using tap water gently to remove the extra crystal violet and the plates left to dry for 24 hours at room temperature. After adding 100µl of 10% acetic acid into the wells, the absorbance was investigated under the plate reading spectrophotometer (BIO-TEK, Elx800, UK) at the wavelength of 595nm.

2.9.3.2 Wounding assay

Cells were seeded on a 24-well-plate overnight to form a confluent monolayer before the scratch assay was performed. Following changing the medium, a 100µl pipette tip was applied to scrape the cell layer to create a wound with clear and straight border. Fresh medium was changed again. The wound was observed under the EVOS (auto imaging system, Thermo Fisher Scientific, Waltham, MA USA) at the indicated times. Image J software was applied to determine the migrated distance.

2.9.4 Invasion assay

Invasion assay applied in this study were modified from methods reported by Parish et al 1992 (Parish et al., 1992).

Transwell inserts (Falcon, pore size 8µm, 24 well format, Greiner Bio-One, Germany) were placed in the 24-well-plate and precoated with 50µg Matrigel in 100µl of serum free medium. The Matrigel coat was air dried at 60ºC followed by a rehydration with 100µl of sterile water for 1 hour before adding cells for the invasion assay. 600µl medium was added to each well containing a transwell insert and also spare wells without an insert to be used as a control. Twenty to thirty thousand of cells in 200µl medium were seeded in the precoated transwell insert and also spares well as a control. Following a 72-hour incubation at 37℃ with 5% CO_2, the inserts were taken out from the plate and non-invaded cells and the Matrigel were gently removed with a cotton swab. Invaded cells on the underside of the inserts were fixed with 4% Formalin for 10 minutes and stained with 0.5% crystal violet for 15 minutes subsequently. The stained cells were washed gently under tap water and left to dry at room temperature for 24 hours. The invaded cells were observed and counted under the microscope. Random 5 fields were acquired and counted. The tests were conducted in triplicates for each cell

line.

2.10 Overexpression of BMP8A using lentiviral vector

Lentiviral expression vector carrying human BMP8A coding sequence and a control vector were purchased from the Vectorbuilder (www.vectorbuilder.com) (Figure 2.2).

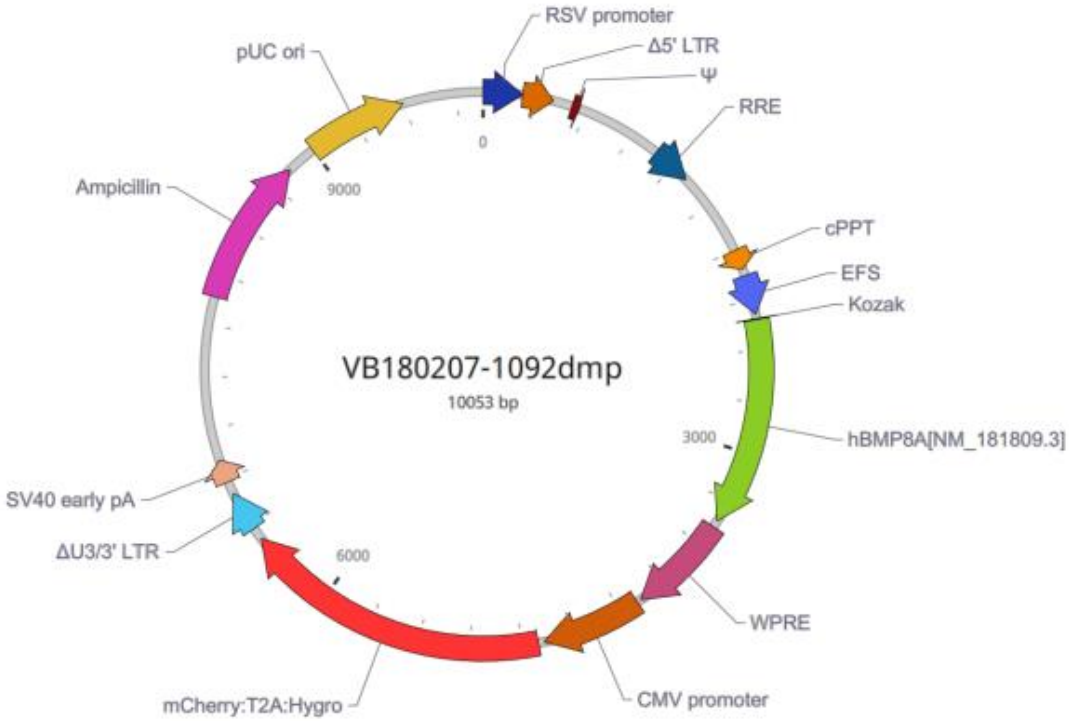

Figure 2.2 Vector map of the lentivirus gene expression vector. As shown in the figure, EFS (232 bp) was designed as the promoter in position 1959-2190, Ampicillin was designed as the drug resistance gene for the *E.coli* selection, hBMP8A (NM_181809.3) was inserted in position 2221-3429 as the gene of interest, mCherry:T2A:Hygro was installed in the vector to allow cells to be visualized by red fluorescence and resistant to hygromycin B. Empty plasmid was installed in the place of hBMP8A to be the control vector. Details of the vector are provided in supplementary file 1.

2.10.1 Plasmid amplification and purification

E. coli cells carrying the lentiviral vectors were grown in an autoclaved flask containing 200ml of LB medium with 100µg/ml ampicillin. After covered by a piece of sterilised foil, the cells were cultured with continuous rotation at a speed of 200 rpm for overnight at 37℃.

Amplified *E. coli* cells were pelleted by a centrifugation at 5000rpm for 15minutes at 4℃, followed by subjection to plasmid extraction using Promega PureYield ™ Plasmid

Midiprep System (Promega, UK). In brief, the cell pellet was resuspended with 6ml of resuspension solution. Cell lysis solution (6ml) was added into the collection tube, then the tube was inverted 5-6 times to mix the suspension inside. The tubes were left at the room temperature for 3 minutes.

Ice cold Neutralisation solution (10ml) was added into the tubes and mixed completely by inverting the tubes 5-10 times followed by a centrifugation at 13,000 rpm for 15 minutes. The supernatant was then transferred to a column stack, which was equipped with a PureYield ^{TM} binding column (the DNA-binding membrane) attached with a blue column to be connected with a vacuum pump. Endotoxin Removal Wash solution (5ml) containing ethanol was used to wash the binding column to clear the endotoxin, followed by a wash with 20ml of column washing solution to remove the excessive ethanol. A microcentrifuge tube (1.5ml) was connected the Eluaotor^{TM} Vacuum Elution Device for a collection of the eluted plasmids in 1ml of Nuclease-Free water or elution buffer provided in the kit. The extracted plasmid vectors were subsequently quantified using the Implen Nanophotometer (Munchen, Germany).

2.10.2 Preparation of lentiviral particles

Prior to the packaging of the lentivirus, HEK-293T cells were prepared. HEK-293T cells were seeded in culture dishes (r= 5cm) with 5ml DMEM and incubated at 37℃ with 5% CO_2 to reach 70-80% confluence. Before transfection, HEK-293T cells were treated with the serum-free medium (OPTI-MEM) for at least one hour, in the meantime, the transfection reagent (Santa Cruz Biotechnology) was prepared according to the protocol as follows:

Vector of interest 4µg + PsPAX2 3µg + pMD2G 1µg

The vectors were added into 1 ml OPTI-MEM followed by vertexing.

Thirty-two µl of Polyethyleneimine (PEI) solution at the concentration of 0.1% was added into the medium with vectors subsequently before vertexing again. The transfection solution was left at room temperature for at least 20 minutes before adding into a dish of HEK-293T cells. Normal medium was changed 24 hours after the transfection. Then supernatant containing lentiviral particles in dishes was collected in 1.5ml sterilized centrifuge tubes every 24 hours. After centrifugation to separate HEK-293T cells, the medium was collected in a universal container and stored in the -80℃

freezer for further use. Once the original medium was harvested, another 5ml fresh medium was added carefully along the wall of the dishes to reduce any disturbance to the transfected cells.

2.10.3 Transduction of breast cancer cell lines with lentiviral particles

Breast cancer cells were seeded in standard growth medium without antibiotics in a 24-well-plate. To ensure good efficiency of the transduction, cells were checked for viability before use. When the confluence of the cells reached 70-80%, cells were washed with PBS twice, and fresh medium (600µl) was changed in each well. After adding 8µg/ml polybrene into the wells, lentiviral particles of 400µl were added into the well drop by drop, followed by gentle shaking. The plate was placed in the incubator at 37℃ with 5% CO_2 for 24 hours.

2.10.4 Screening the stable expression cell line

It is essential to screen out the cell line with stable expression of target gene after transduction. A cherry fluorescent tag was produced by the successfully transduced cells to verify the efficiency. A selection with 200µg/ml hygromycin was conducted for up to two weeks. After verification of the expression of BMP8A, stable cell lines were maintained in a medium with 50µg/ml hygromycin.

2.11 Zymography

Protein sample preparation

Cells with good viability were seeded on the 6-well-plate at the confluence of 80%-90% and cultured for overnight at 37℃ with 5% CO_2. The cells were washed with PBS twice, serum free medium (400 µl per well) was added into the wells to cover the cells on the bottom. Then the cells were incubated at 37℃ with 5% CO_2 for 8 hours. Conditional medium (CM) was collected after the incubation. The non-reducing buffer was added into the supernatant of the CM after a centrifugation at 1300 rpm for 5 mins for a

separation from suspending cells in the CM collected.

Gel preparation

7.5 % SDS-PAGE gel was prepared with gelatin. The formula of the SDS-PAGE was same as the WB. A final concentration of 0.1% gelatin was also added into the gel (Table 2.9).

Table 2.9 Formula for the gel of zymography

Separating gel (7.5 % acrylamide)		Stacking gel	
1.5 M Tris pH 8.8	2 mL	0.5 M Tris pH 6.8	1.25 mL
30% acrylamide	2 mL	30% acrylamide	0.670 mL
H2O	2 mL	H2O	3.075 mL
Gelatin (4 mg/mL)	2 mL	10% SDS	50 µL
10% SDS	80 µL	10 % APS	50 µL
10 % APS	80 µL	TEMED	10 µL
TEMED	10 µL		

Electrophoresis

Once the gelatin SDS-PAGE gels were ready, the prepared protein samples in non-reducing sample buffer were loaded. The amount of the ladder and the protein samples were 15µl and 40µl, respectively. Electrophoresis was performed to separate the proteins, the parameters for the electrophoresis were 120 - 140V, 50mA and 50W. Duration of the electrophoresis was depended on the molecular weight of the target proteins and the concentration of the gel. An ice box was applied during the electrophoresis to avoid protein denaturation caused by the heat generated during electrophoresis.

Gel washing and staining

The gel was soaked in washing buffer twice for 30 minutes for each wash to remove SDS from the gel. After a rinse for 5–10 min in incubation buffer at 37°C with agitation, the gel was incubated in the incubation buffer for 24 hours at 37°C. The gel was then stained in the staining solution for 30 minutes to 1 hour. Destaining was then conducted using the distaining solution until clear bands developed.

Recipes for buffers used for the zymography are outlined below.

Wash buffer:

2.5% Triton X-100

0.02% NaN3

Incubation buffer: pH 8.0

50mM Tris-HCl

5mM CaCl2

0.02% NaN3

Destaining buffer:

100ml Acetic acid

250ml Ethanol

650ml ddH2O

10× gelatin solution

1% gelatin: dissolve 1g gelatin in 100ml distilled water.

5× non-reducing sample buffer

Final concentration for 250 mL

4% SDS 10g

20% glycerol 50 mL of 100%

0.01% bromophenol blue 0.025 g

125 mM Tris-HCl, 4.91g

pH 6.8

2.12 Proteomics

Mass spectrometry is an indispensable method to analyse the protein samples for proteomics research, which can be used to determine the dynamic change of the protein expression, interaction and modification in the samples. Proteomics contains four main procedures including preparation of the cell protein lysis, protein digestion, peptide labelling and sample analysis. After preparation of protein sample using $BT474^{control}$ and $BT474^{BMP8A}$ cells, the last three steps were completed in Bristol University.

- After rinsing the cells twice with cold PBS, cells were harvested using scrapers.
- Cells were pelleted through 1500 rpm centrifugation for 5 mins. RIPA (Radioimmunoprecipitation assay) buffer without SDS and DTT (Dithiothreitol) was applied to lyse the cells (80µl for 10^6 cells) for one hour at 4°C on the roller. Cocktails of protease / phosphatase inhibitors （Cat No. ab201116 and ab201117, respectively） were added in RIPA buffer to reduce the activity of phosphatases.
- Insoluble parts were removed by a centrifugation at 13000 rpm for 15 minutes at 4°C.
- Supernatant was transferred carefully to a new tube.
- After protein quantification (details were depicted in chapter 2.7.2), protein sample concentration was adjusted to a 2µg/µl.
- Protein samples were sent to Bristol University for the following proteomic analysis of total proteins and phosphorylated proteins using TMT approach and mass spectrometry. Three replicates of protein samples extracted from both BT474 BMP8A overexpression and control cell lines were prepared and sent for the proteomic analysis. Alteration of total proteins and phosphorylated proteins including phosphorylation of tyrosine, serine and threonine residues in the BMP8A overexpression BT474 cells were quantitatively analysed in comparison with the control cells through two separate analyses. The first analysis was to compare the total protein levels across the samples whilst the second was to determine phospho-peptide via a phospho-peptide enrichment approach. The processed data was subsequently analysed using Proteome Discoverer v2.1 software for identification of proteins against the Uniport Human database and a 'Common Contaminants' database as a standard procedure. The analyses were conducted by a bioinformatician at the Bristol University.

2.13 Preparation of the bone matrix extract (BME)

Femur bone tissues were collected from patients undergoing total hip replacements at the Trauma and Orthopaedic Department of University Hospital of Wales and Llanddough Hospital.

The collection was performed after receiving written consent from the donors and was implemented with strict adherence to a protocol ethically approved by the Bro Taf Research Ethics Committee (Panel B) for the Bro Taf Health Board, Cardiff, UK. The proximal femur samples collected consisted of the femoral head and part of the femoral neck. Once removed during the hip replacement process, the bone tissues were placed in sterile containers and stored at -20°C until the end of the operation. The samples were then transferred and stored at -80°C until use or further processing. For the extraction of *BME*, the femur samples first needed to be crushed using a Noviomagus bone mill with +/- 0.5 to 1 mm milling drums (Spierings Orthopaedics B.V., Nijmegen, The Netherlands). The resultant fragments were then further crushed by hand (5ml bone fragments: 20 ml of BSS) using a pestle and mortar, while on ice. 2.5ml aliquots of the crushed fragments were then transferred to 15ml centrifuge tubes, to which 10ml of sterile BSS was added. This mixture was placed in a Bioruptor (Diagenode, Seraing, Belgium) and subjected to 5 minutes of uninterrupted pulses, 30 seconds on, 30 seconds off, in an ice-cold water bath. Debris were subsequently removed by centrifuging the samples at 3000 rpm at 4°C for 5 minutes and the supernatants were transferred to fresh tubes. This was repeated five times for each sample. Total protein content of the bone extracts was then quantified using a Bio-Rd DC protein assay kit (Bio-Rad Laboratories, Hemel Hempstead, UK) before being standardised to 2mg/ml. 1ml aliquots were prepared and stored at -80°C.

2.14 Statistical analyses

Normally distributed data was analysed by T-test or one way ANOVA test, whilst non-normally distributed data was assessed using Mann-Whitney tests or Kruskall-Wallis Test. $P<0.05$ was regarded as a statistically significant difference. One way ANOVA, Mann-Whitney test, Spearman correlation test and Kaplan-Meier survival analysis were performed using SPSS 26. 0.

Chapter 3

Aberrant expression of BMP8A/BMP8B in breast cancer and its clinical implication

3.1 Introduction

BMP8A, a member of BMP family that has been poorly studies in the context of cancer, is also named as osteogenic protein 2 (OP2). Mouse OP2 was firstly identified in 1992 (Ozkaynak et al., 1992). Human BMP8A is located at chromosome 1p34.3, whereas BMP8B is located at 1p34.2 being 235kb away from the BMP8A. BMP8A and BMP8B are highly conserved proteins that share 97% homology of their amino acid sequence. The expression of BMP8A is enriched in thyroid (57.449 ± 40.258 RPKM) followed by endometrium (2.571 ± 1.197 RPKM). In an gene expression array assay of hepatocellular carcinoma, BMP8A expression was upregulated in tumour (n=17) compared with adjacent non-tumour liver tissues (Zekri et al., 2008). Aberrant expression of BMP8A in malignant tumours has been associated with methylation status of its promoter. For instance, hypermethylation of BMP8A was detected in rhabdomyosarcomas (Mahoney et al., 2012), whereas hypomethylation of BMP8A was found in oesophageal cancer (Singh et al., 2015). However, in comparison with other members of BMP family, BMP8A and 8B are yet to be investigated for their possible role in breast cancer.

BMP8B signaling protein participates in regulation of thermogenesis and energy expenditure. Silencing of BMP8B diminished thermogenesis contributing to a diet related fatness (Whittle et al., 2012). Further research revealed that BMP8B interacted with NRG4 (Neuregulin-4) to modulate the neuro-vascular network in adipose tissue (Pellegrinelli et al., 2018). It was revealed that BMP8B was associated with regulating the progression of inflammation and cancers. In a study using a tissue microarray of 42 gastric tumour samples paired with adjacent normal controls, BMP8B was presented to be a possible tumour suppressive protein in gastric cancer (Wisnieski et al., 2017). Reduced expression of BMP8B regulated by histone H4 at lysine 16 (H4K16) correlated with poor prognosis in gastric cancer ($P<0.05$) (Wisnieski et al., 2017). In pancreatic cancer, the finding was in clear contrast to that in gastric cancer. Pancreatic cancer tissues had significantly higher expression of BMP8B compared with normal adjacent tissues (Ref?). High expression of BMP8B suppressed the proliferation and promoted the apoptosis of pancreatic cancer while reduced expression of BMP8B accelerated the progression and growth of tumour cells (Cheng et al., 2014). Mutation in BMP8B may promote the metastasis of benign uterine leiomyoma to the pulmonary

metastases. BMP8B has also been shown to interact with BMP4 in inducing the genesis of primordial germ cells in the mouse model (Soritsa et al., 2018).

To date, little is known for the role played by both BMP8A and 8B in breast cancer. The present study aimed to assess the expression of them in breast cancer and their implication in the disease progression of breast cancer.

3.2 Materials and methods

3.2. 1 Cell lines

Wild type cell lines cover all the subtypes, including luminal A (MCF-7 and ZR-751), luminal B (BT474 and MDA-MB-361), Her2 (+) (SKBR3) and triple negative breast cancer (MDA-MB-231, BT20, BT549, MDA-MB-436 and MDA-MB-468) were purchased from the ATCC (American type culture collection, Boulevard Manassas, USA). MCF-7, SKBR3, MDA-MB-231, BT20, BT549, MDA-MB-436, MDA-MB-468 were cultured in DMEM medium (Dulbecco's Modified Eagle Medium) with 10% foetal bovine serum and antibiotic, whilst ZR-751, BT474 and MDA-MB-361 were cultured in RPMI (Sigma-Aldrich, Poole, Dorset, UK) medium with 10% FBS and antibiotics.

3.2.2 RNA isolation, cDNA synthesis and reverse transcript polymerase chain reaction (PCR).

Tri reagent kit (Sigma-Aldrich, Inc., Poole, Dorset, England, UK) was applied to isolate the RNA. Followed by reverse transcription procedure, RNA was translated into the complement DNA using the iScript^{TM} cDNA Synthesis Kit (Bio-Rad Laboratories, California, USA). Conventional PCR reaction was performed according to the protocol in chapter 2 (section 2.7.5). GAPDH was used as the house-keeping gene, Primer sequences for GAPDH, BMP8A and BMP8B were listed in Table 2.2.

3.2.3 Quantitative analysis of BMP8 in breast cancer using real time polymerase chain reaction (PCR)

Total RNA was extracted from the cell lines, followed by the synthesis of the cDNA. Complementary DNA (cDNA) was amplified and detected by QPCR using Amplifluor Uniprimer Universal system (Intergen Company, New York, USA), details could be seen in Chapter 2 (Section 2.7.8). Primer applied in qPCR was listed in Table 2.2. Every sample was repeated for three groups.

3.2.4 Breast cancer databases

RNA sequencing data and quantitative data of proteins for a cohort of breast cancer from the TCGA which comprises 1098 primary tumour and 112 adjacent non-tumour mammary tissues are employed in the present study.

E-MTAB-6703 is a meta-dataset of breast cancer (n=2302) comprising 214 tumour-free mammary tissues and 2088 primary breast carcinomas derived from 20 independent gene expression array datasets.

3.2.5 Tissue collection and quantitative analysis of BMP8 using real time PCR

The levels of gene transcripts of BMP8 were determined in a local cohort of breast cancer (n=144) which had been extensively investigated at the host lab (Bro Taf Health Authority 01/4303 and 01/4046). Breast cancer tissues(n=112) and normal adjacent tissues (n=32) were collected immediately after the resection and stored at -80℃ until required. The clinical follow-up initialled after surgery. Total RNA was extracted from the frozen tissue, followed by the reverse transcription to synthesis the complementary DNA. QPCR was performed to measure the expression of BMP8. Primers used in the research are listed in table 3.1. The clinical information including histological types, histological grade and the clinical implications such as tumour stage, lymph node involvement, distant metastasis and the prognosis were evaluated.

3.2.6 Analysis of protein-protein interaction using STRING.

STRING dataset (https://string-db.org/), an online platform for summarizing and predicting protein-protein interactions. This is employed to identify protein candidates that interacts with BMP8A and BMP8B.

3.2.7 Immunohistochemical staining (IHC) of BMP8 in breast cancer tissue microarray (TMA)

The IHC staining of BMP8A was performed using the TMA (BC 081120f, Biomax, US, details could be seen in supplementary file 1). Vectastain Elite ABC kit (Vector labs, California, US) for HRP was applied in the staining. Primary antibody used in current research was anti-BMP8A/OP-2 antibody (ab60290, abcam), a rabbit polyclonal antibody against human BMP8A/OP-2 (aa 250-350). Low expression of BMP8A in brain tissue was used as the negative control, whilst MDA-MB-231 cells with BMP8A overexpression validated by the Western Blot were applied as the positive control. The IHC staining was evaluated by two pathologists. The semi-quantitative analysis was depended on the staining intensity and the percentage of the cancer cells. The staining intensity of the cells was scored as: 1- weak; 2-medium; 3-strong, whereas

the percentage of the cancer cells on the slices was assessed as follows: 1- less than 1% of cancer cells; 2- 1%-10% of cancer cells; 3- 11%-33% of cancer cells; 4- 34%-66% of tumour cells; 5-67%-100% of tumour cells.

3.2.8 Statistical analysis

Normally distributed data was analysed using t-test for comparison between two groups and one way ANOVA test for statistical analysis of multiple groups, whilst non-normally distributed data was assessed using Mann-Whitney tests or Kruskall-Wallis Test, respectively. Clinical relevance of deregulated BMP8A in breast cancer was assessed using both ANOVA and Kaplan-Meier tests. Kaplan-Meier survival analysis was also performed for the prognosis of BMP8A/8B in breast cancer using an online platform (http://kmplot.com/). Correlation with markers of proliferation and invasion was evaluated using Spearman test. $P<0.05$ was regarded as statistically significant. One way ANOVA, Mann-Whitney test, Spearman correlation test and Kaplan-Meier survival analysis were performed using SPSS 27. 0.

3.3 Results

3.3.1 Aberrant eexpressions of BMP8A and BMP8B in breast cancer.

Expressions of BMP8A and BMP8B were firstly evaluated using the RNA sequencing TCGA-BRCA dataset. Expressions of BMP8A and BMP8B significantly increased in primary tumour lesions comparing with normal adjacent controls. Analysis of BMP8A and BMP8B in E-MDTA-6703 cohort was performed for validation (Figure 3.1). Similar trend was detected in both datasets. Analyse in Cardiff breast cancer dataset was also performed for BMP8 in current study (Table 2), no significant difference was observed between the tumour and normal tissues. BMP8A staining was stronger in breast cancer tissues comparing with the adjacent normal controls (Figure 3.1E). BMP8A protein is mainly distributed in the cytoplasm, few staining can be seen in the cell nuclei, part of BMP8A staining could be observed in carcinoma stroma such as the fibrocytes and the immune cells.

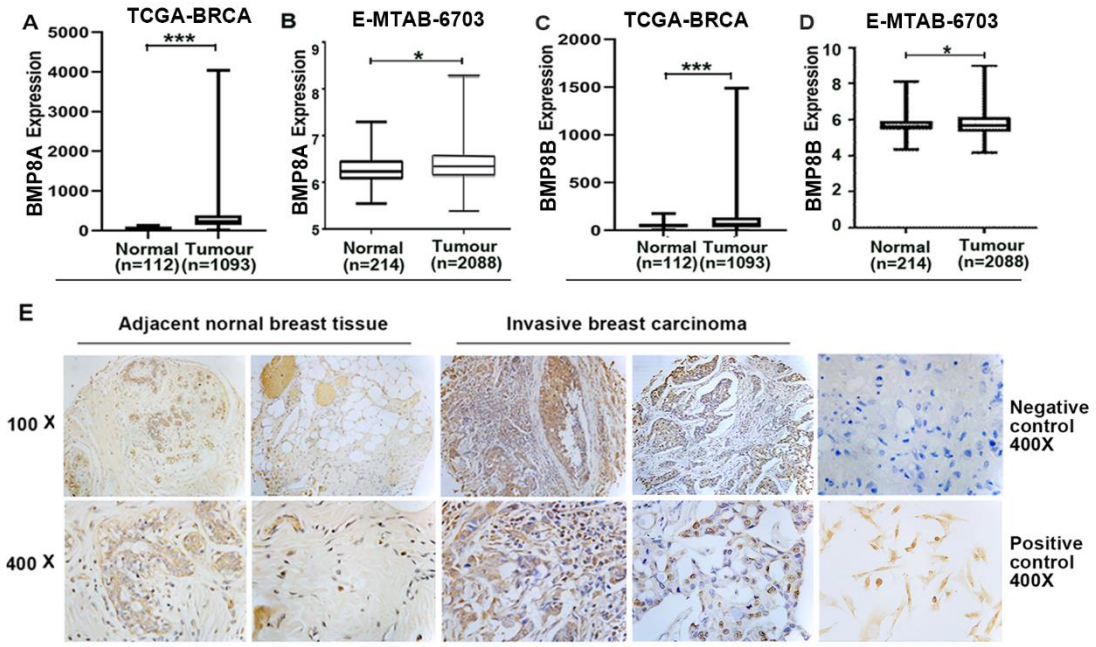

.

Figure 3.1 Aberrant expression of BMP8A and BMP8B in breast cancer. (A) Expression of BMP8A in breast cancer (n=1093) compared with normal tissue (n=112) was assessed at mRNA level in TCGA-BRCA database. (B) Expression of BMP8A in breast cancer (n=2088) compared with the normal tissue (n=214) in the gene-array database (E-MTAB-6703). (C) Expression of BMP8B in breast cancer (n=1093) compared with normal tissue (n=112) was assessed at mRNA level in TCGA-BRCA database. (D) Expression of BMP8A in breast cancer (n=2088) compared with the normal tissue (n=214) in E-MTAB-6703 database (E-MTAB-6703). (E) Immunohistochemical (IHC) staining presented the expression of BMP8A in invasive breast carcinoma compared with the normal adjacent tissue with different magnifications including 100× and 400×. *P＜0.05, **P＜0.01, ***P＜0.001.

3.3.2 BMP8A/8B with the TNM staging of Breast Cancer

Expressions of BMP8A and BMP8B in breast cancer tissues were assessed in TCGA-BRCA dataset. However, when comes to subgrouping by the TNM staging, the samples numbers were rather scarce in some subgroup, especially the tumours of T4 or N3 subgroups from the subtype of HER2 positive tumours. Therefore, tumour subgroups were combined based on what they represented, namely tumours of T1 and T2 stages were grouped together and classified as the early stage, whilst T3 and T4 stage tumours were regarded as local advanced stages. Tumours with lymph node metastases including N1, 2 and 3 were compared with tumours without lymph node metastasis (N0). Increased expression of BMP8A was presented in the early tumour stage (median=239.70), comparing with the advanced tumour stages (median=174.29, $P<0.01$), however, no significant difference was seen in the tumours presented lymph node metastases and distant metastases at the diagnosis of the disease (Figure 3.2).

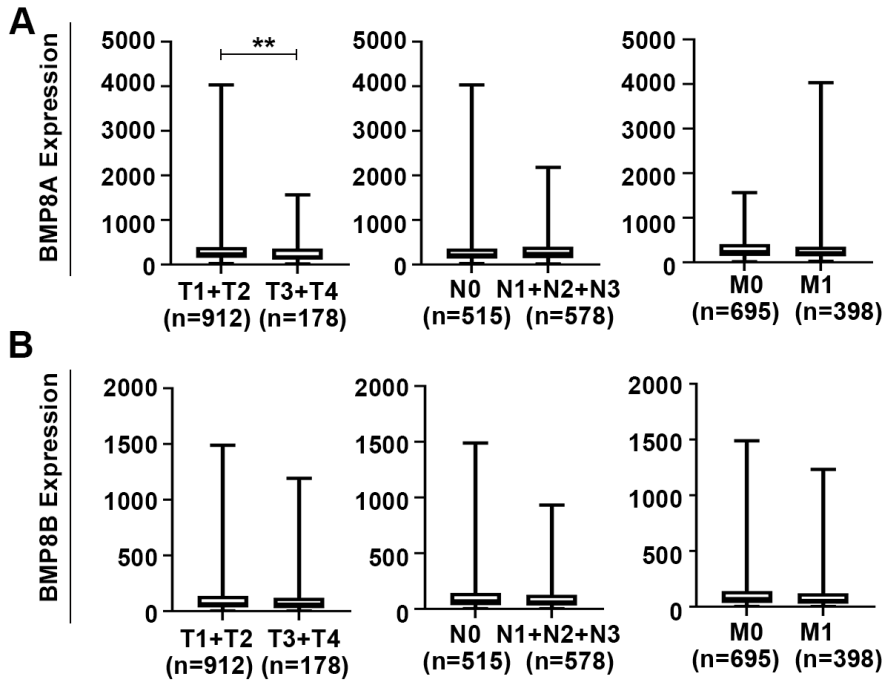

Figure 3.2 Altered expression of BMP8A and BMP8B correlates with the TNM staging of BC. (A)Association between BMP8A mRNA expression and TNM staging of breast cancer in TCGA cohort(n=1093). **P＜0.01. (B) Association between BMP8A mRNA expression and TNM staging of breast cancer in TCGA cohort(n=1093).

3.3.3 BMP8 and clinical outcomes

High levels of expression of BMP8A tends to be associated with the overall survival (OS) of patients with breast cancer, although it does not reach a statistically significant level. High expressions of BMP8A and BMP8B are associated with better relapse free survival (RFS) and post-progression survival (PPS) (Figure 3). It is noteworthy that higher expression of BMP8B is associated with the poorer RFS and distant metastasis free survival (DMFS) (Figure 3.3).

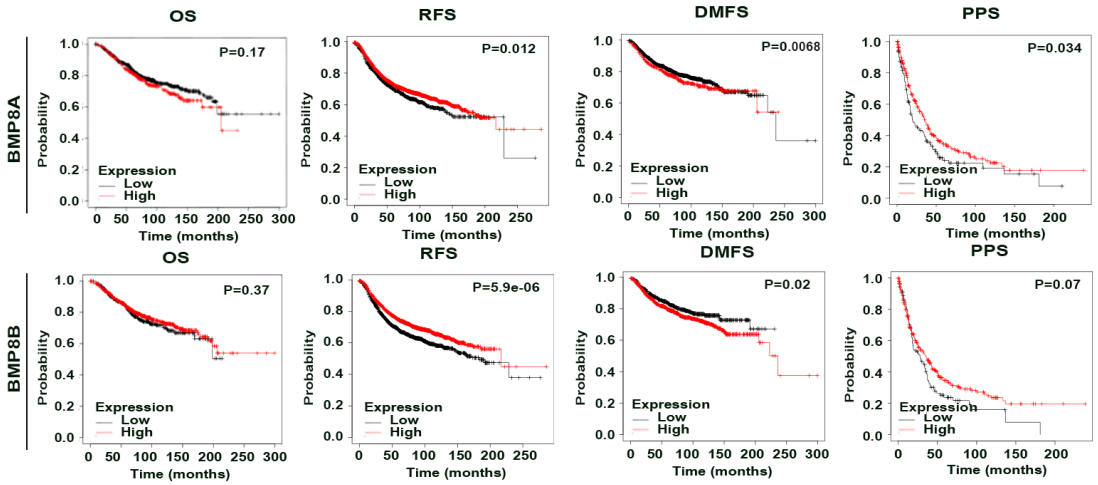

Figure 3.3 Relationship between altered expression of BMP8A/ BMP8B and the prognosis of breast cancer. Kaplan-Meier survival analyses presented the correlation between differential expression of BMP8A/BMP8B and the OS (n=1880), RFS (n=4934), DMFS (n=2767) and PPS (p=458) of breast cancer using the online Kaplan-Meier survival analysis (http://kmplot.com).

3.3.4 Expression of BMP8 and the clinical relevance in breast cancer (Cardiff cohort).

From the quantitative analysis of BMP8 transcripts in the Cardiff cohort of breast cancer (Table 3.1), it was found that expression of BMP8 in poorly differentiated tumours was significantly higher compared with the well-differentiated tumours (P=0.0008). In addition, BMP8 is significantly reduced in ERα (-) tumours (P=0.0027).

Table 3.1 Expression of BMP8 in breast cancer (Cardiff cohort).

Category	Variables	BMP8		
		N	Mean ± SE	P value
Tissue type	Normal	32	12.19±5.30	
	Tumour	112	7.58±1.61	0.6724
Histological types	Duct	90	7.78±1.81	
	Lobule	11	10.36±6.93	0.3921
	Others	5	5.58±3.57	0.5541
Histological Grade	Grade 1	19	0.63±0.447	
	Grade 2	36	7.78±2.52	0.2186
	Grade 3	7	10.12±2.77	0.0008
TNM staging	TNM 1	2	11.8±10.4	
	TNM 2	34	8.75±3.02	0.1445
	TNM 3	7	24.9±16.7	0.0753
	TNM 4	4	4.67±3.90	0.5454
Oestrogen	ERα (-)	67	9.64±2.34	
receptor (ER) status	ERα (+)	33	4.00±2.18	0.0027
	ERβ (-)	82	8.46±2.09	
	ERβ (+)	21	5.16±1.55	0.3679
Nottingham Prognostic Index (NPI)	NPI1	58	7.49±2.42	
	NPI2	34	5.06±2.21	0.4256
	NPI3	15	9.05±3.34	0.2931
Clinical outcome	Disease free	81	6.44±1.87	
	Local recurrence	6	16.14±7.07	0.2121
	Distant metastasis	4	6.23±5.83	0.9586
	Die of breast cancer	16	11.75±5.32	0.36
	Poor prognosis	26	11.92±3.71	0.9363

Note: Normal was adjacent breast tissue.

3.3.5 Differential expression of BMP8 in different subtype BCs

3.3.5.1 Differential expression of BMP8 in different subtypes.

Analyses of the TCGA-BRCA dataset showed that BMP8A was highly expressed in luminal B and Her2 positive tumours in comparison with the other two subtypes, i.e. luminal A and triple negative breast cancer (TNBC). The lowest expression of BMP8A was found in the TNBC tumour group. Expression of BMP8B in luminal B is statistically different from its expression in both luminal A and Her2 (+) tumours whilst the luminal B subtype tumours exhibited the highest expression levels (Fig. 3.4 A). The classification of subtypes of breast cancer was also performed according to the status of ER, PR and Her2. After analysis of frequencies of ER, PR and Her2 in TCGA-BRCA cohort, the cut-off values of these genes were estimated to determine their differential expressions. Expression of BMP8A in the subclasses divided according to the mRNA levels indicates that luminal B subtype is significantly higher than luminal A and TNBC subtypes, whilst expression of BMP8B is significantly higher in luminal B subtype and luminal A subtype than the other two subtypes (Figure 3.4 B). Analysis in E-MTAB-6703 is also applied for the validation (Figure 3.4 C). The overlapping results of the assessment mentioned above are summarized as follows: differential expression of BMP8A was presented in luminal B subtype comparing with luminal A and TNBC subtypes, the median expression was highest in luminal B subtype, whereas the median expression of BMP8B was also the highest in luminal B subtype, BMP8B expression in luminal A presented statistical difference with luminal B and TNBC subclasses.

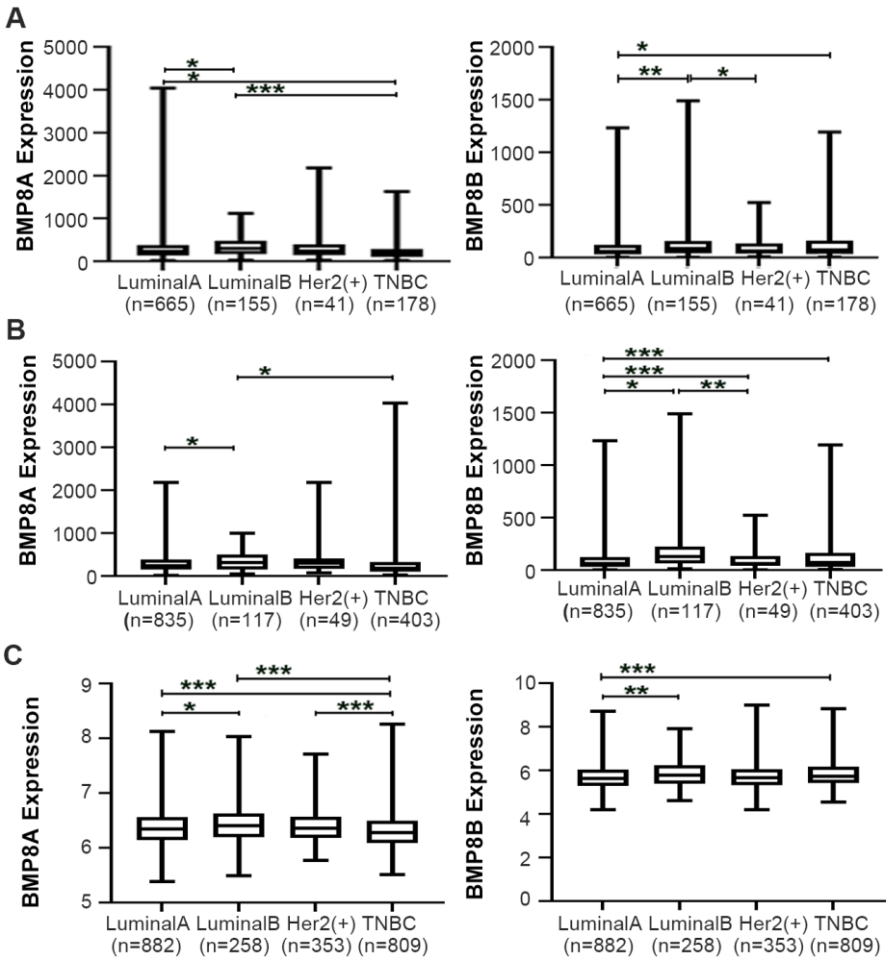

Figure 3.4 Altered expression of BMP8A and BMP8B in different subtypes of breast cancer analysed from the epi-genomic dataset. (A) Differential expression of BMP8A and BMP8B in different subclasses of breast cancer based on the IHC result analysed in TCGA cohort(n=1093). (B) Differential expression of BMP8A and BMP8B in different subclasses of breast cancer based on the mRNA expression levels of ER, PR and Her2 analysed in TCGA cohort(n=1093). (C) Differential expression of BMP8A and BMP8B in different subtypes of breast cancer (classified by the IHC result) analysed in E-MTAB-6703 database (n=2302). *P＜0.05, **P＜0.01, ***P＜0.001.

3.3.5.2 Expression of BMP8A and BMP8B in wild type breast cancer cell lines

Different expressions of BMP8A and BMP8B were observed in all the wild type of cell lines by conventional PCR. Quantitative analysis of the gene transcript by QPCR was also performed to investigate the expressions of BMP8A and BMP8B in all the breast cancer cell lines listed above. QPCR results for the expression of BMP8A and BMP8B were consistent with the β-actin normalised expressions of BMP8A and BMP8B in breast cancer cell lines. High expressions of BMP8A and BMP8B were seen in MCF-7 and ZR 751(luminal A subtype), MDA-MB-361(luminal B subtype) and MDA-MB-436 and MDA-MB-468 cell lines (TNBC subtype), whereas BT474 (luminal B), SKBR3 (Her2 positive), MDA-MB-231, BT20 and BT549 (TNBC) presented low expressions of BMP8A/8B (Figure 3.5).

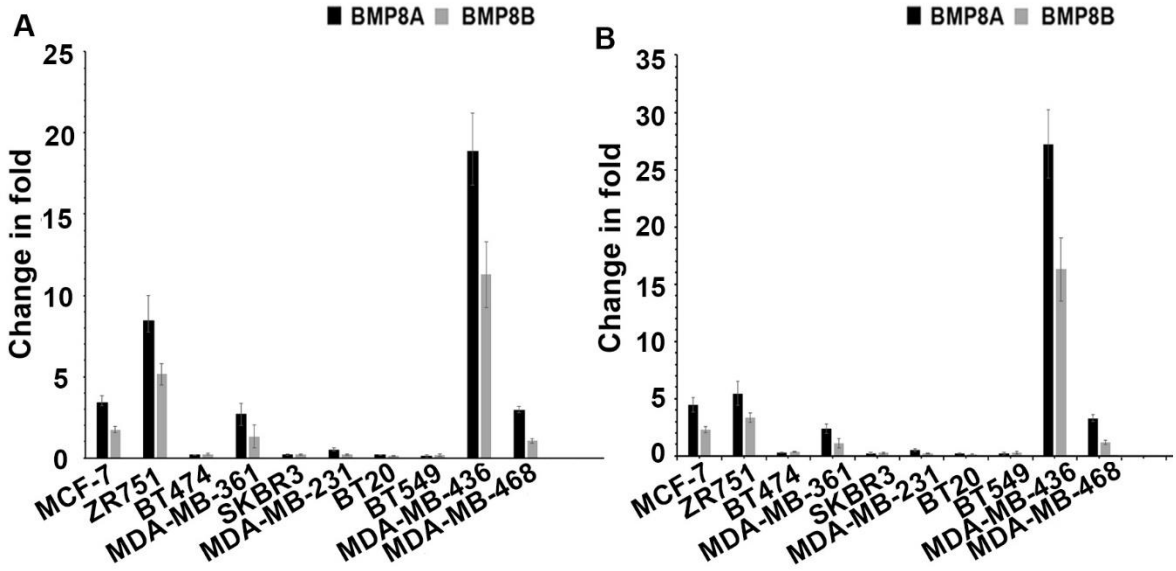

Figure 3.5 Expression of BMP8A and BMP8B in different wild type cell lines of breast cancer. (A) Expression of BMP8A and BMP8B in various wild type cancer cell lines was shown in histogram (QPCR result). (B) Histogram showed β − actin normalised expression of BMP8A and BMP8B in various subtypes of wild breast cancer cell lines (QPCR result). The folds were calculated using ΔCT.

3.3.5.3 Expression of BMP8A in breast cancer tissue microarray (TMA)

Statistically differential expression of BMP8A was presented between the normal tissues and the tumour tissues. Analysis from the current TMA (tissue microarray) showed that protein level of BMP8A was statistically higher in luminal A than Her 2 (+) and TNBC subtypes. BMP8A expressions were increased in luminal A, luminal B and Her 2 (+) subtypes than the normal adjacent tissues.

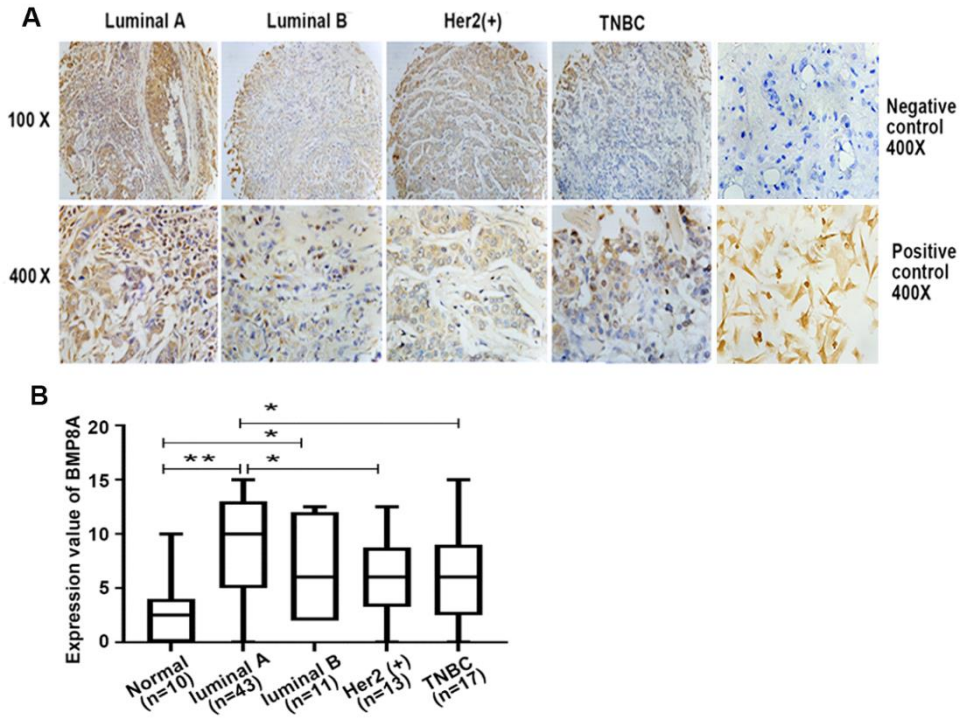

Figure 3.6 Differential expression of BMP8A in breast cancer TMA. (A) Differential expression of BMP8A was assessed using IHC staining. (B) Shown are representative images of IHC staining BMP8A in samples of different subtypes. *P＜0.05, **P＜0.01, ***P＜0.001

3.3.6 Expression of BMP8A/8B and TNM staging in subtypes

Higher expression of BMP8A (from the RNA sequence data) was observed in earlier tumour stages (T1 and T2) compared with the local advanced stages (T3 and T4) in luminal A subtype from the analysis in TCGA dataset in subtypes of breast cancer (classified according to the IHC result of ER, PR and Her2) (Fig. 3.7), however, no other significant difference of either BMP8A or BMP8B was seen within the other TNM stages (Fig. 3.8).

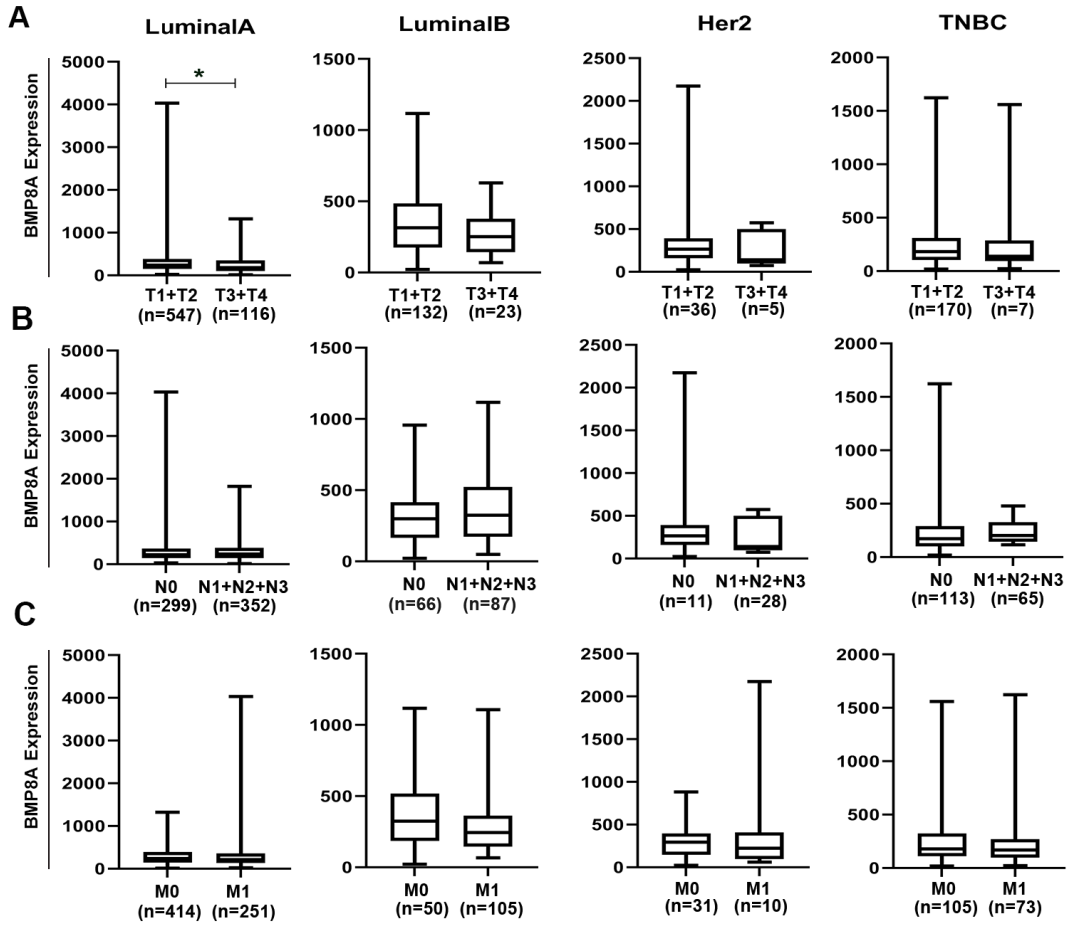

Figure 3.7 Correlation between BMP8A expressions and the TNM staging in different subtypes of breast cancer. (A) Differential expression of BMP8A correlation the tumour staging in different subclasses (classified by IHC result) of breast cancer analysed in TCGA cohort(n=1093). *P＜0.05. (B) Correlation between expression of BMP8A and the lymph node involvement in all the subclasses (classified by IHC result) of breast cancer analysed in TCGA cohort(n=1093). (C)Altered expression of BMP8A associated with distant metastasis in all the subclasses (classified by IHC result) of breast cancer (TCGA n=1093).

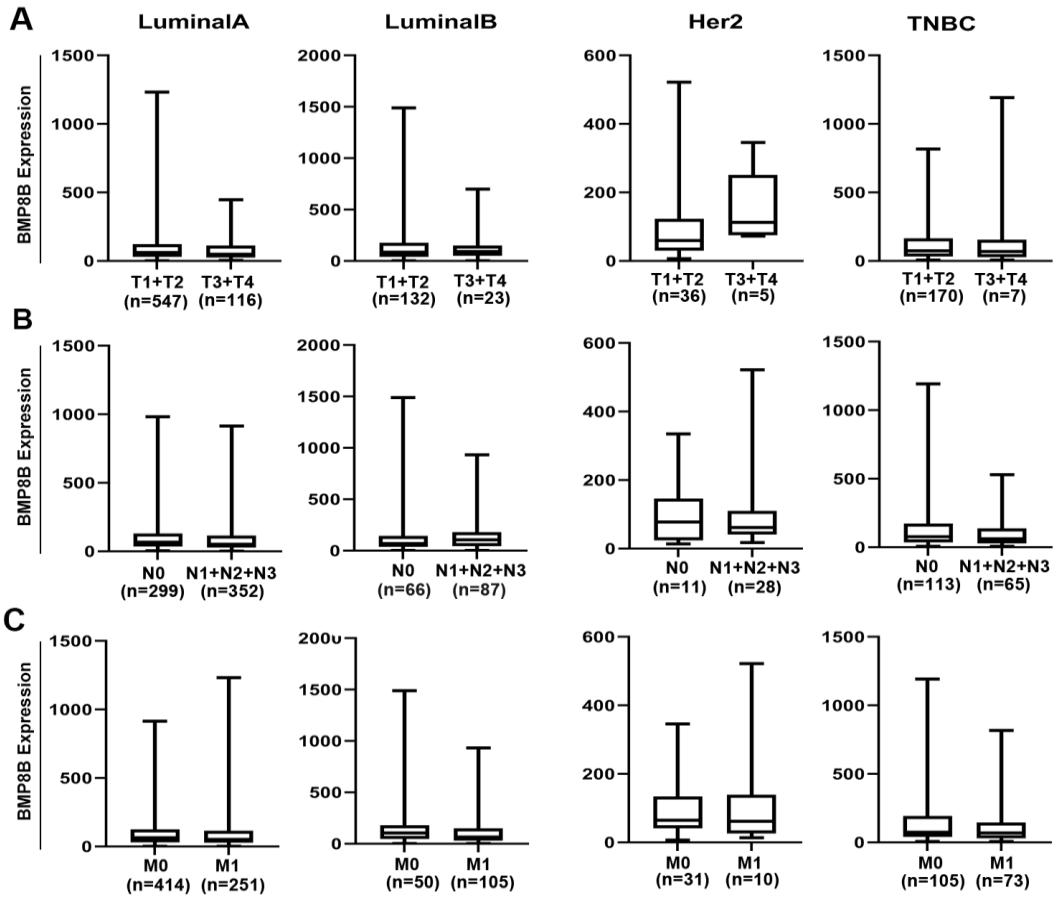

Figure 3.8 Correlation between BMP8B expressions and the TNM staging in different subtypes of breast cancer. (A) Differential expression of BMP8B correlation the tumour staging in different subclasses (classified by IHC result) of breast cancer analysed in TCGA cohort(n=1093). (B) Correlation between expression of BMP8B and the lymph node involvement in all the subclasses (classified by IHC result) of breast cancer analysed in TCGA cohort(n=1093). (C)Altered expression of BMP8B associated with distant metastasis in all the subclasses (classified by IHC result) of breast cancer (TCGA n=1093).

3.3.7 Contrasting relationship with patients' survival in different subtypes of breast cancer

Elevated expression of BMP8A reduced the overall survival (OS) in luminal B subtype ($P<0.01$), whereas in Her2 (+) subtype higher expression of BMP8A was seen with prolonged overall survival. BMP8B did not exhibit an association with OS according to the analyses of different subtypes (Fig. 3.9).

Patients with high levels of BMP8A showed significantly higher DMFS in luminal B ($p=0.0099$) and TNBC ($p=0.048$) subtypes. However, no significant difference was found in luminal A and Her2 (+) subtypes (Fig. 3.9). Elevated expression of BMP8B reduced the DMFS in TNBC group ($P=0.039$), no statistical difference was presented in the other three subtypes (Fig. 3.10).

The elevated expression of BMP8A prolonged the median RFS in overall BC, luminal A, Her2(+) and TNBC subtypes than paired low-expressed cohort, the difference presented more evident in Her2(+) cohort ($P<0.01$). No significant difference was observed in Luminal B subtype (Fig. 3.9). High expression of BMP8B significantly prolonged the RFS in overall, luminal A, luminal B and Her2 (+) groups. High expression of BMP8B in TNBC subtype tended to present a decreasing recurrence rate but did not reach the significant level (Fig. 3.10).

Reduced expression of BMP8A in luminal A BCs is associated with post progression survival (PPS) and overall survival (OS). High BMP8A tended to correlate with poorer post progression survival in the luminal B subtype tumours, however no significant difference was shown. (Fig. 3.9) There is no evident to suggest a relationship between the expression of BMP8B and PPS (Fig. 3.10).

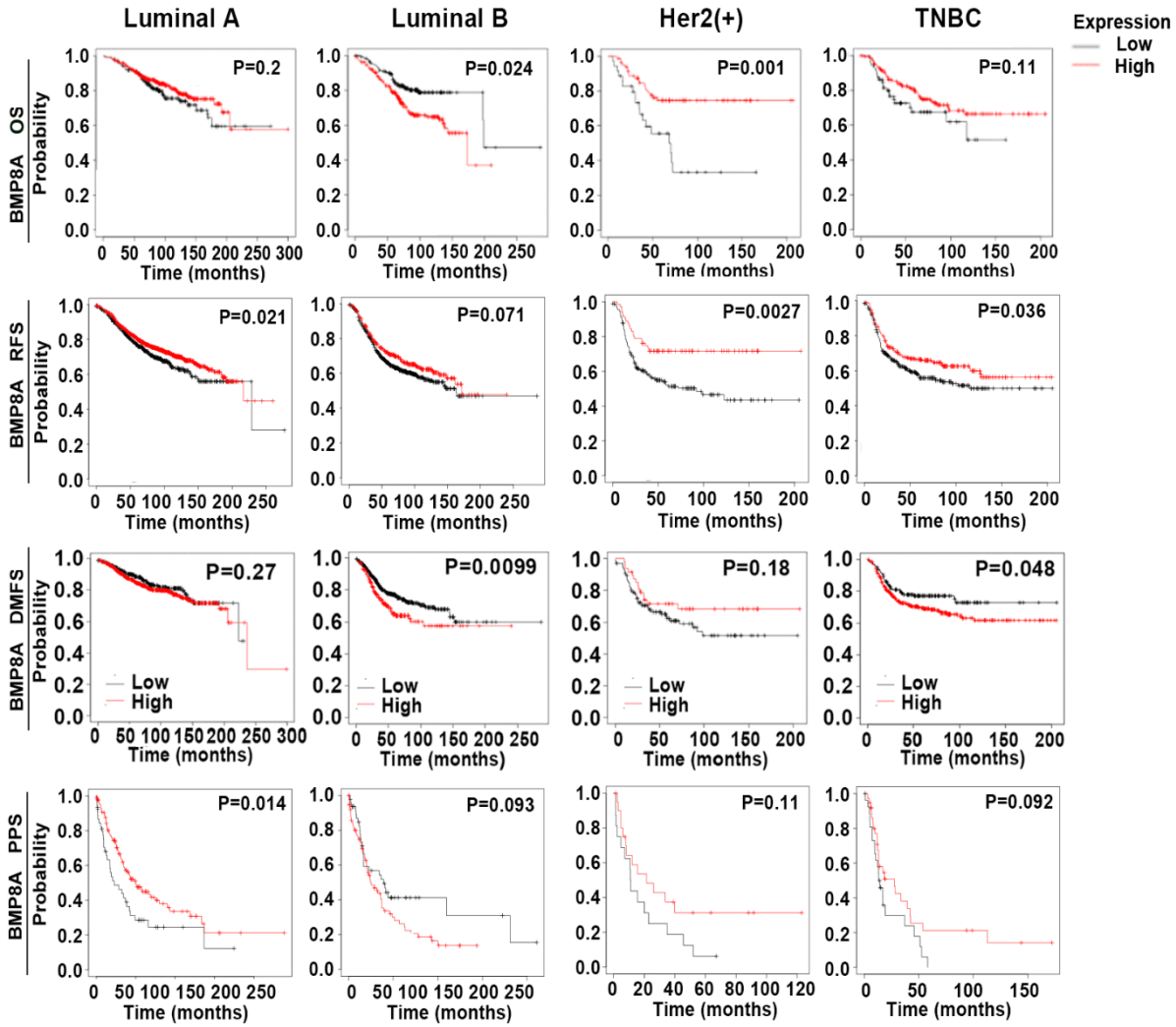

Figure 3.9 Association of altered expression of BMP8Awith the prognosis in different subclasses of breast cancer. Kaplan-Meier survival analyses presented the differential role of BMP8A on the overall survival in different subtypes of breast cancer by the online analysis (http://kmplot.com).

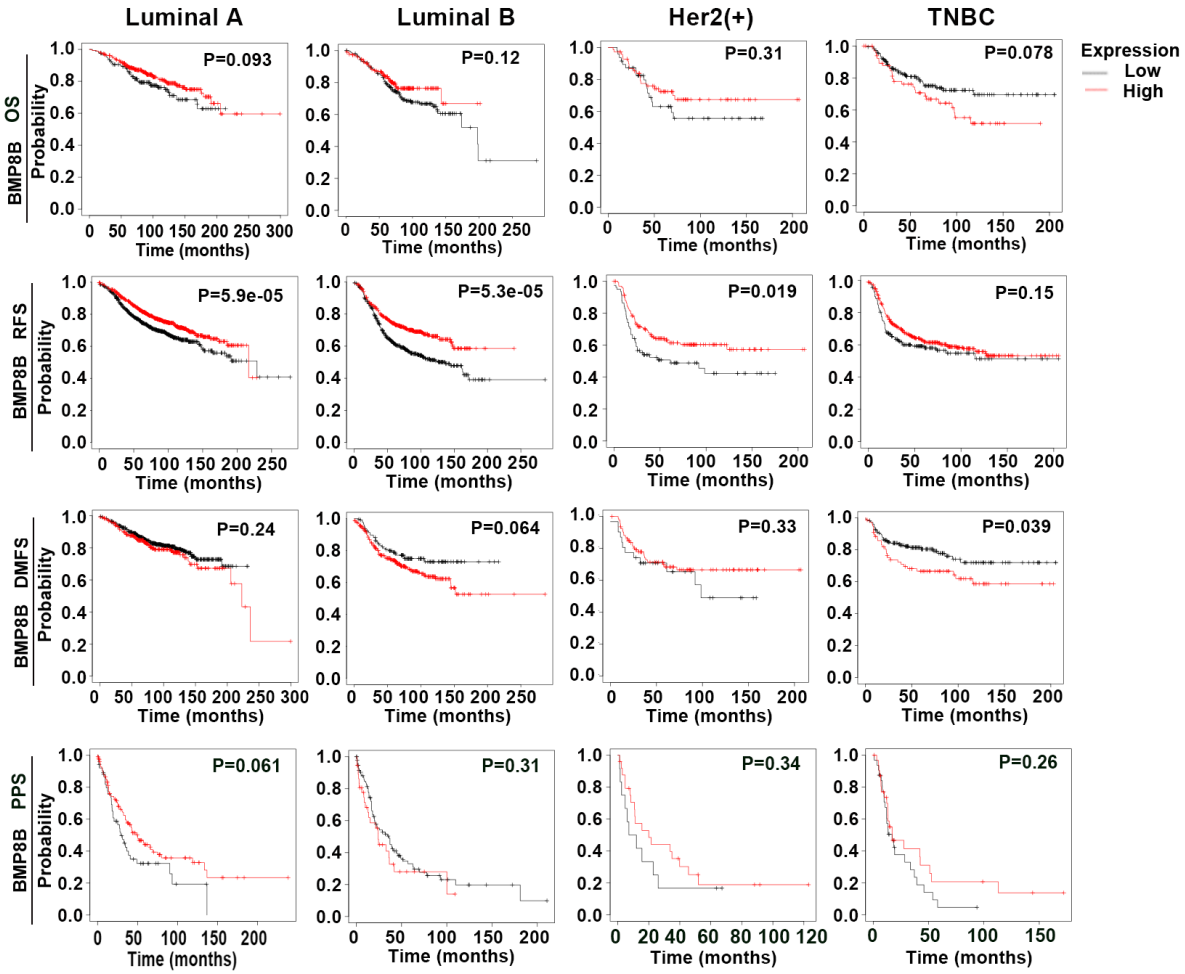

Figure 3.10 Association of altered expression of BMP8Awith the prognosis in different subclasses of breast cancer. Kaplan-Meier survival online analyses presented the association of altered expression of BMP8B on the prognosis of breast cancer in different subtypes (http://kmplot.com).

3.3.8 Correlation of BMP8 with ER, PR and Her2.

Expression of ER, PR and ERBB2 (Her2) in breast cancer.

Due to the wide variance of the expression value of ESR1 (ERα), ESR2 (ERβ), PR and ERBB2 (Her2) in TCGA-BRCA dataset, the log values of their expression were demonstrated in this chapter to aid display and reading. The cohort was then divided into the high and low expression groups according to the cut-off value. The cut-off value was determined according to the morphology and the frequency of the distribution, the cut-off values for ESR1, ESR2, PR and ERBB2 are 2.875, 0.544, 2.333 and 4.672, respectively (Fig. 3.11 A).

Differential expression of BMP8A and BMP8B with altered expression of ESR1, PR and ERBB2.

Analysis in TCGA cohort showed significantly different expression of both BMP8A and BMP8B with altered expression of ERBB2. However, no significant difference of BMP8A or BMP8B expression is seen between the high expression and the low expression group of ESR1 and PR (Fig. 3.11 B).

Correlation of BMP8 with ESR1, ESR2, PGR and ERBB2

From the assessment, BMP8A expression is mildly positively associated with PGR and ERBB2 (the correlation scores are 0.067, $P<0.05$ and 0.092, $P<0.01$, respectively) while negatively correlated ESR2 ($r=-0.115$, $P<0.01$). No statistical correlation is found between BMP8B with ESR1, ESR2, PGR and ERBB2 (Fig. 3.11 C).

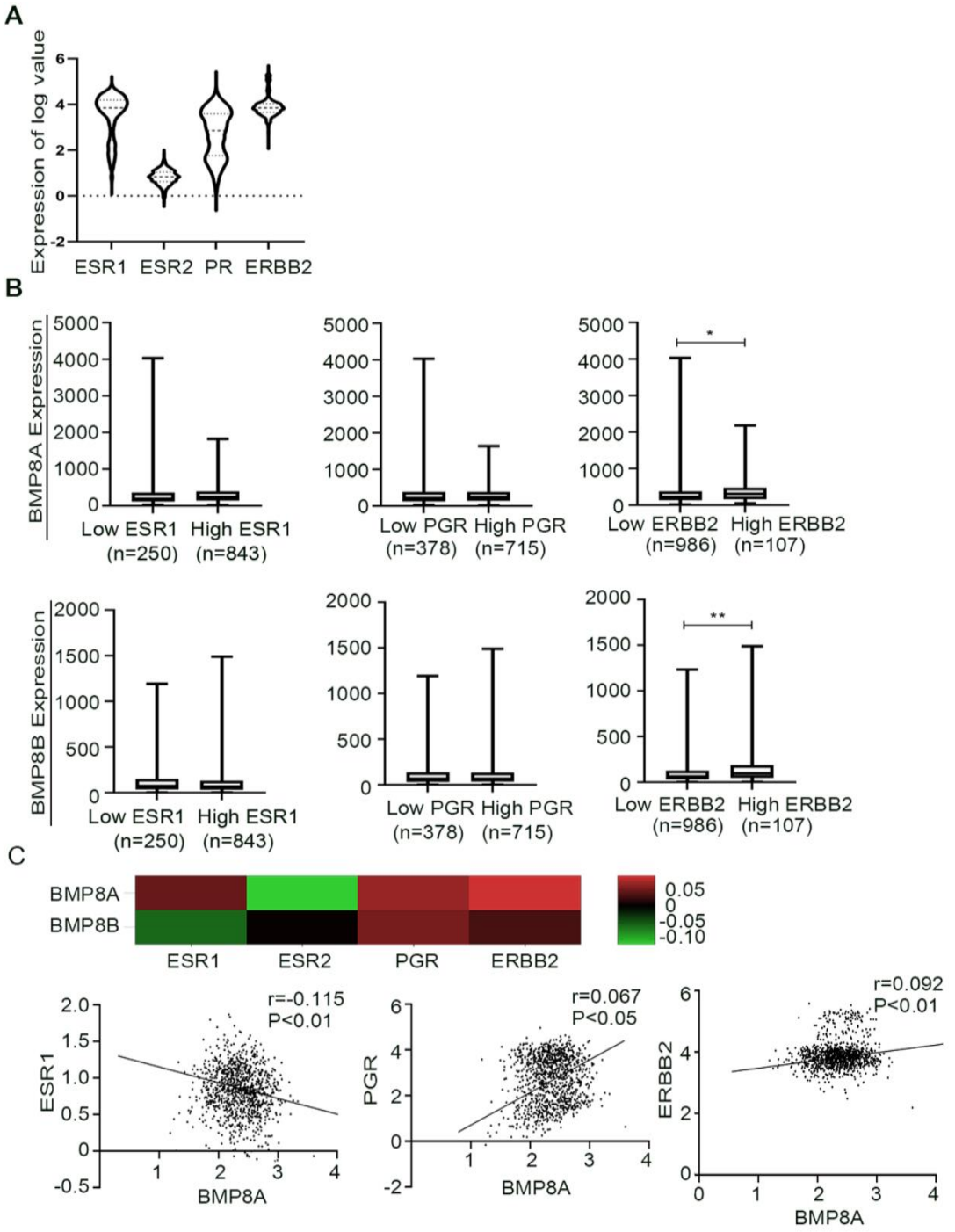

Figure 3.11 Correlation between the mRNA expression of BMP8A/BMP8B and ER/PGR/ERBB2 in breast cancer. (A) Violin plot exhibited the differential expressions of the log value of ESR1, ESR2, PGR and ERBB2 in TCGA-BRCA cohort(n=1093). (B) Altered expression of BMP8A and BMP8B in breast cancer with differential expression of ER, PR and ERBB2. (C) Association of BMP8A/BMP8B with ESR1/ESR2/PGR/ERBB2 was analysed applying spearman tests, the evaluation was shown as the heatmap and the scatter plots. *P＜0.05, **P＜0.01.

3.3.9 Clinical evidence to identify candidate genes (BMPR and antagonist) for diverting signalling of BMP8A in the specific subtypes

STRING dataset is an online analysis platform, correlation with BMP8A can be investigated from known interactions, predicted interactions and others such as co-expression, text mining and protein homology. Overall scores for the BMP8A interacting molecules are (from high to low according to the scores): BMPR1B (0.822), BMPR1A (0.814), BMPR2 (0.814), BMP8B (0.800), NOG (0.740), AMHR2 (0.738), CHRD (0.706), ACVR2A (0.575) and ACVR2B (0.511) (Fig. 3.12).

In order to elucidate the relationship of the BMP8A/BMP8B with the interacting molecules, further evaluation was performed for all BCs and different subtypes. BMP8A expression is positively correlated with BMPR2 ($r=0.283$, $P<0.01$) in overall breast cancer, whilst slightly inversely correlated the expression of BMP1($r=-0.063$, $P<0.05$). BMP1 and BMPR2 are positively correlated with BMP8A in both Luminal A and Luminal B subtypes. ACVR2B is the top molecule positively associated with BMP8B in overall, luminal A and luminal B breast cancer. BMP8A is highly correlated with the antagonist CHRD in Her2 (+) subtype, the correlation coefficient is 0.622, $P<0.01$. AMHR2 is the only interacting molecule associated with BMP8B in Her2 (+) subtype. In TNBC subtype, BMP8A and BMP8B are positively correlated with BMP1 ($r=0.465$, $P<0.01$) and BMPR1B ($r=0.346$, $P<0.01$), respectively. BMP8A and BMP8B expressions are highly associated with the antagonists, the correlation coefficient of BMP8A with CHRD is 0.369 ($P<0.01$) and BMP8B with NOG is 0.265 ($P<0.01$). (Fig. 3.13)

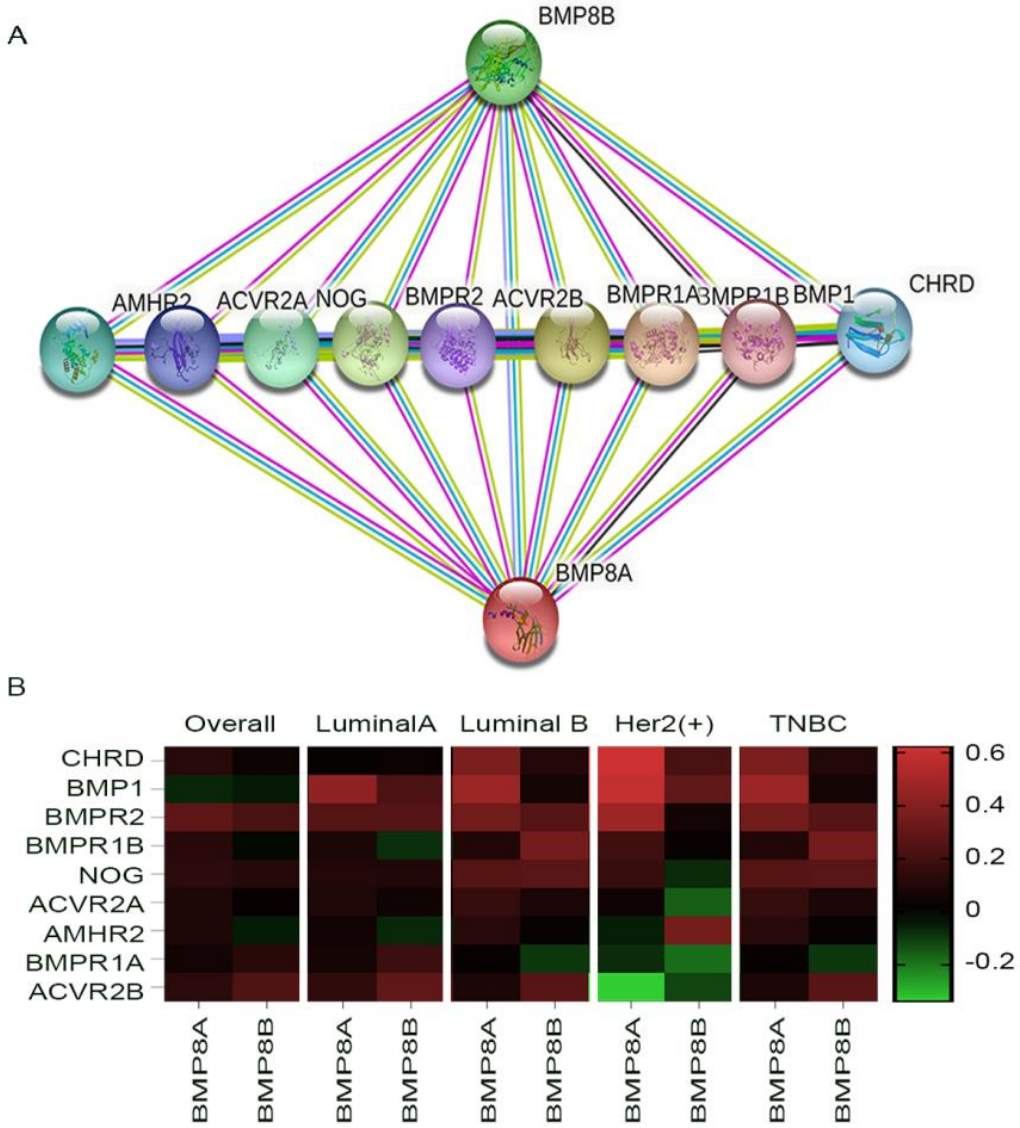

Figure 3.12 Correlation between BMP8A/BMP8B with their interact molecules. (A) Predicted receptors and their correlation with BMP8A were analysed by STRING online database(https://string-db.org/). Known Interactions from curated databases, experimentally determined. Predicted Interactions gene neighborhood gene fusions gene co-occurrence. Others textmining co-expression protein homology. (B) Correlation scores between BMP8 with the interact molecules were analysed using Spearman test and presented with the heatmap.

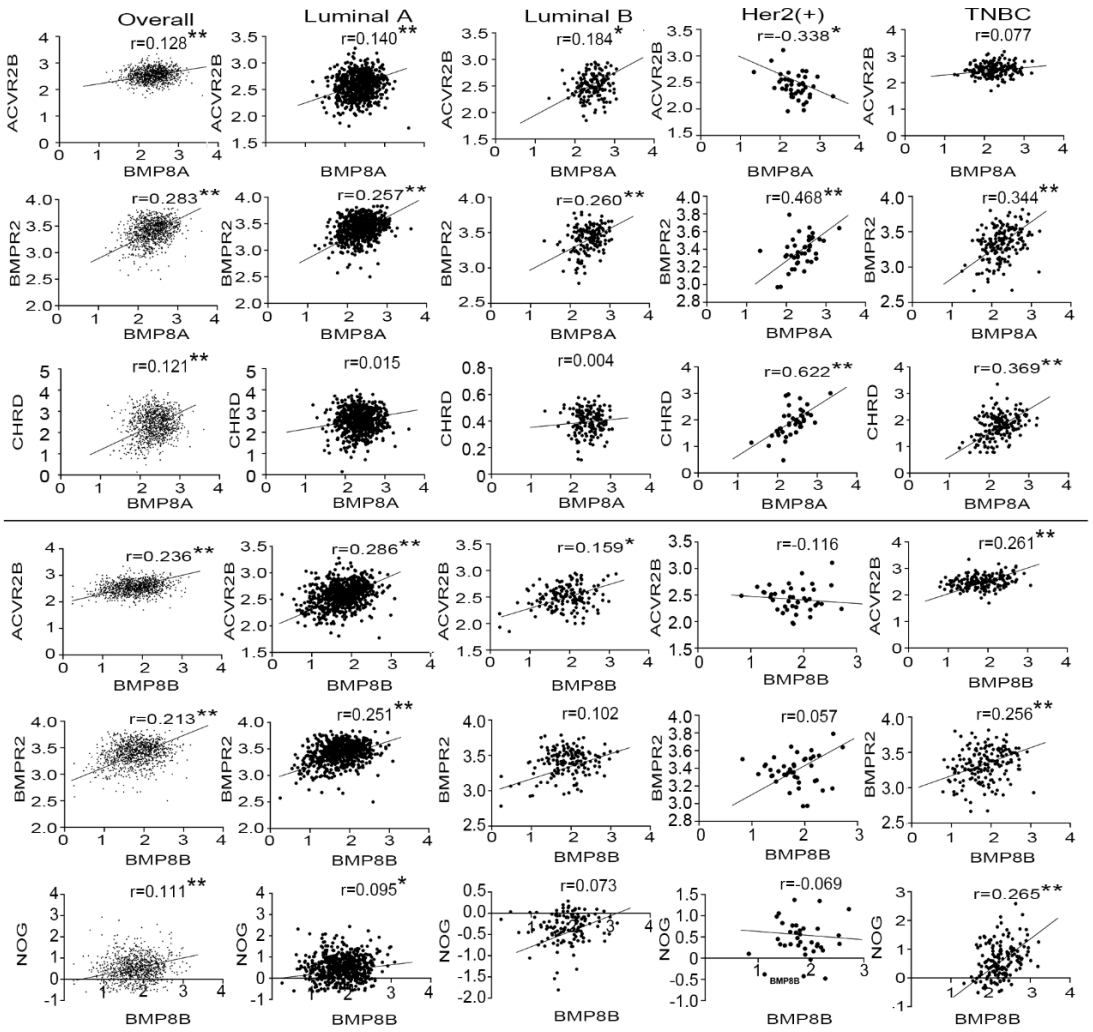

Figure 3.13 Correlation between BMP8A/BMP8B with their interact molecules. Scatter maps showed the significant correlation of BMP8 with interact molecules and their corresponding correlation co-efficient. *P＜0.05, **P＜0.01.

3.4 Discussion

BMP8A actively involved in bone metabolism (Fan et al., 2009b) and the development of the reproductive system (Wu and Luo, 2017). BMP8B signalling participates in the regulation of thermogenesis and energy expenditure (Whittle et al., 2012). Recent years have witnessed an increased research interest in BMP8. It has been reported that both BMP8A and BMP8B participated in the progression of various solid tumours, for instance, BMP8A suppressed the ubiquitination of Nrf2 which modules the expression of TRIM24, leading to the inhibition of apoptosis and drug resistance of renal cancer (Yu et al., 2020). Over-expression of BMP8B suppressed the proliferation and promoted the apoptosis of pancreatic cancer, whilst reduced expression of BMP8B accelerated the disease progression and growth of tumour cells (Cheng et al., 2014). Recent analysis of BMPs in the TCGA-BRCA cohort showed that BMP8A was upregulated in breast cancers. The increased expression of BMP8A was associated with poorer overall survival (Katsuta et al., 2019b).

To date, expressions of BMP8A and BMP8B in subtypes of breast cancer and the clinical implication in these subtypes remain unknown. The present study focused on the aberrant expressions of BMP8A and BMP8B in overall breast cancer and also their specific involvement in different subtypes of the disease. Altered expressions of BMP8A and BMP8B were assessed in three different breast cancer datasets (TCGA_BRCA, E-MTAB-6703 and Cardiff cohort) for their expression in tumour compared with normal or non-tumour adjacent mammary tissues. In the present study, it was found that the expression levels of BMP8A/BMP8B in breast cancer tissues were significantly elevated compared with normal tissues in both TCGA-BRCA and E-MTAB-6703 cohorts. No significant difference was observed for the expression of BMP8 in the analysis of the Cardiff cohort. IHC staining of BMP8A in a breast cancer tissue microarray (Cat NoBC081120f. Biomax) showed a cytoplasmic staining of the protein BMP8A. BMP8A staining is more frequently observed in the BC samples.
Further analyses revealed that there are differential expressions of BMP8A/BMP8B in different subtypes. Initially, the evaluations were performed in different subtypes determined by the IHC result of ER, PR and HER2, however the IHC result is susceptible to the subjective factors. Due to the limited cases of samples, protein level of BMP8a in different subtypes of breast cancer still needs to be further investigated.

In order to reduce the subjective variance, the objective mRNA expressions of ER, PR and Her2 in TCGA cohort were then evaluated to reclassify the subtypes and the differential expressions of BMP8A/8B were analysed subsequently. Finally, analysis in E-MTAB-6703 dataset was applied to validate the result. It was consistently observed in both cohorts that both BMP8A and BMP8B are highly expressed in Luminal B and Luminal A subtypes, whilst Her2 (+) and TNBC subtype tumours present lower expression of both genes. To further verify the findings and make preparation for following cellular experiments, we investigated the expression of BMP8A and BMP8B in a number of breast cancer cell lines comprising different subtypes of BC. QPCR result showed the high expression of BMP8A and BMP8B in current luminal A cell line and part of the luminal B and TNBC cell lines. SKBR3 cell line, belongs to the Her2 (+) subtype, presented low expression of BMP8A and BMP8B. Based on the expression of BMP8A and BMP8B in the wild type of cell lines, overexpression models of BMP8A in BT474 (luminal B), MDA-MB-361(luminal B), SKBR3(Her2 (+)) and MDA-MB-231 cell lines (TNBC), whereas BMP8A knock down is suitable to be constructed in MCF-7 (luminal A), and MDA-MB-436 (TNBC).

It was not until recently that Katsuta et al, by analysing BMPs in the TCGA-BRCA, have reported that higher expression of both BMP8A and BMP8B were correlated with poorer overall survival in breast cancer (Katsuta et al., 2019b). However, studies on the clinical relevance of BMP8A and BMP8B in breast cancer are otherwise lagging. Our analysis for this topic started from the altered expression of BMP8 with TNM staging of BC, significant differential expression of BMP8A was observed between the early and advanced tumour stages. Further analysis within subtypes shows differential expression of BMP8A in luminal A subtype, but not in other subtypes. The association of BMP8 with the clinical outcomes of patients with breast cancer was again performed by KM-plot online analysis. It revealed that high level expression of BMP8A, and not BMP8B, tended to correlate with the poor overall survival. High expression of BMP8B presented a higher possibility of developing distant metastases but less recurrence. This collectively suggests that the relationship between BMP8A and BMP8B and the survival of the patients, are more than just being straight forward correlation. Given the complexity of the biological interactions between BMP8, its receptors, antagonists and diverse signalling events, a combined analysis with these other factors is highly necessary.

Evaluation of BMP8A and BMP8B was also carried out in different subtypes of breast cancer, which have very different biochemical, biological and clinical manifestations. Intriguingly, high expression of BMP8A is associated with the poor overall survival in luminal B subtype (P=0.0024) and with good prognosis in the Her2 (+) subtype (P=0.001). However, we did not find any significant correlation between BMP8B and overall survival in any subtype of breast cancer. Compared with BMP8B, the role of BMP8A in breast cancer seems more relevant and important. BMP8A presents a contrasting relationship with the progression of breast cancer in luminal B and Her2 (+) subtypes, which indicates that BMP8A signalling may interact with the ER and Her2 signalling in a contrasting fashion. ER is capable of modulating the expression and the function of BMP and BMPRs in breast cancer(Takahashi et al., 2008, Katsuta et al., 2019a). Her2 signalling has also exhibited a reciprocal regulation with BMP signalling (Ueda et al., 2004, Mulder, 2000, Ventura et al., 2004). Generally, Her2 signals are transduced as the pattern of heterodimerisation with the co-receptors, that is why Her2 signalling pathway tends to rely on the EGFR signalling pathways and cannot be completely distinguished. EGFR signalling could regulate the expression of BMPs in breast cancer (Clement et al., 1999). Study in the drosophila embryo showed that BMP signal response was inversely modulated by EGFR signalling (Deignan et al., 2016). EGFR signal is capable of modulating the signalling events of the BMP pathway. Under the regulation of EGFR, BMP-7 reduced the progression of liver fibrosis. BMP signal could reversely influence the transduction of EGFR either, in the same study, BMP-7 was shown to reduce the expression and the phosphorylation of EGFR (Wang et al., 2014).The exact impact of BMP8A on breast cancer particularly the subtype specific involvement is yet to be investigated.

In our analysis, significantly altered expressions of BMP8A and BMP8B were observed in tumours with differential expression of HER2. BMP8A expression is positively correlated the expression of HER2.

BMP8 influences the biological events in breast cancer through BMP signalling pathway. To date, little is known about the signalling transduction of BMP8 in BC. Research on the differentiation of spermatogonia proved that BMP8 induced activation of both BMP specific R-Smad1/5/8 and TGF-β specific R-Smad 2/3 signal pathways synchronously. The former pathway was mediated by receptor complexes formed by

type I receptor （ALK3 or ALK6) and type II receptor (ACVR2A or BMPR2). Whilst SMAD2/3 signal pathway was activated through receptor complexes formed by type I receptor (ALK5 or ALK4) and type II receptor(ACVR2A, ACVR2B or TGFBR2)(Wu et al., 2017). Present analysis from STRING dataset reveals that BMPRs such as BMPR1B (0.822), BMPR1A (0.814), BMPR2 (0.814), ACVR2A (0.575) and ACVR2B (0.511) are highly correlated with expression of BMP8A and BMP8B, which are consistent with the research in spermatogonia. These receptors are supposed to be the predicted receptors of BMP8 in BC. Our analysis showed that BMP8A expression was highly positively associated with the BMP1 and BMPR2 expression in the TCGA-BRCA cohort including all subtypes. This indicates that BMPR2 may play a vital role in the signalling transduction of BMP8A of BC. Different from the other members of BMPs, BMP1, possesses a different C-terminal region, works as the proteinases in modulating the formation of ECM and activating the BMP signalling pathway(Hopkins et al., 2007). ACVR2B is positively associated with BMP8A in Luminal A and B subtypes, whilst an inversely correlation is observed in Her2 (+) subtype ($r=-0.338$ $P<0.05$). CHRD, the antagonist of BMPs, is highly positively correlated with expression of BMP8A in Her2(+) and TNBC subtypes, in addition, another antagonist of BMPs, NOG, is significantly correlated with the expression of BMP8A too ($r=0.255$ $P<0.01$). It is speculated that the activity of BMP8A may be inhibited in Her2(+) and TNBC subtypes. BMP8B is positively correlated with ACVR2B in breast cancer excluding Her2(+) subtype. BMPR2 is positively correlated with BMP8B in overall breast cancer ($r=0.213$ $P<0.01$), luminal A ($r=0.251$ $P<0.01$) and TNBC subtypes ($r=0.256$ $P<0.01$). Notably, NOG expression is also positively correlated with BMP8B expression in overall, luminal A and TNBC subtypes, especially in TNBC subtype ($r=0.265$ $P<0.01$), which implied that function of BMP8B may be suppressed by the antagonist, especially in TNBC subtypes.

3.5 Conclusion:

BMP8A and BMP8B expression are significantly elevated in breast cancer compared with adjacent normal breast tissues, especially in luminal B and Her2(+) subclasses from the analyses in the database, however, Result from IHC staining of the current TMA showed that BMP8A is highly expression in luminal A subtype. Further

investigation of BMP8A in breast cancer cell lines presented those high expressions of BMP8A in MCF-7 (luminal A), MDA-MB-436 cells (TNBC).

BMP8A may involve in tumour staging in luminal A subtype of breast cancer.

BMP8A presents the contrasting role in luminal B and Her2 positive subtypes of BC, which is yet to be investigated in the following research.

Differential expression of ERBB2 is correlated with significantly altered expression of BMP8A and BMP8B in breast cancer and ERBB2 is positively associated with the expression of BMP8A.

BMPR2 and ACVR2B seem to closely correlate with BMP8A and BMP8B signalling in breast cancer. BMP8 signalling transduction is to be further investigated in the following chapter.

Function of BMP8 is possible to be inhibited by the antagonists in Her2(+) and TNBC subtypes of breast cancer. To detect the exact regulation for BMP8 and the antagonists, further study is required.

Chapter 4

BMP8A regulates cellular functions of luminal B breast cancer cells by enhancing invasiveness and epithelial mesenchymal transition (EMT)

4.1 Introduction

The luminal subtype (including luminal A and Luminal B) accounts for 80% of breast cancer and is characterised by having positive endocrine receptors, including oestrogen receptor (ER) and progesterone receptor (PR). In addition to the ER and PR, luminal B subtype is also positive for HER2 expression, differing from the luminal A subtype which is HER2 negative. Luminal B subtype is an aggressive phenotype presenting less responsive to endocrine therapies (Nelson et al., 2017). Luminal B subtype is more likely to occur in older women (over 75 years of age) and is correlated with poor prognosis (Mills et al., 2021).

The roles played by BMPs in breast cancer, particularly in Luminal-B subtype, remain under intensive investigation. It has been indicated that BMP signalling may be epigenetically pivotal, with increased tendency of deregulation in luminal B subtype (Gao et al., 2015). BMP signalling has also been shown to modulate the EMT (Epithelial to Mesenchymal Transition) process and promote tumour invasion (Buijs et al., 2007a, Naber et al., 2012, Ying et al., 2015). EMT, a process whereby tumour cells forfeit epithelial morphology and obtain mesenchymal phenotype, is critical for indolent cells acquiring metastatic propensity (Gonzalez and Medici, 2014). The other key feature of BMPs' signalling is their stimulatory effect on the expression of, or increase in the activity of certain MMPs including MMP1, MMP2 and MMP9, (Wang et al., 2015). Collectively, there is evidence to argue the potential importance of BMPs in the progression of breast cancer.

Amongst the BMP family members, BMP8A is one of the poorest understood BMPs in cancer. It was found to suppress tumour apoptosis and is associated with drug resistance in renal cancer (Yu et al., 2020). In clinical breast cancer, it has been shown that higher expression of BMP8A is associated with shorter overall survival (OS) of breast cancer patients (TCGA) (Katsuta et al., 2019c).

Analysis of BMP8A for its implication in breast cancer, as presented in Chapter3, reveals that upregulated BMP8A is associated with poor overall survival and poor DMFS in luminal B subtype breast cancers, which indicates a possible involvement of BMP8A in disease progression. The work presented in the present chapter aimed to

investigate the impact of BMP8A on the cellular functions of luminal B subtype breast cancer cells. For this study I developed a set of sub-models from luminal B breast cancer cells, BT474 and MDA-MB-361, by genetically modifying the expression of BMP8A using a Lentiviral vector system. These new cell models were then used to evaluate the impact of modified expression of BMP8A on cellular functions including proliferation, adhesion, migration and invasion. On discovering that BMP8A influenced functions that are hallmarks of EMT in these cells, using both the cell models and a clinical database (TCGA), I went on to further explore the links between BMP8A and EMT molecular events.

4.2 Materials and methods

4.2.1 **Breast cancer database**

RNA sequencing data (TCGA_BRCA) was applied in this study to investigate the correlation between BMP8A and tumour biological markers. TCGA-BRCA is an mRNA sequencing cohort, with quantitative data of genomic DNA, mRNA, microRNA and protein, for a cohort of breast cancer comprising 1098 tumours and 112 adjacent non-tumour mammary tissues.

4.2.2 Cell lines

BT474 and MDA-MB-361 cell lines were used to investigate the impact of BMP8A in breast cancer cells. Wild type BT474 and MDA-MB-361 cell lines were cultured in RPMI-1640 medium, with 10% FBS and antibiotics. The stably transfected MDA-MB-361 and BT474 cell lines were cultured with selection medium, adding 100µg/ml hygromycin. After selection for about one week, selection medium with 50µg/ml hygromycin was used to maintain the cells.

4.2.3 Overexpression model in BT474 and MDA-MB-361 cell lines

Lentivirus BMP8A expression vector was ordered from the vector builder (VB180207-1092dmp). After the same procedures of amplification, purification and packaging of the lentiviral particles, BT 474 and MDA-MB-361 cells were transduced with lentiviral BMP8A vectors or control vectors, respectively. The transduced cell lines were subject

to selection using hygromycin and verified for the expression of BMP8A.

4.2.4 RNA isolation, cDNA synthesis, RT-PCR, and Q-PCR

Tri Reagent kit (Sigma-Aldrich, Inc., Poole, Dorset, England, UK) was utilised to extract the RNA, followed by the synthesis of complete DNA using GoScriptTM Reverse Transcription System kit (details could be seen in Chapter2 section 2.6.1). Conventional and QPCR were then accomplished according to the protocols in Chapter 2. Details of primers including GAPDH, β-actin, BMP8A and other responsive genes are given in Chapter 2 (Table 2.3).

4.2.5 Protein extraction, SDS-PAGE, and Western blot analysis

After protein extraction using a lysis buffer and quantification by the DC Protein Assay kit (BIO-RAD, USA), the proteins were separated by SDS-PAGE and then transferred onto PVDF membranes (pre-treated by methanol for 1 minute and the running buffer for 15 minutes). After blocking with a blocking buffer, the membrane was incubated with the respective primary antibody at 1:1000 dilution overnight (4^{o}C) to probe the target protein. After washing, the respective HRP conjugate secondary antibody was added and incubated for another hour, followed by more washings. The protein bands were eventually visualised using the chemiluminescence detection kit (Luminate Forta Western HRP substrate (Cat. No. WBLUF0500, Merk-Millipore, Hertfordshire, UK)) and the chemiluminescent tagged bands was visualised with UVITech Imager (UVITech Inc., Cambridge, UK). Details for procedures and the antibodies applied in the current study are listed in chapter 2 (Table 2.4).

4.2.6 *In vitro* cell proliferation assay

Ten thousand cells, in 200 µl medium, were seeded in three 96-well-plates, (each cell type in six repeats) and incubated at 37°C with 5% CO2 for 1, 4 and 7 days respectively. Following incubation, the cells were fixed using 4% formalin for 15 minutes and stained with crystal violet (0.5% w/v) for 10 minutes. After washing with tap water to remove excess crystal violet, 100µl of 10% acetic acid was added into each well to extract the crystal staining and the absorbance was measured using a spectrophotometer (BIO-TEK, Elx800, UK) at a wavelength of 590nm.

4.2.7 *In vitro* cell adhesion assay

A ninety-six well plate was precoated with Matrigel at a concentration of 5µg per 100µl,

followed by seeding the cells on the bottom of the plate. Details have been previously described in chapter 2 (Section 2.9.2). The cells were then incubated, to adhere to the matrix protein on the bottom of the plate, for 40 minutes at 37℃ with 5% CO2, prior to being fixed in formalin (4%) and stained with crystal violet (1% w/v). Cell counting procedure was then performed.

4.2.8 *In vitro* cell invasion assay

After precoating the 8μm pore transwell inserts with Matrigel, at a concentration of 50μg per 100μl on the 24-well-plate, 30000 cells were seeded into the upper chapter of inserts and incubated for 72 hours at 37℃ with 5% CO2. After three days, cells which had invaded the Matrigel layer and migrated thought the pores to the other side of the insert were fixed with formalin (4%). After removing the Matrigel on the bottom of the insert gently, the cells were stained with crystal violet (1%) and the cell counting procedure was subsequently performed.

4.2.9 *In vitro* cell motility assay

One million BT474 and MDA-MB-361 cells, in 5ml of RPMI, were transferred to a UC tube, together with 500μl of Cytodex bead solution (5g in 75ml PBS) and incubated at 37℃ at 5% CO2 overnight. This would allow cells to adhere to the surface of the cytocarrier beads. After washing the cell/bead pellet with PBS twice, the beads with attached cells were resuspended in 2ml of fresh medium and transferred to the 96-well-plate (200μl per well) and incubated at 37℃ at 5% CO2 for 6 hours. Beads and non-adherent cells were then removed, and the plate washed. The cells, which had migrated off the carrier beads and had adhered to the bottom of the wells, were fixed with formalin and stained with crystal violet. Absorbance was read at a wavelength of 590nM.

4.2.10 Preparation of protein samples for TMT Mass Spectrometry for Proteomics

Cells at an approximate 90% confluence were harvested using a cell scraper. RIPA buffer was used to lyse the cells at 4℃ for one hour. After centrifugation at 13000rpm for 15mins, supernatant with protein inside was collected. The protein concentrations were then quantified and were standardised to 2μg/μl. Three individual 150μl protein samples were sent to Bristol university for analysis, preserved by the dry ice based, on the blind principle. Two separate analyses were performed, comparison between the

total protein levels across the samples and the phosphor-peptide enrichment. Online analysis software, Enrichr, was applied to identify the pathway involved for the altered BMP8A in BT474 cells.

4.2.11 Statistical analyses

Student's T-test was applied to compare the normally distributed data, whilst the non-normally distributed data was analysed by Manny-Whitney Test. SPSS software was applied in the current statistical analysis.

4.3 Results

4.3.1 Overexpression of BMP8A was established in BT474 and MDA-MB-361 cell lines

As presented in Chapter 3, BT474 and MDA-MB-361 cells exhibited low levels of BMP8A. The two cells, luminal B subtype in nature, were chosen to produce overexpression models, using lentivirus vector system. Following successful selection, both cells were found to have successfully over-expressed BMP8A transcript, as shown by conventional PCR (Fig. 4.1 A) and QPCR (Fig. 4.1 B). These cells also expressed high levels of BMP8A protein. These cells were used in the subsequent functional analyses.

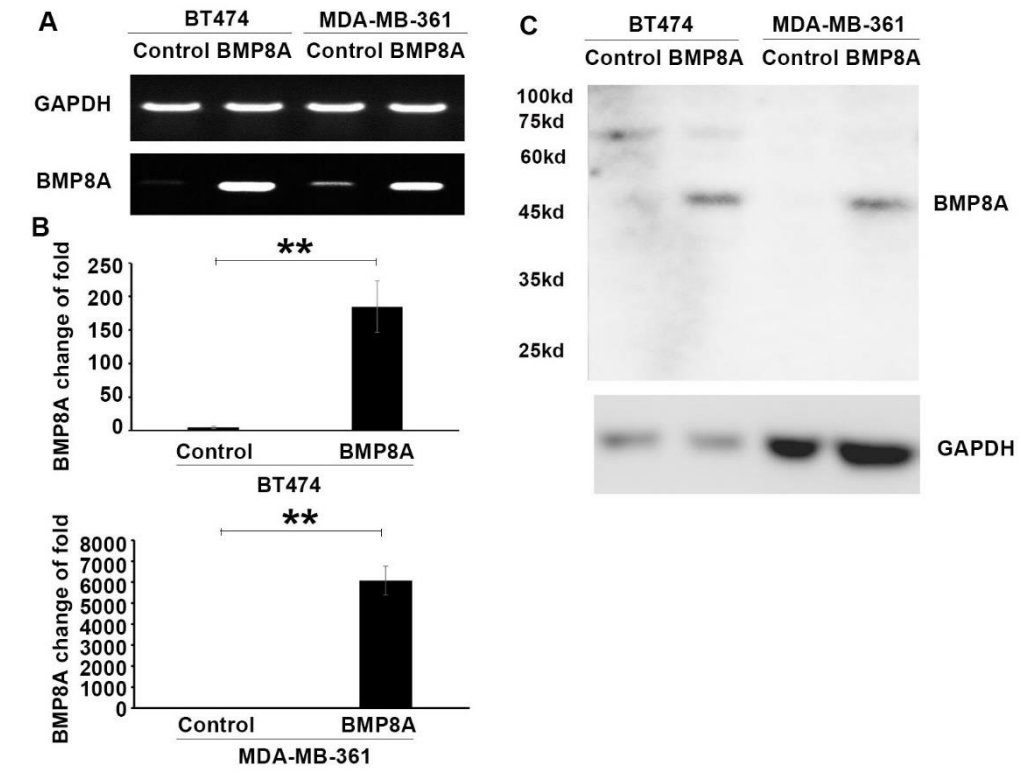

,

Figure 4.1 Validation of BMP8A expression after successful transfection and selection. BMP8A overexpression in BT474 and MDA-MB-361 cell lines was verified by conventional PCR (A), QPCR (B) and Western blot (C). ** P<0.01.

4.3.2 BMP8A regulates cellular functions of luminal B breast cancer cells

Following the creation of the overexpression cell models in BT474 and MDA-MB-361 cells, *in vitro* cell function assays, including proliferation, adhesion, invasion, and migration were performed. After 7 days' incubation, no significant difference in cell growth was found between BT474 cell models, whilst slightly increased growth rate was shown in MDA-MB-361 cells with upregulated BMP8A expression (Fig. 4.2 A). Cell invasion increased significantly in both cell lines with high expression of BMP8A, especially for the BT474 cells. Invaded cells increased by approximately 50% in the $BT474^{BMP8Aexp}$ cells compared with the control cells. No significant change in adhesion was observed in BT474 cells whilst adhesion was marginally increased in MDA-MB-361 cells. Differently from the adhesion, cell migration increased significantly in BT474 cell with high expression of BMP8A, no statistical difference was seen in MDA-MB-361 cells.

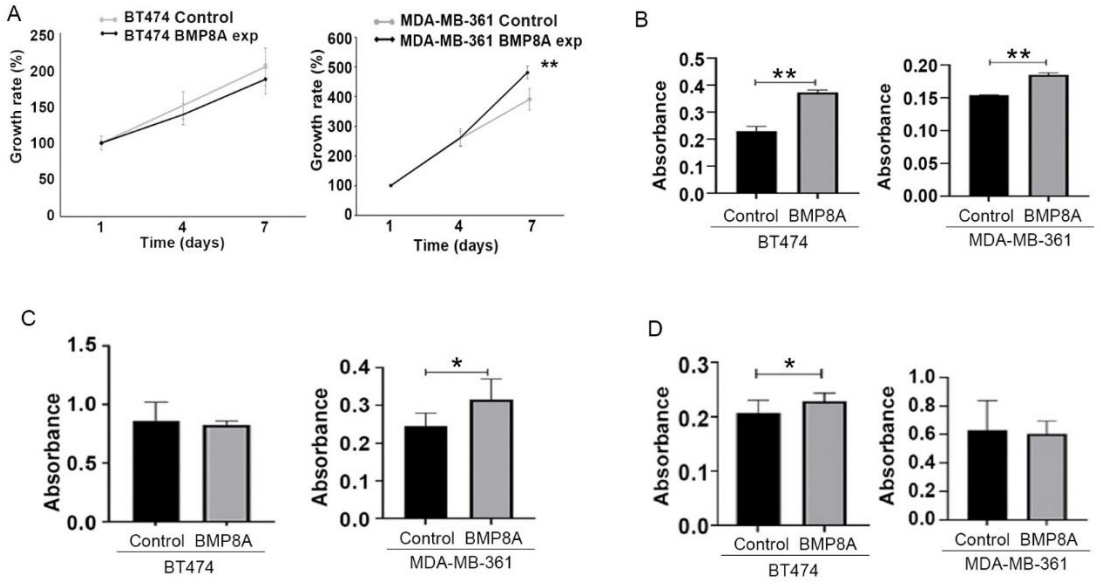

Figure 4.2 *In vitro* cell function test of two luminal B cell lines with altered BMP8A expression. (A) Proliferation assay in BT474 and MDA-MB-361 cells with differential BMP8A expression. (B) Invasion assay in BT474 and MDA-MB-361 cell models. (C) Adhesion assay in BT474 and MDA-MB-361 cell models. (D) Cytocarrier Beads assay in BT474 and MDA-MB-361 cell models.

4.3.3 Differential expression of MMPs in Luminal B breast cancer stratified by BMP8A expression levels: a TCGA database analysis.

To investigate the mechanism of enhanced invasion in BMP8A upregulated BT474 and MDA-MB-361 cells, correlation of BMP8A with MMPs was analysed in the TCGA-BRCA cohort. Differentially expressed MMPs/TIMPs/ADAMs were identified and summarised according to BMP8A expression as shown in Figure 4.3A and B). Correlation between these differentially expressed MMPs/ADAMs/TIMPs and BMP8A was further analysed using Spearman test (Figure 4.3C). Relatively higher expression levels were evident for MMP11, MMP13, MMP14, ADAM12, TIMP2 and TIMP3 in comparison with others (Figure 4.3D).

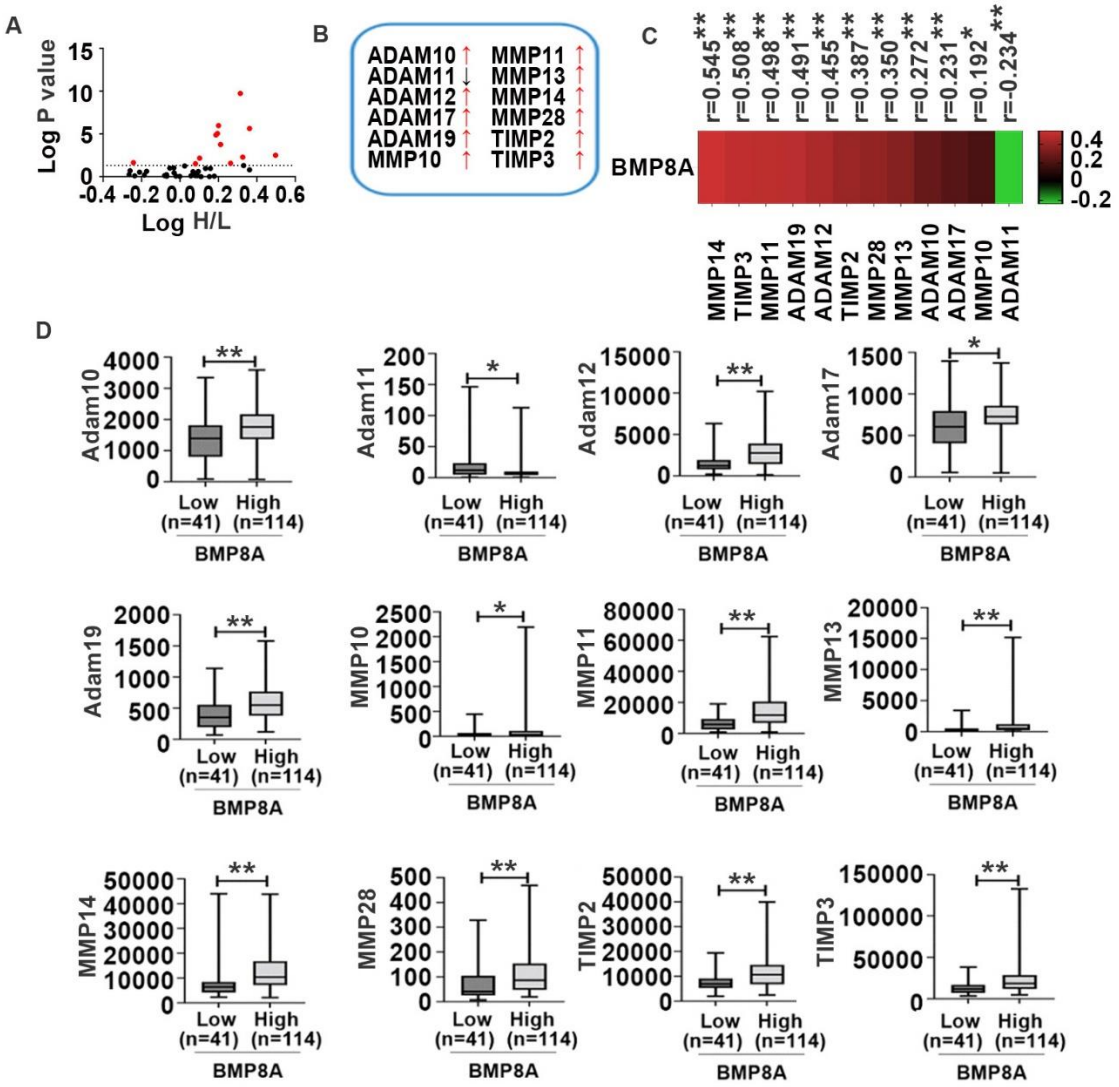

Figure 4.3 Differential expression of MMPs/TIMPs/ADAMs in luminal B breast cancer (TCGA) according to BMP8A expression. (A) Volcano plot to show the differential expression of MMPs/TIMPs/ADAMs in luminal B breast cancer (TCGA) according to BMP8A expression. A cut off value of BMP8A = 179.3775 was employed for the DEGs analysis. Shown are log values of ratios of expression values of each gene in the group of tumours with higher expression of BMP8A against their values in the tumours with lower expression of BMP8A. (B) List of differentially expressed MMPs/TIMPs/ADAMs in luminal B breast cancer (TCGA) according to BMP8A expression. (C) Heatmap to show the correlation of listed molecules with BMP8A. (D) Shown are box plots for the differential expression MMPs/ADAMs/TIMPs individually in luminal B breast cancers according to the expression of BMP8A (cut off value=179.3775).

4.3.4 Alteration of the candidate MMPs in BMP8A overexpressing luminal B breast cancer cell lines.

Expression profiles of MMPs in the BMP8A expression cell models were verified, in BT474 and MDA-MB-361 cell lines, by conventional PCR and QPCR. Increased MMP7 and MMP1 levels were found via conventional PCR, with significantly increased MMP1 and MMP11 seen in BT474 cells with upregulated BMP8A expression. Increased MMP1 was also found in MDA-MB-361 BMP8A overexpressed cells. However, results of the protein levels via zymography, using the collected conditional medium, showed no significant differential expression in the activated protein levels of MMP1 or MMP2 in BT474 and MDA-MB-361 cell lines with BMP8A overexpression.

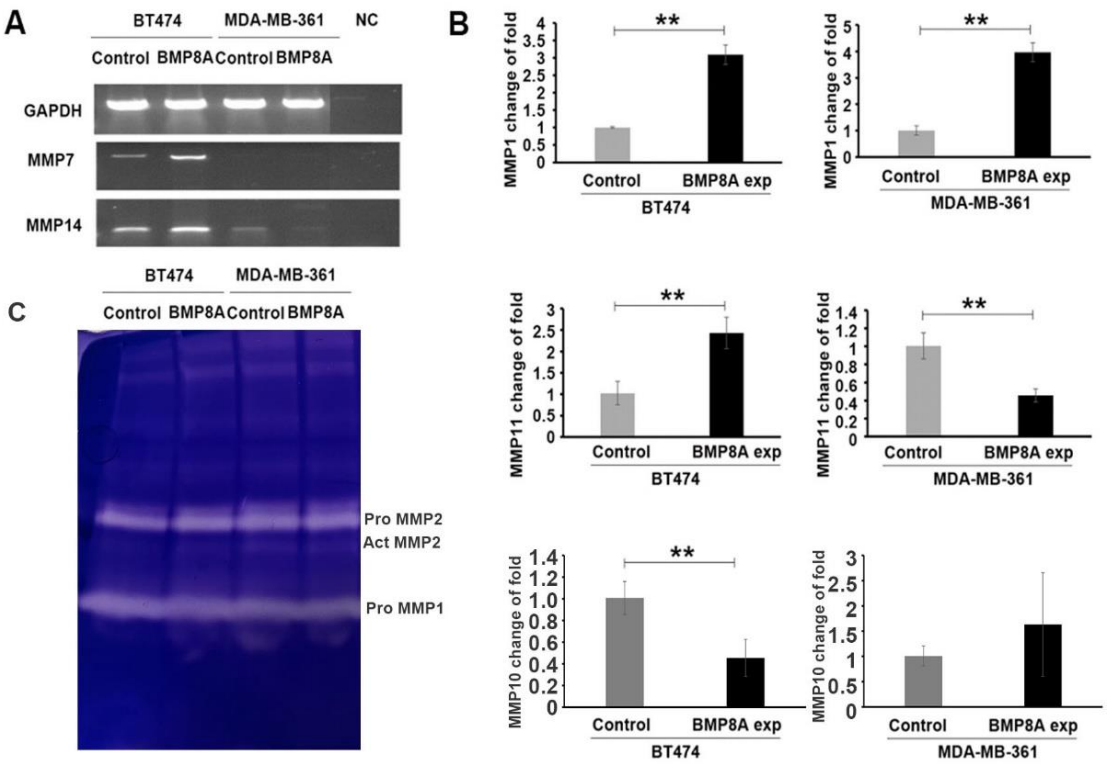

Figure 4.4 Alteration of the candidate MMPs in BMP8A overexpressing luminal B breast cancer cell lines. (A) Differential expression of MMP7 and MMP14 in BT474 and MDA-MB-361 cell models using conventional PCR. (B) QPCR to show the alteration of MMP1, MMP11 and MMP10 in BT474 and MDA-MB-361 cell models. Individual experiments were performed three times. (C) Zymography to determine the expression of MMPs from the protein level. ** *P<0.01*.

4.3.5 **Influence of BMP8A on EMT in luminal B subtype**

Influence of BMP8A on EMT in both BT474 and MDA-MB-361 cells.

To identify the responsive genes for enhanced cell invasion, EMT markers were determined in the BT474 and MDA-MB-361 cells, using both conventional PCR and QPCR. As shown in Figures4.5A and B, increased Slug transcripts were seen in both BT474 and MDA-MB-361 cells, following BMP8A overexpression. Again, following BMP8A overexpression, CDH2 expression reduced significantly in BT474 cells, whereas VIM increased markedly in MDA-MB-361 cells.

Differential expression of EMT markers/regulators in luminal B breast tumours stratified by BMP8A expression levels (TCGA database).

As EMT exhibits a key influence in the invasion of breast cancer, correlation of BMP8A with the EMT markers including VIM, SNAIL, SLUG, CDH2, CDH1 and TWIST were analysed in the TCGA-BRCA dataset. From the analysis, BMP8A expression was positively correlated with all EMT markers, in which, CDH2 ($r=0.483$, $P<0.01$) and SLUG ($r=0.407$, $P<0.01$) presented the high correlation scores (Figure-4.5 C). Investigation of the protein level, significantly increased Vimentin and Slug were found in BT474 cells and MDA-MB-361 cells with upregulated BMP8A expression (Figure-4.5 D).

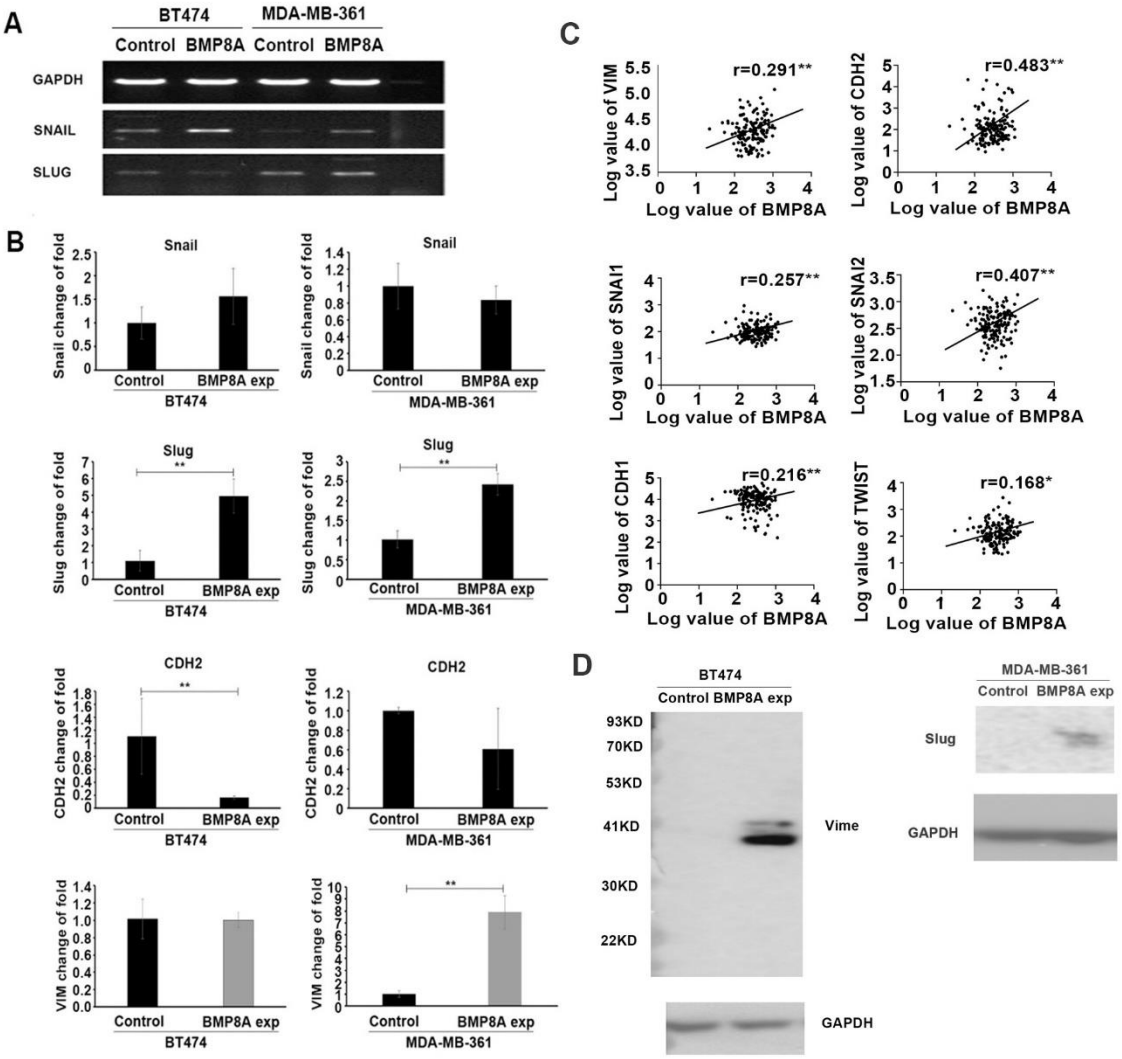

Figure 4.5 Impact of BMP8A on EMT in the luminal B tumours. (A) Differentially expressed Snail and Slug in BT474 and MDA-MB-361 cells detected by conventional PCR. (B) QPCR to determine the altered expression of Snail, Slug, CDH2 and VIM in BT474 and MDA-MB-361 cells. (C) Scatter plots to show the correlation between BMP8A and EMT markers in TCGA-BRCA cohort. (D) Differentially expressed Vimentin and Slug in BT474 and MDA-MB-361 cells by Western Blot.

4.3.6. Identification of Differentially expressed molecules and signalling molecules in BT474 cells in response to BMP8A over-expression, a proteomics-based analysis

The proteomics analysis found that 3639 molecules were differentially present between the BT474/BMP8A over-expressing cells and BT474 control cells. Of the differentially expressed molecules, 1861 significantly decreased and 1778 proteins significantly increased following BMP8A over-expression (Fig. 4.6A). LGALS1 (Lectin, Galactoside-Binding, Soluble, 1), VIM (Vimentin), IFI16 (Interferon Gamma Inducible Protein 16), CAVIN1 (Caveolae Associated Protein 1) and GSTP1 (Glutathione S-Transferase Pi 1) were the top five increased molecules. Notably, vimentin was one of the central molecules mediating the EMT. The change of vimentin seen with proteomics analysis was further verified by Western blot (Fig 4.6 B). The top twenty significantly increased molecules and the top 10 up-phosphorylated proteins, as well as their biological functions, are summarised in Table 4.1 and Table 4.2, respectively.

I went on to analyse the possible signalling pathways involved with the upregulated molecules through Enrichr online analysis (https://maayanlab.cloud/Enrichr/). With BioCarta 2016 and the metabolic pathways from BioCarta, ERK and PI-3K signalling pathways were found to be the main pathways involved. The top ten potential signalling pathways involved are otherwise listed in Fig. 4.6 C.

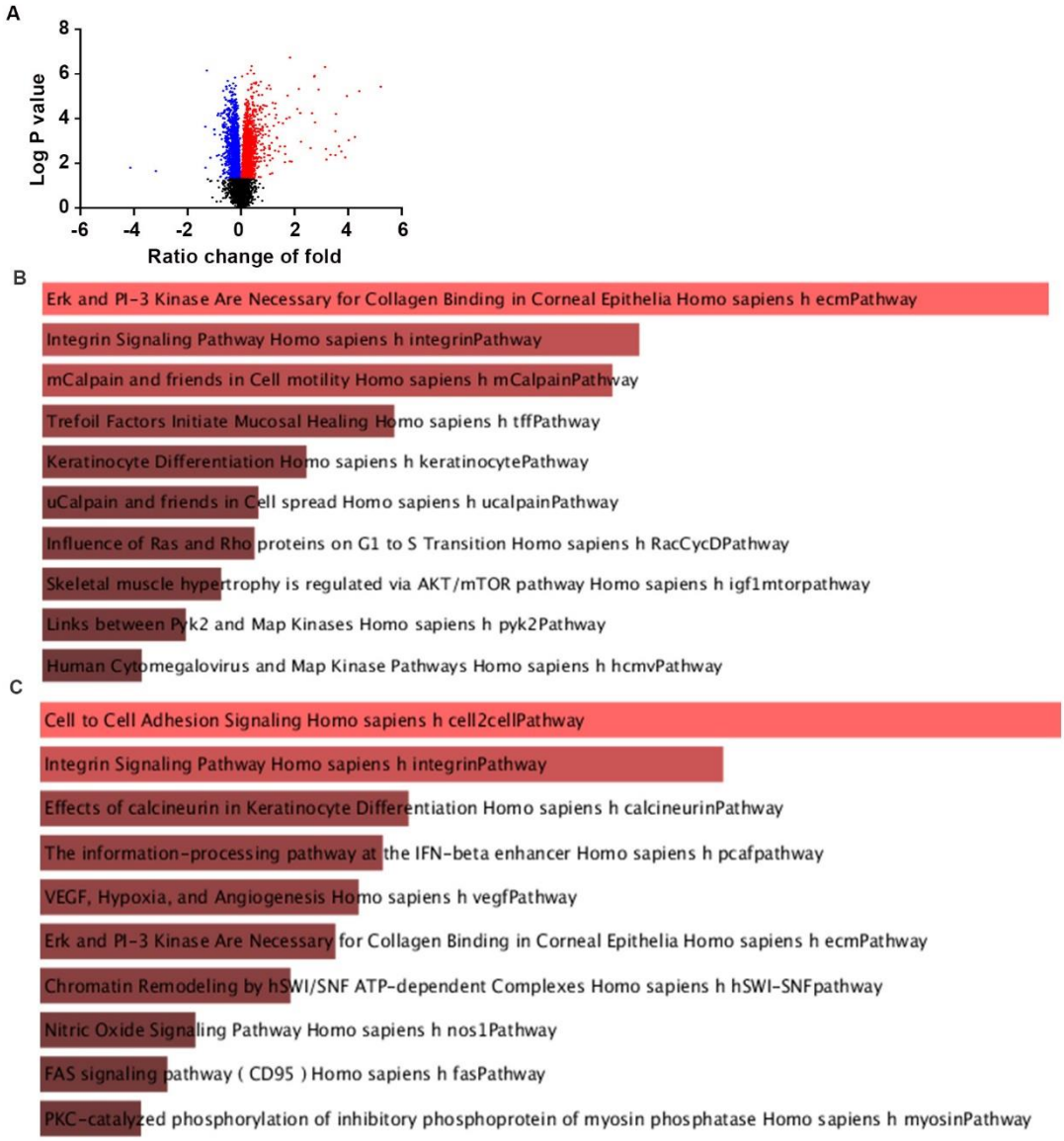

Figure 4.6 Differentially expressed molecules and signalling pathways in BT474 cells. (A) Volcano plot to present differentially expressed molecules with altered BMP8A expression in BT474 cells. (B) Potential signalling pathways correlated BMP8A overexpression in BT474 cells. (C) Candidate signalling pathways associated with the phosphorylated molecules in BT474 cells.

Table 4.1 Top twenty upregulated proteins identified in BT474 cells with BMP8A overexpression.

Gene name	LogFC	P-value	FDR	Function
LGALS1	5.22	3.74e-06	0.00113	An autocrine negative growth factor regulates cell proliferation, apoptosis, and differentiation. Related pathways are apoptosis and autophagy and validated targes of C-MYC transcriptional repression
VIM	4.42	5.87e-06	0.001223	Important marker in various non-epithelial cells, especially mesenchymal cells. Related pathways are ERK signalling and apoptosis - related network
IFI16	4.25	0.000667	0.007994	P53 function regulator. Inhibit cell proliferation via Ras/Raf signalling pathway.
CAVIN1	4.02	0.000918	0.009331	Important role in Caveolae formation and organization. Promotes ribosomal transcriptional activity in response to metabolic challenges in the adipocytes.
GSTP1	3.95	9.63e-06	0.001498	Involved in the formation of glutathione conjugate of prostaglandin A2 and prostaglandin J2. Inversely regulating CDK5 activity through p25/p35 translocation to prevent neurodegeneration.
BMP8A	3.89	0.005388	0.024819	Target molecule in the present study. Related pathways are Phospholipase-C pathway and ERK signalling.
ZNF100	3.75	0.002912	0.017252	Transcriptional regulator.
FERMT3	3.66	0.001711	0.01261	Exerts a pivotal role in cell adhesion in hematopoietic cells. May also act as a repressor of NF-kappa-B and apoptosis
MT1E	3.54	6.14e-05	0.002881	Binds with various heavy metals. Related pathways are Copper homeostasis and Metal ion SLC transporters.
CBR1	3.52	0.004274	0.021916	NAPDH-dependent reductase with broad substrate specificity.
PYGL	3.35	0.000367	0.006133	catalyses the cleavage of alpha-1,4-glucosidic bonds to release glucose-1-phosphate from liver glycogen stores. This protein switches from inactive phosphorylase B to active phosphorylase A by phosphorylation of serine residue 15. Related pathways are Glucose

				metabolism and Activation of cAMP-Dependent PKA
HLA-A	3.35	0.004134	0.021525	Important role in the immune system. Related pathways are Interferon gamma signalling and CDK-mediated phosphorylation and removal of Cdc6.
GSDME	3.19	0.006765	0.028466	Expressed in foetal cochlea, no syndromic hearing impairment is associated with a mutation in this gene. May regulate p53/TP53 associated cell response to DNA damage.
CD44	3.17	0.002273	0.014877	Cell-surface glycoprotein involved in cell-cell interactions, cell adhesion and migration. Relate pathways are Wnt signalling pathway and interferon gamma signalling.
BAG2	3.13	4.79e-07	0.000921	Interacts with Hsc70 ATPase domain in mammalian cells. Related pathways are cell response to heat stress and regulation of degradation of deltaF508 CFTR in CF.
CAV1	2.90	4.94e-06	0.001152	Scaffolding protein links integrin subunits to the tyrosine kinase FYN, which is the initiating step in coupling integrins to the Ras-ERK pathway and promoting cell cycle progression. Related pathways are development ERBB signalling and G-Beta Gamma Signalling.
RNF34	2.76	0.000146	0.004023	Interacts with apoptosis regulating protein. Presents anti-apoptosis function in Hela cells.
FLNC	2.75	1.21e-06	0.000944	Involves in the anchoring of membrane proteins for the actin cytoskeleton. Related pathways are cell junction organization and ERK signalling.
MSN	2.73	1.31e-06	0.000944	Cross-linkers between plasma membranes and actin-based cytoskeletons. Related pathways are ERK signalling and AGE/RAGE pathway.
CALD1	2.65	5.72e-05	0.002801	Central regulators for the smooth muscle and non-muscle contraction.

Table 4.2 Top 10 up-phosphorylated molecules in BT474 BMP8A overexpressed-cells.

Gene name	LogFC	P-value	FDR	Function
SMARCA4	2.40	8.76302E-05	0.039568415	Activation of the transcriptional genes repressed by chromatin. Regulation of CD44, the tumorigenic protein.
CCDC86	1.61	0.00146901	0.070035229	RNA binding molecule.
SEC16A	1.51	0.02389101	0.191054854	Organizing the endoplasmic reticulum (ERES). RAB10 regulator for insulin-induced SLC2A4/GLUT4 glucose transporter-enriched vesicles delivery.
NAA15	1.47	0.02969449	0.210317757	Presenting (N-terminal) acetyltransferase (NAT) activity, which is pivotal for vascular, neuronal growth and development.
SNX29	1.28	0.019532015	0.18453508	Microtubule motor activity and phosphatidylinositol binding.
SETD2	1.21	0.023753476	0.191054854	Histone methyltransferase and associated with hyperphosphorylated RNA polymerase II.
TNS3	1.14	0.004646896	0.107767166	MET promotes cell motility and signalling by GPCR
TUT4	1.10	0.038613187	0.234595438	RNA uridylyl transferase.
TRIM3	1.03	0.006320496	0.123915201	Involved in *ubiquitin-protein* transferase activity and protein C-*terminus binding. Its* related pathways are Interferon gamma signalling and Innate Immune System.
DDX27	1.03	0.015931668	0.17077036	Putative RNA helicases, which are implicated in a number of cellular processes involving alteration of RNA secondary structure.

4.4 Discussion

BMPs have been implicated in regulating cellular differentiation, proliferation, apoptosis and motility in some solid tumours, especially in hormone related malignancies, such as breast cancer and prostate cancer (Davis et al., 2016, Ye et al., 2009a). However, the role of BMP8A in the tumourigenesis and progression of breast cancer in luminal B subtype remains unclear. Based on the bioinformatical analysis for the potential role of BMP8A in luminal B subtype breast cancer, cell models with altered BMP8A expression were created according to the BMP8A expression in the wild type cells. After the validation of the BMP8A overexpression cell models in BT474 and MDA-MB-361 cells, the *in vitro* cell function assays, including proliferation, adhesion, invasion, and migration, were performed. From the analysis of these cell function assays, the major impact of BMP8A in luminal B breast cancer cells appeared to be mainly on invasion; upregulated BMP8A was associated with enhanced cell invasion in both cell lines used, especially in BT474 cells.

In previous research, BMP signalling has been shown to regulate the dissemination of breast cancer through a variety of mechanisms. BMP signalling alters the expression and activity of matrix metalloproteinases (MMPs), contributing to tumour invasion and metastatic spread. BMP2 has been shown to up-regulate the expression of MMP11 (Huang et al., 2017), whilst BMP4 was found to stimulate the expression, or increase the activity, of MMP1(Guo et al., 2012).

From the clinical cohort study, expression of MMPs, including MMP11, MMP14, MMP13, MMP28, ADAM10, ADAM12, ADAM17 and ADAM19, were found to be at an increased level in luminal B subtype with higher BMP8A expression. These candidate molecules, when further validated in the cell models. MMP7, MMP14, MMP2 and MMP11, were found upregulated in BT474 cells with high BMP8A expression, and BMP1 was upregulated in BMP8A highly expressed MDA-MB-361 cells. However, protein production and activation are yet to be further investigated in both *in vitro* 3D spheroid/organoid models and *in vivo* xenograft/metastatic models and, also in corresponding tumour samples which represent this subtype and distant metastases associated.

Metastasis is the most typical property of malignant tumours, which accounts for the leading cause of death in cancer patients. Metastasis is initiated from the detachment of

the individual cancer cell from the primary tumour and invasion of adjacent tissue, , then migration through blood or lymphatic circulation to the subsequent sites. Epithelial mesenchymal transition is critical for cancerous cells acquiring invasiveness and aggressive traits to spread. BMP signalling is also found to regulate EMT mediated invasion and migration of the tumour cells. Research has shown that BMP2 could downregulate the expression of Rb leading to ubiquitin-mediated degradation, which reduced the polyubiquitination of EMT factors and promoted EMT and bone metastasis (Huang et al., 2017). BMP4 signalling was found to be involved in the EMT process in many cancers (Kestens et al., 2016). Expression of BMP4 has been found to be significantly higher in invasive cancer tissue compared with normal tissue. BMP4 could promote EMT and tumour progression by suppressing the expression of E-cadherin and elevating the expression of N-cadherin and SNAIL2 (Park et al., 2015), resulting in progressive motility and invasiveness (Serrao et al., 2018). It is worth mentioning that BMP4 also inhibited EMT through restraining the Notch signalling pathway, which augmented the EMT properties in epithelial cells of the breast (Choi et al., 2019). Differently from BMP4, BMP6 exerted an inhibitory effect on EMT, which restrained the metastasis of breast cancer cells, by downregulating the expression of miR-21 and δEF1 (ZEB1) and restoring the expression of E-cadherin(de Boeck et al., 2016). Lower expression of BMP6 in MCF7 cells enhanced the expression of mesenchymal proteins and silenced E-cadherin, giving rise to increased invasiveness (Liu et al., 2014).

Analysis in TCGA-BRCA cohort shows that BMP8A expression is highly positively correlated with the EMT markers in luminal B subtype, which indicates the potential role for BMP8A in regulating the expression of EMT markers. Further research in cell models revealed that enhanced BMP8A expression was associated with upregulated SLUG expression at the gene level. Results from the proteomics study also showed the significantly increased vimentin in BMP8A high-expressed BT474 cells and was validated by Western Blot.

There are also some interesting findings from the proteomics study. ERK/PI3K signalling was found to be associated with BMP8A in BioCarta analysed from the up-regulated proteins. Analysis of the up-phosphorylated molecules showed involvement with cell adhesion. Activation of integrin signalling was found to be correlated with the up-regulated BMP8A. ERK/PI3K signalling was also identified for the up-phosphorylated molecules, which indicated that ERK/PI3K signalling may actively

interact with BMP8A signalling.

Taken together, higher expression of BMP8A is associated with a panel of upregulated MMPs including MMP11and MMP14, as well as the increased EMT molecules including SLUG and Vimentin in luminal B subtype, leading to enhanced invasion. Analysis from the proteomic study showed that the ERK and PI3K signalling pathway may be actively involved in BMP8A mediated cell function. Further mechanisms of BMP8A signalling transduction in luminal B subtype will be elucidated in Chapter 7.

Chapter 5

BMP8A and cellular functions of HER2 positive breast cancer cells

5.1 Introduction

HER2 positive subtype breast cancer is characterised by the positive expression of the ERBB2 receptor and comprises of approximately 15-20% of all breast cancers (Loibl and Gianni, 2017). Due to the improvement of HER2 target therapy in the past decades, the survival rate for patients with metastatic HER2 positive breast cancer has risen to almost 5 years and a pathological complete response to the treatment can be achieved in over 70% of the patients (Loibl and Gianni, 2017)). Although this represents a remarkable achievement in the target therapy of HER2 positive breast cancer, its long-term survival over 10 years is still lower than luminal subtypes. Better understanding of the cellular and molecular mechanisms of HER2 positive tumours will further improve the treatment.

Although BMP signalling is involved in the tumorigenesis and progression of breast cancer, the specific role of BMP signalling in subtypes of breast cancer, including the HER2 positive subtype, remains largely unknown. Emerging evidence has indicated the importance of BMPs in this subtype. For example, proliferation and metastasis of Her2 (+) SKBR3 breast cancer cells were impeded by BMP9 via the ERK1/2 and PI3K/AKT signalling pathways (Ren et al., 2014a). It has also been shown that BMP4 can suppress *Anoikis* resistance, cell proliferation and colony formation of SKBR3 cells (Sharma et al., 2022).

As presented in Chapter 3, high expression of BMP8A was associated with better overall survival in Her2 subtype, which is in clear contrast to luminal B and TNBC subtypes, indicating differential roles of BMP8A in the different subtypes of breast cancer. In the present chapter, the impact of BMP8A on the cellular functions of two HER2 (+) breast cancer cell lines, SKBR3 and HCC1419, was examined using a BMP8A overexpression model.

5.2 Materials and Methods

5.2.1 Cell lines

Both SKBR3 and HCC1419 cell lines are derived from HER2 positive breast cancer. Wild type HCC1419 cell line was cultured in RPMI-1640 medium with 10% FBS and antibiotics, whilst the SKBR3 cell line was maintained in DMEM medium with 10% FBS and antibiotics.

5.2.2 BMP8A overexpression in HCC1419 and SKBR3 cell lines

Lentiviral particles for BMP8A overexpression were prepared following a procedure described in Chapter 2 (section?) and were used to transduce both HCC1419 and SKBR3 cell lines. Following transduction, the cells were subject to selection with hygromycin before verification of BMP8A expression using both PCR and Western blot. Empty lentiviral vector was also used as a control. The selected HCC1419 and SKBR3 cell lines were cultured with the corresponding medium, containing 100μg/ml hygromycin.

5.2.3 RNA isolation, cDNA synthesis, RT-PCR, and Q-PCR

RNA extraction and cDNA synthesis was accomplished from the cell models, strictly according to the protocols. Then conventional PCR and QPCR were performed (details are depicted in Chapter 2.6). GAPDH was used as the house-keeping gene, the primer sequences for GAPDH, BMP8A and other target genes are listed in Chapter 2 (Table 2.2).

5.2.4 Protein extraction, SDS-PAGE, and Western blot analysis

After protein extraction using lysis buffer and the quantification by the DC Protein Assay kit (BIO-RAD, USA), the protein samples separated by the SDS-PAGE were transferred onto PVDF membranes (Pre-treated with methanol for 1 minute and running buffer for 15 minutes). Following membrane blocking, the membrane was incubated with primary antibody at 1:1000 dilution overnight and corresponding secondary antibodies, to probe the target protein. Finally, after membrane washing, the protein bands were visualised using the chemiluminescence detection kit (Luminate Forta Western HRP substrate, Cat. No. WBLUF0500, Merk-Millipore, Hertfordshire, UK) and the chemiluminescent tagged bands were visualised with UVITech Imager (UVITech Inc., Cambridge, UK). Details for procedures and the antibodies applied in the current study are listed in Chapter 2, Table 2.4.

5.2.5 *In vitro* cell proliferation assay

Five thousand SKBR3 cells in 200μl medium were seeded in three 96-well-plates and incubated at 37℃ with 5% CO2 for 1, 4, 7 days respectively. Six repeats were included for each cell line per plate. Following incubation, the cells were fixed and stained as previously described in Chapter 2 (Section 2.9.1). Absorbance was determined at a

wavelength of 590nm.

5.2.6 *In vitro* cell adhesion assay

Ninety-six well plates were precoated with the Matrigel, then the cell adhesion assay was performed by seeding 30000 SKBR3 or HCC1419 cells in the plate as described in Chapter 2 (Section 2.9.2). The absorbance was read to assess the cell adhesion.

5.2.7 Cell invasion assay

Thirty thousand cells (SKBR3 and HCC1419) were seeded in the inserts, precoated with Matrigel, on a 24-well plate. After three days' incubation at 37℃ with 5% CO2, the insert and control wells were fixed and stained with crystal violet. Absorbance was read to determine the cell invasion as described in Chapter 2 (Section 2.9.4).

5.2.8 Cell migration assay

Wound assay

SKBR3 cells were seeded in a 24-well-plate followed by overnight culture allowing the cells to form a monolayer. Wounds were created using a pipette tip. Closure of the wounds was monitored using the EVOS system, over a duration up to 28 hours as described in Chapter 2 (Section 2.9.3.2).

Cell motility assay using cytocarrier beads

For HCC1419 cells, a cytocarrier beads assay was applied to assess the impact of BMP8A on the cell migration (Chapter 2 Section 2.9.3.1). After overnight incubation with the microcarriers, the cells and the beads were washed twice with 5ml of PBS, followed by resuspension with 2ml fresh medium. Two hundred microlitres of cell suspension was seeded in each well, on a 96-well-plate, with minimal 6 repeats per testing cell line. After further incubation for 8 hours, cells were fixed and stained. The absorbance was then read to assess the impact on the migration as described in Chapter 2 (Section 2.9.3.1).

5.2.9 Cell viability test

SKBR3 cells and HCC1419 cells were seeded in a 96-well-plate, at a cell density of 5000 cells per well and 10000 cells per well, respectively. After a 3-day incubation for SKBR3 and 4 days' incubation for HCC1419, 20μl of CCK8 reagent was added into

each well followed by further culture for 70 minutes. The optical density (OD) value was read at a wavelength of 450 nm.

5.2.10 Zymography

Both control and BMP8A over-expression cells (SKBR3 and HCC1419) were seeded on the 6-well-plate at approximately 90% confluence. After overnight incubation, fresh medium (400 µl) was added into the wells. Medium (conditional medium) was collected after 8 hours incubation. Non-reducing buffer was added into the conditional medium. Following electrophoresis in an SDS-PAGE gelatin gel, the gel was washed, using a washing buffer, then incubated with incubation (activation) buffer at 37℃ with 5% CO2 overnight, to renature the proteins. The gel was stained with Coomassie brilliant blue and washed with destaining buffer. The stained gels were then photographed to visualise the enzymatic degradation of the substrate (Gelatin). (Chapter 2 Section 2.9)

5.3 Results

5.3.1 Creation of the cell models in Her2(+) cell lines

As shown in Figure 5.1, SKBR3 and HCC1419 cells expressed very low levels of BMP8A transcript (A) and were undetectable for BMP8A protein (B). After transduction using the lentiviral vectors and selection using hygromycin (100 µg/ml) for one-week, stable cell lines were established. The validation experiments clearly showed that both SKBR3 and HCC1419 cell lines had significantly increased expression of BMP8A at both mRNA and protein levels (Figure 5.1).

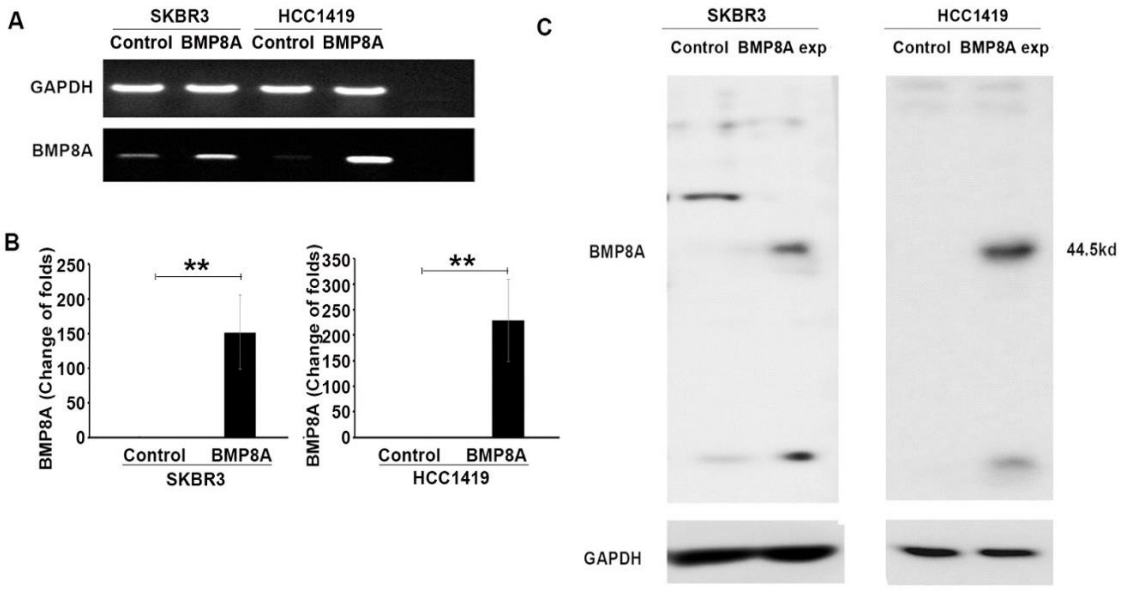

Figure 5.1 Validation of the BMP8A overexpression cell models in Her2(+) cell lines. (A) BMP8A overexpression in SKBR3 and HCC1419 cell models verified using conventional PCR (A), QPCR (B) and Western blot (C). ** P<0.01 vs control cells.

5.3.2 Influence of BMP8A on cellular functions of HER2 positive breast cancer cell lines.

Upregulated BMP8A appears to present a contrasting effect on the growth of SKBR3 and HCC1419. The growth of SKBR3 cells was significantly increased following the over-expression of BMP8A, whilst HCC1419 BMP8A overexpression cells exhibited a reduced growth (Figure 5.2A). No impact on the cell adhesion to Matrigel was observed in either SKBR3 or HCC1419 cell lines following the overexpression of BMP8A (Figure 5.2B).

An increased number of invaded cells was seen in both SKBR3 and HCC1419 cell lines with BMP8A overexpression (Figure 5.2C). However, BMP8A promoted cell proliferation had significant impact on the results of the invasion assay, normalised invasion against corresponding control showed little change in invasiveness of SKBR3 with BMP8A overexpression. In contrast to the SKBR3, the HCC1419 BMP8A overexpression cells presented a remarked increase of invasion, though both SKBR3 and HCC1419 cell lines are less invasive in comparison with some cell lines derived from TNBC and other subtype tumours.

As shown in Figure 5.2D, cell migration was significantly increased following BMP8A over-expression. This increase was evident in the SKBR3 cells over a time course of 28 hours after the wound. For HCC1419 cells, migration was tested using cytocarrier bead assay. Over-expression of BMP8A in HCC1419 cells significantly increased the number of migrated cells when compared with the control cells. Thus, BMP8A demonstrated a profound influence on the migration of HER2 positive breast cancer cells.

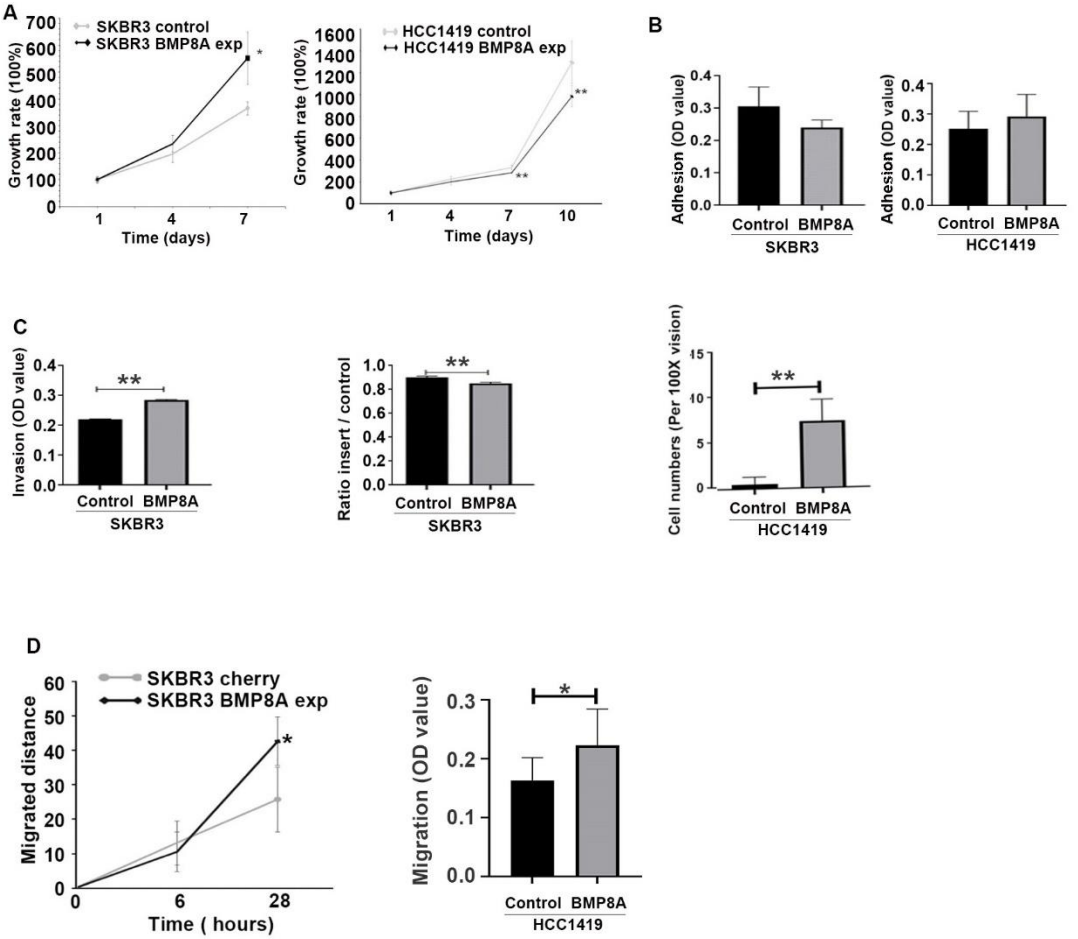

Figure 5.2 Impact of BMP8A on the cell functions of SKBR3 and HCC1419 cells. (A) Influence of BMP8A on the proliferation of SKBR3 and HCC1419 cells. (B) Impact of BMP8A on the cell matrix adhesion of SKBR3 and HCC1419 cells. (C) Invasion of SKBR3 and HCC1419 cells was determined using transwell invasion assay. Normalisation of invasion was performed by calculating a ratio of invasion against corresponding control, where the same number of cells were seeded on a 24-well plate and cultured over the same time course. (D) Cell migration assessed by wound assay in SKBR3 cells and beads assay in HCC1419 cells. * $p<0.05$ vs control.

5.3.3 Involvement of BMP responsive genes in the BMP8A-regulated proliferation of HER2 positive breast cancer cell lines.

BMP8A exhibited contrasting effects proliferation of the two Her2 positive breast cancer cell lines. Some regulatory genes of proliferation are BMP responsive genes including c-MYC, CCND1, ID1 and CCNE1(Clement et al., 2000, Chen et al., 2019). Transcripts of these genes were determined in both SKBR3 and HCC1419 cell lines using QPCR (Figure 5.3 A).

Significantly increased c-MYC and ID1 was found in SKBR3^{BMP8A} cells. This is consistent with the increased cell growth *in vitro* (Figure 5.3). Expression of CCND1 tends to reduce in BMP8A overexpressed SKBR3 cells but did not reach statistical significance. No change was seen for expression of c-MYC, CCNE1 and ID1in HCC1419 sublines.

To further assess the protein expression of these responsive genes, c-MYC was determined by Western blot. From the results, (shown in Figure 5.3B), enhanced c-MYC expression was found in SKBR3^{BMP8A}, whilst decreased c-MYC protein level was found in HCC1419^{BMP8A}.

Expressions of P21 and P27, negative regulators of the cell growth, were also determined by Western blot (shown in Figure 5.3B). A subtle decrease of P27 protein was seen in HCC1419^{BMP8A} cells, whilst P27 protein was undetectable in both SKBR3^{BMP8A} and the control cells. Meanwhile, P21 protein was not visible on the Western blots for neither SKBR3 nor HCC1419 cell lines.

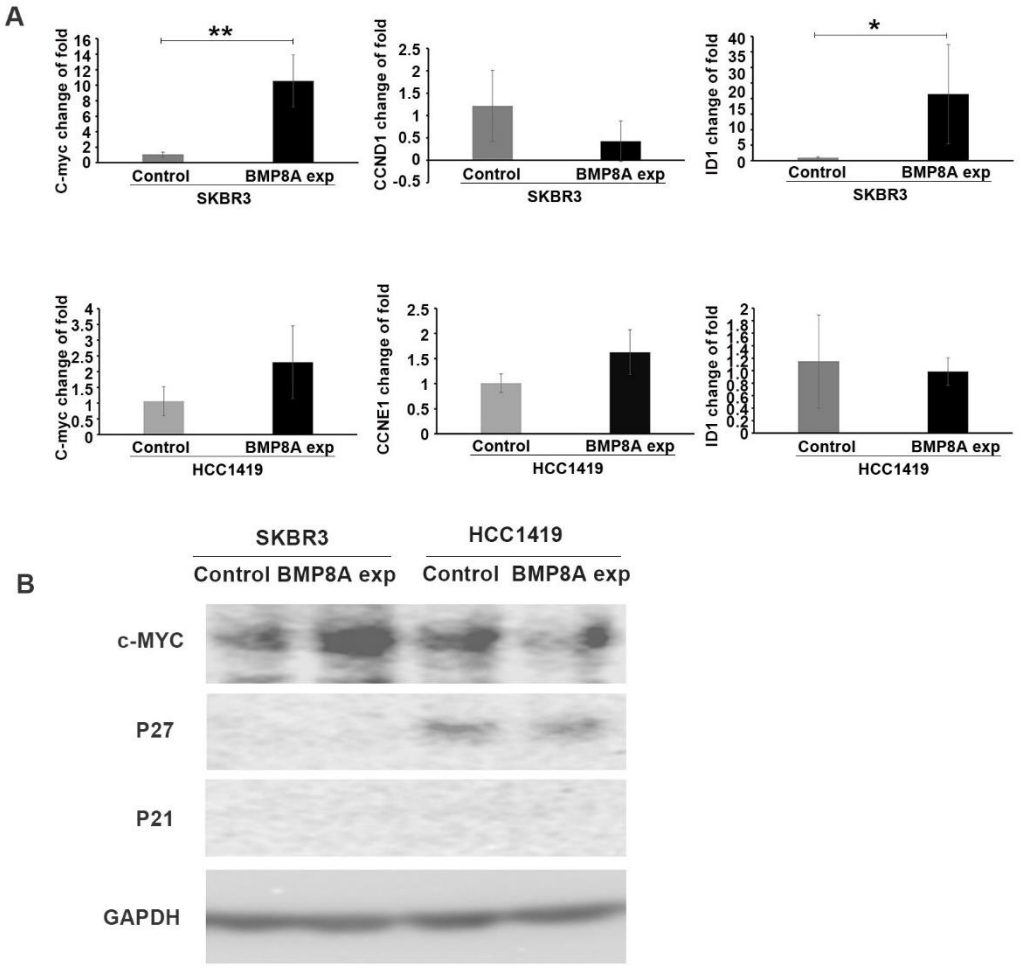

Figure 5.3 Influence of BMP8A on growth regulators in SKBR3 and HCC1419 cells. (A) QPCR presents differential expression of proliferation markers in SKBR3 and HCC1419 cells. (B) Differential expressions of c-MYC, P27 and P21 in SKBR3 and HCC1419 cells by Western blot. ** $P<0.01$, * $P<0.05$.

5.3.4 Influence of BMP8A on cell viability in SKBR3 and HCC1419 cells.

In addition to determining cell population with crystal violet staining, cell counting kit 8 (CCK8) was also employed to assess the influence of BMP8A on the cell viability in HER2 positive cell lines. After 4 days' incubation, absorbance (representing cell viability) in SKBR3^{BMP8A} cells increased significantly compared with the control cells, and the cell viability was also higher in SKBR3^{BMP8A} cells after 7 days' incubation (Figure 5.4A). No significant difference in absorbance was found in HCC1419 cell lines (Figure 5.4B). This indicated that no significant impact on the cell viability was exerted by BMP8A in the HCC1419 cell line, under general culture condition, whilst the cell viability was enhanced significantly by BMP8A in SKBR3 cell line.

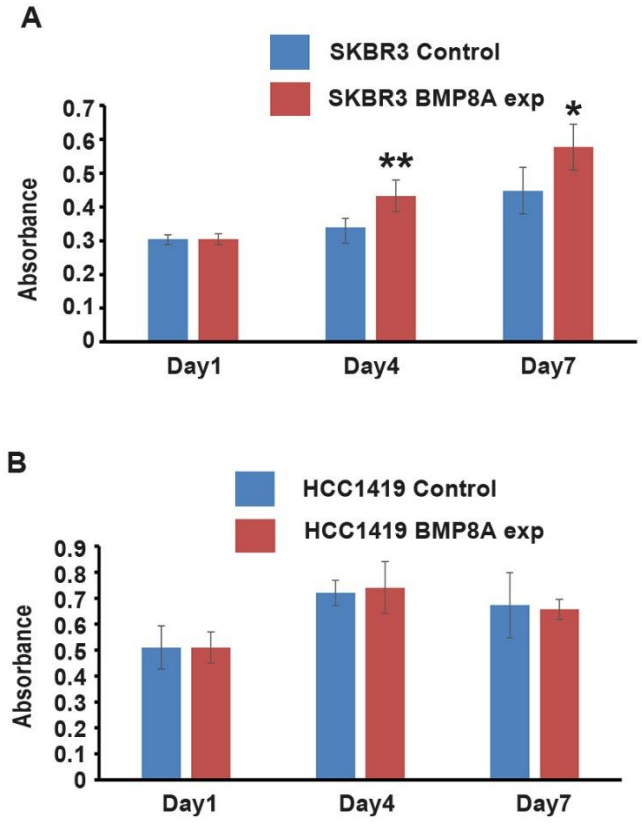

Figure 5.4 Impact of BMP8A on cell viability in HER2 positive cells was determined using CCK8. (A) Absorbance of SKBR3 cells were read after incubation at a wavelength of 450nm. (B) Absorbance of HCC1419 cells were read after incubation at a wavelength of 450nm.

5.3.5 Differential expression of proliferation markers in HER2 positive subtype breast cancer

To further understand if and how BMP8A correlated with the proliferation biomarkers in the HER2 positive breast cancer subtype, bioinformatical analysis was performed in the TCGA-BRCA cohort. Cell proliferation markers and cell cycle markers were analysed for their differential expression in the HER2 positive tumours, from the TCGA cohort according to BMP8A expression. An expression value of BMP8A =370 was employed as a threshold. Their correlation with BMP8A was also analysed using Spearman ranked correlation test. Compared with the BMP8A low expression group, 13 cycle markers were significantly upregulated, whilst 3 genes were also downregulated in the tumours with higher expression of BMP8A (Figure 5.5A and B). Levels of cell proliferation markers, including MKI67 ($r=-0.110$, $P>0.05$) and PCNA ($r=-0.458$, $P<0.01$) were inversely correlated with BMP8A expression (Figure 5.5C). CCNB3 ($r=-0.466$, $p<0.01$), CCNC ($r=-0.488$, $P<0.01$) and CCNA2 ($r=-0.414$ $P<0.01$) were the top three cell cycle regulators inversely correlated with BMP8A expression (Figure 5.5). CDKs are also important cell cycle regulators, from the present analysis, CDK1 ($r=-0.387$, $P<0.05$) and CDK20 ($r=-0.393$, $P<0.05$) were also highly negatively associated with BMP8A (Figure 5.5 D).

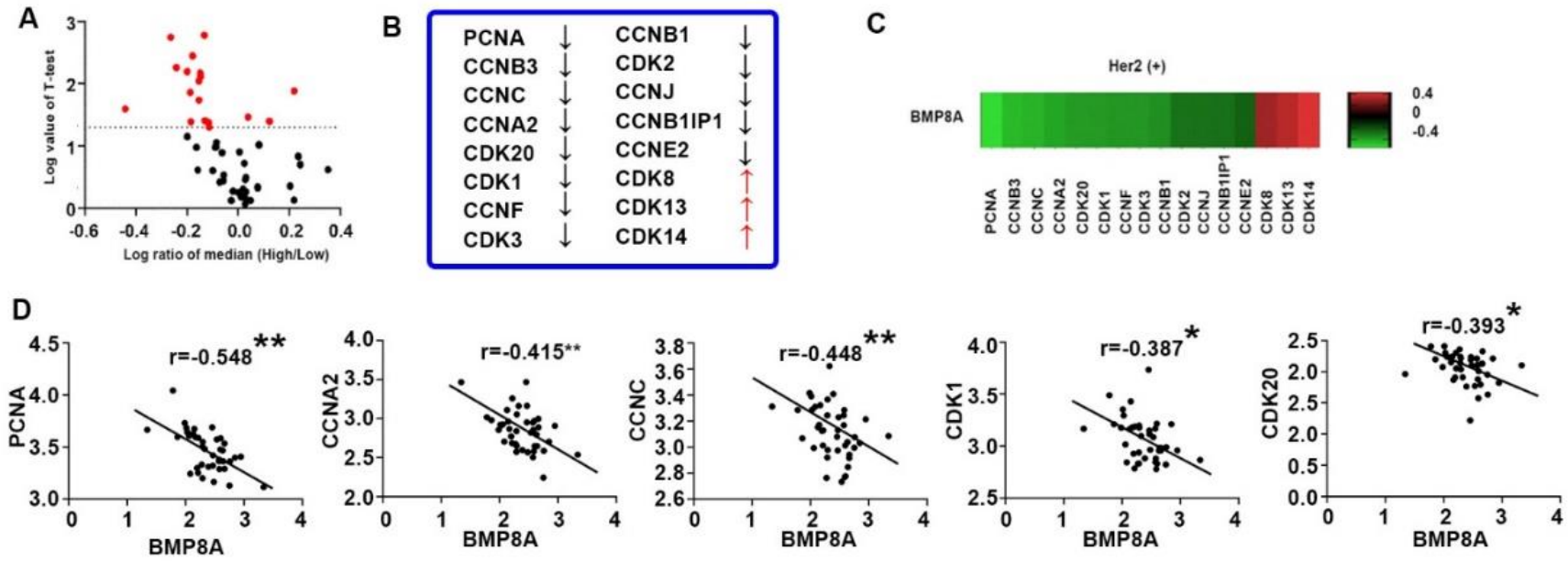

Figure 5.5 Cell cycling regulators associated with BMP8A in TCGA-BRCA cohort of HER2 positive breast cancer. (A) Volcano plot to show differential expression of cell proliferation markers with altered BMP8A expression. A cut off value of BMP8A=370 was employed for the analysis of differentially expressed genes. (B) Summary of the differential expression of cell proliferation markers. (C) Heatmap to present the correlation between BMP8A and the candidate proliferation markers. (D) Scatter plot to show the association between BMP8A and the candidate proliferation markers. ** $p<0.01$, * $p<0.05$.

5.3.6 BMP8A and cell's responses to cytotoxic drugs in Her2(+) breast cancer cells

As demonstrated in the last few sections, BMP8A influenced cell growth of HER2 positive subtype cancer. The question arose as to whether BMP8A influences the response of the cancer cells to chemotherapy? Analyses were performed to evaluate a possible role for BMP8A, in patients with HER2 positive tumours, on their responses to systemic therapy, including adjuvant chemotherapy, neoadjuvant chemotherapy and endocrine therapy, using the KM-plot. Higher expression of BMP8A is associated with poorer overall survival in patients with HER2 positive tumours, who received systemic therapy (including endocrine therapy, target therapy and chemotherapy) and neoadjuvant chemotherapy only (Figure 5.6A, B, C). To further explore the possible mechanism of chemotherapeutic resistance in HER2 positive tumours, expressions of cell stemness markers including CD34, CD133 and CD44 were determined in SKBR3 and HCC1419 cells (Figure 5.6D). Increased CD133 expression was seen in $HCC1419^{BMP8A}$ cells, whilst CD44 expression decreased in association with upregulated BMP8A expression in HCC1419 cells. CD133 expression reduced in $SKBR3^{BMP8A}$ cells, with no significant differential expression of CD34 nor CD44 observed in SKBR3 cells, with altered BMP8A expression.

Response to chemotherapy drugs was determined in the current study. No obvious change was seen in the cell viability of either SKBR3 or HCC1419 cells after exposure to DTX over 3 days. (Figure 5.7A and 5.7B). However, over-expression of BMP8A in both SKBR3 and HCC1419 cell lines rendered them more sensitive to 5-FU in which the response was more prominent in SKBR3 cells in comparison with the HCC1419 cells (Figure 5.7C). This would thus indicate that high BMP8A expression increased the sensitivity to 5-FU in HER2 positive cells, at least in SKBR3 and HCC1419 cells.

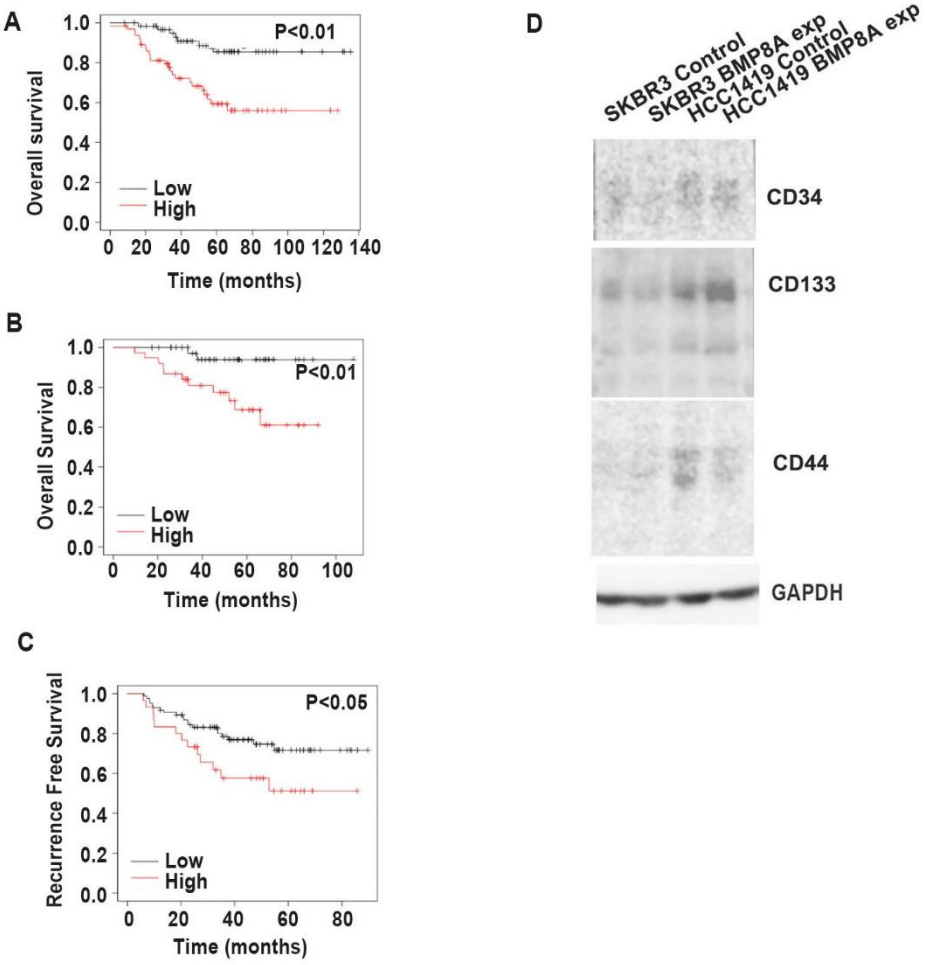

Figure 5.6 Cell's responses to cytotoxic drugs in Her2(+) breast cancer cells with altered BMP8A. (A) Differential overall survival of patients who accepted systemic treatment. (B) Differential overall survival for patients with following neoadjuvant therapy only. (C) Recurrence free survival for the patients following neoadjuvant therapy. (D) Expression of Stemness markers in HER2 positive cells with altered BMP8A expression.

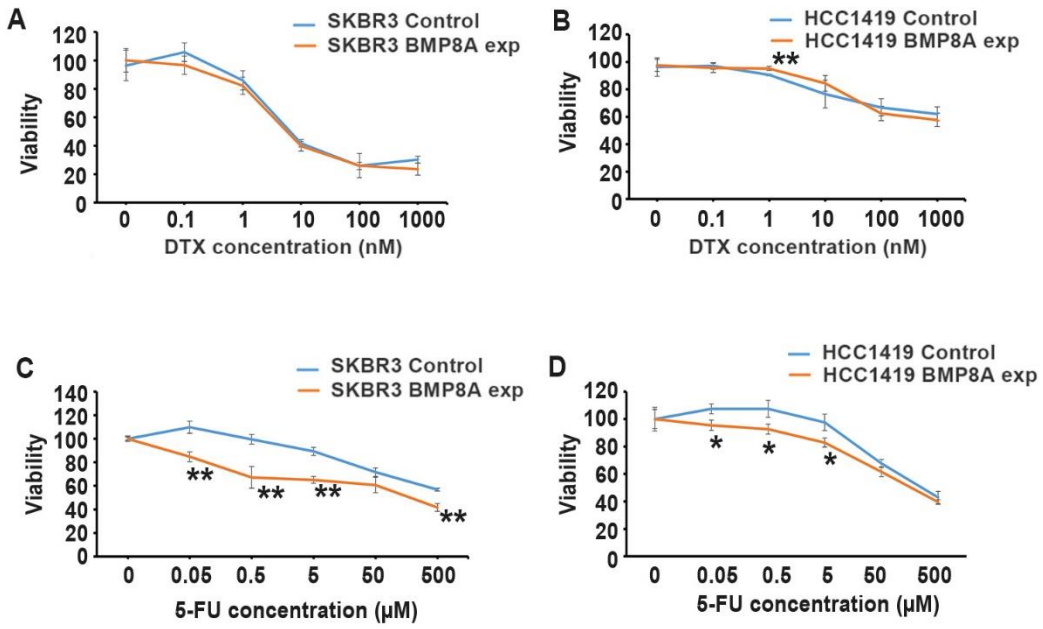

Figure 5.7 Influence of BMP8A on chemotherapeutic drugs. Cell response to DTX (A) and 5FU (C) in SKBR3 cells. Cell response to DTX (B) and 5FU (D) in HCC1419 cells.

5.3.7 Influence of BMP8A on EMT in HER2 positive breast cancer cells

As presented in Section 5.3.2, over-expression of BMP8A in HER2 positive breast cancer cells elicited changes in cellular migration and, to a minor degree, on cell invasion. EMT markers including Snail, Slug, CDH2 and VIM were determined, at gene transcript level by QPCR and at protein level by Western blot, in SKBR3 and HCC1419 cells and in the sublines with BMP8A over-expression. Upregulated Snail, but not Slug, was found in $SKBR3^{BMP8A}$ cells (Figure 5.8A). Downregulated Vimentin was also found in in $SKBR3^{BMP8A}$ cells (Figure 5.8A). Snail and Slug transcripts were also increased in HCC1419 cells (Figure 5.8A). At protein level, upregulated Snail and Slug expression were also found in HCC1419 cells at the protein level (Figure 5.8B), whilst little change at protein levels for both Snail and Slug was evident in the $SKBR3^{BMP8A}$ cells, though high abundance of Snail protein was seen in the SKBR3 sublines. No significant differential expression of CDH2 was found at gene or protein level in either cell line. Analysis from the TCGA-BRCA cohort was also performed to validate the current finding, both Snail ($r=0.474$, $P<0.01$) and Slug ($r=0.36$, $P<0.01$) presented high correlation scores with BMP8A in HER2 positive tumours from the TCGA cohort (Figure 5.8C).

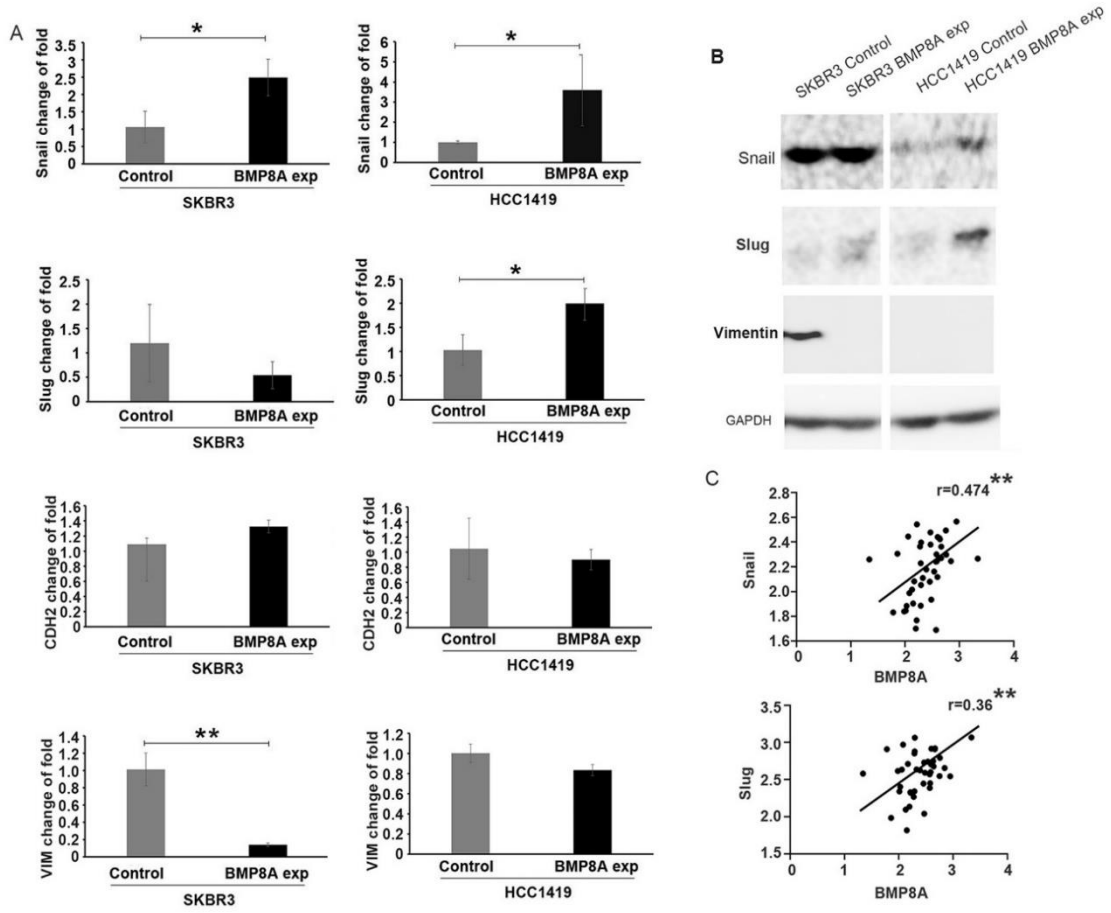

Figure 5.8: Impact of BMP8A on EMT in HER2 positive cells. (A) Altered EMT marker transcripts in SKBR3 cells and HCC1419 cells. (B) Differential Snail, Slug and Vimentin expression in SKBR3 and HCC1419 cells. (C) Scatter plot to show the correlation of BMP8A with Snail and Slug in TCGA-BRCA cohort. * P<0.05, ** P<0.01.

5.3.8 Involvement of MMPs in BMP8A promoted cell motility

In addition to EMT, the influence of BMP8A on MMPs has also been evaluated for their possible involvement in BMP8A coordinated cell motility of HER2 positive breast cancer cells. Over-expression of BMP8A resulted in increased expression of MMP3, MMP7 and MMP14 in SKBR3 cells, whilst these MMPs were barely detectable in HCC1419 cells (Figure 5.9A). Increased expression of MMP3 in SKBR3 was also evident in the following QPCR analyses (Figure 5.9B). Furthermore, zymography analysis, with gelatine as substrate, showed increased activity of MMP2 and MMP9 in the SKBR3^{BMP8A} cells (Figure 5.9C).

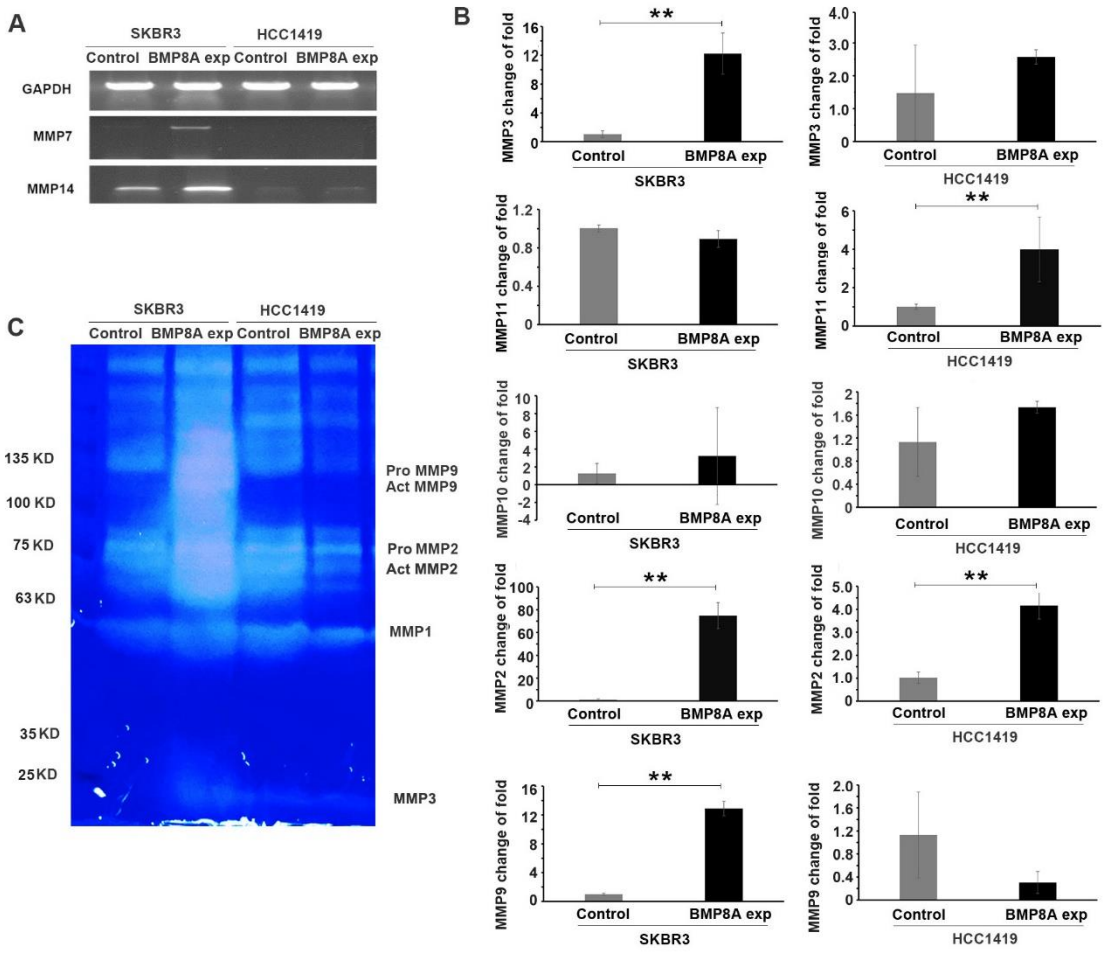

Figure 5.9 Influence of BMP8A on MMPs in HER2 positive cells. (A) Conventional PCR to show the differentially expressed MMPs in SKBR3 and HCC1419 cells. (B) QPCR to present differential expression of MMPs in SKBR3 cells and HCC1419 cells. (C) Expressions of MMPs were determined by zymography with gelatine as substrate.

5.4 Discussion:

The BMP signalling pathway has been shown to cooperate with Her2 signalling to promote cancer progression (Siegel and Massague, 2003). Highly expressed BMPs, or BMPRs in the Her2 (+) breast cancer murine model, increased the mortality caused by metastases (Muraoka et al., 2003, Muraoka-Cook et al., 2006, Seton-Rogers et al., 2004). Following treatment with trastuzumab, a specific antibody of Her2, migration induced by BMP signalling was intercepted in Her2 (+) breast cancer cells (Ueda et al., 2004), suggesting that the Her2 signal is essential for the transforming effect elicited by BMP signalling.

On the other hand, BMP proteins have been shown to reciprocally regulate the Her2 signal by activating the downstream receptor tyrosine kinases of ErbBs, such as Ras/MAPK (Mulder, 2000) and PI3K/AKT (Yi et al., 2005, Wilkes et al., 2005). Silencing of endogenous BMP signals significantly reduced the proliferation of Ras-transformed cancers (Ventura et al., 2004), indicating that Her2 signal induced tumour progression at least partly relies on the function of the BMP signalling pathway. BMP signals in Her2 (+) breast cancer induced the activation of PI3K to form the Her2/actin/actinin complex, with recruited actin and actinin to phosphorylated Her2. The protein complex coordinates cytoskeletal reformation via Pak2, Rac1 and Vav2 to facilitate cell motility and invasiveness (Wang et al., 2006). BMP signals also facilitate the phosphorylation of Tumour Necrosis Factor, Alpha, Converting Enzyme (TACE) to promote the maturation of EGFR ligands. Activation of EGFR stimulates the Src-FAK pathway to form a complex with integrin and Her2 (Wang et al., 2009) and the further heterodimerisation with Her2 (Wang et al., 2009). Integrin/EGFR/Her2 signalling is closely acting together to regulate invasiveness and morphology of cancer cells (Kass et al., 2007).

The data presented in this chapter has demonstrated a causal relationship between BMP8A expression and two of the key cell functions, namely cell growth and EMT related cell traits (cell invasion and migration) in Her2 (+) breast cancer cells.

BMP8A, cell growth and drug sensitivity

The findings that BMP8A influences the growth and growth regulators are very interesting and appear to be different from that seen with Luminal-B subtype of breast cancer cells to some degree. Whilst possible mechanisms behind this difference between the two subtypes are to be explored in a later chapter (Chapter 7), the impacts on Her2 (+) cells are valuable observations in terms of cancer treatment. One of the consequences of this change may well contribute to the increased sensitivity of Her2 (+) breast cancer to chemotherapy drugs. As shown here, BMP8A over-expression markedly increased the toxicity manifested by 5-FU, arguing a clinical value. On the other hand, this had little impact on the other drug tested, namely DTX. This may suggest that BMP8A may impinge on a mechanism critical to 5-FU and not DTX, thus the effect appears to be drug specific. One possibility may also be that Her2 (+) breast cancer patients tend to have better survival, as a results of improved drug response, in line with BMP8A expression. This would make a worthwhile future study.

The molecular events underlying BMP8A induced cell growth are interesting and may be part of a complex network of cell growth/death signalling. BMP signalling is associated with the proliferation of a variety of tumour cell types. Aberrant BMP expression could make demonstrable alterations in cell-regulation factors, such as cyclinD1 and CDK-interacting protein p27. Increased expression of cyclinD1 and decreased expression of CDK-interacting protein p27 accelerate the cell cycle from the G0/G1 phases toward the S-phase (Besson et al., 2008, Garcia-Alvaro et al., 2015). Activated BMP signalling pathways also modulate expression of other key factors of mitotic checkpoint, including MAD2, TTK, BUB3 and Hec1, which can significantly reverse the mitotic arrest defect (Yan et al., 2012). BMPs also promote tumour proliferation by co-acting with tumour stimulating factors. In the presence of conditioned media, derived from cancer-related fibroblasts *in vitro*, BMP2 enhanced the proliferation, as well as multi-drug resistance, of breast cancer cells (Tan et al., 2016). Co-acting with epidermal growth factor (EGF), fibroblast growth factor (FGF) and hepatocyte growth factor (HGF), BMP4 facilitated the proliferation of breast epithelial cells (Montesano et al., 2008).

The present study presented a more complex picture on BMP8A and cell growth, for example a contrasting role for BMP8A was found in SKBR3 and HCC1419 cells, despite both being Her2 (+). Further investigation of the molecular mechanism of BMP8A signalling transduction, in SKBR3 and HCC1419 cells, will be further

investigated in Chapter 7.

Cancer stem-like cells (CSCs) are a small proportion of tumour-initiating cells, presenting properties of classic stem cells, which are depicted as immortal, possessing self-renewal capacity (Dalerba and Clarke, 2007, Liu et al., 2016a) and are resistant to chemotherapies (Liu et al., 2016b). CSCs remain in a mainly dormant status in both the primary lesion and secondary lesion, which are often insensitive to chemotherapy (Yang et al., 2016, Martinez and Zhang, 2013). This indicates a small number of CSCs survive after chemotherapy, leading to drug resistance and high rates of recurrence. In the present study, Increased CD133 expression was observed in HCC1419^{BMP8A} cells, which indicated that upregulated BMP8A may help some HER2 positive cells remain in a dormant status, to escape elimination by chemotherapeutic drugs and lead to a recurrence in the future.

The data presented here, on BMP8A and EMT related cell traits, has some degree of similarity to the data presented in Chapter 4 on luminal-B breast cancer cells, mainly seen as changes of cellular migration and *in vitro* invasiveness. The two subtypes also share some common mechanisms underlying BMP8A, namely metalloproteinases and EMT transcription factors, Snail and Slug. These are known factors that drive the EMT process and appear to be a commonly adopted mechanism by both Her2(+) and Luminal-B breast cancer cells.

In summary, upregulated BMP8A expression promotes the migration of SKBR3 and HCC1419 cells *in vitro* via influencing MMPs and EMT, BMP8A also regulates cell proliferation and their sensitivity to chemotherapy drugs. C-MYC appears to play a role here. BMP8A also enhances the cancer stemness in HER2 positive cells, which is likely associated with recurrence of the disease. The regulatory mechanism, underlying the contrasting roles of BMP8A in the two HER2 positive cell lines, will be further explored in Chapter 7.

Chapter 6

Role of BMP8A in TNBC and its involvement in bone metastasis

6.1 Introduction

Triple-negative breast cancer (TNBC) is a heterogeneous group of breast cancers characterised as the absence of ER, PR and HER2. It is more frequently seen in younger patients (less than 50 years), accounting for 10% to 20% of invasive breast cancers (Kumar and Aggarwal, 2016). Although TNBC is sensitive to chemotherapy, prognosis of this subtype is the worst compared with other subtypes due to lack of therapeutic targets. According to a follow-up study, the recurrence risk reaches the peak at 3 years after surgery and metastatic relapse is higher than the other subtypes with shorter survival (Kumar and Aggarwal, 2016).

BMP signalling is actively involved in disease progression and metastasis of TNBC. For example, BMP6 was found to promote the expression of E-cadherin in MDA-MB-231 cells, mediating cell adhesion (Yang et al., 2007). Hypermethylation of BMP6 was observed in the ER negative breast cancer specimens and was also detected in MDA-MB-231 cells (Zhang et al., 2007). BMP6 reduced invasiveness of MDA-MB-231 cells through a downregulation of MMP1 at both mRNA and protein level (Hu et al., 2016). Similarly, BMP4 reduced the expression of MMP9 in TNBC cell lines including MDA-MB-231 and MDA-MB-468 (Laulan and St-Pierre, 2015). In addition to regulating MMPs, BMP2 enhanced oestradiol-stimulated proliferation of MDA-MB-231 cells via an upregulation of ERα-36 (Wang et al., 2012).

Previous analysis in Chapter 3 revealed that high BMP8A expression was associated with poorer overall survival and poorer distant metastasis free survival in the TNBC subtype. To further elucidate the subtype specific role of BMP8A and its involvement in bone metastasis in TNBC cells (the subtype with the highest incidence of bone metastasis), lentiviral vector carrying the coding sequence of human BMP8A was also employed to manually alter BMP8A expression in MDA-MB-231 cells. Following cell functional analysis *in vitro,* the responsive genes for the altered cell function(s) and signalling pathway(s) were investigated. Furthermore, the cells were also exposed to the bone environment (mimicked by the conditional medium from the hFOB1.19 cell line and bone matrix extract) to determine the differential cell response and altered cellular function.

6.2 Material and Method

6.2.1 Cell lines

MDA-MB-231 cell lines were used in the current research to investigate the impact of BMP8A in TNBC. Wild type MDA-MB-231 cell line were cultured in DMEM medium with 10% FBS and antibiotics. The stably transfected MDA-MB-231 cell lines were cultured in selection medium containing 100µg/ml hygromycin. After approximately one week of selection, maintenance medium with 50µg/ml hygromycin was used to maintain the cells. An osteoblast cell line, hFOB1.19 (ATCC) was also employed in the present study to evaluate its impact on the cellular functions of breast cancer cells.

6.2.2 Overexpression of BMP8A in MDA-MB-231 cells

Both lentiviral BMP8A expression vector and corresponding control vector were used to facilitate BMP8A overexpression in MDA-MB-231 cells following a previously described procedure (Chapter 2 section 2.10.3).

6.2.3 RNA isolation, cDNA synthesis, RT-PCR, and Q-PCR

RNA extraction and subsequent cDNA synthesis from the cell models was undertaken strictly according to the protocol (Chapter 2 section 2.6.1). Following this, conventional PCR and Q-PCR were performed (details were depicted in chapter 2 section 2.1). GAPDH was used as the house-keeping gene, the primer sequences designed for GAPDH, BMP8A and other target genes are listed in chapter 2 (Table 2.2).

6.2.4 Protein extraction, SDS-PAGE, and Western blot analysis

Following protein extraction using lysis buffer and protein quantification using the DC Protein Assay kit (BIO-RAD, USA), the proteins were separated by SDS-PAGE and transferred onto PVDF membranes using a semi-dry transfer method. Followed transfer, the membrane was blocked, incubated with specific primary antibodies overnight and, subsequently, the corresponding secondary antibodies to probe the target protein. Finally, after membrane washing, the protein bands were visualised using the chemiluminescence detection kit (Luminate Forta Western HRP substrate, Cat. No. WBLUF0500, Merck-Millipore, Hertfordshire, UK) and the chemiluminescent tagged bands was visualised with UVITech Imager (UVITech Inc., Cambridge, UK). Details for procedures and the antibodies applied in current study are listed in chapter 2 (Table 2.4).

6.2.5 *In vitro* cell proliferation assay

Three thousand MDA-MB-231 cells in 200 µl medium were seeded in three 96-well-plates and incubated at 37℃ with 5% CO2 for 1, 3, 5 days respectively. Each cell line was repeated for six wells. Following incubation, the cells were fixed using 4% formalin and stained using crystal as documented in chapter 2. After dissolving the crystal violet stain using acetic acid, the absorbance was read using a spectrophotometer (BIO-TEK, Elx800, UK) at the wavelength of 590nm (Full details outlined in chapter2 section 2.9.1).

6.2.6 *In vitro* cell adhesion assay

Ninety-six well plates were precoated with Matrigel before performing the cell adhesion assay through seeding 30,000 MDA-MB-231 cells onto the plate, as depicted in chapter 2 (Section 2.9.2). The absorbance was read to assess the cell adhesion.

6.2.7 Cell invasion assay

Thirty thousand cells (MDA-MB-231) were seeded in the insert on 24-well plate, precoated with Matrigel. After three days' incubation at 37℃ with 5% CO_2, the insert and control well were fixed and further stained with crystal violet. Absorbance was read to determine the levels of cell invasion within control and BMP8A overexpression cells.

6.2.8 Cell migration assay

MDA-MB-231 cells were seeded on a 24-well-plate followed by an overnight culture to form a monolayer. Wounds were made using a fine pipette tip. Migration of cells was monitored using the EVOS over a course of up to 6 hours. Full protocol details are outlined in chapter 2 (Section 2.9.3).

6.2.9 Zymography

Following quantification of cell numbers, the same amount of control and BMP8A overexpression MDA-MB-231 cells were seeded onto a 6-well-plate to achieve 90% confluence overnight. Fresh medium (400 µl) was added into the well and collected after 8 hours' incubation. Non-reducing buffer was added into the conditional medium. This was followed by electrophoresis with gelatin in the SDS-PAGE. The gel was then washed with washing buffer and incubated with incubation buffer at 37℃ with 5% CO_2 overnight. The gel was stained with Coomassie brilliant blue and washed with

destaining buffer before capturing images of the developed bands.

6.2.10 Preparation of bone matrix extract (BME)

Femoral heads were taken following hip replacement in the Trauma and Orthopaedic Department of University Hospital of Wales and Llanddough Hospital and was crushed into fragments. The fragments were further processed using a Bioruptor (Diagenode, Seraing, Belgium) before adding PBS buffer. After centrifugation at 1600rpm for 10 minutes, supernatant was collected. Total protein content of the bone matrix extracts (BME) was then quantified using a Bio-Rd DC protein assay kit (Bio-Rad Laboratories, Hemel Hempstead, UK) before being standardised to 2 mg/ml. The BME was stored at -80°C for further use (full details are described in chapter 2, section 2.13).

6.2.11 Collection of the conditional medium (CM) from hFOB cells

Once cell confluence of hFOB cells reached 80% of the T25 flask, medium was aspired and fresh medium, without phenol red, was added after rinsing with PBS twice. Following incubation with the fresh medium for 6 hours at 37℃ with 5% CO_2, the supernatant was collected, filtered to remove the debris and stored at -80℃ for further use.

6.3 Results

6.3.1 Creation of the cell models in MDA-MB-231 cells

The early screening of BMP8A in breast cancer cell lines (shown in the Chapter 3) indicated that MDA-MB-231 cells presented low expression of BMP8A. An overexpression model was employed to examine the role of BMP8A using the MDA-MB-231 cell line and the lentiviral BMP8A expression vector as described in previous chapters. Following selection using hygromycin, increased expression of BMP8A in the transduced MDA-MB-231 cells was confirmed with both conventional PCR (Fig. 6.1 A) and QPCR (Fig. 6.1 B). These cells also produced high levels of BMP8A protein (Fig. 6.1C).

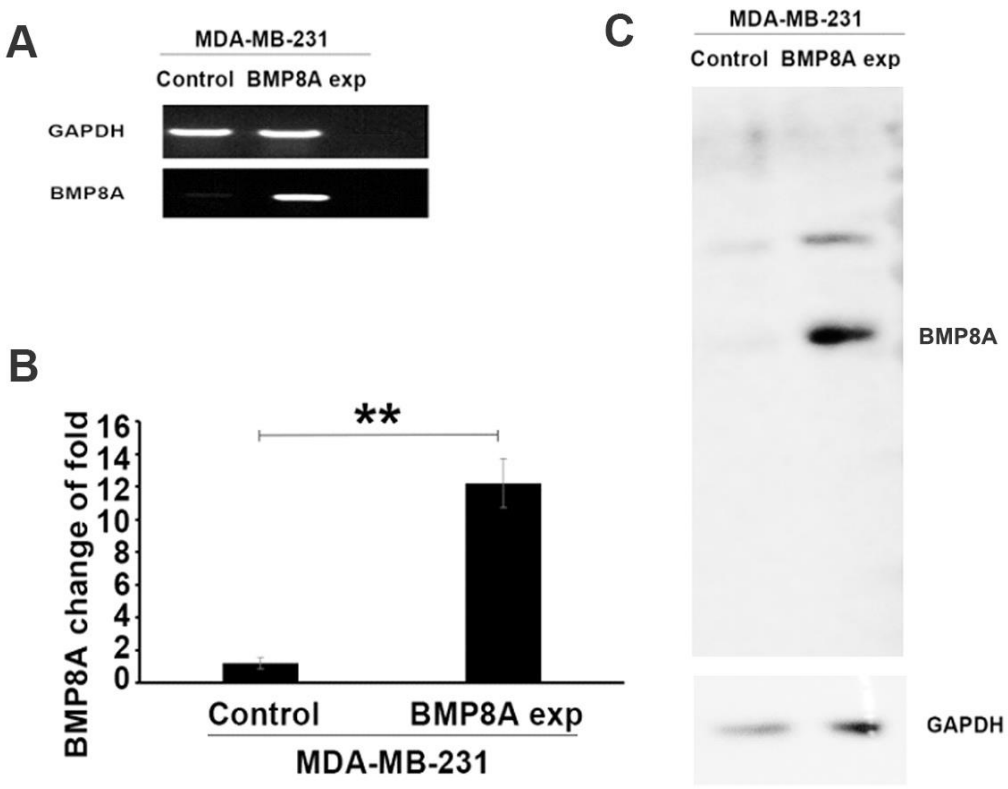

Figure 6.1 BMP8A overexpression in MDA-MB-231 cell line was verified using conventional PCR (A), QPCR (B) and Western blot (C). The values of QPCR were shown as mean and STD. ** $P<0.01$. The folds were calculated using ΔCT.

6.3.2 Impact of BMP8A on cellular functions of MDA-MB-231 cells.

Following the establishment of the MDA-MB-231 BMP8A overexpression model, *in vitro* cellular function assays including proliferation, adhesion, invasion, and migration were performed. After an incubation up to 5 days, no significant change in cell growth was seen in the MDA-MB-231 BMP8A overexpression cells (Fig. 6.2 A). BMP8A overexpression resulted in an increase of invasiveness in the MDA-MB-231 cells (Fig. 6.2 B). No significant change was observed in the adhesion of MDA-MB-231 BMP8A cells to Matrigel compared with the control cells (Fig. 6.2 C). In addition to the enhanced invasion, cell migration was also increased significantly in MDA-MB-231 cell with high expression of BMP8A (Fig. 6.2 D).

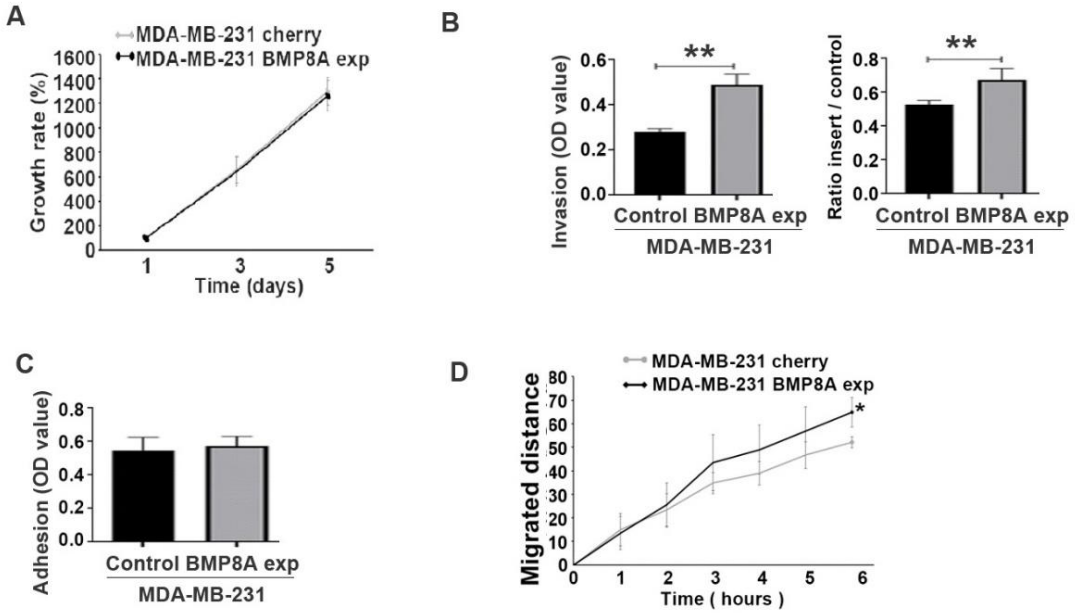

Figure 6.2 Influence of BMP8A overexpression on *in vitro* cellular functions of MDA-MB-231 cells. (A) A colorimetric proliferation assay using crystal violet was employed for the evaluation of proliferation affected by BMP8A overexpression. (B) Effect on invasiveness of MDA-MB-231 cells was determined using the transwell invasion assay. (C) Adhesion assays were conducted to assess adhesion of MDA-MB-231 cells to Matrigel. (D) Influence of BMP8A on migration of MDA-MB-231 cells was determined using the migration assay (wound assay). Values presented in the figures are mean and STD. ** $P<0.01$, * $P<0.05$.

6.3.3 Impact of BMP8A on EMT in MDA-MB-231 cells

To explore the influence of BMP8A on EMT, one of the pivotal processes affecting cell motility, expression of the EMT markers including Snail, Slug, Vim and CDH2 were determined for their expression at both mRNA and protein levels. Conventional PCR showed increased expression of vimentin (VIM) and Slug in the MDA-MB-231 BMP8A cells (Fig. 6.3 A), whilst little change was evident in the expression of Snail and N-cadherin (Fig. 6.3 B). A further analysis using Western blot showed increased protein levels of both Slug and vimentin in the MDA-MB-231 BMP8A overexpression cells (Fig. 6.3 C). Correlation between BMP8A and the EMT markers in breast cancer tumours was then analysed using RNA sequencing data of the TCGA breast cancer cohort. BMP8A transcript levels are positively correlated with most the EMT markers including Snai2 (Slug), Twist, Vimentin and N-cadherin, but not Snail (Fig. 6.3 D). Expression of Snai2 (Slug) and Vimentin is also significantly higher in the tumours with higher expression of BMP8A (Fig 6.3 E).

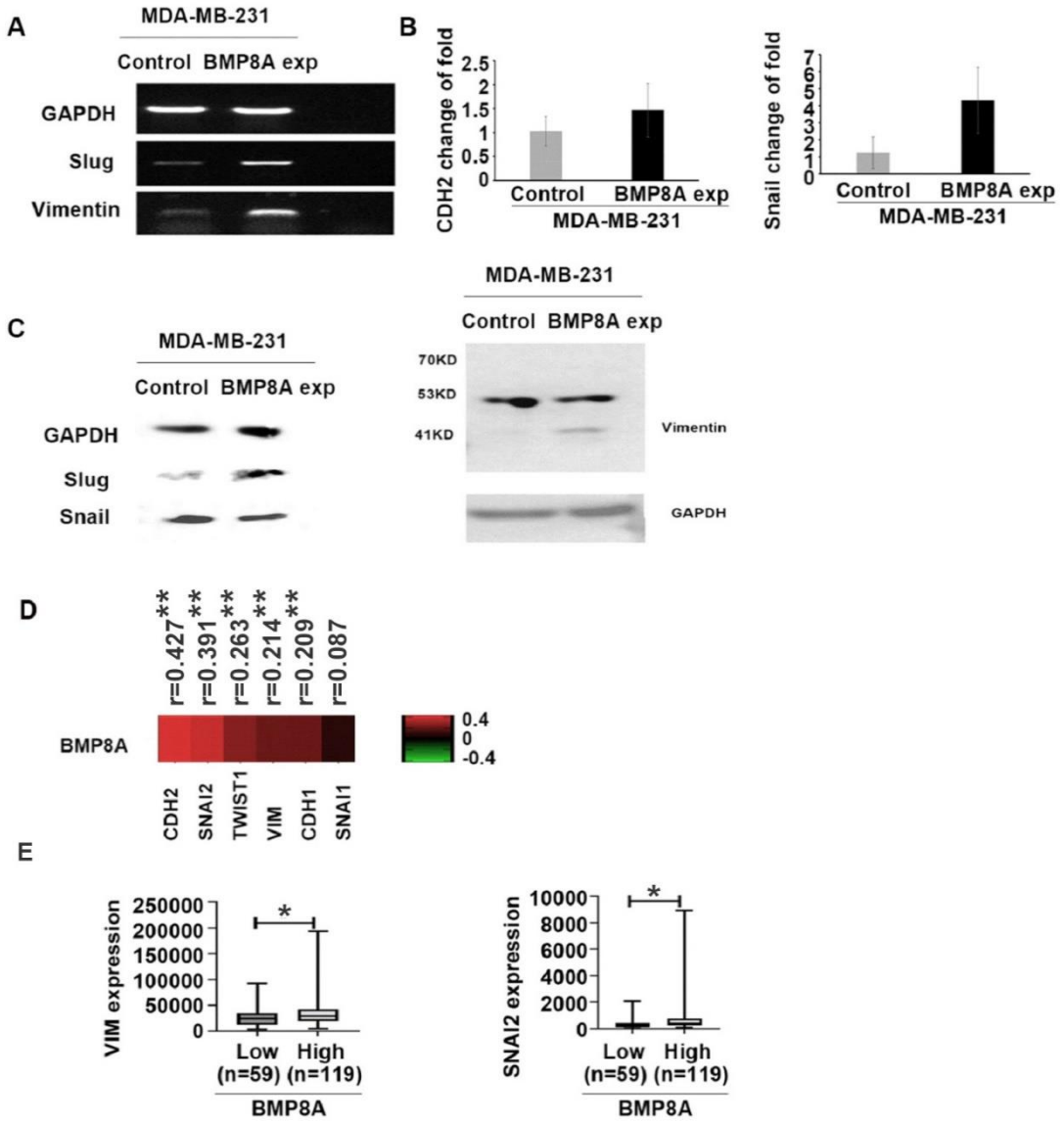

Figure 6.3 Impact of BMP8A on EMT in MDA-MB-231 cell line. (A) Differently expressed Slug and Vimentin were detected using conventional PCR. (B) QPCR shows the expressions of CDH2 and Snai1 in MDA-MB-231 cells. (C) WB presents the expression of EMT markers in MDA-MB-231 cells. (D) Heatmap shows the correlation efficiency between BMP8A and EMT markers in TCGA-BRCA cohort. (E) Differentially expressed VIM and SNAI2 in TCGA-BRCA cohort according to BMP8A expression (cut-off value =128.1).

6.3.4 Influence of BMP8A on MMPs in TNBC.

Influence of BMP8A on the enhanced invasiveness in MDA-MB-231 cells was also investigated by determining the expression of a number of MMPs (Figure 6.4 A and B). Although no significant increases in MMP2 transcript was determined by QPCR (Figure 6.4 B), enhanced MMP2 excretion was observed in MDA-MB-231^{BMP8A} cells compared to control cells according to a gelatin zymography analysis (Figure 6.4 C). There was no obvious change seen for the other MMPs determined in the MDA-MB-231 BMP8A overexpression cells in comparison with the control cells including conventional PCR, QPCR and a gelatin zymography analysis of MMPs released from the MDA-MB-231 cells.

Analysis for the expression of MMPs in TNBC tumours with higher expression of BMP8A was conducted in comparison with TNBC tumours with lower BMP8A expression, similarly to the previous analysis of Snai2 and Vimentin in the TCGA TNBC tumours. A number of MMPs exhibited higher expression in the TNBC tumours with higher expression of BMP8A including MMP2, MMP3, MMP11, MMP14, MMP15 and MMP19. Those MMPs also have a significantly positive correlation with BMP8A in the TNBC tumours of the TCGA cohort (Figure 6.4 C and D). MMP2 was identified as the top molecule associated with BMP8A ($r=0.549$ $P<0.01$), which was consistent with the result in the MDA-MB-231 cell models (Figure 6.4 D).

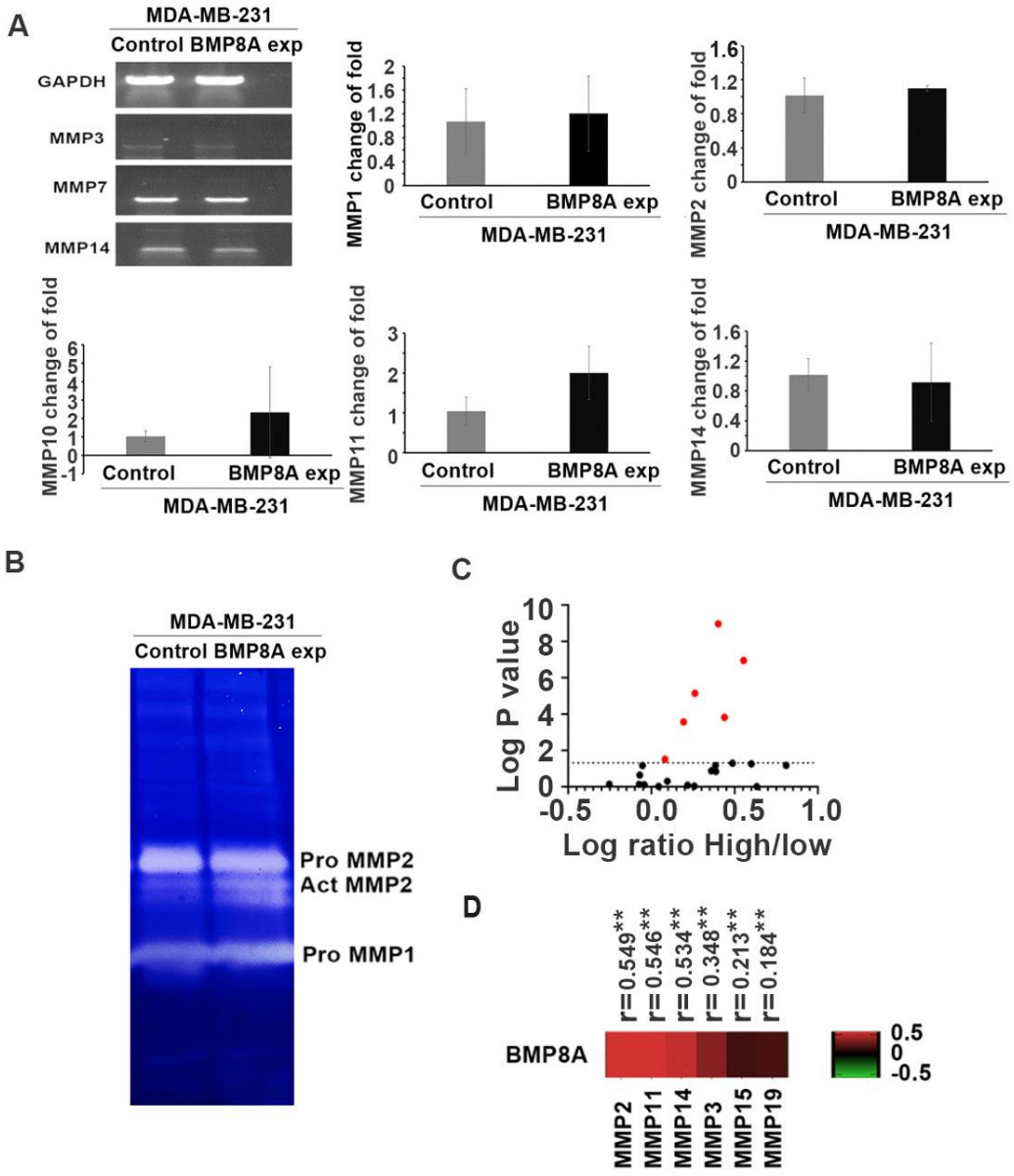

Figure 6.4 BMP8A induced differential MMPs in MDA-MB-231 cell line. (A) Expressions of MMPs in MDA-MB-231 cells determined from conventional PCR and QPCR. (B) Differential MMPs were determined from protein level by Zymography. (C) Differential MMPs identified from TCGA-BRCA cohort according to the BMP8A expression. (D) Heatmap shows the association between BMP8A and differentially expressed MMPs (The red points in figure 6.4 C). ** P<0.01.

6.3.5 BMP8A and bone metastasis in breast cancer (TNBC)

As elucidated in chapter 3, high BMP8A expression in luminal B and TNBC presented poorer distant metastasis free survival (Figure 3.9). To determine the involvement of BMP8A in bone metastasis, expressions of BMP8A in breast cancer with bone metastasis, distant metastasis and no metastasis were analysed in the TCGA-BRCA cohort. No significant differential expression of BMP8A was seen among these groups (Figure 6.5 A). Further analysis was performed to detect the impact of BMP8A in the bone metastasis free survival in the TCGA-BRCA cohort, from the present study, where again no significant difference was found in breast cancer with altered BMP8A expression (Figure 6.5 B).

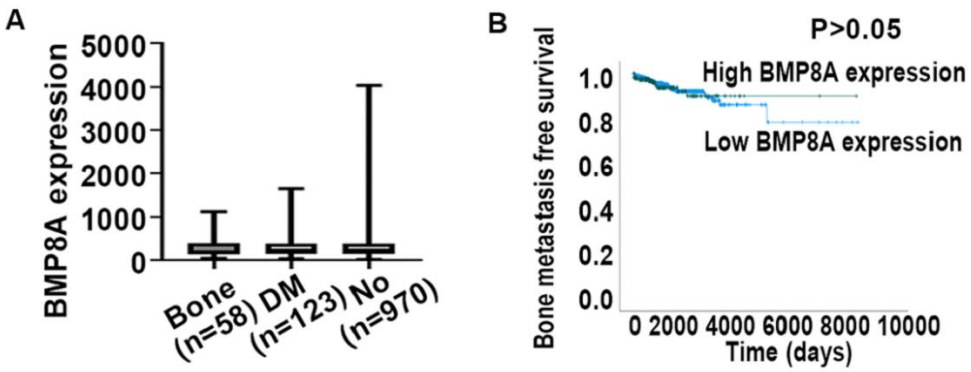

Figure 6.5 Involvement of BMP8A in bone metastasis. (A) Expression profile of BMP8A in patients who developed bone metastases, distant metastases, and no metastases. (B) Correlation between BMP8A and bone metastasis free survival.

To further explore the involvement of BMP8A in bone metastasis, one of the most common complications of BC, in luminal B and TNBC subtypes, the correlation between BMP8A with important biomarkers in bone metastases, including osteoblastogenesis, osteoclastogenesis, homing, immuno-escape and angiogenesis, was analysed. According to the present analysis, BMP8A was highly correlated with most of the osteolytic and osteoblastic markers in both luminal B and TNBC subtypes, especially in TNBC (Figure 6.6 A). High correlation efficiency was also seen with markers for homing and angiogenesis in TNBC. The correlation coefficients were summed up to assess an overall relation between BMP8A and those markers of bone metastasis (Figure 6.6 B), high correlations were found with osteoclastic and osteoblastic markers, especially in TNBC. Correlations of the top three osteoclastic and osteoblastic markers with BMP8A were presented as a scatter plot. Compared with the luminal B subtype, correlation scores were markedly higher in TNBC (Figure 6.6 C), which indicated the potential involvement of BMP8A in bone metastasis in TNBC.

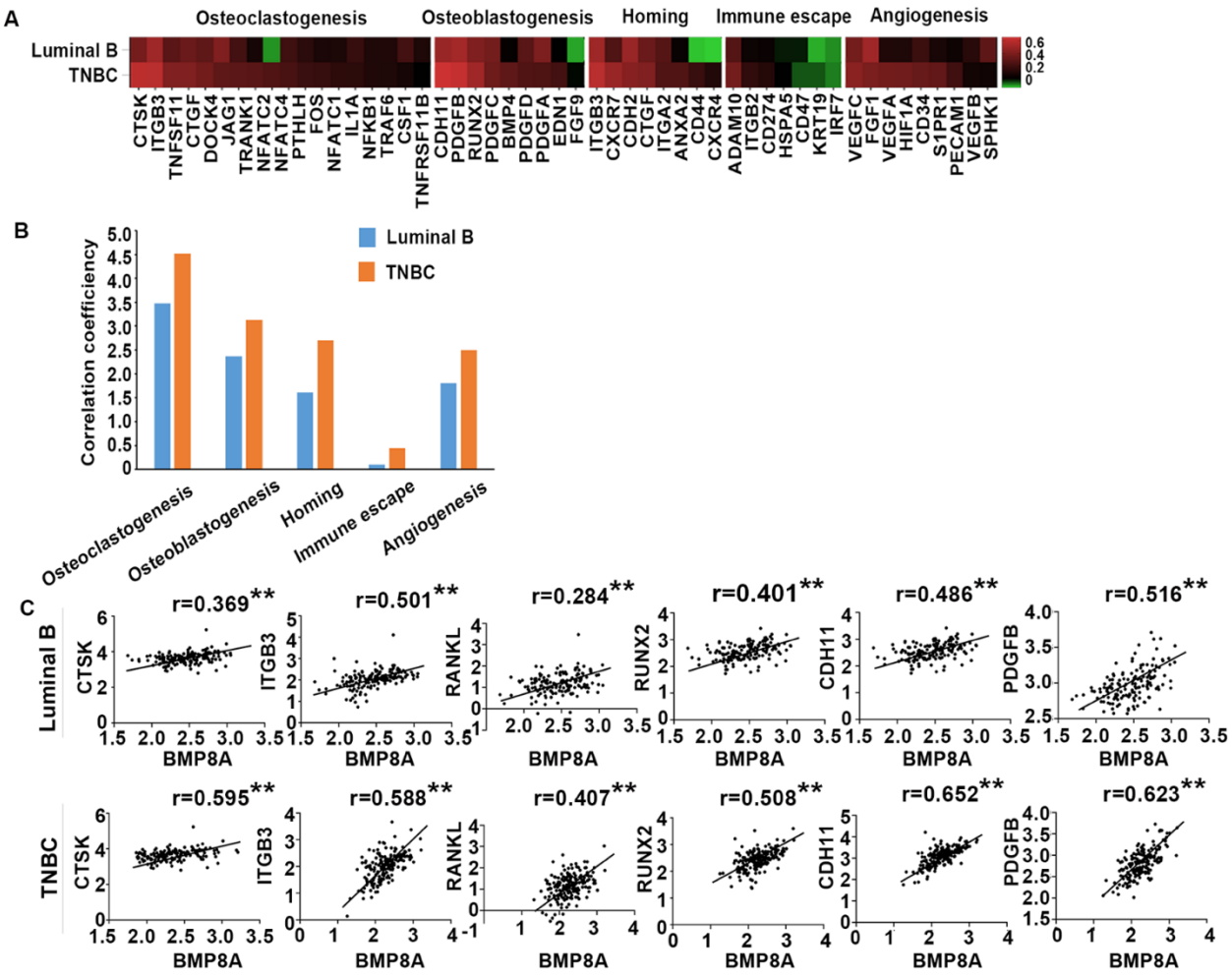

Figure 6.6 Correlation of BMP8A with biomarkers in bone metastasis. (A) Heatmap to show the correlation of BMP8A with bone metastasis in luminal B and TNBC subtypes. (B) Correlation coefficients of BMP8A with biomarkers were summed and presented by bar graph. (C) Scatter plot to show the association between BMP8A and most responsive markers in bone metastasis.

6.3.6 Influence of BMP8A on proliferation and invasion of MDA-MB-231 cells exposed to bone environment *in vitro*

To investigate the involvement of BMP8A in bone metastasis, bone matrix extract (BME) and conditional medium (CM) collected from the supernatant of hFOB cells were utilised to mimic the bone environment. Six thousand MDA-MB-231 cells were seeded in the 96-well-plate and treated with CM in different concentrations (25% and 50%). After 3 days' incubation, proliferation in MDA-MB-231 $^{BMP8A\ exp}$ cells significantly reduced compared with the control cells under the 25% CM concentration ($P<0.05$). Under 50% CM concentration, decreased cell growth was even more obvious when comparing with both control cells and MDA-MB-231 $^{BMP8A\ exp}$ cells maintained in normal medium ($P<0.01$) (Figure 6.7 A). hFOB CM exhibited an inhibitory effect on cell proliferation of MDA-MB-231 cells when BMP8A was overexpressed but not in control cells.

In addition to the tests using the hFOB CM, proliferation assays were also conducted by exposing the MDA-MB-231 cells to BME. After a culture of 5 days, the proliferation of MDA-MB-231 $^{BMP8A\ exp}$ cells was reduced significantly when they were exposed to BME ($P<0.01$), whereas no reduction was seen in the control cells that were treated with the BME. Instead, an increase of proliferation was seen in the control cells when they were cultured in medium containing 50µg/ml of BME (Figure 6.7 B).

Invasion of the MDA-MB-231 cells was assessed *in vitro* with the exposure to the bone environment. Thirty thousand cells were seeded in the plate with conditional medium (50%) and BME (50ug/ml). After 3 days, significantly enhanced cell invasion was found in MDA-MB-231 $^{BMP8A\ exp}$ cells comparing with the corresponding control group (Figure 6.7 C).

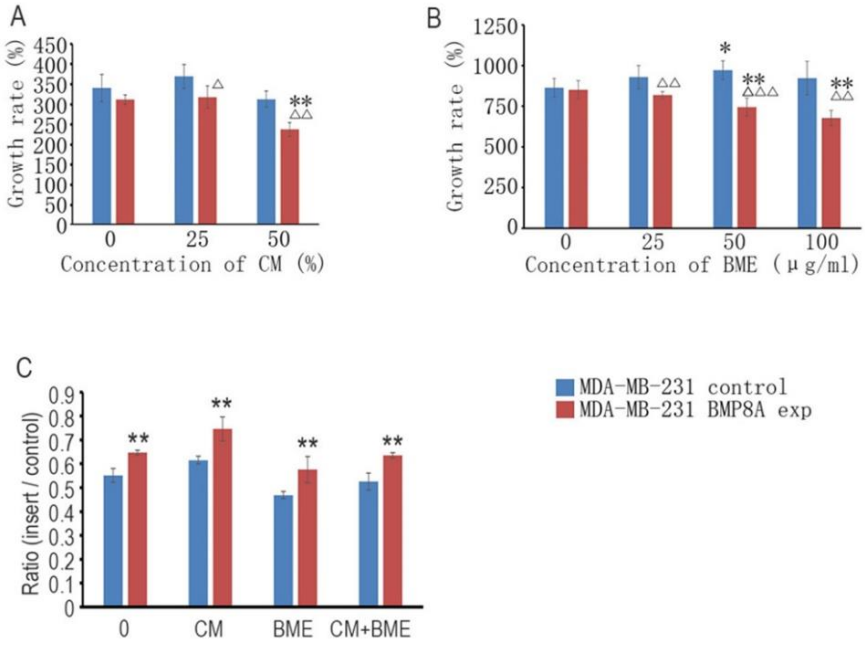

Figure 6.7 Cell response to the bone environment. (A) Impact of BMP8A on cell growth following exposure to different concentrations of conditional medium over a 3-day incubation. (B) Cell growth response to different concentrations of BME after 5 days' incubation. (C) Altered cell invasion following exposure to a bone environment. Δ P<0.05 *VS* concentration 0, ΔΔ P<0.01 *VS* concentration 0, * P<0.05 *VS* MDA-MB-231 ^{control}, ** P<0.01 *VS* MDA-MB-231 ^{control}.

6.3.7 Expression of osteolytic/osteoblastic markers in MDA-MB-231 cells with BMP8A overexpression

To assess the possible role of BMP8A in bone metastasis, expression of promising biomarkers including osteolytic, osteoblastic and angiogenesis were determined in MDA-MB-231 cells. From the present research, increased RANKL expression was found in MDA-MB-231 BMP8A exp cells, which strongly indicated that BMP8A may take part in the bone metastasis via RANKL-OPG signalling (Figure 6.8 A). No differential CTSK, PTHrP, RANK, and VEGF expressions were detected (Figure 6.8 A and C). CDH11, a pivotal molecule mediating the osteoblastogenesis, was increased in the cells with BMP8A overexpression (Figure 6.8 B).

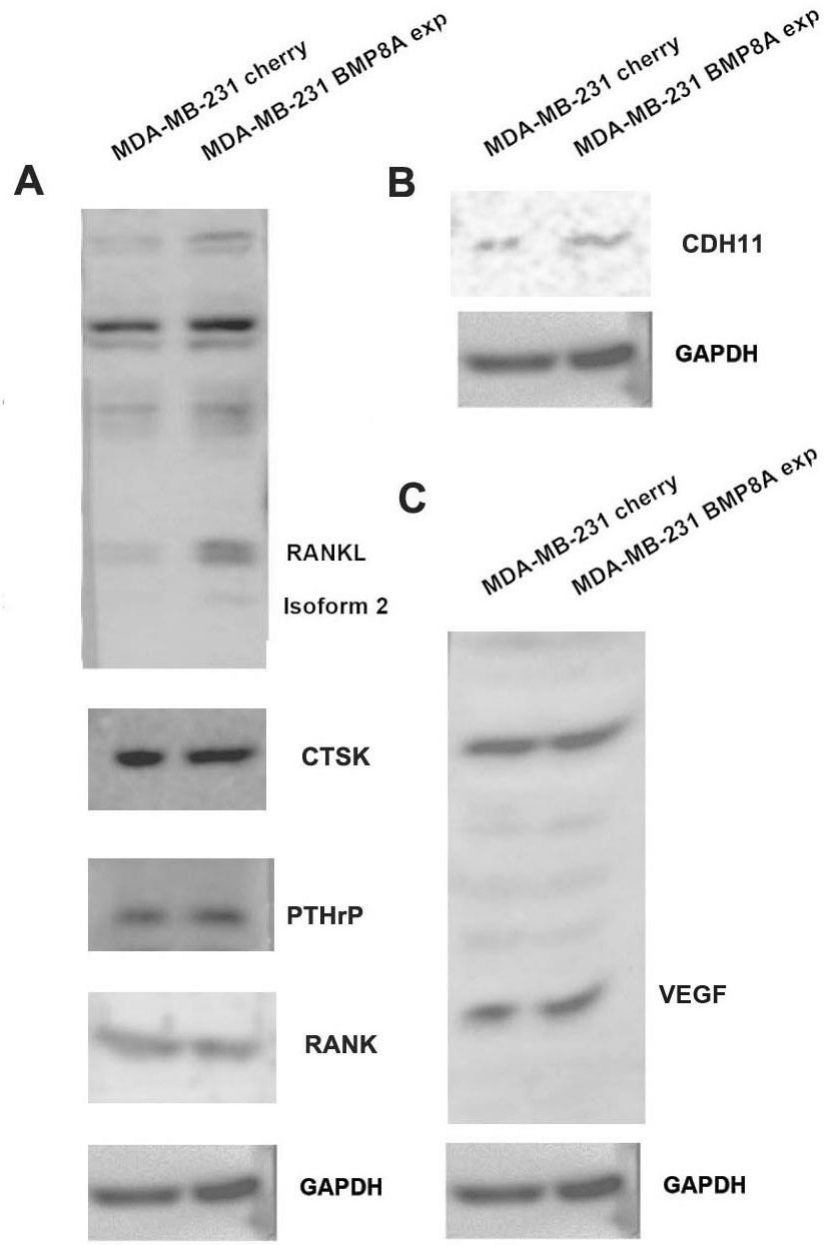

Figure 6.8 Involvement of BMP8A in the bone metastasis of MDA-MB-231 cells. (A) Impact of BMP8A on the expression of the osteolytic marker RANKL. (B) Impact of BMP8A on CDH11 expression, an osteoblastic marker. (C) Expression of VEGF in MDA-MB-231 cells with altered BMP8A expression.

6.4 Discussion

BMP signalling has been evident in the regulation of both proliferation and invasion in TNBC cells. BMP2 exerts an inhibitory effect on cell growth and induces cellular apoptosis of MDA-MB-231 cells (Chen et al., 2012a). By upregulating the expression of microRNA-192, BMP6 was found to induce cell cycle arrest in MDA-MB-231 cells. Cell growth in MMP9 overexpressed MDA-MB-231 cells was significantly inhibited compared to the control cells due to a downregulation of PI3K/AKT signalling pathway (Li et al., 2018). Tumour invasion and migration of TNBC cells were suppressed by interfering BMP signalling (Di et al., 2019). Besides the inhibition on the cell growth, BMP6 was also found to suppress the metastasis of MDA-MB-231 cells by downregulating the expression of MMP1 (Hu et al., 2016) and upregulating E-cadherin (Yang et al., 2007). Cell growth, invasion and motility in MDA-MB-231 BMP10 overexpression cells were significantly suppressed compared with the control cells (Ye et al., 2010). However, the impact of BMP8A in TNBC subtype remains largely unknown.

The present research was the first study to examine the influence of BMP8A on cellular functions of TNBC cells. *In vitro* cellular function tests showed that BMP8A promoted both invasion and migration of MDA-MB-231 cells. This is in line with a finding in chapter 3, that higher expression of BMP8A in TNBC was associated with poorer DMFS, as both invasion and migration are essential for the spread of the disease. Along with this finding, further research on BMP8A mediated cell invasion was performed. As no significant difference was seen in the cell adhesion, the present study focused on the impact of BMP8A on MMPs and EMT transcript factors. BMP8A overexpression resulted in increased expression of certain MMPs including MMP2 and a transcription factor Slug, which is an important EMT factor. It suggests that BMP8A regulated MMPs and EMT may account for the promoted invasion in MDA-MB-231.

In addition to their direct regulation of proliferation, migration and invasion of cancer cells, BMP signalling also exerts fundamental effects during the osteogenic differentiation and homeostasis through regulating the balance of osteoblasts and osteoclasts. BMPs, such as BMP-2, BMP-4 and BMP-7 have been proved to promote the differentiation of the mesenchymal stem cells (MSCs) into osteoblasts (Alarmo and Kallioniemi, 2010, Carreira et al., 2014). BMPs can impact the maturation and the

activation of osteoclasts through RANKL-OPG pathway (Yahiro et al., 2020). In osteolysis caused by osteoclasts, BMPs in the bone matrix are released, which could regulate the expression of CX43/GJA1 through the BMP signalling pathway to interact with osteoblast to adjust mineralization (Shi et al., 2016).

Since BMP8A played a pivotal role in the progression of breast cancer, and breast cancer is well known as a disease prone to bone metastasis, the role of BMP8A in the bone metastasis of BC was explored in the current study. To assess the potential role BMP8A involved in the bone metastasis in BC, bioinformatical analysis in TCGA-BRCA cohort was performed. From the analysis, BMP8A was highly correlated with the biomarkers being profound in the process of bone metastasis, especially osteoblastic (RUNX2, CDH11 and PDGFB) and osteolytic (CTSK, ITGB3 and RANKL) markers, which strongly indicated the promising role of BMP8A in the bone metastasis of BC in TNBC. The influence of BMP8A on cellular functions in the bone environment including cell proliferation and invasion was further evaluated. Following exposure to *in vitro* bone environment, including the conditional medium from hFOB cells and bone matrix extract (BME), the proliferation of BMP8A overexpressing cells was significantly reduced comparing with control cells. The mechanism for the suppressed cell proliferation of MDA-MB-231$^{BMP8A\ exp}$ is yet to be elucidated. As in the present study, enhanced cell invasiveness was found in MDA-MB-231 with BMP8A overexpression, which was even more obvious in an exposure to the *in vitro* bone environment. Preliminary investigations aiming to identify possible responsive genes for TNBC bone metastasis were undertaken and the expression profiles of a panel of osteolytic, osteoblastic and angiogenesis markers were determined. Increased RANKL and CDH11 expressions were seen in the MDA-MB-231 $^{BMP8A\ exp}$ cells. RANKL-OPG signalling is renowned for its importance in osteoclastogenesis, whilst CDH11 is an important molecule for the activation of the osteoblast, being critical for cancer cells to colonise the bone.

Taken together, BMP8A can promote invasiveness of TNBC cells in which MMP2 and EMT are involved. Related signal transduction events will be investigated in the following chapter. BMP8A may act as pivotal molecule responsible for the progression of bone metastasis in breast cancer, both for the initiation of the osteoblast genesis and the activation of the osteolytic bone metastasis. RANKL signalling may be involved in BMP8A mediated bone metastasis. Further research focused on elucidating the

mechanisms underlying the impact of BMP8A in bone metastasis is required in the future. Notably, EGFR signalling is highly expressed in TNBC subtype, which is closely related with tumour progression and survival (Masuda et al., 2012). Involvement of EGFR signalling and its interaction with the BMP8A signalling in TNBC will be further explored in Chapter 7.

Chapter 7

Signal transduction of BMP8A in breast cancer cells

7.1 Introduction

As elucidated in chapter 1, BMP signalling has two patterns of signal transduction, the canonical BMP signalling pathway (Smad dependent pathway) and the non-canonical signalling pathway (Smad-independent pathway). In canonical signal transduction, BMP ligands bind to a complex of serine-threonine kinase transmembrane receptors including type I receptors (BMPRIA, BMPRIB, ActR1, ACVR1B, ACVR1C and ACVRLI) and type II receptors (BMPRII, ActRIIA, and ActRIIB), resulting in a phosphorylation of the type I receptors. The activated receptor complex then recruits and phosphorylates the downstream transcription factors, Smad 1, 5, and 8. Subsequently, phosphorylated Smads1/5/8 form a heteromeric complex with Smad4 which acts as a shuttle to transport the Smad complex into the nucleus (Nickel and Mueller, 2019). In the Smad-independent signalling pathway, BMP ligands present higher affinity for type I receptors than type II receptors. BMP ligands preferentially bind to BMPR1A or BMPR1B, then recruit BMPRII to form the hetero-oligomeric complexes known as BMP-induced signal complex (BISC) (da Silva Madaleno et al., 2020). Depending on the ligands and receptors recruited, the Smad-independent pathway involves the transmission of a variety of other signal pathways, including the MAPK pathway, RAS pathway, PI3K/Akt pathway, Rho-GTPases pathway and so on (Zabkiewicz et al., 2017). Different from the other BMPs, BMP8A can induce activation of both BMP specific R-Smad1/5/8 and TGF-β specific R-Smad 2/3 signal pathways in spermatogonia synchronously (Wu et al., 2017). The former pathway was mediated by receptor complexes formed by the type I receptor（BMPR1A or BMPR1B) and type II receptor (ACVR2A or BMPR2) Whilst Smad2/3 signal pathway was activated through receptor complexes formed by type I receptor (TGFBR1 or ACVR1B) and type II receptor (ACVR2A, ACVR2B or TGFBR2).

As the key molecules to mediate BMP signalling transduction, BMP receptors are quite important in modulating the progression of breast cancer. BMPR1B was identified as the key downstream receptor mediating the activation of BMP/Smad signalling to induce the dedifferentiation and progression of ER positive breast cancer (Helms et al., 2005). Silencing BMPR1A in breast cancer was found to intercept the osteolytic bone metastasis via suppressing the RANKL/P38 signalling pathway (Liu et al., 2018). Upregulated BMP4 transcripts were observed to be correlated with increased

BMPR2 expression in the advanced stage of breast cancer (Gul et al., 2015). N-acetyl-α-galactosaminyltransferase 8 (GALNT8) and its regulated O-glycosylation of BMPR1A can regulate BMP/Smad/RUNX2 signalling to coordinate growth of breast cancer cells (Huang et al., 2022).

Although BMP8A signal transduction in spermatogonia has been well investigated, the role of BMP8A in breast cancer and the mechanism for BMP8A induced altered cell functions have been less studied. Previous analysis of BMPs in the TCGA breast cancer cohort illustrated the higher expression of BMP8A in breast cancers was also correlated with poorer overall survival (Katsuta et al., 2019a). However, no research was performed to test the impact of BMP8A on cellular function of breast cancer. Our research is the first study to evaluate the biological function and the molecular mechanism of BMP8A involved in breast cancer. The present study reveals the subtype involvement of BMP8A in the progression of BC, mainly through its impact on invasion and proliferation *in vitro* and has been summarised in Table 7.1. BMP8A induced cell invasion is mainly through promoting EMT event and degradation of cell matrix via upregulation of MMPs in luminal B, HER2 positive and TNBC subtypes. Contrasting effects on cell proliferation were observed in the HER2 positive cell lines with BMP8A overexpression. The mechanism for the altered cell function and the signalling transduction of BMP8A in breast cancer will be examined in the current chapter.

Table 7.1 Alteration of BMP8A responsive genes in breast cancer cell lines.

		Luminal B				Her2 (+)				TNBC	
		BT474		MDA-MB-361		SKBR3		HCC1419		MDA-MB-231	
		Control	BMP8A exp	Control	BMP8A exp	Control	BMP8A exp	Control	BMP8A exp	Control	BMP8A exp
Cell function Test	Proliferation		—		↑ 20%		↑↑（100%）		↓（30%）		—
	Adhesion		—		↑（15%-30%）		—		—		—
	Invasion		↑30%		↑10%		↑20%		↑		↑ 40%
	Migration		↑10%		—		↑		↑		↑
Responsive genes	MYC		—		↑		↑		↓		—
	CCND-1		—		—		—		—		—
	ID-1		—		—		—		—		—
	Ki67		—		—		↓		—		—
	PCNA		—		—		↑		↓		—
	Snail		—		—		—		↑		—
	Slug		—		↑		↑		↑		↑
	Vimentin		↑		—		—		—		—
	P21		—		—		—		—		—
	MMP1		—		—		—		—		—
	MMP3		—		—		↑		—		—
	MMP2		—		—		↑		—		↑
	MMP7		↑		—		↑		—		—
	MMP9		—		—		↑		—		↑
	MMP11		↑		↓		↓		↑		—
	MMP14		↑		—		↑		—		—

7.2 Materials and methods

7.2.1 Breast cancer database

RNA sequencing data (TCGA_BRCA) was utilised in this study to investigate the differential expression of BMPRs in different subtypes. TCGA-BRCA is an mRNA sequencing cohort, with quantitative data of genomic DNA, mRNA, microRNA and protein, for a cohort of breast cancer comprising 1098 tumours and 112 adjacent non-tumour mammary tissues.

7.2.2 Cell lines

Cell lines including luminal A (MCF-7 and ZR571), luminal B (BT474 and MDA-MB-361), Her2 (+) (SKBR3 and HCC1419) and TNBC (MDA-MB-231, BT20, BT549, MDA-MB-436 and MDA-MB-468) subtypes were used to determine the differential expression of BMP receptors and ERBBs in breast cancer cells. ZR751, BT474, MDA-MB-361, HCC1419 cell lines were cultured in RPMI-1640 medium, with 10% FBS and antibiotics, whilst the others including MCF-7, SKBR3, BT20, BT549, MDA-MB-231, MDA-MB-436 and MDA-MB-468 were maintained in DMEM medium with 10% FBS and antibiotics as previously described in the method section.

7.2.3 Overexpression model in breast cancer cell lines

BMP8A overexpression cell models were created in luminal B (BT474 and MDA-MB-361), Her2 (+) (SKBR3 and HCC1419) and TNBC (MDA-MB-231) cell lines using lentiviral vectors as described in previous chapters. After selection for about one week, medium with 50µg/ml hygromycin was used to maintain the cells.

7.2.4 RNA isolation, cDNA synthesis, RT-PCR, and Q-PCR

Tri Reagent (Sigma-Aldrich, Inc., Poole, Dorset, England, UK) was utilised to extract RNA, followed by the synthesis of complete DNA using reverse transcription kit (Promega, Southampton, UK) (Chapter 2 section 2.6.1). Conventional and QPCR were then accomplished according to the protocols outlined in chapter 2 (section 2.2). Details of primers including GAPDH, β-actin, BMP8A and other responsive genes are given in chapter 2 (Table2.2).

7.2.5 Western blot analysis

After protein extraction using a lysis buffer and quantification by the DC Protein Assay

kit (BIO-RAD, USA), the proteins were separated by SDS-PAGE and then transferred onto PVDF membranes (Pre-treated by methanol for 1 minute and the running buffer for 15 minutes). After blocking with a blocking buffer, the membrane was incubated with the respective primary antibody at 1:1000 dilution overnight (4℃) to probe the target protein. After washing, the respective HRP conjugate secondary antibody was added and incubated for another hour, followed by more washings. The protein bands were eventually visualised using the chemiluminescence detection kit, Luminate Forta Western HRP substrate (Cat. No. WBLUF0500, Merk-Millipore, Hertfordshire, UK) and the chemiluminescent tagged bands were visualised with a UVITech Imager (UVITech Inc., Cambridge, UK). Details for procedures and the antibodies applied in current study are listed in Table 2.3 and 2.4.

7.2.6 Statistical analyses

Student's T-test was applied to compare the normally distributed data, whilst the non-normally distributed data was analysed using a Manny-Whitney Test. ANOVA test was employed for statistical comparison of data comprising multiple groups. SPSS software was used to undertake statistical analysis.

7.3 Result

7.3.1 BMP8A induced Smad signalling in breast cancer cells

Activation of Smad1/5/8 in breast cancer cell lines with BMP8A overexpression

Enhanced Smad 1/5/8 phosphorylation was detected in MDA-MB-361^{BMP8A} and BT474^{BMP8A} cells, both these two cell lines belong to luminal B subtype. A reduced level of phosphorylated Smad1/5/8 was seen in the SKBR3^{BMP8A} cells. No significant change was observed in other cell lines (Figure 7.1).

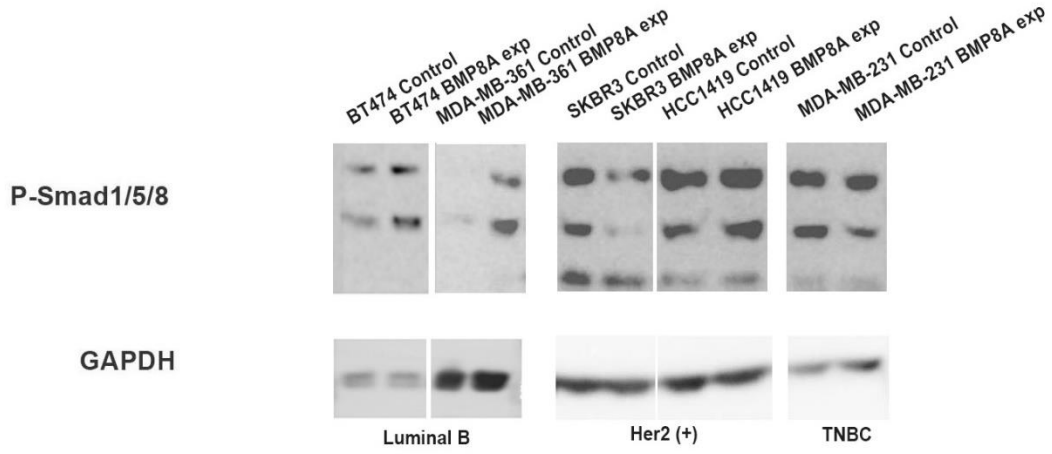

Figure 7.1 Phosphorylated Smad 1/5/8 in breast cancer cell lines with altered BMP8A expression.

Activation of Smad3 in breast cancer lines with BMP8A overexpression

Different from other BMP signalling, phosphorylation of Smad 2/3 was also observed in BMP8A signalling. Enhanced Smad 2/3 activation was found in SKBR3^{BMP8A} andMDA-MB-231^{BMP8A} cells comparing to the control cells respectively, whilst reduced Smad 2/3 phosphorylation was found in MDA-MB-361^{BMP8A} and HCC1419^{BMP8A} cells (Figure 7.2). Interestingly, those cell lines had enhanced activation of Smad1/5/8 presented lower or reduced levels of P-Smad3, such as MD-MB-361 and HCC1419, whilst SKBR3 exhibited a possibly increase in P-Smad3 and similarly the MDA-MB-231 cell line.

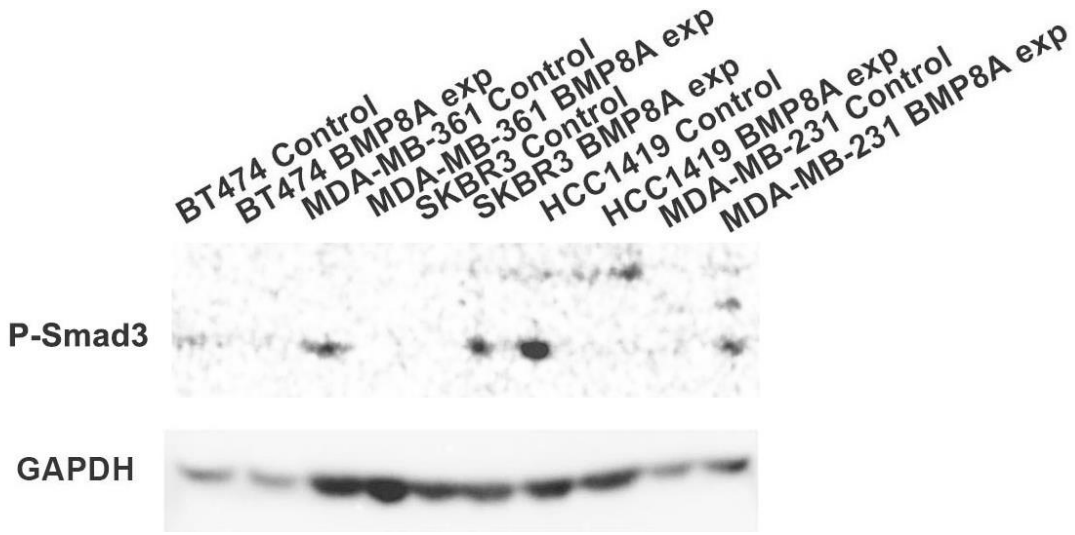

Figure 7.2 Smad 2/3 phosphorylation in breast cancer cell lines with differential BMP8A expressions.

7.3.2 Influence of BMP8A on Smad independent signalling

The influence of BMP8A on Smad independent signalling, including AKT and MAPK (ERK, P38, JNK) signalling was also determined in the present study (Figure7.3). Although upregulated AKT expressions were observed in MDA-MB-361, HCC1419 and MDA-MB-231 cells with BMP8A overexpression, phosphorylated AKT appeared to be undetectable in most of the cell lines tested except the HCC1419 and AKT activation tended to be enhanced in HCC1419^{BMP8A} cells. In comparison with other cell lines, ERK protein is highly activated in SKBR3^{BMP8A} cells compared with the control. A weak increase of phosphorylated ERK was noticed in BT474^{BMP8A}, whilst no obvious change was seen in ERK phosphorylation in other cell lines. P38 expression significantly increased in MDA-MB-231^{BMP8A} and MDA-MB-361^{BMP8A}. Comparing to the control cells, increased JNK expression was found in HCC1419^{BMP8A} and MDA-MB-361^{BMP8A}, however, subtly enhanced JNK phosphorylation was seen in BT474^{BMP8A}, MDA-MB-361^{BMP8A}, SKBR3^{BMP8A} and MDA-MB-231^{BMP8A}cells.

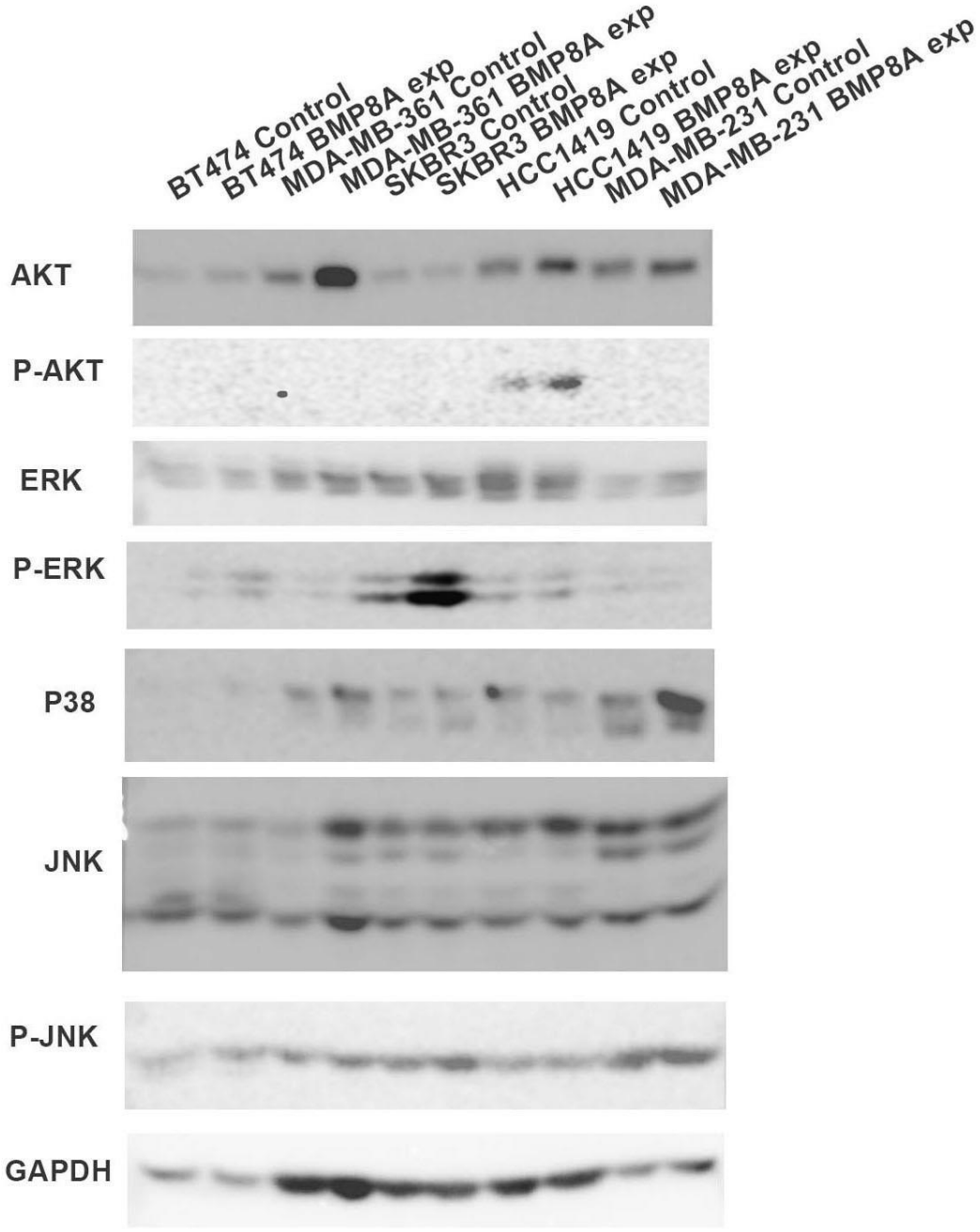

Figure 7.3 Influence of the BMP8A on the Smad independent signalling was evaluated using Western blot analysis.

7.3.3 Expression of BMP receptors in different subtypes of the disease

Expression of BMP receptors in different subtype breast cancers

To determine the receptors of BMP8A in breast cancer, expressions of candidate BMPRs including type I and type II receptors were analysed in the TCGA-BRCA cohort (Figure 7.4). ACVR1 expression was found to be significantly different between certain subtype groups. Levels of ACVR1 were found to be significantly higher in Her2 (+) ($P < 0.05$), luminal A ($P < 0.01$) and luminal B ($P < 0.05$) compared to TNBC subtypes. Elevated ACVR1B expression was seen in both luminal A and luminal B subtypes comparing with ER (-) subtypes, namely Her2 (+) and TNBC subtypes. Level of ACVR1B is the lowest in TNBC than the other three subtypes. Higher ACVR2A and lower ACVR2B expressions were shown in Her2 (+) subtype compared to the other subtypes. BMPR1A was highly expressed in Her2 (+) subtype comparing to luminal subtypes. Compared with ER (-) subtype, BMPR2 and BMPR1B expressions were higher in luminal subtypes. Expression of the BMP receptors in the TCGA cohort is also summarised in the Table 7.2.

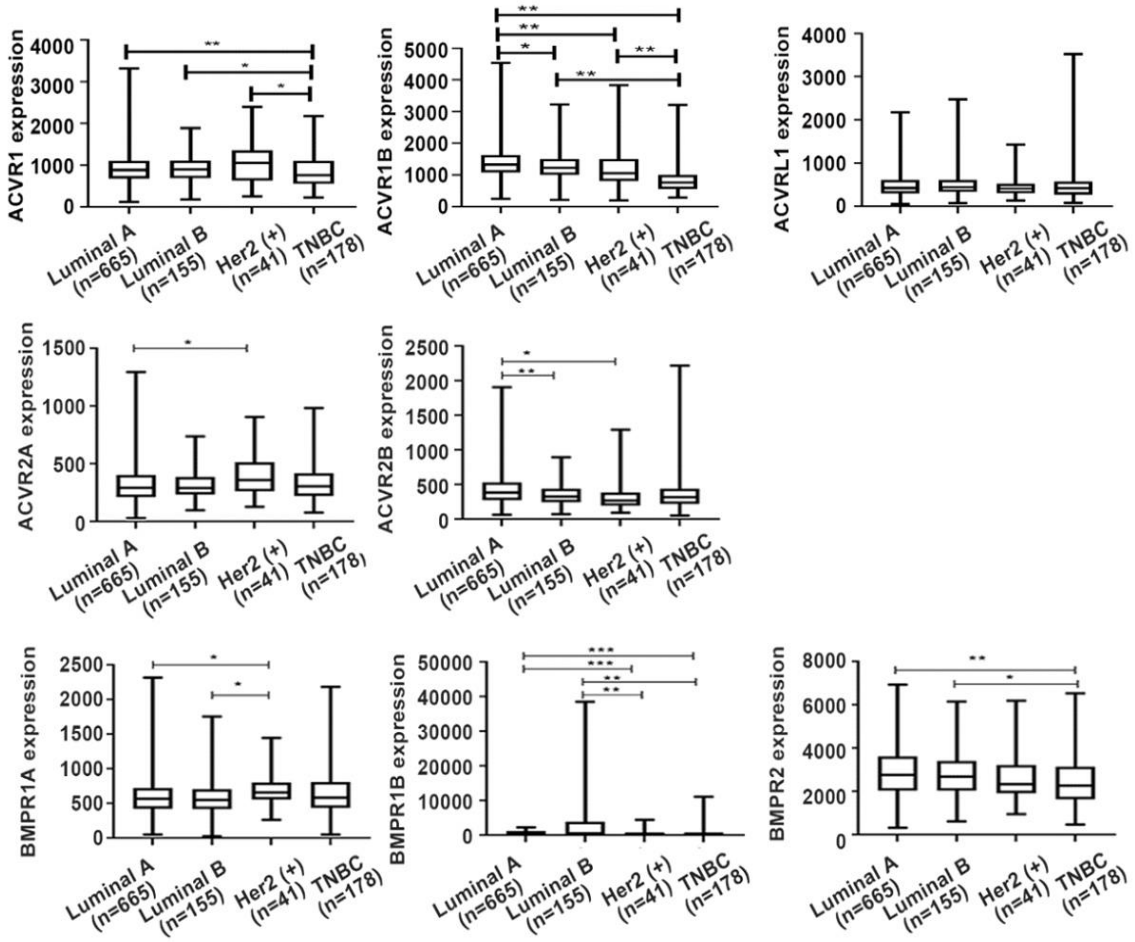

Figure 7.4 Differential expression of BMPRs in different subtypes of breast cancer analyses from TCGA-BRCA cohort. Values presented in the figures are median and interquartile range. * P<0.05, **P<0.01.

Table 7.2 Differential expression of BMPRs in different subtypes of breast cancer analyses from TCGA-BRCA cohort.

	Luminal A		**Luminal B**			**Her2 positive**			**TNBC**		
	Median	(IQR: Q1-Q3)	Median	(IQR: Q1-Q3)		Median	(IQR: Q1-Q3)		Median	(IQR: Q1-Q3)	
ACVRL1	417.45	(290.84-605.50)	429.50	(338.80-603.49)		401.7782	(303.56-517.98)		414.6238	(272.19-573.60)	
ACVR1	885.47	(677.76-1102.74)	899.90	(689.14-1107.27)		1053.904	(647.21-1317.33)		762.4559	(558.62-1096.30)	#*Δ
BMPR1A	563.97	(419.92-722.12)	549.47	(416.67-700.62)		657.2411	(556.53-797.13)	#*	581.3553	(436.37-803.74)	
ACVR1B	1332.89	(1072.25-1623.05)	1216.87	(1002.21-1500.89)	#	1050.98	(818.40-1502.82)	#	759.4324	(562.87-991.84)	#*Δ
BMPR1B	977.80	(85.78-6788.58)	471.42	(98.46-3693.34)		83.57	(31.80-249.63)	#*	80.13935	(26.42-222.39)	#*
BMPR2	2757.92	(2026.94-3611.08)	2668.06	(2051.76-3392.14)		2327.094	(1971.94-3189.37)		2265.878	(1631.29-3130.28)	#*
ACVR2A	292.06	(209.15-403.49)	287.72	(231.33-384.24)		357.8093	(262.00-500.68)	#	303.7473	(220.91-417.22)	
ACVR2B	380.77	(270.53-527.48)	323.00	(242.12-438.18)	#	265.3865	(192.36-363.89)	#	314.3501	(220.33-437.69)	

Note: Shown are median (IQR), IQR interquartile range = Q1 – Q3; #P *vs* luminal A; *P *vs* luminal B; ΔP *vs* Her2 positive.

Expression of BMP receptors in breast cancer cell lines

Expression levels of candidate BMP receptors were also determined in wild type breast cancer cell lines (Figure 7.5). Following amplification over 30 cycles, high expressions of ACVR1, ACVR2B, BMPR1A and BMPR2 were found to be present in the majority of tested cell lines. Compared with others, relatively higher expression of ACVR1B was seen in BT474, MDA-MB-361 and SKBR3 cell lines. BMPR1B expression was relatively high in luminal A cell lines (MCF-7 and ZR751), MDA-MB-361 and SKBR3 cells. Although both belong to the luminal B subtype, lower BMP1B expression was observed in BT474 cells compared to the MDA-MB-361 cell line. Compared with HCC1419 cells, higher expressions of ACVR1B and BMPR1B were seen in SKBR3 cells.

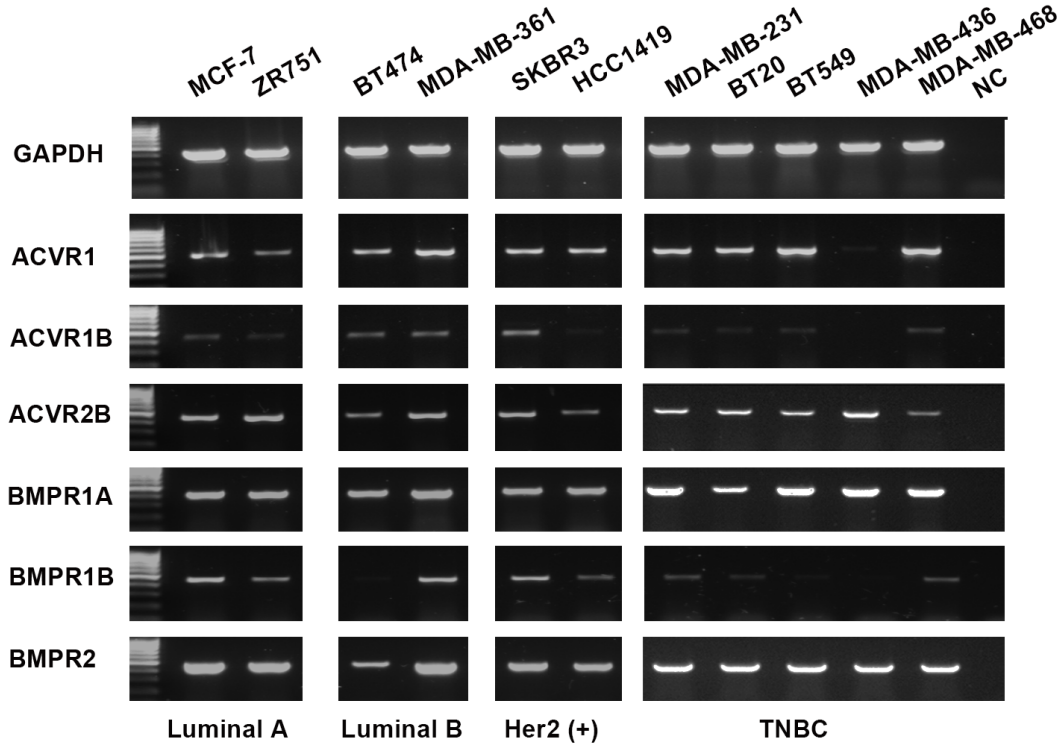

Figure 7.5 Expression of candidate BMP receptors in wild type cells of breast cancer cell lines was determined using conventional PCR.

Altered BMPR expression in breast cancer cell models.

To further determine the promising receptors involved in BMP8A signal transduction, altered expression of the BMPRs were investigated in the breast cancer cell models with BMP8A overexpression using both conventional PCR (Figure 7.6) and QPCR (Figure 7.7). In luminal B cells, reduced ACVR1 was observed in MDA-MB-361^{BMP8A}, whilst significantly induced BMPR2 and BMPR1A expressions were found in both BT474^{BMP8A} and MDA-MB-361^{BMP8A} cells (Figure 7.7). In Her2 (+) subtype, significantly reduced ACVR1B, BMPR1B, BMPR1A and BMPR2 expressions were associated high BMP8A expression in SKBR3 cells, whilst increased ACVR2B was associated BMP8A expression in SKBR3 cells. Significantly increased ACVR1, BMPR1A and BMPR2 expressions were observed in HCC1418^{BMP8A} cells. For MDA-MB-231 cells, induced expression of ACVR2B and reduced BMPR1A expression were associated with upregulated BMP8A expression.

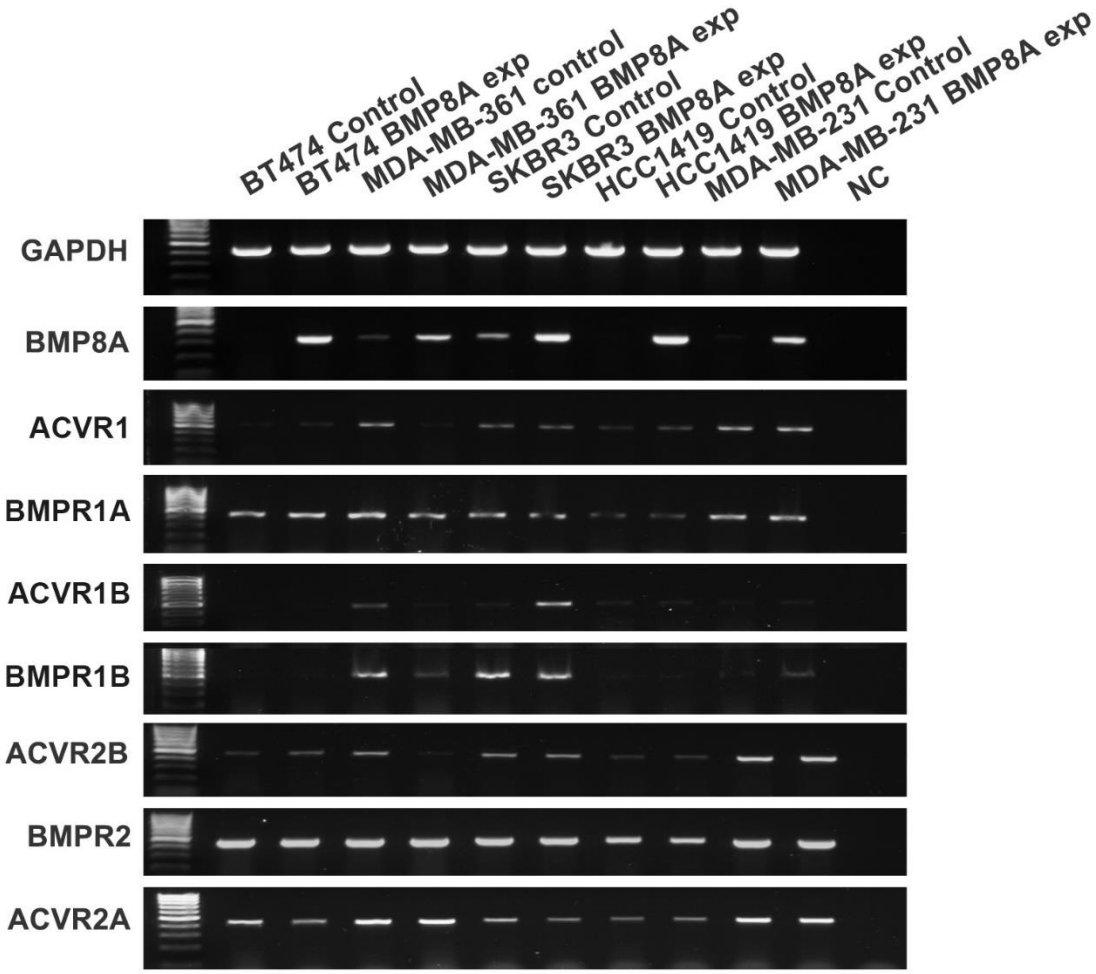

Figure 7.6 Altered BMPRs expression in breast cancer cell models was examined using conventional PCR.

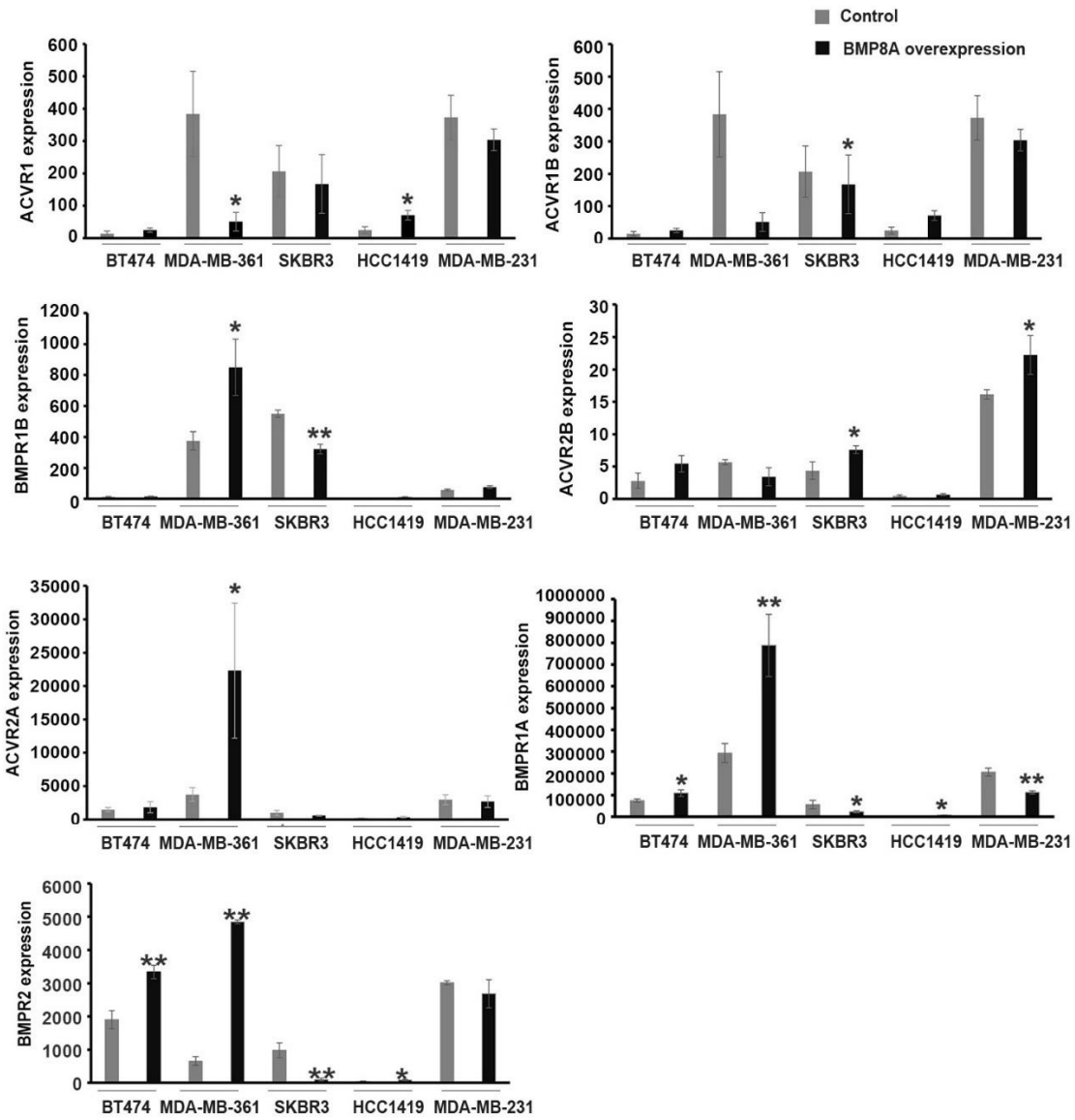

Figure 7.7 Transcripts of BMPRs in breast cancer cell models were determined using QPCR. Values presented in the figures are mean and STD. **P<0.01 *VS* control group, *P<0.05 *VS* control group.

7.3.4 Possible influence of BMP8A on ERBBs in different subtypes of breast cancer

Expression of ERBBS in breast cancer cell lines

To determine the interaction between ERBBs and BMP8A signalling, expressions of ERBBs were investigated in the wild type of breast cancer cell lines, covering all of the subtypes (Figure 7.8). According to the present results, high expressions of EGFR were seen in BT474 cells, SKBR3 cells and almost all the cells belonging to the TNBC subtype. ERBB2 were found to be highly expressed in luminal B (BT474 and MDA-MB-361) and Her2 (+) (SKBR3 and HCC1419) cell lines. High expression of ERBB3 was seen in MDA-MB-361, SKBR3 and HCC1419 cells but was only found to be weakly expressed in TNBC cells. Comparing with the other cells, high expression of ERBB4 was seen in HCC1419 cells.

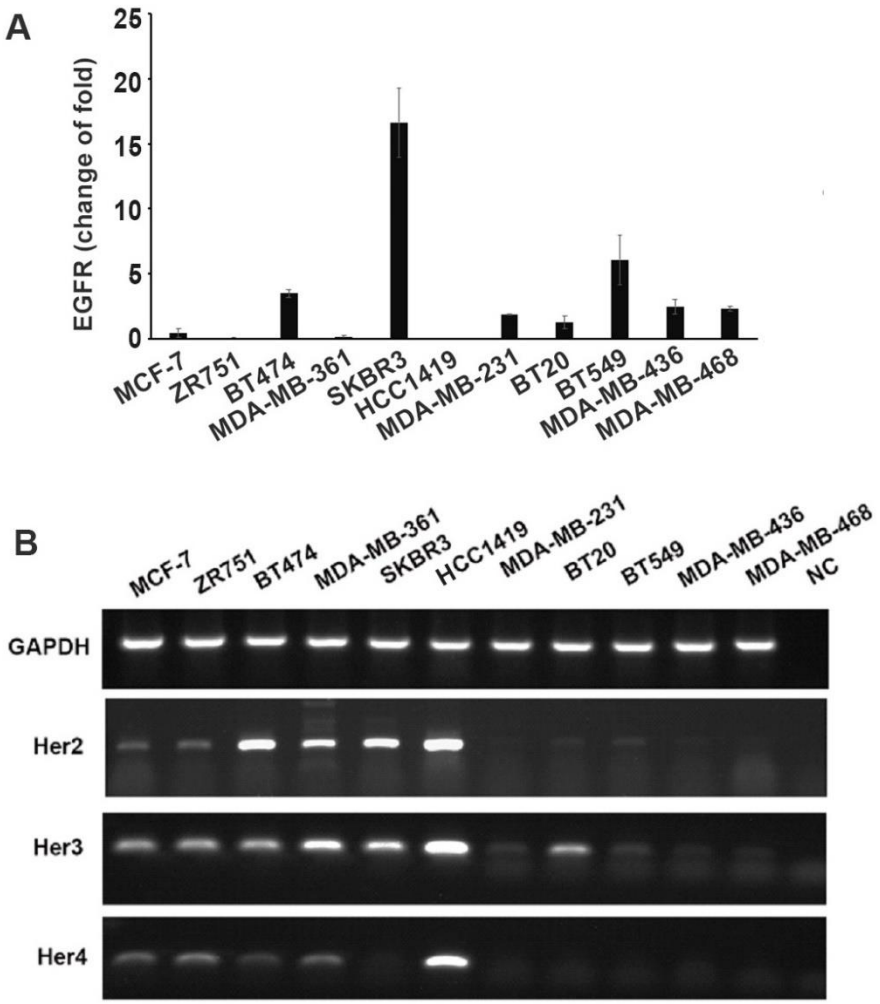

Figure 7.8 Expression of ERBBs in breast cancer cell lines. (A) EGFR transcripts in wild type breast cancer cell lines determined by QPCR. (B) Conventional PCR to show the different expression of ERBB2, ERBB3 and ERBB4 in wild type breast cancer cells.

Differential expression of EGFR/ERBB2 in the BMP8A overexpression cell line models

Differential expressions of EGFR were investigated in BMP8A modified cell models in the present study (Figure 7.9) using QPCR and western blot analysis. Decreased EGFR transcripts were seen in MDA-MB-361^{BMP8A} cells, whilst increased EGFR expression was observed in both SKBR3^{BMP8A} and MDA-MB-231^{BMP8A} cells. No significant change in EGFR expression was seen in BT474 and HCC1419 cells following BMP8A overexpression (Figure 7.9 A). Increased EGFR protein levels were observed in SKBR3 and MDA-MB-231 cells following overexpression of BMP8A, however, no band was seen in other three cell lines examined (Figure 7.9 B).

Differential ERBB2 expression following BMP8A overexpression was also determined in the present study using QPCR and western blot analysis (Figure 7.10). Significantly decreased ERBB2 and increased ERBB2 expressions were seen in MDA-MB-361^{BMP8A} and SKBR3^{BMP8A} cells respectively. No obvious, significant change in ERBB2 transcript expression was observed in the other three cell lines following BMP8A overexpression (Figure 7.10 A). At a protein level, significantly decreased ERBB2 and increased ERBB2 expressions were seen in MDA-MB-361^{BMP8A} and SKBR3^{BMP8A} cells, compared to their controls, respectively. No ERBB2 expression was observed in MDA-MB-231 cells (Figure 7.10 B).

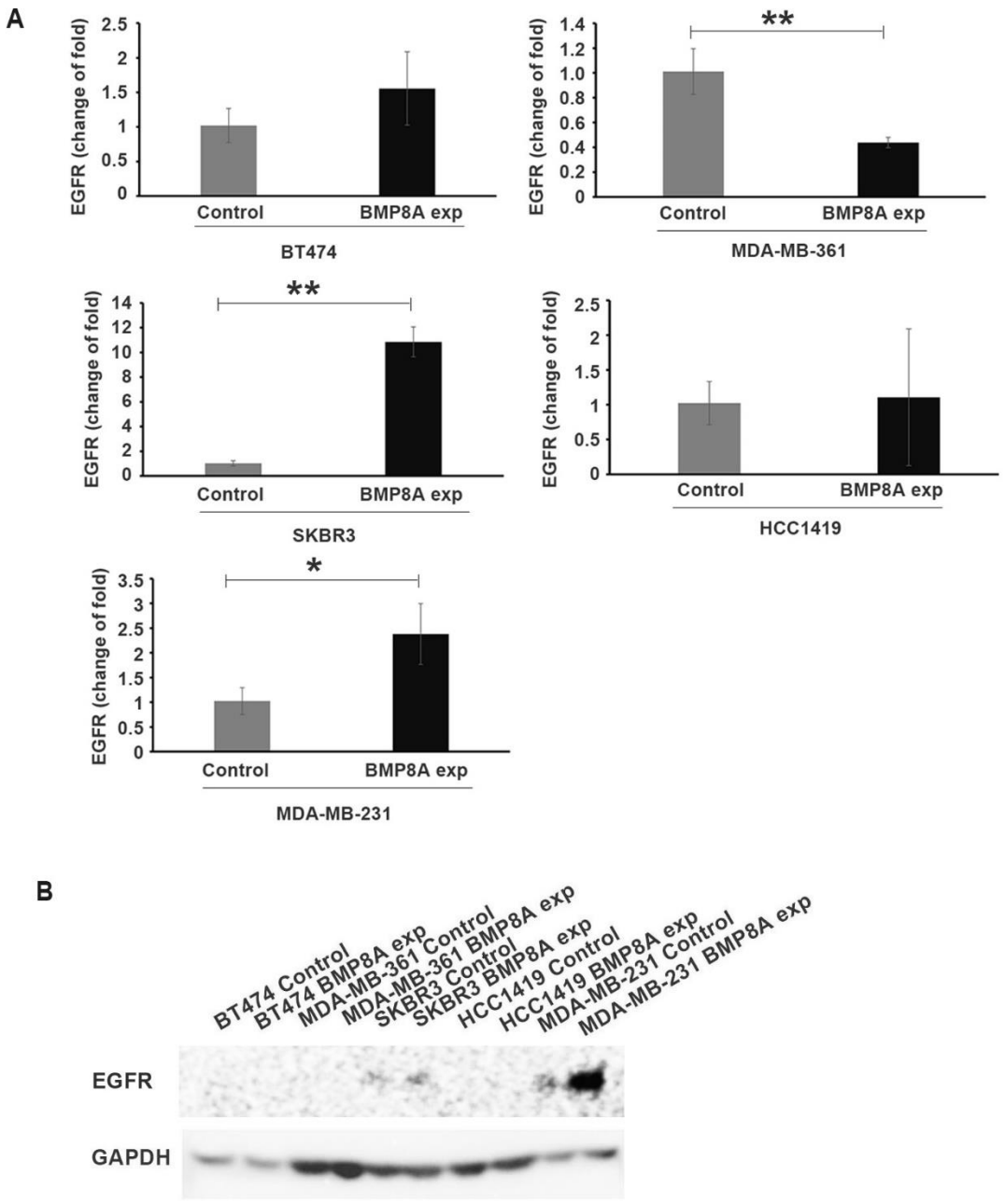

Figure 7.9 Differential EGFR expression in breast cancer cell models. (A) EGFR transcripts in cell models were determined by QPCR. Values presented in the figures are mean and STD. ** P<0.01, * P<0.05. (B) Protein levels of EGFR in breast cancer cell models.

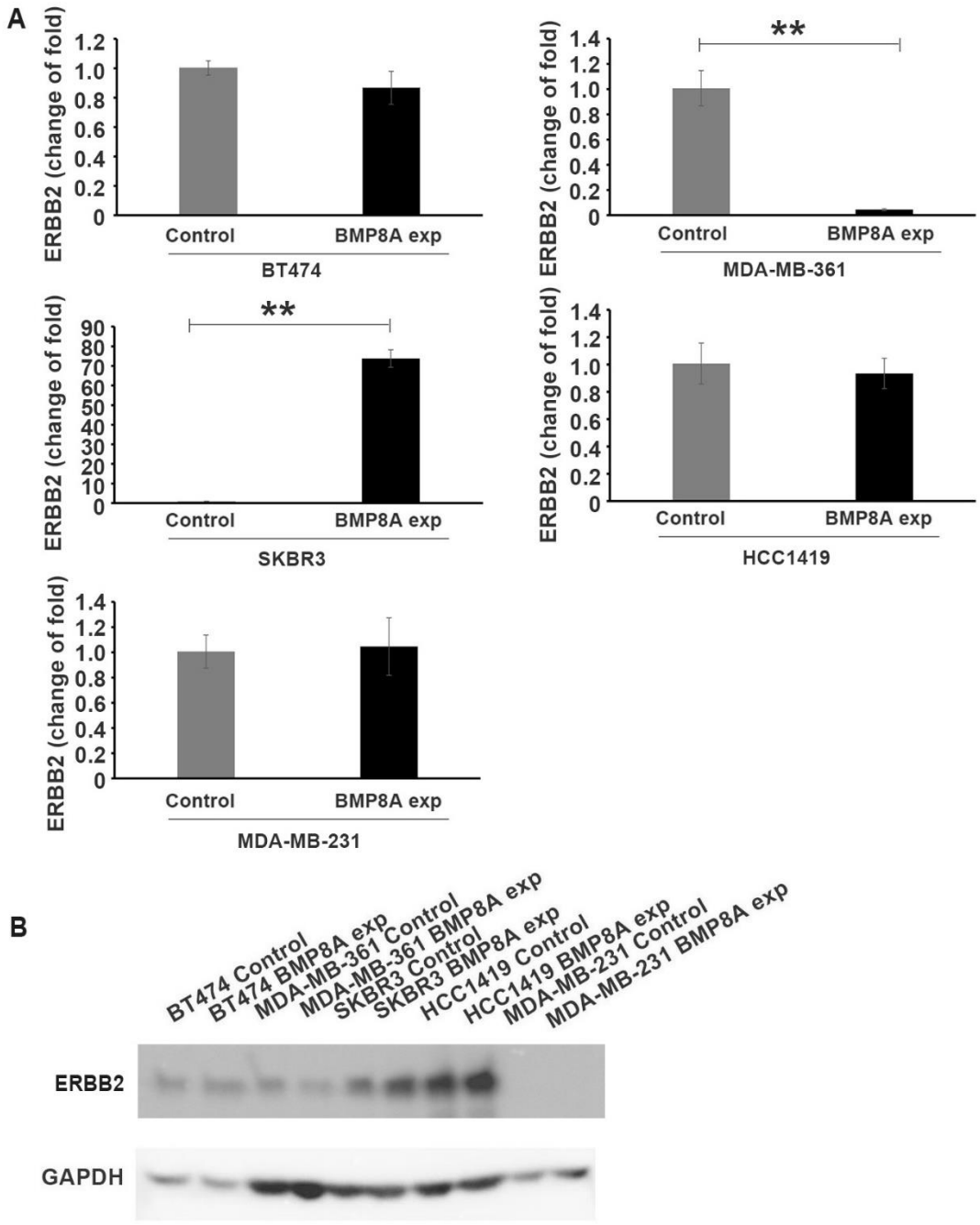

Figure 7.10 Differential expressions of ERBB2 in breast cancer cell models with altered BMP8A expression. (A) ERBB2 transcripts were determined by the QPCR. ** P<0.01, * P<0.05. (B) ERBB2 expressions in breast cancer cell models determined by western blot. Values presented in the figures are mean and STD.

7.4 Discussion

As elucidated in the previous chapters, BMP8A presented subtype specific roles in breast cancer. Survival analyses showed that high BMP8A expression is associated with poor overall survival in luminal B subtype but is correlated with a better overall survival in patients with Her2 (+) tumours. Overexpression of BMP8A in two luminal B breast cancer cell lines (BT474 and MDA-MB-361) enhanced their invasiveness, in which increased MMPs and EMT markers were observed. However, in addition to a similar effect on invasion, BMP8A exhibited different influences on cell proliferation in two Her2 positive cell lines, SKBR3 and HCC1419. It suggests that diverse influences of BMP8A on cellular/molecular events and response to the current therapy may all contribute to the different role of BMP8A in the HER2 positive tumours in comparison with its role in luminal B tumours. The present study also showed that BMP8A can also enhance the invasiveness of MDA-MB-231 cells through a regulation of both MMPs and EMT. These BMP8A induced changes in cellular functions are executed through different signal transductions in cancer cells.

Two patterns of signal transduction have been identified in BMP signalling, the Smad-dependent pathway and Smad-independent pathway. In the current research, elevated phosphorylation of Smad1/5/8 was evident in both BT474 and MDA-MB-361 cells with BMP8A overexpression suggesting the canonical Smad dependent signalling via Smad1/5/8 can be induced in the two luminal B cancer cell lines.

In addition to signalling through BMP specific R-Smads, i.e. Smad1/5/8, BMP8A may also induce activation of TGF-β specific R-Smads (Smad2/3) which is evident in spermatogonia (Wu et al., 2017). Therefore, the present study also determined the expression of phosphorylated Smad3 in those breast cancer cell line models. Interestingly, those cell lines with enhanced activation of Smad1/5/8 had lower or reduced levels of P-Smad3, such as MD-MB-361 and HCC1419, whilst SKBR3 exhibited a possible increase in P-Smad3 and similarly in the MDA-MB-231 cell line (Figure 7.2). The role of Smad 2/3 phosphorylation and its correlation with the phosphorylation of Smad1/5/8 in breast cancer still need to be further investigated. Furthermore, non-canonical signalling via Smad-independent signalling transduction is also assessed in the current study. Upregulated P38 expression was seen in MDA-MB-231^{BMP8A} whilst increased AKT expression was shown in MDA-MB-361^{BMP8A} cells

comparing to the corresponding control cells, respectively. Elevated Erk phosphorylation and AKT phosphorylation were seen in SKBR3^{BMP8A} and HCC1419^{BMP8A}, respectively. Increased JNK expression was found in HCC1419^{BMP8A} and MDA-MB-361^{BMP8A}. Meanwhile, subtly enhanced JNK phosphorylation was seen in BT474^{BMP8A}, MDA-MB-361^{BMP8A}, SKBR3^{BMP8A} and MDA-MB-231^{BMP8A} cells (Figure 7.3). However, involvement of these MAPK pathways and AKT pathway in the BMP8A regulated cellular function and corresponding implication in the subtype specific role of BMP8A requires further investigation.

BMP signalling transduction initiates from the binding with the receptors on the membrane. In Wu's report, P-Smad 1/5/8 was mediated by receptor complexes formed by type I receptor（BMPR1A or BMPR1B) and type II receptor (ACVR2A or BMPR2). Whilst Smad2/3 signal pathway was activated through receptor complexes formed by type I receptor (TGFBR1 or ACVR1B) and type II receptor (ACVR2A, ACVR2B or TGFBR2) (Wu et al., 2017). Influenced by the ER, EGFR and ERBB2 signalling, BMP8A mediated signalling transduction seems to be more complex in breast cancer.

BMP receptors are detectable in most breast cancer cell lines (Arnold et al., 1999). BMP receptors such as BMPRIA and BMPR2 mediated regulation of proliferation and invasiveness have also been revealed in breast cancer (Katsuno et al., 2008) (Pouliot et al., 2003). However, exact expression of BMP receptors in breast cancer regarding different subtypes remains largely unknown. From the current analyses in TCGA-BRCA cohort, high expressions of ACVR1B and BMPR2 were seen in luminal subtypes. Compared with Her2 (+) subtype, ACVR2B expression is highly expressed in luminal subtype. BMPR1B is also highly expressed in luminal subtypes compared with both Her2 (+) and TNBC subtypes. ACVR1 and BMPR1A present higher expression in Her2 (+) tumours than other subtype tumours. Conventional PCR showed that ACVR1, ACVR2B, BMPR1A and BMPR2 were expressed at relatively higher levels in the panel of breast cancer cell lines examined in comparison with other receptors. It suggests that the differential expression patterns of BMP receptors are more likely mediating diverse signalling for the BMP ligands in different subtypes of breast cancer. This opened a new avenue for further exploration to shed light on their role in breast cancer, particularly for the subtype specific roles of BMP8A.

Luminal subtypes including luminal A and luminal B subtypes account for approximate

70% of breast cancer (Lukasiewicz et al., 2021), are positive for ER expression in comparison with the HER2 (+) and TNBC tumours. ER signalling is capable of modulating the expression of BMP and BMPRs in breast cancer (Takahashi et al., 2008). Several BMPs and BMPRs are differentially expressed in different subtypes of breast cancer with different ER status. For example, BMP2 expression was markedly higher in ER negative subtypes and expression of BMP2 was elevated when ER expression was silenced in ER positive breast cancer (Al Saleh et al., 2011). Elevated expression of BMP6 contributed to immunological surveillance and prolonged the overall survival in ER-positive patients, however the survival time reduced in ER negative cases with high expression of BMP6 (Katsuta et al., 2019b). In addition to the BMP ligands, ERα also exhibited a capacity of binding to BMPR2 promoter to upregulate BMPR2 expression, contributing to a protection of right ventricular function (Frump et al., 2021), though it remains controversial as BMPR2 transcripts were also reduced as a result of stimulating ER (Austin et al., 2012). Moreover, O-glycosylation of BMPR1A was found to increase the expression of ERα to modulate the BMP/RUNX2 signalling in breast cancer (Huang et al., 2022). The cross talk between ER and BMP signalling represents an interesting and profound area for further investigation to elucidate molecular and cellular mechanism in ER positive breast cancers and also current challenges in chemotherapy and endocrine therapy.

HER2 is a key marker for HER2 (+) breast cancer and is also present in luminal B tumours. The BMP signalling pathway has been shown to cooperate with that of the Her2 signalling pathway to promote cancer progression (Siegel and Massague, 2003). Highly expressed BMPs or BMPRs in the Her2(+) breast cancer murine model increased the mortality caused by metastases (Muraoka et al., 2003, Muraoka-Cook et al., 2006, Seton-Rogers et al., 2004). On the other hand, BMP proteins have been shown to reciprocally regulate Her2 signalling by activating the downstream receptor tyrosine kinases of ErbB, such as Ras/MAPK (Mulder, 2000) and PI3K/Akt (Yi et al., 2005, Wilkes et al., 2005). Silencing of endogenous BMP signals significantly reduced the proliferation of Ras-transformed cancers (Ventura et al., 2004), indicating that Her2 signal induced tumour progression at least partly relies on the function of the BMP signalling pathway. Notably, EGFR/ErbB2 heterodimers, but not the homodimers, could induce cell invasion in mammary epithelial cells (Zhan et al., 2006).

Although both SKBR3 and HCC1419 cells belong to the Her2 (+) subtype, presenting

high expression of ERBB2, the mechanism for the altered cell functions in SKBR3 and HCC1419 appears to be different. ERBB2 is an orphan receptor, it has to rely on the EGFR signalling to form the heterodimer EGFR/HER2 to exert biological function (Ferguson, 2008). With the lack of ER signalling in Her2 (+) subtype, EGFR and HER2 signalling tends to be the dominant. However, EGFR/HER2 signalling is not well conducted due to an absence of EGFR in HCC1419 cells (Figure 7.9), as a result, BMP signalling seems to be the dominant signalling induced by BMP8A as increased phosphorylation of P-Smad1/5/8 was seen in HCC1419^{BMP8A} cells. In comparison with HCC1419, EGFR was detectable in the SKBR3 cells (Figure 7.9) which may mediate the enhanced activation of the ERK pathway in the SKBR3^{BMP8A} cells (Figure 7.3). Contrasting effects on the activation of Smad3 were also evident those two HER2 (+) cell lines. P-Smad3 was reduced in the HCC1419^{BMP8A} cells whilst it appeared to be marginally increased in the SKBR3 cells with BMP8A overexpression indicating in addition to EGFR, differentially expressed BMP receptors may also rely on signalling of BMP8A through different Smads. Furthermore, upregulated ACVR2B and downregulated BMPR1 and BMPR2 were seen in SKBR3^{BMP8A}, whilst upregulated ACVR1, BMPR1A and BMPR2 were observed in HCC1419^{BMP8A} cells mediating BMP signal transduction (Figure 7.6). Those BMP receptors bear an answer at least for the specific signalling events of BMP8A in those two HER2 (+) cell lines.

Apart from oestrogen receptors and HER2, EGFR also plays an important role in breast cancer. Study in the drosophila embryo showed that BMP signal response was inversely modulated by EGFR signalling (Deignan et al., 2016). In breast cancer, high EGFR expression is found in TNBC subtype, however BMP8A expression is low in the TNBC subtype analysed from the TCGA-BRCA cohort and comparing to the other three subtypes. The present quantitative analysis of EGFR showed high expression of EGFR in the TNBC cell lines including MDA-MB-231, BT20 and BT549.

Crosstalk has been evident between EGFR and BMP which was recently reviewed (Sun et al., 2020). Enhanced EGFR activity has been shown to modulate the activity of BMP downstream signalling molecules such as MAPK and PI3K/Akt to facilitate tumour invasion and motility (Barr et al., 2008). BMP may modulate EGFR signalling via a regulation of PTEN and PI3K/Akt (Zhang et al., 2006). In the present study, significantly

increased EGFR expression was seen in MDA-MB-231^{BMP8A} cells which indicated an enhanced EGFR signalling may also occur in MDA-MB-231 cells as a result of BMP8A overexpression. Activation of EGFR can promote cell migration and invasion in ameloblastoma cells by enhancing MMP2 and MMP9 activity (da Rosa et al., 2014). In line with our findings in a previous chapter, BMP8A promoted invasion and upregulated MMP2 in MDA-MB-231 cells. It suggests that BMP8A may promote the invasiveness of TNBC cells through dual mechanisms including both BMP signalling and the regulation of EGFR which are yet to be fully evaluated. Furthermore, increased P38 was observed in MDA-MB-231^{BMP8A} cells, together with elevated RANKL expression and their implication in BMP8A related activities in bone metastasis warrants further investigation since RANKL/P38 signalling pathway is renowned for the osteolytic bone metastasis in breast cancer (Lim et al., 2020).

In addition to the differential expression of BMP receptors in breast cancer, the influence of BMP8A on the expression of BMP receptors was also assessed in the present study. In luminal B subtype, increased BMPR1A, BMPR1B, ACVR2A and BMPR2 were seen in MDA-MB-361^{BMP8A}, whilst increased BMPR1A and BMPR2 were found in BT474 cell with high BMP8A expression. In MDA-MB-231^{BMP8A} cells, increased ACVR2B and reduced BMPR1A were observed compared to the control cells. In Her2 (+) cell lines, upregulated ACVR2B and downregulated BMPR1 and BMPR2 were seen in SKBR3^{BMP8A}, whilst upregulated ACVR1, BMPR1A and BMPR2 were observed in HCC1419^{BMP8A} cells mediating BMP signal transduction. This suggests that BMP receptors are altered as a result of BMP8A overexpression although the exact regulatory mechanism is yet to be revealed in which both Smad dependent and independent pathways might be involved. Certainly, this also adds a challenge and difficulty to what are already complicated signal transduction cascades underlying the subtype specific role of BMP8A.

Taken together, the subtype specific role of BMP8A was completed by the interaction of ER, EGFR and HER2 signalling in breast cancer. Two patterns including Smad dependent and Smad independent signalling pathway were transduced in BMP8A signalling. Besides phosphorylation of Smad1/5/8, activation of Smad2/3 was also found in the Smad dependent BMP8A signalling pathway. Altered Smad independent

signalling was also evident in the BMP8A overexpression cell lines. BMP receptors will be an area of focus in future studies for dissecting the specific role of BMP8A in different subtypes in addition to the influence from ER, EGFR and HER2.

Chapter 8

General Discussion

Increasing evidence has revealed the role of BMPs in the development and progression of tumours (Gonzalez and Medici, 2014), especially endocrine related tumours, such as breast cancer (Chi et al., 2019) and prostate cancer (Ye et al., 2007b). The present study aimed to investigate the role played by BMP8A in breast cancer.

8.1 Key findings from the current study

Elevated expression and subtype specific roles of BMP8A in breast cancer

In the initial analysis of BMP8A expression in breast cancer and its clinical relevance, an upregulated expression of BMP8A was revealed in breast cancers compared with that in adjacent tissues. IHC staining showed that BMP8A was mainly stained in the cytoplasm of breast cancer cells and was differentially expressed in subtypes. The increased expression of BMP8A in luminal B tumours was associated with poorer overall survival but appears to be positive marker for the prognosis in HER2 (+) tumours. High BMP8A expression was correlated with poorer distant metastases free survival in both luminal B and TNBC subtypes. Such findings suggest that BMP8A plays different roles, being specific to certain subtype tumours.

To further explore the subtype specific role of BMP8A in breast cancer, a panel of breast cancer cell lines derived from different subtypes of the disease was employed to dissect the cellular and molecular machinery involved in BMP8A's subtype specific roles. Luminal B, HER2 (+) and TNBC were investigated in the present study using a range of *in vitro* cell line models. Interestingly, enhanced cell invasion was observed in all the cell lines with high BMP8A expression, however contrasting impacts on cell growth was seen in Her2 (+) cell lines.

BMP8A promoted invasiveness of luminal B cancer cell lines (BT474 and MDA-MB-361)

Different downstream cascades induced by BMP8A were investigated in the present study, although enhanced cell invasion was seen in both $BT474^{BMP8A}$ and $MDA\text{-}MB\text{-}361^{BMP8A}$ cells. Increased expression of Vimentin and MMPs including MMP7, MMP11 and MMP14 were seen in $BT474^{BMP8A}$ cells. This suggests that BMP8A promotes invasiveness and migration of BT474 cells through the regulation of both EMT and MMPs. Subsequent experiments revealed an activation of both Smad1/5/8 and JNK pathways. BMP signalling can promote invasion and EMT via Smad

signalling (Gonzalez and Medici, 2014). EGFR and its downstream MAPK and Akt pathways are also able to promote invasion and migration by regulating MMPs and EMT (Hardy et al., 2010). Since both EGFR and HER2 are highly expressed in BT474 cells, the exact role of JNK as a downstream pathway of both EGFR/HER2 and BMP Smad independent signalling is yet to fully elucidated in future study. The other luminal B cell line used in the present study, MDA-MB-361 exhibits relatively lower expression of EGFR comparing with BT474. An increased Smad signalling and elevated expression of one of its responsive genes, Slug, were evident in the MDA-MB-361^{BMP8A} cells, indicating a likely involvement in the BMP8A promoted invasion (Figure 8.1). Future study will further validate their involvement in BMP8A promoted invasion in luminal B cancer cells.

Influence of BMP8A on cellular functions of Her2 (+) breast cancer cell lines (SKBR3 and HCC1419)

Opposite effects on cell proliferation were observed in the BMP8A overexpression SKBR3 and HCC1419 cells; an increased and decreased cell proliferation were seen in SKBR3^{BMP8A} and HCC1419^{BMP8A} cells respectively. Increased expression of c-Myc was seen in the SKBR3^{BMP8A} cells but appeared to be decreased in the HCC1419^{BMP8A} cells. Both BMP signalling and EGFR/AKT pathway are able to induce c-Myc and consequently regulate proliferation of cancer cells (Wang et al., 2018, Yang et al., 2021). Increased expression of HER2 was seen in the SKBR3^{BMP8A} cells in which both activation of Smad3 and ERK1/2 were evident together with a marginal reduction in activation of Smad1/5/8. In comparison with SKBR3, a markedly increased activation of Smad1/5/8 and also reduced c-Myc and PCNA were seen in the HCC1419^{BMP8A} cells. This suggests that BMP8A elicits opposite regulation of c-Myc and cell proliferation through different signalling pathways in which the exact role of Smad3, Smad1/5/8 and the MAPK pathways are yet to fully established. Furthermore, different levels of EGFR expressed in SKBR3 and HCC1419 cell lines may bear another cause for the contrasting effects on both proliferation and signalling. Whether HER2/EGFR or BMP receptors mediate the BMP8A induced c-Myc expression and consequent influence on cell proliferation are yet to be investigated fully by blocking either EGFR/HER2 or BMP receptors with specific inhibitors. In comparison with the contrasting effects on proliferation, BMP8A elicited a promotive effect on invasiveness of the two HER2 (+) cell lines accompanied with increased expression of both MMPs and EMT markers

(Figure 8.1).

BMP8A regulated cell functions of TNBC cells (MDA-MB-231) and its involvement in bone metastasis

Enhanced cell invasion and migration were seen in MDA-MB-231BMP8A cells together with increased expression of Slug and MMPs including MMP2 and MMP9. This suggests that BMP8A promotes invasiveness and migration of MDA-MB-231 cells through a regulation of both EMT and MMPs. EGFR, being frequently upregulated in TNBC tumours, can promote both invasion and EMT through both MAPK and Akt pathways (Hardy et al., 2010). EGFR signalling is closely related with tumour progression and survival (Masuda et al., 2012). In the present study, significantly elevated EGFR expression was also seen in MDA-MB-231BMP8A cells as well as upregulated P38 expression and activation of Smad3. It appears that upregulated BMP8A in MDA-MB-231 cells is capable of promoting the expression of MMPs and EMT, in which the exact role EGFR signalling and Smad 3 signalling play is yet to be determined by blocking either EGFR/HER2 or BMP receptors with specific inhibitors.

Preliminary investigation of BMP8A in the bone metastasis of BC was performed in the current study. Following exposure to a mimicked bone environment, significantly reduced cell growth and increased invasiveness were observed in MDA-MB-231^{BMP8A} cells. Additional research revealed upregulated P38 and RANKL expression in MDA-MB-231^{BMP8A} cells. BMP signalling was found to upregulate P38 signalling and downregulate ERK signalling to induce tumour cell quiescence in the bone environment (Sosa et al., 2011), which is in line with the current findings. The invasiveness of MDA-MB-231^{BMP8A} cells was further enhanced while they were exposed to the *in vitro* bone environment. Increased RANKL and CDH11 expressions were also found in MDA-MB-231^{BMP8A} cells. RANKL-OPG signalling is renowned for osteoclastogenesis, activated RANKL-P38/ERK signalling pathway is associated with activation of osteoclasts and subsequent bone loss (Zhang et al., 2022), whilst CDH11 is a key molecule for the activation of osteoblasts, inducing the premetastatic niche for bone colonization of breast cancer (Li et al., 2022). This indicates that BMP8A may act as an important molecule to mediate the osteolytic bone metastasis and the initiation of the osteoblastogenesis in MDA-MB-231 cells through the RANKL/P38 signalling

pathway. However, this still needs to be fully investigated to elucidate the exact role of BMP8A in the spread of breast cancer cells to the bone and also their subsequent colonisation.

BMP8A signalling transduction and interaction with ER, EGFR, EGFR/HER2 signalling

Different from the other BMPs, BMP8A can induce activation of both BMP specific R-Smad1/5/8 and TGF-β specific R-Smad 2/3 signal pathways in spermatogonia synchronously (Wu et al., 2017). The former pathway is mediated by receptor complexes formed by the type I receptor （BMPR1A or BMPR1B) and type II receptor (ACVR2A or BMPR2). Whilst the SMAD2/3 signal pathway is activated through receptor complexes formed by the type I receptors (TGFBR1 or ACVR1B) and type II receptor (ACVR2A, ACVR2B or TGFBR2). Influenced by ER, EGFR, and EGFR/ERBB2 signalling, BMP8A mediated signalling transduction seems to be more complex in breast cancer. In the ER (+) luminal B cell lines, Smad dependant and independent BMP signalling were activated in the BMP8A overexpression cell lines in which the putative role of both BMPR2 and BMPR1A in the signal transduction of BMP8A warrants further elucidation in regard to its subtype specific role. Being from the luminal B cell lines, EGFR and HER2 signalling tend to be more active in the in TNBC and Her2 (+) breast cancer cell lines, respectively being absent from ER. Upregulated ACVR2B and downregulated BMPR1 were seen in MDA-MB-231^{BMP8A}, whilst reduced ACVR1B, BMPR1B and BMPR2 were detected in SKBR3^{BMP8A}. Key receptors mediating the subtype specific signalling of BMP8A are proposed (Figure 8.1). BMPR1A, BMPR1B and BMPR2 may act as pivotal receptors to deliver the BMP8A signalling in luminal B tumours whilst BMPR1A, ACVR1, BMPR2 and ACVR2B are the putative receptors in HER2 positive tumours in addition to the common phenotype of HER2. Comparing with luminal B and HER2 (+) tumours, candidate type I receptors in TNBC are yet to be discovered. Further investigations will clarify the exact involvement of these putative receptors in the subtype specific signalling of BMP8A in breast cancer.

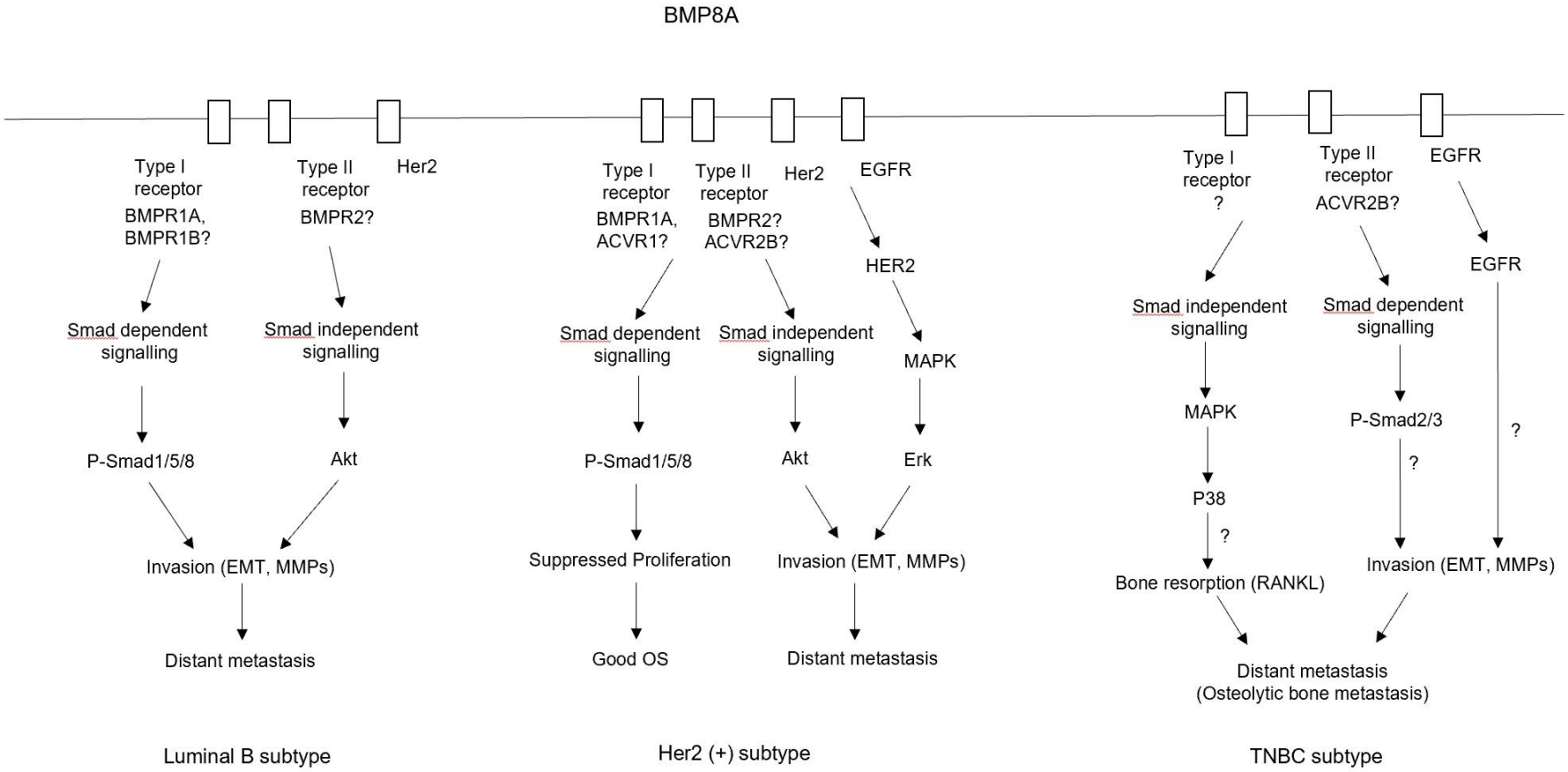

Figure 8.1 Proposed signal transduction and molecular mechanisms for the subtype specific involvement of BMP8A in breast cancer.

8.2 Perspectives and future study

To elucidate the subtype specific roles of BMP8A, the responsive genes for the altered cellular functions and the downstream signalling induced by BMP8A in breast cancer cells were examined in the present study. The influence of BMP8A on chemoresistance in Her2 (+) cancer cells and the involvement of BMP8A in bone metastasis were also preliminarily evaluated. However, there are still many questions yet to be answered in order to gain a better understanding of the subtype specific roles of BMP8A in breast cancer and to tackle clinical challenges encountered to aid disease management.

Receptors for the BMP8A signalling cascade.

According to the current study, interacting with ER, EGFR and ERBB2 signalling, different downstream signalling cascades were induced by BMP8A in breast cancer. However, further investigation is essential for identification of what BMP receptors are activated upon binding with BMP8A ligands leading to subtype specific signalling and subsequently regulation of responsive genes and alterations of cellular functions.

Bone metastasis in MDA-MB-231 cells

BMP8A presents contrasting roles for the bone metastasis in MDA-MB-231 cells. Cell growth was significantly suppressed whereas cell invasion was promoted while exposed to the bone environment *in vitro* for MDA-MB-231^{BMP8A}. On the other hand, RANKL (osteolytic molecule) and CDH11 (osteoblastic molecule) expression were significantly increased in MDA-MB-231^{BMP8A}. More experiments are urged, including both *in vitro* and *in vivo* metastatic models to shed light on the role of BMP8A in bone metastasis.

Potential of BMP8A in diagnosis and prediction of prognosis

BMP8A tends to be a good marker to predict the prognosis of breast cancer. Overall, high BMP8A expression is correlated with a poor prognosis in breast cancer. According to the analysis in luminal A subtype, high expression of BMP8A tends to be associated with higher recurrence of the disease, which may be caused by the resistance to chemotherapeutic drugs in luminal A subtypes. Analyses in luminal B and TNBC subtypes indicate that high BMP8A expression is correlated with enhanced tumour

invasion and migration, leading to poor prognosis. As one of the most common distant metastases, bone metastasis is common in TNBC tumours and presents a correlation with elevated BMP8A expression. Although proliferation of migrated cells in the bone environment was not that active with high BMP8A expression, it suggests a possible role of BMP8A in cell dormancy when the metastatic cancer cells spread to the bone. Although high BMP8A expression is associated with better overall survival in patients with Her2 positive tumours, the diagnostic value of BMP8A should be further evaluated in future study. Upregulated BMP8A expression induces EMT events and secretion of MMPs, which facilitate tumour invasion and migration. These warrants further study using both *in vitro* and *in vivo* models to elucidate its role in distant metastases. The contrasting effects of BMP8A on proliferation of the two HER2 positive cell lines, together with different expression of both EGFR and BMP receptors observed in those two cell lines, requires further investigation and should shed light on EGFR and BMP receptor mediated biphasic effects of BMP8A on proliferation. Furthermore, high BMP8A may also act an indicator for enhanced cell sensitivity to some chemotherapeutic drugs in EGFR highly expressed cells, however, for the EGFR-low-expressed cancer cells, high BMP8A may not be a good indication for the use of chemotherapy, due to the cell stemness induced by BMP8A which may lead to resistance to chemotherapy and targeted therapy. This will be an important area for future study.

Clinical therapeutic value of BMP8A in breast cancer

As revealed in the present research, BMP8A is an important molecule mediating the enhanced cell invasion in luminal B, TNBC and Her2 (+) subtype via EMT and MMPs. BMP8A tends to be a potential target to impede tumour invasion and migration in the subtypes listed above. In TNBC, BMP8A acts as an important molecule to induce osteolytic bone metastasis through RANKL/P38 signalling pathway, which indicates that BMP8A is also a possible target for the treatment of bone metastases from TNBC tumours. Anti-BMP8A neutralising antibody, small inhibitors targeting BMP8A, or BMP receptors and BMP antagonists can be considered for the further exploration.

Taken together, BMP8A is elevated in breast cancer primary tumours comparing to the adjacent normal tissues. The increased BMP8A expression is associated with poorer

survival of patients with luminal B tumours but is associated with longer survival in patients with HER2 positive tumours. Upregulated BMP8A expression is correlated with high incidence of distant metastases in luminal B and TNBC subtypes. Signal transductions are yet to be fully investigated to shed light on BMP8A promoted invasion and its regulation of proliferation in different breast cancer subtypes, which warrants further development of better disease management.

Bibliography

AGUIRRE-GHISO, J. A. 2007. Models, mechanisms and clinical evidence for cancer dormancy. *Nat Rev Cancer,* 7**,** 834-46.

AHMED, N., SAMMONS, J., CARSON, R. J., KHOKHER, M. A. & HASSAN, H. T. 2001. Effect of bone morphogenetic protein-6 on haemopoietic stem cells and cytokine production in normal human bone marrow stroma. *Cell Biol Int,* 25**,** 429-35.

AKRAM, M., IQBAL, M., DANIYAL, M. & KHAN, A. U. 2017. Awareness and current knowledge of breast cancer. *Biol Res,* 50**,** 33.

AL-HAJJ, M., WICHA, M. S., BENITO-HERNANDEZ, A., MORRISON, S. J. & CLARKE, M. F. 2003. Prospective identification of tumorigenic breast cancer cells. *Proc Natl Acad Sci U S A,* 100**,** 3983-8.

AL SALEH, S., AL MULLA, F. & LUQMANI, Y. A. 2011. Estrogen receptor silencing induces epithelial to mesenchymal transition in human breast cancer cells. *PLoS One,* 6**,** e20610.

ALARMO, E. L. & KALLIONIEMI, A. 2010. Bone morphogenetic proteins in breast cancer: dual role in tumourigenesis? *Endocr Relat Cancer,* 17**,** R123-39.

AMIN, R., MORITA-FUJIMURA, Y., TAWARAYAMA, H., SEMBA, K., CHIBA, N., FUKUMOTO, M. & IKAWA, S. 2016. DeltaNp63alpha induces quiescence and downregulates the BRCA1 pathway in estrogen receptor-positive luminal breast cancer cell line MCF7 but not in other breast cancer cell lines. *Mol Oncol,* 10**,** 575-93.

AMPUJA, M., JOKIMAKI, R., JUUTI-UUSITALO, K., RODRIGUEZ-MARTINEZ, A., ALARMO, E. L. & KALLIONIEMI, A. 2013. BMP4 inhibits the proliferation of breast cancer cells and induces an MMP-dependent migratory phenotype in MDA-MB-231 cells in 3D environment. *BMC Cancer,* 13**,** 429.

ANDERSSON, O., REISSMANN, E., JORNVALL, H. & IBANEZ, C. F. 2006. Synergistic interaction between Gdf1 and Nodal during anterior axis development. *Dev Biol,* 293**,** 370-81.

AOKI, H., FUJII, M., IMAMURA, T., YAGI, K., TAKEHARA, K., KATO, M. & MIYAZONO, K. 2001. Synergistic effects of different bone morphogenetic protein type I receptors on alkaline phosphatase induction. *J Cell Sci,* 114**,** 1483-9.

ARA, T. & DECLERCK, Y. A. 2010. Interleukin-6 in bone metastasis and cancer progression. *Eur J Cancer,* 46**,** 1223-31.

ARNETT, T. R. 2010. Acidosis, hypoxia and bone. *Arch Biochem Biophys,* 503**,** 103-9.

ARNOLD, S. F., TIMS, E. & MCGRATH, B. E. 1999. Identification of bone morphogenetic proteins and their receptors in human breast cancer cell lines: importance of BMP2. *Cytokine,* 11**,** 1031-7.

ARONSON, K. J., MILLER, A. B., WOOLCOTT, C. G., STERNS, E. E., MCCREADY, D. R., LICKLEY, L. A., FISH, E. B., HIRAKI, G. Y., HOLLOWAY, C., ROSS, T., HANNA, W. M., SENGUPTA, S. K. & WEBER, J. P. 2000. Breast adipose tissue concentrations of polychlorinated biphenyls and other organochlorines and breast cancer risk. *Cancer Epidemiol Biomarkers Prev,* 9**,** 55-63.

ARORA, K. & WARRIOR, R. 2001. A new Smurf in the village. *Dev Cell,* 1**,** 441-2.

ARVATZ, G., SHAFAT, I., LEVY-ADAM, F., ILAN, N. & VLODAVSKY, I. 2011. The heparanase system and tumor metastasis: is heparanase the seed and soil? *Cancer Metastasis Rev,* 30**,** 253-68.

AUSTIN, E. D., HAMID, R., HEMNES, A. R., LOYD, J. E., BLACKWELL, T., YU, C., PHILLIPS III, J. A., GADDIPATI, R., GLADSON, S., GU, E., WEST, J. & LANE, K. B. 2012. BMPR2 expression is suppressed by signaling through the estrogen receptor. *Biol Sex Differ,* 3**,** 6.

AVNET, S., DI POMPO, G., CHANO, T., ERRANI, C., IBRAHIM-HASHIM, A., GILLIES, R. J., DONATI, D. M. & BALDINI, N. 2017. Cancer-associated mesenchymal stroma fosters the stemness of osteosarcoma cells in response to intratumoral acidosis via NF-kappaB activation. *Int J Cancer,* 140**,** 1331-1345.

AZMI, P. & SETH, A. 2005. RNF11 is a multifunctional modulator of growth factor receptor signalling and transcriptional regulation. *Eur J Cancer,* 41**,** 2549-60.

BABITT, J. L., ZHANG, Y., SAMAD, T. A., XIA, Y., TANG, J., CAMPAGNA, J. A., SCHNEYER, A. L., WOOLF, C. J. & LIN, H. Y. 2005. Repulsive guidance molecule (RGMa), a DRAGON homologue, is a bone morphogenetic protein co-receptor. *J Biol Chem,* 280**,** 29820-7.

BACCELLI, I. & TRUMPP, A. 2012. The evolving concept of cancer and metastasis stem cells. *J Cell Biol,* 198**,** 281-93.

BACH, D. H., PARK, H. J. & LEE, S. K. 2018. The Dual Role of Bone Morphogenetic Proteins in Cancer. *Mol Ther Oncolytics,* 8**,** 1-13.

BADVE, S., TURBIN, D., THORAT, M. A., MORIMIYA, A., NIELSEN, T. O., PEROU, C. M., DUNN, S., HUNTSMAN, D. G. & NAKSHATRI, H. 2007. FOXA1 expression in breast cancer--correlation with luminal subtype A and survival. *Clin Cancer Res,* 13**,** 4415-21.

BAHENA-OCAMPO, I., ESPINOSA, M., CEBALLOS-CANCINO, G., LIZARRAGA, F., CAMPOS-ARROYO, D., SCHWARZ, A., GARCIA-LOPEZ, P., MALDONADO, V. & MELENDEZ-ZAJGLA, J. 2016. miR-10b

expression in breast cancer stem cells supports self-renewal through negative PTEN regulation and sustained AKT activation. *EMBO Rep,* 17**,** 1081.

BALBONI, A. L., HUTCHINSON, J. A., DECASTRO, A. J., CHERUKURI, P., LIBY, K., SPORN, M. B., SCHWARTZ, G. N., WELLS, W. A., SEMPERE, L. F., YU, P. B. & DIRENZO, J. 2013. DeltaNp63alpha-mediated activation of bone morphogenetic protein signaling governs stem cell activity and plasticity in normal and malignant mammary epithelial cells. *Cancer Res,* 73**,** 1020-30.

BALEMANS, W. & VAN HUL, W. 2002. Extracellular regulation of BMP signaling in vertebrates: a cocktail of modulators. *Dev Biol,* 250**,** 231-50.

BANIWAL, S. K., KHALID, O., GABET, Y., SHAH, R. R., PURCELL, D. J., MAV, D., KOHN-GABET, A. E., SHI, Y., COETZEE, G. A. & FRENKEL, B. 2010. Runx2 transcriptome of prostate cancer cells: insights into invasiveness and bone metastasis. *Mol Cancer,* 9**,** 258.

BANYS, M., SOLOMAYER, E. F., BECKER, S., KRAWCZYK, N., GARDANIS, K., STAEBLER, A., NEUBAUER, H., WALLWIENER, D. & FEHM, T. 2009. Disseminated tumor cells in bone marrow may affect prognosis of patients with gynecologic malignancies. *Int J Gynecol Cancer,* 19**,** 948-52.

BARAJAS-CASTANEDA, L. M., CORTES-GUTIERREZ, E., GARCIA-RODRIGUEZ, F. M., CAMPOS-RODRIGUEZ, R., LARA-PADILLA, E., ENRIQUEZ-RINCON, F., CASTRO-MUSSOT, M. E. & FIGUEROA-ARREDONDO, P. 2016. Overexpression of MMP-3 and uPA with Diminished PAI-1 Related to Metastasis in Ductal Breast Cancer Patients Attending a Public Hospital in Mexico City. *J Immunol Res,* 2016**,** 8519648.

BARR, S., THOMSON, S., BUCK, E., RUSSO, S., PETTI, F., SUJKA-KWOK, I., EYZAGUIRRE, A., ROSENFELD-FRANKLIN, M., GIBSON, N. W., MIGLARESE, M., EPSTEIN, D., IWATA, K. K. & HALEY, J. D. 2008. Bypassing cellular EGF receptor dependence through epithelial-to-mesenchymal-like transitions. *Clin Exp Metastasis,* 25**,** 685-93.

BECK, H. N., DRAHUSHUK, K., JACOBY, D. B., HIGGINS, D. & LEIN, P. J. 2001. Bone morphogenetic protein-5 (BMP-5) promotes dendritic growth in cultured sympathetic neurons. *BMC Neurosci,* 2**,** 12.

BEDNAREK, A. K., SAHIN, A., BRENNER, A. J., JOHNSTON, D. A. & ALDAZ, C. M. 1997. Analysis of telomerase activity levels in breast cancer: positive detection at the in situ breast carcinoma stage. *Clin Cancer Res,* 3**,** 11-6.

BELLACOSA, A., KUMAR, C. C., DI CRISTOFANO, A. & TESTA, J. R. 2005. Activation of AKT kinases in cancer: implications for therapeutic targeting. *Adv Cancer Res,* 94**,** 29-86.

BEN-ZVI, D., SHILO, B. Z., FAINSOD, A. & BARKAI, N. 2008. Scaling of the BMP activation gradient in Xenopus embryos. *Nature,* 453**,** 1205-11.

BERTUCCI, F., NG, C. K. Y., PATSOURIS, A., DROIN, N., PISCUOGLIO, S., CARBUCCIA, N., SORIA, J. C., DIEN, A. T., ADNANI, Y., KAMAL, M., GARNIER, S., MEURICE, G., JIMENEZ, M., DOGAN, S., VERRET, B., CHAFFANET, M., BACHELOT, T., CAMPONE, M., LEFEUVRE, C., BONNEFOI, H., DALENC, F., JACQUET, A., DE FILIPPO, M. R., BABBAR, N., BIRNBAUM, D., FILLERON, T., LE TOURNEAU, C. & ANDRE, F. 2019. Genomic characterization of metastatic breast cancers. *Nature,* 569**,** 560-564.

BESSON, A., DOWDY, S. F. & ROBERTS, J. M. 2008. CDK inhibitors: cell cycle regulators and beyond. *Dev Cell,* 14**,** 159-69.

BIRNBAUM, D., BERTUCCI, F., GINESTIER, C., TAGETT, R., JACQUEMIER, J. & CHARAFE-JAUFFRET, E. 2004. Basal and luminal breast cancers: basic or luminous? (review). *Int J Oncol,* 25**,** 249-58.

BOKOBZA, S. M., YE, L., KYNASTON, H. E., MANSEL, R. E. & JIANG, W. G. 2009. Reduced expression of BMPR-IB correlates with poor prognosis and increased proliferation of breast cancer cells. *Cancer Genomics Proteomics,* 6**,** 101-8.

BONNOMET, A., BRYSSE, A., TACHSIDIS, A., WALTHAM, M., THOMPSON, E. W., POLETTE, M. & GILLES, C. 2010. Epithelial-to-mesenchymal transitions and circulating tumor cells. *J Mammary Gland Biol Neoplasia,* 15**,** 261-73.

BORGEN, E., RYPDAL, M. C., SOSA, M. S., RENOLEN, A., SCHLICHTING, E., LONNING, P. E., SYNNESTVEDT, M., AGUIRRE-GHISO, J. A. & NAUME, B. 2018. NR2F1 stratifies dormant disseminated tumor cells in breast cancer patients. *Breast Cancer Res,* 20**,** 120.

BREWER, H. R., JONES, M. E., SCHOEMAKER, M. J., ASHWORTH, A. & SWERDLOW, A. J. 2017. Family history and risk of breast cancer: an analysis accounting for family structure. *Breast Cancer Res Treat,* 165**,** 193-200.

BROWN, J. D., DICHIARA, M. R., ANDERSON, K. R., GIMBRONE, M. A., JR. & TOPPER, J. N. 1999. MEKK-1, a component of the stress (stress-activated protein kinase/c-Jun N-terminal kinase) pathway, can selectively activate Smad2-mediated transcriptional activation in endothelial cells. *J Biol Chem,* 274**,** 8797-805.

BROWN, M. A., ZHAO, Q., BAKER, K. A., NAIK, C., CHEN, C., PUKAC, L., SINGH, M., TSAREVA, T., PARICE, Y., MAHONEY, A., ROSCHKE, V., SANYAL, I. & CHOE, S. 2005. Crystal structure of BMP-9 and functional interactions with pro-region and receptors. *J Biol Chem,* 280**,** 25111-8.

BUCKLEY, S., SHI, W., DRISCOLL, B., FERRARIO, A., ANDERSON, K. & WARBURTON, D. 2004. BMP4 signaling induces senescence and modulates the oncogenic phenotype of A549 lung adenocarcinoma cells. *Am J Physiol Lung Cell Mol Physiol,* 286**,** L81-6.

BUIJS, J. T., HENRIQUEZ, N. V., VAN OVERVELD, P. G., VAN DER HORST, G., QUE, I., SCHWANINGER, R., RENTSCH, C., TEN DIJKE, P., CLETON-JANSEN, A. M., DRIOUCH, K., LIDEREAU, R., BACHELIER, R., VUKICEVIC, S., CLEZARDIN, P., PAPAPOULOS, S. E., CECCHINI, M. G., LOWIK, C. W. & VAN DER PLUIJM, G. 2007a. Bone morphogenetic protein 7 in the development and treatment of bone metastases from breast cancer. *Cancer Res,* 67**,** 8742-51.

BUIJS, J. T., HENRIQUEZ, N. V., VAN OVERVELD, P. G., VAN DER HORST, G., TEN DIJKE, P. & VAN DER PLUIJM, G. 2007b. TGF-beta and BMP7 interactions in tumour progression and bone metastasis. *Clin Exp Metastasis,* 24**,** 609-17.

BUIJS, J. T., RENTSCH, C. A., VAN DER HORST, G., VAN OVERVELD, P. G., WETTERWALD, A., SCHWANINGER, R., HENRIQUEZ, N. V., TEN DIJKE, P., BOROVECKI, F., MARKWALDER, R., THALMANN, G. N., PAPAPOULOS, S. E., PELGER, R. C., VUKICEVIC, S., CECCHINI, M. G., LOWIK, C. W. & VAN DER PLUIJM, G. 2007c. BMP7, a putative regulator of epithelial homeostasis in the human prostate, is a potent inhibitor of prostate cancer bone metastasis in vivo. *Am J Pathol,* 171**,** 1047-57.

BUIJS, J. T., VAN DER HORST, G., VAN DEN HOOGEN, C., CHEUNG, H., DE ROOIJ, B., KROON, J., PETERSEN, M., VAN OVERVELD, P. G., PELGER, R. C. & VAN DER PLUIJM, G. 2012. The BMP2/7 heterodimer inhibits the human breast cancer stem cell subpopulation and bone metastases formation. *Oncogene,* 31**,** 2164-74.

BUNYARATAVEJ, P., HULLINGER, T. G. & SOMERMAN, M. J. 2000. Bone morphogenetic proteins secreted by breast cancer cells upregulate bone sialoprotein expression in preosteoblast cells. *Exp Cell Res,* 260**,** 324-33.

BUTLER, S. J. & DODD, J. 2003. A role for BMP heterodimers in roof plate-mediated repulsion of commissural axons. *Neuron,* 38**,** 389-401.

CARREIRA, A. C., ALVES, G. G., ZAMBUZZI, W. F., SOGAYAR, M. C. & GRANJEIRO, J. M. 2014. Bone Morphogenetic Proteins: structure, biological function and therapeutic applications. *Arch Biochem Biophys,* 561**,** 64-73.

CAVALLARO, U. & CHRISTOFORI, G. 2004. Cell adhesion and signalling by cadherins and Ig-CAMs in cancer. *Nat Rev Cancer,* 4**,** 118-32.

CELESTE, A. J., IANNAZZI, J. A., TAYLOR, R. C., HEWICK, R. M., ROSEN, V., WANG, E. A. & WOZNEY, J. M. 1990. Identification of transforming growth factor beta family members present in bone-inductive protein purified from bovine bone. *Proc Natl Acad Sci U S A,* 87**,** 9843-7.

CELESTE, A. J., SONG, J. J., COX, K., ROSEN, V. & WOZNEY, J. M. 1994. Bone morphogenetic protein-9, a new member of the TGF-beta superfamily. *J Bone Min Res,* Suppl 1**,** S136.

CHANDARLAPATY, S. & RAZAVI, P. 2019. Cyclin E mRNA: Assessing Cyclin-Dependent Kinase (CDK) Activation State to Elucidate Breast Cancer Resistance to CDK4/6 Inhibitors. *J Clin Oncol,* 37**,** 1148-1150.

CHANG, C. & HEMMATI-BRIVANLOU, A. 1999. Xenopus GDF6, a new antagonist of noggin and a partner of BMPs. *Development,* 126**,** 3347-57.

CHANG, C., HOLTZMAN, D. A., CHAU, S., CHICKERING, T., WOOLF, E. A., HOLMGREN, L. M., BODOROVA, J., GEARING, D. P., HOLMES, W. E. & BRIVANLOU, A. H. 2001. Twisted gastrulation can function as a BMP antagonist. *Nature,* 410**,** 483-7.

CHAVEZ-MACGREGOR, M., MITTENDORF, E. A., CLARKE, C. A., LICHTENSZTAJN, D. Y., HUNT, K. K. & GIORDANO, S. H. 2017. Incorporating Tumor Characteristics to the American Joint Committee on Cancer Breast Cancer Staging System. *Oncologist,* 22**,** 1292-1300.

CHEN, A., WANG, D., LIU, X., HE, S., YU, Z. & WANG, J. 2012a. Inhibitory effect of BMP-2 on the proliferation of breast cancer cells. *Mol Med Rep,* 6**,** 615-20.

CHEN, D., ZHAO, M. & MUNDY, G. R. 2004. Bone morphogenetic proteins. *Growth Factors,* 22**,** 233-41.

CHEN, G., DENG, C. & LI, Y. P. 2012b. TGF-beta and BMP signaling in osteoblast differentiation and bone formation. *Int J Biol Sci,* 8**,** 272-88.

CHEN, X., ZANKL, A., NIROOMAND, F., LIU, Z., KATUS, H. A., JAHN, L. & TIEFENBACHER, C. 2006. Upregulation of ID protein by growth and differentiation factor 5 (GDF5) through a smad-dependent and MAPK-independent pathway in HUVSMC. *J Mol Cell Cardiol,* 41**,** 26-33.

CHEN, X., ZHI, X., WANG, J. & SU, J. 2018. RANKL signaling in bone marrow mesenchymal stem cells negatively regulates osteoblastic bone formation. *Bone Res,* 6**,** 34.

CHEN, X. J., SHEN, Y. S., HE, M. C., YANG, F., YANG, P., PANG, F. X., HE, W., CAO, Y. M. & WEI, Q. S. 2019. Polydatin promotes the osteogenic differentiation of human bone mesenchymal stem cells by activating the BMP2-Wnt/beta-catenin signaling pathway. *Biomed Pharmacother,* 112**,** 108746.

CHENG, H., JIANG, W., PHILLIPS, F. M., HAYDON, R. C., PENG, Y., ZHOU, L., LUU, H. H., AN, N., BREYER, B., VANICHAKARN, P., SZATKOWSKI, J. P., PARK, J. Y. & HE, T. C. 2003. Osteogenic activity of the fourteen types of human bone morphogenetic proteins (BMPs). *J Bone Joint Surg Am,* 85**,** 1544-52.

CHENG, Z., CUI, W., DING, Y., LIU, T., LIU, W., QIN, Y., XIA, W., XU, J., ZHANG, Y. & ZOU, X. 2014. BMP8B mediates the survival of pancreatic cancer cells and regulates the progression of pancreatic cancer. *Oncol Rep,* 32**,** 1861-6.

CHI, L. H., BURROWS, A. D. & ANDERSON, R. L. 2019. Bone morphogenetic protein signaling in breast cancer progression. *Growth Factors,* 37**,** 12-28.

CHOI, S., YU, J., PARK, A., DUBON, M. J., DO, J., KIM, Y., NAM, D., NOH, J. & PARK, K. S. 2019. BMP-4 enhances epithelial mesenchymal transition and cancer stem cell properties of breast cancer cells via Notch signaling. *Sci Rep,* 9**,** 11724.

CHU, K., CHENG, C. J., YE, X., LEE, Y. C., ZURITA, A. J., CHEN, D. T., YU-LEE, L. Y., ZHANG, S., YEH, E. T., HU, M. C., LOGOTHETIS, C. J. & LIN, S. H. 2008. Cadherin-11 promotes the metastasis of prostate cancer cells to bone. *Mol Cancer Res,* 6**,** 1259-67.

CLAVEL-CHAPELON, F. & GERBER, M. 2002. Reproductive factors and breast cancer risk. Do they differ according to age at diagnosis? *Breast Cancer Res Treat,* 72**,** 107-15.

CLEMENT, F., XU, X., DONINI, C. F., CLEMENT, A., OMARJEE, S., DELAY, E., TREILLEUX, I., FERVERS, B., LE ROMANCER, M., COHEN, P. A. & MAGUER-SATTA, V. 2017. Long-term exposure to bisphenol A or benzo(a)pyrene alters the fate of human mammary epithelial stem cells in response to BMP2 and BMP4, by pre-activating BMP signaling. *Cell Death Differ,* 24**,** 155-166.

CLEMENT, J. H., MARR, N., MEISSNER, A., SCHWALBE, M., SEBALD, W., KLICHE, K. O., HOFFKEN, K. & WOLFL, S. 2000. Bone morphogenetic protein 2 (BMP-2) induces sequential changes of Id gene expression in the breast cancer cell line MCF-7. *J Cancer Res Clin Oncol,* 126**,** 271-9.

CLEMENT, J. H., SANGER, J. & HOFFKEN, K. 1999. Expression of bone morphogenetic protein 6 in normal mammary tissue and breast cancer cell lines and its regulation by epidermal growth factor. *Int J Cancer,* 80**,** 250-6.

CLEVERS, H. 2006. Wnt/beta-catenin signaling in development and disease. *Cell,* 127**,** 469-80.

CLEZARDIN, P. 2011. Therapeutic targets for bone metastases in breast cancer. *Breast Cancer Res,* 13**,** 207.

COGHLIN, C. & MURRAY, G. I. 2010. Current and emerging concepts in tumour metastasis. *J Pathol,* 222**,** 1-15.

COHEN, I., PAPPO, O., ELKIN, M., SAN, T., BAR-SHAVIT, R., HAZAN, R., PERETZ, T., VLODAVSKY, I. & ABRAMOVITCH, R. 2006. Heparanase promotes growth, angiogenesis and survival of primary breast tumors. *Int J Cancer,* 118**,** 1609-17.

COLEMAN, R. E. 2006. Clinical features of metastatic bone disease and risk of skeletal morbidity. *Clin Cancer Res,* 12**,** 6243s-6249s.

COLEMAN, R. E., MAJOR, P., LIPTON, A., BROWN, J. E., LEE, K. A., SMITH, M., SAAD, F., ZHENG, M., HEI, Y. J., SEAMAN, J. & COOK, R. 2005. Predictive value of bone resorption and formation markers in cancer patients with bone metastases receiving the bisphosphonate zoledronic acid. *J Clin Oncol,* 23**,** 4925-35.

COLLEONI, M., O'NEILL, A., GOLDHIRSCH, A., GELBER, R. D., BONETTI, M., THURLIMANN, B., PRICE, K. N., CASTIGLIONE-GERTSCH, M., COATES, A. S., LINDTNER, J., COLLINS, J., SENN, H. J., CAVALLI, F., FORBES, J., GUDGEON, A., SIMONCINI, E., CORTES-FUNES, H., VERONESI, A., FEY, M. & RUDENSTAM, C. M. 2000. Identifying breast cancer patients at high risk for bone metastases. *J Clin Oncol,* 18**,** 3925-35.

COX, T. R., RUMNEY, R. M. H., SCHOOF, E. M., PERRYMAN, L., HOYE, A. M., AGRAWAL, A., BIRD, D., LATIF, N. A., FORREST, H., EVANS, H. R., HUGGINS, I. D., LANG, G., LINDING, R., GARTLAND, A. & ERLER, J. T. 2015. The hypoxic cancer secretome induces pre-metastatic bone lesions through lysyl oxidase. *Nature,* 522**,** 106-110.

CRANE, G. M., JEFFERY, E. & MORRISON, S. J. 2017. Adult haematopoietic stem cell niches. *Nat Rev Immunol,* 17**,** 573-590.

CUNNINGHAM, N. S., JENKINS, N. A., GILBERT, D. J., COPELAND, N. G., REDDI, A. H. & LEE, S. J. 1995. Growth/differentiation factor-10: a new member of the transforming growth factor-beta superfamily related to bone morphogenetic protein-3. *Growth Factors,* 12**,** 99-109.

CYR-DEPAUW, C., NORTHEY, J. J., TABARIES, S., ANNIS, M. G., DONG, Z., CORY, S., HALLETT, M., RENNHACK, J. P., ANDRECHEK, E. R. & SIEGEL, P. M. 2016. Chordin-Like 1 Suppresses Bone Morphogenetic Protein 4-Induced Breast Cancer Cell Migration and Invasion. *Mol Cell Biol,* 36**,** 1509-25.

CZERWINSKA, P. & KAMINSKA, B. 2015. Regulation of breast cancer stem cell features. *Contemp Oncol (Pozn),* 19**,** A7-A15.

DA ROSA, M. R., FALCAO, A. S., FUZII, H. T., DA SILVA KATAOKA, M. S., RIBEIRO, A. L., BOCCARDO, E., DE SIQUEIRA, A. S., JAEGER, R. G., DE JESUS VIANA PINHEIRO, J. & DE MELO ALVES JUNIOR, S. 2014. EGFR signaling downstream of EGF regulates migration, invasion, and MMP secretion of immortalized cells derived from human ameloblastoma. *Tumour Biol,* 35**,** 11107-20.

DA SILVA MADALENO, C., JATZLAU, J. & KNAUS, P. 2020. BMP signalling in a mechanical context - Implications for bone biology. *Bone,* 137**,** 115416.

DAI, J., KITAGAWA, Y., ZHANG, J., YAO, Z., MIZOKAMI, A., CHENG, S., NOR, J., MCCAULEY, L. K., TAICHMAN, R. S. & KELLER, E. T. 2004. Vascular endothelial growth factor contributes to the prostate cancer-induced osteoblast

differentiation mediated by bone morphogenetic protein. *Cancer Res,* 64**,** 994-9.

DALE, K., SATTAR, N., HEEMSKERK, J., CLARKE, J. D., PLACZEK, M. & DODD, J. 1999. Differential patterning of ventral midline cells by axial mesoderm is regulated by BMP7 and chordin. *Development,* 126**,** 397-408.

DALERBA, P. & CLARKE, M. F. 2007. Cancer stem cells and tumor metastasis: first steps into uncharted territory. *Cell Stem Cell,* 1**,** 241-2.

DALUISKI, A., ENGSTRAND, T., BAHAMONDE, M. E., GAMER, L. W., AGIUS, E., STEVENSON, S. L., COX, K., ROSEN, V. & LYONS, K. M. 2001. Bone morphogenetic protein-3 is a negative regulator of bone density. *Nat Genet,* 27**,** 84-8.

DANO, K., BEHRENDT, N., HOYER-HANSEN, G., JOHNSEN, M., LUND, L. R., PLOUG, M. & ROMER, J. 2005. Plasminogen activation and cancer. *Thromb Haemost,* 93**,** 676-81.

DARDAEI, L., SHAHSAVANI, R., GHAVAMZADEH, A., BEHMANESH, M., ASLANKOOHI, E., ALIMOGHADDAM, K. & GHAFFARI, S. H. 2011. The detection of disseminated tumor cells in bone marrow and peripheral blood of gastric cancer patients by multimarker (CEA, CK20, TFF1 and MUC2) quantitative real-time PCR. *Clin Biochem,* 44**,** 325-30.

DAVIDSON, A. J., POSTLETHWAIT, J. H., YAN, Y. L., BEIER, D. R., VAN DOREN, C., FOERNZLER, D., CELESTE, A. J., CROSIER, K. E. & CROSIER, P. S. 1999. Isolation of zebrafish gdf7 and comparative genetic mapping of genes belonging to the growth/differentiation factor 5, 6, 7 subgroup of the TGF-beta superfamily. *Genome Res,* 9**,** 121-9.

DAVIS, H., RAJA, E., MIYAZONO, K., TSUBAKIHARA, Y. & MOUSTAKAS, A. 2016. Mechanisms of action of bone morphogenetic proteins in cancer. *Cytokine Growth Factor Rev,* 27**,** 81-92.

DE BOECK, M., CUI, C., MULDER, A. A., JOST, C. R., IKENO, S. & TEN DIJKE, P. 2016. Smad6 determines BMP-regulated invasive behaviour of breast cancer cells in a zebrafish xenograft model. *Sci Rep,* 6**,** 24968.

DE CAESTECKER, M. P., PARKS, W. T., FRANK, C. J., CASTAGNINO, P., BOTTARO, D. P., ROBERTS, A. B. & LECHLEIDER, R. J. 1998. Smad2 transduces common signals from receptor serine-threonine and tyrosine kinases. *Genes Dev,* 12**,** 1587-92.

DE CASTRO JUNIOR, G., PUGLISI, F., DE AZAMBUJA, E., EL SAGHIR, N. S. & AWADA, A. 2006. Angiogenesis and cancer: A cross-talk between basic science and clinical trials (the "do ut des" paradigm). *Crit Rev Oncol Hematol,* 59**,** 40-50.

DE KEULENAER, G. W., DOGGEN, K. & LEMMENS, K. 2010. The vulnerability of the heart as a pluricellular paracrine organ: lessons from unexpected triggers of heart failure in targeted ErbB2 anticancer therapy. *Circ Res,* 106**,** 35-46.

DEIGNAN, L., PINHEIRO, M. T., SUTCLIFFE, C., SAUNDERS, A., WILCOCKSON, S. G., ZEEF, L. A., DONALDSON, I. J. & ASHE, H. L. 2016. Regulation of the BMP Signaling-Responsive Transcriptional Network in the Drosophila Embryo. *PLoS Genet,* 12**,** e1006164.

DELIGIORGI, M. V., PANAYIOTIDIS, M. I., GRINIATSOS, J. & TRAFALIS, D. T. 2020. Harnessing the versatile role of OPG in bone oncology: counterbalancing RANKL and TRAIL signaling and beyond. *Clin Exp Metastasis,* 37**,** 13-30.

DEVIGNES, C. S., ASLAN, Y., BRENOT, A., DEVILLERS, A., SCHEPERS, K., FABRE, S., CHOU, J., CASBON, A. J., WERB, Z. & PROVOT, S. 2018. HIF signaling in osteoblast-lineage cells promotes systemic breast cancer growth and metastasis in mice. *Proc Natl Acad Sci U S A,* 115**,** E992-E1001.

DI, L., LIU, L. J., YAN, Y. M., FU, R., LI, Y., XU, Y., CHENG, Y. X. & WU, Z. Q. 2019. Discovery of a natural small-molecule compound that suppresses tumor EMT, stemness and metastasis by inhibiting TGFbeta/BMP signaling in triple-negative breast cancer. *J Exp Clin Cancer Res,* 38**,** 134.

DIONNE, M. S., SKARNES, W. C. & HARLAND, R. M. 2001. Mutation and analysis of Dan, the founding member of the Dan family of transforming growth factor beta antagonists. *Mol Cell Biol,* 21**,** 636-43.

DORAI, H., VUKICEVIC, S. & SAMPATH, T. K. 2000. Bone morphogenetic protein-7 (osteogenic protein-1) inhibits smooth muscle cell proliferation and stimulates the expression of markers that are characteristic of SMC phenotype in vitro. *J Cell Physiol,* 184**,** 37-45.

DUBE, J. L., WANG, P., ELVIN, J., LYONS, K. M., CELESTE, A. J. & MATZUK, M. M. 1998. The bone morphogenetic protein 15 gene is X-linked and expressed in oocytes. *Mol Endocrinol,* 12**,** 1809-17.

DUCHARTRE, Y., KIM, Y. M. & KAHN, M. 2016. The Wnt signaling pathway in cancer. *Crit Rev Oncol Hematol,* 99**,** 141-9.

DVORAK, H. F. 2002. Vascular permeability factor/vascular endothelial growth factor: a critical cytokine in tumor angiogenesis and a potential target for diagnosis and therapy. *J Clin Oncol,* 20**,** 4368-80.

DYER, L. A., PI, X. & PATTERSON, C. 2014. The role of BMPs in endothelial cell function and dysfunction. *Trends Endocrinol Metab,* 25**,** 472-80.

EBISAWA, T., TADA, K., KITAJIMA, I., TOJO, K., SAMPATH, T. K., KAWABATA, M., MIYAZONO, K. & IMAMURA, T. 1999. Characterization of bone morphogenetic protein-6 signaling pathways in osteoblast differentiation. *J Cell Sci,* 112 (Pt 20)**,** 3519-27.

EIVERS, E., FUENTEALBA, L. C. & DE ROBERTIS, E. M. 2008. Integrating positional information at the level of Smad1/5/8. *Curr Opin Genet Dev,* 18**,** 304-10.

ELLIS, M. J., COOP, A., SINGH, B., MAURIAC, L., LLOMBERT-CUSSAC, A., JANICKE, F., MILLER, W. R., EVANS, D. B., DUGAN, M., BRADY, C., QUEBE-FEHLING, E. & BORGS, M. 2001. Letrozole is more effective neoadjuvant endocrine therapy than tamoxifen for ErbB-1- and/or ErbB-2-positive, estrogen receptor-positive primary breast cancer: evidence from a phase III randomized trial. *J Clin Oncol,* 19**,** 3808-16.

ENDO, H. & INOUE, M. 2019. Dormancy in cancer. *Cancer Sci,* 110**,** 474-480.

FAINSOD, A., DEISSLER, K., YELIN, R., MAROM, K., EPSTEIN, M., PILLEMER, G., STEINBEISSER, H. & BLUM, M. 1997. The dorsalizing and neural inducing gene follistatin is an antagonist of BMP-4. *Mech Dev,* 63**,** 39-50.

FAN, B., ONTERU, S. K., MOTE, B. E., SERENIUS, T., STALDER, K. J. & ROTHSCHILD, M. F. 2009a. Large-scale association study for structural soundness and leg locomotion traits in the pig. *Genet Sel Evol,* 41**,** 14.

FAN, B., ONTERU, S. K., NIKKILA, M. T., STALDER, K. J. & ROTHSCHILD, M. F. 2009b. Identification of genetic markers associated with fatness and leg weakness traits in the pig. *Anim Genet,* 40**,** 967-70.

FERGUSON, K. M. 2008. Structure-based view of epidermal growth factor receptor regulation. *Annu Rev Biophys,* 37**,** 353-73.

FERRER, A., ROSER, C. T., EL-FAR, M. H., SAVANUR, V. H., ELJARRAH, A., GERGUES, M., KRA, J. A., ETCHEGARAY, J. P. & RAMESHWAR, P. 2020. Hypoxia-mediated changes in bone marrow microenvironment in breast cancer dormancy. *Cancer Lett,* 488**,** 9-17.

FIDLER, I. J. 1973. The relationship of embolic homogeneity, number, size and viability to the incidence of experimental metastasis. *Eur J Cancer,* 9**,** 223-7.

FINN, R. S., MARTIN, M., RUGO, H. S., JONES, S., IM, S. A., GELMON, K., HARBECK, N., LIPATOV, O. N., WALSHE, J. M., MOULDER, S., GAUTHIER, E., LU, D. R., RANDOLPH, S., DIERAS, V. & SLAMON, D. J. 2016. Palbociclib and Letrozole in Advanced Breast Cancer. *N Engl J Med,* 375**,** 1925-1936.

FLUEGEN, G., AVIVAR-VALDERAS, A., WANG, Y., PADGEN, M. R., WILLIAMS, J. K., NOBRE, A. R., CALVO, V., CHEUNG, J. F., BRAVO-CORDERO, J. J., ENTENBERG, D., CASTRACANE, J., VERKHUSHA, V., KEELY, P. J., CONDEELIS, J. & AGUIRRE-GHISO, J. A. 2017. Phenotypic heterogeneity of disseminated tumour cells is preset by primary tumour hypoxic microenvironments. *Nat Cell Biol,* 19**,** 120-132.

FOLKMAN, J. & KALLURI, R. 2004. Cancer without disease. *Nature,* 427**,** 787.

FORNETTI, J., WELM, A. L. & STEWART, S. A. 2018. Understanding the Bone in Cancer Metastasis. *J Bone Miner Res,* 33**,** 2099-2113.

FREES, S., BREUKSCH, I., HABER, T., BAUER, H. K., CHAVEZ-MUNOZ, C., RAVEN, P., MOSKALEV, I., N, D. C., TAN, Z., DAUGAARD, M., THUROFF, J. W., HAFERKAMP, A., PRAWITT, D., SO, A. & BRENNER, W. 2018. Calcium-sensing receptor (CaSR) promotes development of bone metastasis in renal cell carcinoma. *Oncotarget,* 9**,** 15766-15779.

FRUMP, A. L., ALBRECHT, M., YAKUBOV, B., BREUILS-BONNET, S., NADEAU, V., TREMBLAY, E., POTUS, F., OMURA, J., COOK, T., FISHER, A., RODRIGUEZ, B., BROWN, R. D., STENMARK, K. R., RUBINSTEIN, C. D., KRENTZ, K., TABIMA, D. M., LI, R., SUN, X., CHESLER, N. C., PROVENCHER, S., BONNET, S. & LAHM, T. 2021. 17beta-Estradiol and estrogen receptor alpha protect right ventricular function in pulmonary hypertension via BMPR2 and apelin. *J Clin Invest,* 131.

FU, Q., MANOLAGAS, S. C. & O'BRIEN, C. A. 2006. Parathyroid hormone controls receptor activator of NF-kappaB ligand gene expression via a distant transcriptional enhancer. *Mol Cell Biol,* 26**,** 6453-68.

FUENTES, N. & SILVEYRA, P. 2019. Estrogen receptor signaling mechanisms. *Adv Protein Chem Struct Biol,* 116**,** 135-170.

GALLIHER, A. J. & SCHIEMANN, W. P. 2007. Src phosphorylates Tyr284 in TGF-beta type II receptor and regulates TGF-beta stimulation of p38 MAPK during breast cancer cell proliferation and invasion. *Cancer Res,* 67**,** 3752-8.

GAMER, L. W., WOLFMAN, N. M., CELESTE, A. J., HATTERSLEY, G., HEWICK, R. & ROSEN, V. 1999. A novel BMP expressed in developing mouse limb, spinal cord, and tail bud is a potent mesoderm inducer in Xenopus embryos. *Dev Biol,* 208**,** 222-32.

GAO, D. & MITTAL, V. 2009. The role of bone-marrow-derived cells in tumor growth, metastasis initiation and progression. *Trends Mol Med,* 15**,** 333-43.

GAO, H., CHAKRABORTY, G., LEE-LIM, A. P., MO, Q., DECKER, M., VONICA, A., SHEN, R., BROGI, E., BRIVANLOU, A. H. & GIANCOTTI, F. G. 2012. The BMP inhibitor Coco reactivates breast cancer cells at lung metastatic sites. *Cell,* 150**,** 764-79.

GAO, Y., JONES, A., FASCHING, P. A., RUEBNER, M., BECKMANN, M. W., WIDSCHWENDTER, M. & TESCHENDORFF, A. E. 2015. The integrative epigenomic-transcriptomic landscape of ER positive breast cancer. *Clin Epigenetics,* 7**,** 126.

GARCIA-ALVARO, M., ADDANTE, A., RONCERO, C., FERNANDEZ, M., FABREGAT, I., SANCHEZ, A. & HERRERA, B. 2015. BMP9-Induced Survival Effect in Liver Tumor Cells Requires p38MAPK Activation. *Int J Mol Sci,* 16**,** 20431-48.

GARRETT, J. T., OLIVARES, M. G., RINEHART, C., GRANJA-INGRAM, N. D., SANCHEZ, V., CHAKRABARTY, A., DAVE, B., COOK, R. S., PAO, W., MCKINELY, E., MANNING, H. C., CHANG, J. & ARTEAGA, C. L. 2011. Transcriptional and posttranslational up-regulation of HER3 (ErbB3) compensates for inhibition of the HER2 tyrosine kinase. *Proc Natl Acad Sci U S A,* 108**,** 5021-6.

GARULLI, C., KALOGRIS, C., PIETRELLA, L., BARTOLACCI, C., ANDREANI, C., FALCONI, M., MARCHINI, C. & AMICI, A. 2014. Dorsomorphin reverses the mesenchymal phenotype of breast cancer initiating cells by inhibition of bone morphogenetic protein signaling. *Cell Signal,* 26**,** 352-62.

GATZA, C. E., ELDERBROOM, J. L., OH, S. Y., STARR, M. D., NIXON, A. B. & BLOBE, G. C. 2014. The balance of cell surface and soluble type III TGF-beta receptor regulates BMP signaling in normal and cancerous mammary epithelial cells. *Neoplasia,* 16**,** 489-500.

GAWRZAK, S., RINALDI, L., GREGORIO, S., ARENAS, E. J., SALVADOR, F., UROSEVIC, J., FIGUERAS-PUIG, C., ROJO, F., DEL BARCO BARRANTES, I., CEJALVO, J. M., PALAFOX, M., GUIU, M., BERENGUER-LLERGO, A., SYMEONIDI, A., BELLMUNT, A., KALAFATOVIC, D., ARNAL-ESTAPE, A., FERNANDEZ, E., MULLAUER, B., GROENEVELD, R., SLOBODNYUK, K., STEPHAN-OTTO ATTOLINI, C., SAURA, C., ARRIBAS, J., CORTES, J., ROVIRA, A., MUNOZ, M., LLUCH, A., SERRA, V., ALBANELL, J., PRAT, A., NEBREDA, A. R., BENITAH, S. A. & GOMIS, R. R. 2018. MSK1 regulates luminal cell differentiation and metastatic dormancy in ER(+) breast cancer. *Nat Cell Biol,* 20**,** 211-221.

GAZZERRO, E., GANGJI, V. & CANALIS, E. 1998. Bone morphogenetic proteins induce the expression of noggin, which limits their activity in cultured rat osteoblasts. *J Clin Invest,* 102**,** 2106-14.

GERLACH-BANK, L. M., CLEVELAND, A. R. & BARALD, K. F. 2004. DAN directs endolymphatic sac and duct outgrowth in the avian inner ear. *Dev Dyn,* 229**,** 219-30.

GHAJAR, C. M., PEINADO, H., MORI, H., MATEI, I. R., EVASON, K. J., BRAZIER, H., ALMEIDA, D., KOLLER, A., HAJJAR, K. A., STAINIER, D. Y., CHEN, E. I., LYDEN, D. & BISSELL, M. J. 2013. The perivascular niche regulates breast tumour dormancy. *Nat Cell Biol,* 15**,** 807-17.

GHOSH-CHOUDHURY, N., GHOSH-CHOUDHURY, G., CELESTE, A., GHOSH, P. M., MOYER, M., ABBOUD, S. L. & KREISBERG, J. 2000. Bone morphogenetic protein-2 induces cyclin kinase inhibitor p21 and hypophosphorylation of retinoblastoma protein in estradiol-treated MCF-7 human breast cancer cells. *Biochim Biophys Acta,* 1497**,** 186-96.

GOMEZ DE CEDRON, M., MOUHID, L., GARCIA-CARRASCOSA, E., FORNARI, T., REGLERO, G. & RAMIREZ DE MOLINA, A. 2019. Marigold

Supercritical Extract as Potential Co-adjuvant in Pancreatic Cancer: The Energetic Catastrophe Induced via BMP8B Ends Up With Autophagy-Induced Cell Death. *Front Bioeng Biotechnol,* 7**,** 455.

GOMIS, R. R. & GAWRZAK, S. 2017. Tumor cell dormancy. *Mol Oncol,* 11**,** 62-78.

GONZALEZ, D. M. & MEDICI, D. 2014. Signaling mechanisms of the epithelial-mesenchymal transition. *Sci Signal,* 7**,** re8.

GOTO, K., KAMIYA, Y., IMAMURA, T., MIYAZONO, K. & MIYAZAWA, K. 2007. Selective inhibitory effects of Smad6 on bone morphogenetic protein type I receptors. *J Biol Chem,* 282**,** 20603-11.

GOTTE, M. & YIP, G. W. 2006. Heparanase, hyaluronan, and CD44 in cancers: a breast carcinoma perspective. *Cancer Res,* 66**,** 10233-7.

GOULD ROTHBERG, B. E. & BRACKEN, M. B. 2006. E-cadherin immunohistochemical expression as a prognostic factor in infiltrating ductal carcinoma of the breast: a systematic review and meta-analysis. *Breast Cancer Res Treat,* 100**,** 139-48.

GOUMANS, M. J., VALDIMARSDOTTIR, G., ITOH, S., ROSENDAHL, A., SIDERAS, P. & TEN DIJKE, P. 2002. Balancing the activation state of the endothelium via two distinct TGF-beta type I receptors. *EMBO J,* 21**,** 1743-53.

GRAHAM, T. R., AGRAWAL, K. C. & ABDEL-MAGEED, A. B. 2010. Independent and cooperative roles of tumor necrosis factor-alpha, nuclear factor-kappaB, and bone morphogenetic protein-2 in regulation of metastasis and osteomimicry of prostate cancer cells and differentiation and mineralization of MC3T3-E1 osteoblast-like cells. *Cancer Sci,* 101**,** 103-11.

GROTEWOLD, L., PLUM, M., DILDROP, R., PETERS, T. & RUTHER, U. 2001. Bambi is coexpressed with Bmp-4 during mouse embryogenesis. *Mech Dev,* 100**,** 327-30.

GUISE, T. A., YIN, J. J. & MOHAMMAD, K. S. 2003. Role of endothelin-1 in osteoblastic bone metastases. *Cancer,* 97**,** 779-84.

GUL, S., MURAD, S., EHSAN, N., BLOODSWORTH, P., SULTAN, A. & FAHEEM, M. 2015. Transcriptional up-regulation of BMP-4 and BMPR-II genes in the peripheral blood of breast cancer patients: A pilot study. *Cancer Biomark,* 15**,** 551-7.

GUO, D., HUANG, J. & GONG, J. 2012. Bone morphogenetic protein 4 (BMP4) is required for migration and invasion of breast cancer. *Mol Cell Biochem,* 363**,** 179-90.

GUO, X. & WANG, X. F. 2009. Signaling cross-talk between TGF-beta/BMP and other pathways. *Cell Res,* 19**,** 71-88.

HALLAHAN, A. R., PRITCHARD, J. I., CHANDRARATNA, R. A., ELLENBOGEN, R. G., GEYER, J. R., OVERLAND, R. P., STRAND, A. D., TAPSCOTT, S. J. & OLSON, J. M. 2003. BMP-2 mediates retinoid-induced apoptosis in medulloblastoma cells through a paracrine effect. *Nat Med,* 9**,** 1033-8.

HANKER, A. B., SUDHAN, D. R. & ARTEAGA, C. L. 2020. Overcoming Endocrine Resistance in Breast Cancer. *Cancer Cell,* 37**,** 496-513.

HANYU, A., ISHIDOU, Y., EBISAWA, T., SHIMANUKI, T., IMAMURA, T. & MIYAZONO, K. 2001. The N domain of Smad7 is essential for specific inhibition of transforming growth factor-beta signaling. *J Cell Biol,* 155**,** 1017-27.

HARBECK, N. & GNANT, M. 2017. Breast cancer. *Lancet,* 389**,** 1134-1150.

HARBECK, N., SAUPE, S., JAGER, E., SCHMIDT, M., KREIENBERG, R., MULLER, L., OTREMBA, B. J., WALDENMAIER, D., DORN, J., WARM, M., SCHOLZ, M., UNTCH, M., DE WIT, M., BARINOFF, J., LUCK, H. J., HARTER, P., AUGUSTIN, D., HARNETT, P., BECKMANN, M. W., AL-BATRAN, S. E. & INVESTIGATORS, P. 2017. A randomized phase III study evaluating pegylated liposomal doxorubicin versus capecitabine as first-line therapy for metastatic breast cancer: results of the PELICAN study. *Breast Cancer Res Treat,* 161**,** 63-72.

HARDY, K. M., BOOTH, B. W., HENDRIX, M. J., SALOMON, D. S. & STRIZZI, L. 2010. ErbB/EGF signaling and EMT in mammary development and breast cancer. *J Mammary Gland Biol Neoplasia,* 15**,** 191-9.

HATA, A., LAGNA, G., MASSAGUE, J. & HEMMATI-BRIVANLOU, A. 1998. Smad6 inhibits BMP/Smad1 signaling by specifically competing with the Smad4 tumor suppressor. *Genes Dev,* 12**,** 186-97.

HAUDENSCHILD, D. R., PALMER, S. M., MOSELEY, T. A., YOU, Z. & REDDI, A. H. 2004. Bone morphogenetic protein (BMP)-6 signaling and BMP antagonist noggin in prostate cancer. *Cancer Res,* 64**,** 8276-84.

HAWINKELS, L. J., DE VINUESA, A. G., PAAUWE, M., KRUITHOF-DE JULIO, M., WIERCINSKA, E., PARDALI, E., MEZZANOTTE, L., KEEREWEER, S., BRAUMULLER, T. M., HEIJKANTS, R. C., JONKERS, J., LOWIK, C. W., GOUMANS, M. J., TEN HAGEN, T. L. & TEN DIJKE, P. 2016. Activin Receptor-like Kinase 1 Ligand Trap Reduces Microvascular Density and Improves Chemotherapy Efficiency to Various Solid Tumors. *Clin Cancer Res,* 22**,** 96-106.

HE, X. C., ZHANG, J., TONG, W. G., TAWFIK, O., ROSS, J., SCOVILLE, D. H., TIAN, Q., ZENG, X., HE, X., WIEDEMANN, L. M., MISHINA, Y. & LI, L. 2004. BMP signaling inhibits intestinal stem cell self-renewal through suppression of Wnt-beta-catenin signaling. *Nat Genet,* 36**,** 1117-21.

HEIM, E., VALACH, L. & SCHAFFNER, L. 1997. Coping and psychosocial adaptation: longitudinal effects over time and stages in breast cancer. *Psychosom Med,* 59**,** 408-18.

HELMS, M. W., PACKEISEN, J., AUGUST, C., SCHITTEK, B., BOECKER, W., BRANDT, B. H. & BUERGER, H. 2005. First evidence supporting a potential role for the BMP/SMAD pathway in the progression of oestrogen receptor-positive breast cancer. *J Pathol,* 206**,** 366-76.

HERNANDEZ, R. K., WADE, S. W., REICH, A., PIROLLI, M., LIEDE, A. & LYMAN, G. H. 2018. Incidence of bone metastases in patients with solid tumors: analysis of oncology electronic medical records in the United States. *BMC Cancer,* 18**,** 44.

HIGGINS, D. F., EWART, L. M., MASTERSON, E., TENNANT, S., GREBNEV, G., PRUNOTTO, M., POMPOSIELLO, S., CONDE-KNAPE, K., MARTIN, F. M. & GODSON, C. 2017. BMP7-induced-Pten inhibits Akt and prevents renal fibrosis. *Biochim Biophys Acta Mol Basis Dis,* 1863**,** 3095-3104.

HIRAGA, T., KIZAKA-KONDOH, S., HIROTA, K., HIRAOKA, M. & YONEDA, T. 2007. Hypoxia and hypoxia-inducible factor-1 expression enhance osteolytic bone metastases of breast cancer. *Cancer Res,* 67**,** 4157-63.

HOPKINS, D. R., KELES, S. & GREENSPAN, D. S. 2007. The bone morphogenetic protein 1/Tolloid-like metalloproteinases. *Matrix Biol,* 26**,** 508-23.

HOPPLER, S. & MOON, R. T. 1998. BMP-2/-4 and Wnt-8 cooperatively pattern the Xenopus mesoderm. *Mech Dev,* 71**,** 119-29.

HOTTEN, G., NEIDHARDT, H., JACOBOWSKY, B. & POHL, J. 1994. Cloning and expression of recombinant human growth/differentiation factor 5. *Biochem Biophys Res Commun,* 204**,** 646-52.

HSU, D. R., ECONOMIDES, A. N., WANG, X., EIMON, P. M. & HARLAND, R. M. 1998. The Xenopus dorsalizing factor Gremlin identifies a novel family of secreted proteins that antagonize BMP activities. *Mol Cell,* 1**,** 673-83.

HU, F., ZHANG, Y., LI, M., ZHAO, L., CHEN, J., YANG, S. & ZHANG, X. 2016. BMP-6 inhibits the metastasis of MDA-MB-231 breast cancer cells by regulating MMP-1 expression. *Oncol Rep,* 35**,** 1823-30.

HUANG, H. Y., JIANG, Z. F., LI, Q. X., LIU, J. Y., WANG, T., ZHANG, R., ZHAO, J., XU, Y. M., BAO, W., ZHANG, Y., JIA, L. T. & YANG, A. G. 2010. Inhibition of human breast cancer cell invasion by siRNA against urokinase-type plasminogen activator. *Cancer Invest,* 28**,** 689-97.

HUANG, P., CHEN, A., HE, W., LI, Z., ZHANG, G., LIU, Z., LIU, G., LIU, X., HE, S., XIAO, G., HUANG, F., STENVANG, J., BRUNNER, N., HONG, A. & WANG, J. 2017. BMP-2 induces EMT and breast cancer stemness through Rb and CD44. *Cell Death Discov,* 3**,** 17039.

HUANG, T., WU, Q., HUANG, H., ZHANG, C., WANG, L., WANG, L., LIU, Y., LI, W., ZHANG, J. & LIU, Y. 2022. Expression of GALNT8 and O-glycosylation of BMP receptor 1A suppress breast cancer cell proliferation by upregulating ERalpha levels. *Biochim Biophys Acta Gen Subj,* 1866**,** 130046.

HUNTER, K. W., CRAWFORD, N. P. & ALSARRAJ, J. 2008. Mechanisms of metastasis. *Breast Cancer Res,* 10 Suppl 1**,** S2.

IBRAHIM, T., LEONG, I., SANCHEZ-SWEATMAN, O., KHOKHA, R., SODEK, J., TENENBAUM, H. C., GANSS, B. & CHEIFETZ, S. 2000. Expression of bone sialoprotein and osteopontin in breast cancer bone metastases. *Clin Exp Metastasis,* 18**,** 253-60.

IEMURA, S., YAMAMOTO, T. S., TAKAGI, C., UCHIYAMA, H., NATSUME, T., SHIMASAKI, S., SUGINO, H. & UENO, N. 1998. Direct binding of follistatin to a complex of bone-morphogenetic protein and its receptor inhibits ventral and epidermal cell fates in early Xenopus embryo. *Proc Natl Acad Sci U S A,* 95**,** 9337-42.

ITOH, F., ASAO, H., SUGAMURA, K., HELDIN, C. H., TEN DIJKE, P. & ITOH, S. 2001. Promoting bone morphogenetic protein signaling through negative regulation of inhibitory Smads. *Embo J,* 20**,** 4132-42.

ITOH, S., ITOH, F., GOUMANS, M. J. & TEN DIJKE, P. 2000. Signaling of transforming growth factor-beta family members through Smad proteins. *Eur J Biochem,* 267**,** 6954-67.

JACQUILLAT, C., WEIL, M., BAILLET, F., BOREL, C., AUCLERC, G., DE MAUBLANC, M. A., HOUSSET, M., FORGET, G., THILL, L., SOUBRANE, C. & ET AL. 1990. Results of neoadjuvant chemotherapy and radiation therapy in the breast-conserving treatment of 250 patients with all stages of infiltrative breast cancer. *Cancer,* 66**,** 119-29.

JAIN, R. K. 2005. Normalization of tumor vasculature: an emerging concept in antiangiogenic therapy. *Science,* 307**,** 58-62.

JAMES, J. J., EVANS, A. J., PINDER, S. E., GUTTERIDGE, E., CHEUNG, K. L., CHAN, S. & ROBERTSON, J. F. 2003. Bone metastases from breast carcinoma: histopathological - radiological correlations and prognostic features. *Br J Cancer,* 89**,** 660-5.

JANDA, E., LEHMANN, K., KILLISCH, I., JECHLINGER, M., HERZIG, M., DOWNWARD, J., BEUG, H. & GRUNERT, S. 2002. Ras and TGF[beta] cooperatively regulate epithelial cell plasticity and metastasis: dissection of Ras signaling pathways. *J Cell Biol,* 156**,** 299-313.

JAWORSKA, D., KROL, W. & SZLISZKA, E. 2015. Prostate Cancer Stem Cells: Research Advances. *Int J Mol Sci,* 16**,** 27433-49.

JI, H., WANG, J., NIKA, H., HAWKE, D., KEEZER, S., GE, Q., FANG, B., FANG, X., FANG, D., LITCHFIELD, D. W., ALDAPE, K. & LU, Z. 2009. EGF-induced ERK activation promotes CK2-mediated disassociation of alpha-Catenin from beta-Catenin and transactivation of beta-Catenin. *Mol Cell,* 36**,** 547-59.

JIANG, W. G., GRIMSHAW, D., MARTIN, T. A., DAVIES, G., PARR, C., WATKINS, G., LANE, J., ABOUNADER, R., LATERRA, J. & MANSEL, R. E. 2003. Reduction of stromal fibroblast-induced mammary tumor growth, by retroviral ribozyme transgenes to hepatocyte growth factor/scatter factor and its receptor, c-MET. *Clin Cancer Res,* 9**,** 4274-81.

JIANG, W. G., HISCOX, S., HALLETT, M. B., MANSEL, R. E. & PUNTIS, M. C. 1995. Regulation of motility and invasion of cancer cells by human monocytic cells. *Anticancer Res,* 15**,** 1303-10.

JIANG, W. G., MARTIN, T. A., PARR, C., DAVIES, G., MATSUMOTO, K. & NAKAMURA, T. 2005. Hepatocyte growth factor, its receptor, and their potential value in cancer therapies. *Crit Rev Oncol Hematol,* 53**,** 35-69.

JIN, C., YANG, Y. A., ANVER, M. R., MORRIS, N., WANG, X. & ZHANG, Y. E. 2009. Smad ubiquitination regulatory factor 2 promotes metastasis of breast cancer cells by enhancing migration and invasiveness. *Cancer Res,* 69**,** 735-40.

JIN, E. J., LEE, S. Y., CHOI, Y. A., JUNG, J. C., BANG, O. S. & KANG, S. S. 2006. BMP-2-enhanced chondrogenesis involves p38 MAPK-mediated down-regulation of Wnt-7a pathway. *Mol Cells,* 22**,** 353-9.

JONES, D. H., NAKASHIMA, T., SANCHEZ, O. H., KOZIERADZKI, I., KOMAROVA, S. V., SAROSI, I., MORONY, S., RUBIN, E., SARAO, R., HOJILLA, C. V., KOMNENOVIC, V., KONG, Y. Y., SCHREIBER, M., DIXON, S. J., SIMS, S. M., KHOKHA, R., WADA, T. & PENNINGER, J. M. 2006. Regulation of cancer cell migration and bone metastasis by RANKL. *Nature,* 440**,** 692-6.

JUAREZ, P. & GUISE, T. A. 2011. TGF-beta in cancer and bone: implications for treatment of bone metastases. *Bone,* 48**,** 23-9.

JUHL, H., STRITZEL, M., WROBLEWSKI, A., HENNE-BRUNS, D., KREMER, B., SCHMIEGEL, W., NEUMAIER, M., WAGENER, C., SCHREIBER, H. W. & KALTHOFF, H. 1994. Immunocytological detection of micrometastatic cells: comparative evaluation of findings in the peritoneal cavity and the bone marrow of gastric, colorectal and pancreatic cancer patients. *Int J Cancer,* 57**,** 330-5.

JULIEN, S., PUIG, I., CARETTI, E., BONAVENTURE, J., NELLES, L., VAN ROY, F., DARGEMONT, C., DE HERREROS, A. G., BELLACOSA, A. & LARUE, L. 2007. Activation of NF-kappaB by Akt upregulates Snail expression and induces epithelium mesenchyme transition. *Oncogene,* 26**,** 7445-56.

KACZANOWSKI, S. 2016. Apoptosis: its origin, history, maintenance and the medical implications for cancer and aging. *Phys Biol,* 13**,** 031001.

KALLURI, R. & ZEISBERG, M. 2006. Fibroblasts in cancer. *Nat Rev Cancer,* 6**,** 392-401.

KAMARAJU, A. K. & ROBERTS, A. B. 2005. Role of Rho/ROCK and p38 MAP kinase pathways in transforming growth factor-beta-mediated Smad-dependent growth inhibition of human breast carcinoma cells in vivo. *J Biol Chem,* 280**,** 1024-36.

KANG, M. H., KANG, H. N., KIM, J. L., KIM, J. S., OH, S. C. & YOO, Y. A. 2009. Inhibition of PI3 kinase/Akt pathway is required for BMP2-induced EMT and invasion. *Oncol Rep,* 22**,** 525-34.

KANG, M. H., OH, S. C., LEE, H. J., KANG, H. N., KIM, J. L., KIM, J. S. & YOO, Y. A. 2011. Metastatic function of BMP-2 in gastric cancer cells: the role of PI3K/AKT, MAPK, the NF-kappaB pathway, and MMP-9 expression. *Exp Cell Res,* 317**,** 1746-62.

KAPOOR, P., SUVA, L. J., WELCH, D. R. & DONAHUE, H. J. 2008. Osteoprotegrin and the bone homing and colonization potential of breast cancer cells. *J Cell Biochem,* 103**,** 30-41.

KASS, L., ERLER, J. T., DEMBO, M. & WEAVER, V. M. 2007. Mammary epithelial cell: influence of extracellular matrix composition and organization during development and tumorigenesis. *Int J Biochem Cell Biol,* 39**,** 1987-94.

KATSUNO, Y., HANYU, A., KANDA, H., ISHIKAWA, Y., AKIYAMA, F., IWASE, T., OGATA, E., EHATA, S., MIYAZONO, K. & IMAMURA, T. 2008. Bone morphogenetic protein signaling enhances invasion and bone metastasis of breast cancer cells through Smad pathway. *Oncogene,* 27**,** 6322-33.

KATSUTA, E., MAAWY, A. A., YAN, L. & TAKABE, K. 2019a. High expression of bone morphogenetic protein (BMP) 6 and BMP7 are associated with higher immune cell infiltration and better survival in estrogen receptorpositive breast cancer. *Oncol Rep,* 42**,** 1413-1421.

KATSUTA, E., MAAWY, A. A., YAN, L. & TAKABE, K. 2019b. High expression of bone morphogenetic protein (BMP) 6 and BMP7 are associated with higher immune cell infiltration and better survival in estrogen receptorpositive breast cancer. *Oncol Rep*.

KATSUTA, E., QI, Q., PENG, X., HOCHWALD, S. N., YAN, L. & TAKABE, K. 2019c. Pancreatic adenocarcinomas with mature blood vessels have better overall survival. *Sci Rep,* 9**,** 1310.

KELLY, T., YAN, Y., OSBORNE, R. L., ATHOTA, A. B., ROZYPAL, T. L., COLCLASURE, J. C. & CHU, W. S. 1998. Proteolysis of extracellular matrix

by invadopodia facilitates human breast cancer cell invasion and is mediated by matrix metalloproteinases. *Clin Exp Metastasis,* 16**,** 501-12.

KENNECKE, H., YERUSHALMI, R., WOODS, R., CHEANG, M. C., VODUC, D., SPEERS, C. H., NIELSEN, T. O. & GELMON, K. 2010. Metastatic behavior of breast cancer subtypes. *J Clin Oncol,* 28**,** 3271-7.

KESTENS, C., SIERSEMA, P. D., OFFERHAUS, G. J. & VAN BAAL, J. W. 2016. BMP4 Signaling Is Able to Induce an Epithelial-Mesenchymal Transition-Like Phenotype in Barrett's Esophagus and Esophageal Adenocarcinoma through Induction of SNAIL2. *PLoS One,* 11**,** e0155754.

KIM, B. R., OH, S. C., LEE, D. H., KIM, J. L., LEE, S. Y., KANG, M. H., LEE, S. I., KANG, S., JOUNG, S. Y. & MIN, B. W. 2015. BMP-2 induces motility and invasiveness by promoting colon cancer stemness through STAT3 activation. *Tumour Biol,* 36**,** 9475-86.

KIM, J. H. & KIM, N. 2016. Signaling Pathways in Osteoclast Differentiation. *Chonnam Med J,* 52**,** 12-7.

KIM, R. S., AVIVAR-VALDERAS, A., ESTRADA, Y., BRAGADO, P., SOSA, M. S., AGUIRRE-GHISO, J. A. & SEGALL, J. E. 2012a. Dormancy signatures and metastasis in estrogen receptor positive and negative breast cancer. *PLoS One,* 7**,** e35569.

KIM, S. & JHO, E. H. 2010. The protein stability of Axin, a negative regulator of Wnt signaling, is regulated by Smad ubiquitination regulatory factor 2 (Smurf2). *J Biol Chem,* 285**,** 36420-6.

KIM, S., KANG, Y., KRUEGER, C. A., SEN, M., HOLCOMB, J. B., CHEN, D., WENKE, J. C. & YANG, Y. 2012b. Sequential delivery of BMP-2 and IGF-1 using a chitosan gel with gelatin microspheres enhances early osteoblastic differentiation. *Acta Biomater,* 8**,** 1768-77.

KIMURA, N., MATSUO, R., SHIBUYA, H., NAKASHIMA, K. & TAGA, T. 2000. BMP2-induced apoptosis is mediated by activation of the TAK1-p38 kinase pathway that is negatively regulated by Smad6. *J Biol Chem,* 275**,** 17647-52.

KOBAYASHI, A., OKUDA, H., XING, F., PANDEY, P. R., WATABE, M., HIROTA, S., PAI, S. K., LIU, W., FUKUDA, K., CHAMBERS, C., WILBER, A. & WATABE, K. 2011. Bone morphogenetic protein 7 in dormancy and metastasis of prostate cancer stem-like cells in bone. *J Exp Med,* 208**,** 2641-55.

KOENIG, B. B., COOK, J. S., WOLSING, D. H., TING, J., TIESMAN, J. P., CORREA, P. E., OLSON, C. A., PECQUET, A. L., VENTURA, F., GRANT, R. A. & ET AL. 1994. Characterization and cloning of a receptor for BMP-2 and BMP-4 from NIH 3T3 cells. *Mol Cell Biol,* 14**,** 5961-74.

KORCHYNSKYI, O., DECHERING, K. J., SIJBERS, A. M., OLIJVE, W. & TEN DIJKE, P. 2003. Gene array analysis of bone morphogenetic protein type I receptor-induced osteoblast differentiation. *J Bone Miner Res,* 18**,** 1177-85.

KOTB, A. M., HIERHOLZER, A. & KEMLER, R. 2011. Replacement of E-cadherin by N-cadherin in the mammary gland leads to fibrocystic changes and tumor formation. *Breast Cancer Res,* 13**,** R104.

KOVACHEVA, M., ZEPP, M., BERGER, S. M. & BERGER, M. R. 2014. Sustained conditional knockdown reveals intracellular bone sialoprotein as essential for breast cancer skeletal metastasis. *Oncotarget,* 5**,** 5510-22.

KOZLOW, W. & GUISE, T. A. 2005. Breast cancer metastasis to bone: mechanisms of osteolysis and implications for therapy. *J Mammary Gland Biol Neoplasia,* 10**,** 169-80.

KRETZSCHMAR, M., DOODY, J., TIMOKHINA, I. & MASSAGUE, J. 1999. A mechanism of repression of TGFbeta/ Smad signaling by oncogenic Ras. *Genes Dev,* 13**,** 804-16.

KRUGER, T. E., MILLER, A. H., GODWIN, A. K. & WANG, J. 2014. Bone sialoprotein and osteopontin in bone metastasis of osteotropic cancers. *Crit Rev Oncol Hematol,* 89**,** 330-41.

KUMAR, P. & AGGARWAL, R. 2016. An overview of triple-negative breast cancer. *Arch Gynecol Obstet,* 293**,** 247-69.

KURATOMI, G., KOMURO, A., GOTO, K., SHINOZAKI, M., MIYAZAWA, K., MIYAZONO, K. & IMAMURA, T. 2005. NEDD4-2 (neural precursor cell expressed, developmentally down-regulated 4-2) negatively regulates TGF-beta (transforming growth factor-beta) signalling by inducing ubiquitin-mediated degradation of Smad2 and TGF-beta type I receptor. *Biochem J,* 386**,** 461-70.

KUSU, N., LAURIKKALA, J., IMANISHI, M., USUI, H., KONISHI, M., MIYAKE, A., THESLEFF, I. & ITOH, N. 2003. Sclerostin is a novel secreted osteoclast-derived bone morphogenetic protein antagonist with unique ligand specificity. *J Biol Chem,* 278**,** 24113-7.

LAULAN, N. B. & ST-PIERRE, Y. 2015. Bone morphogenetic protein 4 (BMP-4) and epidermal growth factor (EGF) inhibit metalloproteinase-9 (MMP-9) expression in cancer cells. *Oncoscience,* 2**,** 309-16.

LEE, H. S., MOON, C., LEE, H. W., PARK, E. M., CHO, M. S. & KANG, J. L. 2007. Src tyrosine kinases mediate activations of NF-kappaB and integrin signal during lipopolysaccharide-induced acute lung injury. *J Immunol,* 179**,** 7001-11.

LEE, K. J., MENDELSOHN, M. & JESSELL, T. M. 1998. Neuronal patterning by BMPs: a requirement for GDF7 in the generation of a discrete class of commissural interneurons in the mouse spinal cord. *Genes Dev,* 12**,** 3394-407.

LEE, S. J. 1990. Identification of a novel member (GDF-1) of the transforming growth factor-beta superfamily. *Mol Endocrinol,* 4**,** 1034-40.

LEE, W., KO, K. R., KIM, H. K., LEE, D. S., NAM, I. J., LIM, S. & KIM, S. 2018. Dehydrodiconiferyl Alcohol Inhibits Osteoclast Differentiation and Ovariectomy-Induced Bone Loss through Acting as an Estrogen Receptor Agonist. *J Nat Prod,* 81**,** 1343-1356.

LEHMANN, K., JANDA, E., PIERREUX, C. E., RYTOMAA, M., SCHULZE, A., MCMAHON, M., HILL, C. S., BEUG, H. & DOWNWARD, J. 2000. Raf induces TGFbeta production while blocking its apoptotic but not invasive responses: a mechanism leading to increased malignancy in epithelial cells. *Genes Dev,* 14**,** 2610-22.

LI, D. M. & FENG, Y. M. 2011. Signaling mechanism of cell adhesion molecules in breast cancer metastasis: potential therapeutic targets. *Breast Cancer Res Treat,* 128**,** 7-21.

LI, J., YE, L., SANDERS, A. J. & JIANG, W. G. 2012. Repulsive guidance molecule B (RGMB) plays negative roles in breast cancer by coordinating BMP signaling. *J Cell Biochem,* 113**,** 2523-31.

LI, S., DAI, H., HE, Y., PENG, S., ZHU, T., WU, Y., LI, C. & WANG, K. 2018. BMP9 inhibits the growth of breast cancer cells by downregulation of the PI3K/Akt signaling pathway. *Oncol Rep,* 40**,** 1743-1751.

LI, X. Q., DU, X., LI, D. M., KONG, P. Z., SUN, Y., LIU, P. F., WANG, Q. S. & FENG, Y. M. 2015. ITGBL1 Is a Runx2 Transcriptional Target and Promotes Breast Cancer Bone Metastasis by Activating the TGFbeta Signaling Pathway. *Cancer Res,* 75**,** 3302-13.

LI, X. Q., ZHANG, R., LU, H., YUE, X. M. & HUANG, Y. F. 2022. Extracellular Vesicle-Packaged CDH11 and ITGA5 Induce the Premetastatic Niche for Bone Colonization of Breast Cancer Cells. *Cancer Res,* 82**,** 1560-1574.

LIM, S., KIM, T. H., IHN, H. J., LIM, J., KIM, G. Y., CHOI, Y. H., BAE, J. S., JUNG, J. C., SHIN, H. I., KIM, J. E. & PARK, E. K. 2020. Inhibitory effect of oolonghomobisflavan B on osteoclastogenesis by suppressing p38 MAPK activation. *Bioorg Med Chem Lett,* 30**,** 127429.

LIN, J., PATEL, S. R., CHENG, X., CHO, E. A., LEVITAN, I., ULLENBRUCH, M., PHAN, S. H., PARK, J. M. & DRESSLER, G. R. 2005. Kielin/chordin-like protein, a novel enhancer of BMP signaling, attenuates renal fibrotic disease. *Nat Med,* 11**,** 387-93.

LIU, C., LIU, L., CHEN, X., CHENG, J., ZHANG, H., SHEN, J., SHAN, J., XU, Y., YANG, Z., LAI, M. & QIAN, C. 2016a. Sox9 regulates self-renewal and tumorigenicity by promoting symmetrical cell division of cancer stem cells in hepatocellular carcinoma. *Hepatology,* 64**,** 117-29.

LIU, F., VENTURA, F., DOODY, J. & MASSAGUE, J. 1995. Human type II receptor for bone morphogenic proteins (BMPs): extension of the two-kinase receptor model to the BMPs. *Mol Cell Biol,* 15**,** 3479-86.

LIU, G., LIU, Y. J., LIAN, W. J., ZHAO, Z. W., YI, T. & ZHOU, H. Y. 2014. Reduced BMP6 expression by DNA methylation contributes to EMT and drug resistance in breast cancer cells. *Oncol Rep,* 32**,** 581-8.

LIU, H., WANG, Y. J., BIAN, L., FANG, Z. H., ZHANG, Q. Y. & CHENG, J. X. 2016b. CD44+/CD24+ cervical cancer cells resist radiotherapy and exhibit properties of cancer stem cells. *Eur Rev Med Pharmacol Sci,* 20**,** 1745-54.

LIU, Y., ZHANG, R. X., YUAN, W., CHEN, H. Q., TIAN, D. D., LI, H., JIANG, X., DENG, Z. L. & WANG, Y. 2018. Knockdown of Bone Morphogenetic Proteins Type 1a Receptor (BMPR1a) in Breast Cancer Cells Protects Bone from Breast Cancer-Induced Osteolysis by Suppressing RANKL Expression. *Cell Physiol Biochem,* 45**,** 1759-1771.

LOIBL, S. & GIANNI, L. 2017. HER2-positive breast cancer. *Lancet,* 389**,** 2415-2429.

LOMBARDO, Y., SCOPELLITI, A., CAMMARERI, P., TODARO, M., IOVINO, F., RICCI-VITIANI, L., GULOTTA, G., DIELI, F., DE MARIA, R. & STASSI, G. 2011. Bone morphogenetic protein 4 induces differentiation of colorectal cancer stem cells and increases their response to chemotherapy in mice. *Gastroenterology,* 140**,** 297-309.

LOPEZ-COVIELLA, I., MELLOTT, T. M., KOVACHEVA, V. P., BERSE, B., SLACK, B. E., ZEMELKO, V., SCHNITZLER, A. & BLUSZTAJN, J. K. 2006. Developmental pattern of expression of BMP receptors and Smads and activation of Smad1 and Smad5 by BMP9 in mouse basal forebrain. *Brain Res,* 1088**,** 49-56.

LU, Z., GHOSH, S., WANG, Z. & HUNTER, T. 2003. Downregulation of caveolin-1 function by EGF leads to the loss of E-cadherin, increased transcriptional activity of beta-catenin, and enhanced tumor cell invasion. *Cancer Cell,* 4**,** 499-515.

LUKASIEWICZ, S., CZECZELEWSKI, M., FORMA, A., BAJ, J., SITARZ, R. & STANISLAWEK, A. 2021. Breast Cancer-Epidemiology, Risk Factors, Classification, Prognostic Markers, and Current Treatment Strategies-An Updated Review. *Cancers (Basel),* 13.

LUO, K. 2017. Signaling Cross Talk between TGF-beta/Smad and Other Signaling Pathways. *Cold Spring Harb Perspect Biol,* 9.

LUO, K., STROSCHEIN, S. L., WANG, W., CHEN, D., MARTENS, E., ZHOU, S. & ZHOU, Q. 1999. The Ski oncoprotein interacts with the Smad proteins to repress TGFbeta signaling. *Genes Dev,* 13**,** 2196-206.

LV, J., XIU, P., TAN, J., JIA, Z., CAI, H. & LIU, Z. 2015. Enhanced angiogenesis and osteogenesis in critical bone defects by the controlled release of BMP-2 and VEGF: implantation of electron beam melting-fabricated porous Ti6Al4V scaffolds incorporating growth factor-doped fibrin glue. *Biomed Mater,* 10**,** 035013.

MAHLI, A., SEITZ, T., BECKROGE, T., FREESE, K., THASLER, W. E., BENKERT, M., DIETRICH, P., WEISKIRCHEN, R., BOSSERHOFF, A. & HELLERBRAND, C. 2019. Bone Morphogenetic Protein-8B Expression is Induced in Steatotic Hepatocytes and Promotes Hepatic Steatosis and Inflammation In Vitro. *Cells,* 8.

MAHONEY, S. E., YAO, Z., KEYES, C. C., TAPSCOTT, S. J. & DIEDE, S. J. 2012. Genome-wide DNA methylation studies suggest distinct DNA methylation patterns in pediatric embryonal and alveolar rhabdomyosarcomas. *Epigenetics,* 7**,** 400-8.

MALIREDDI, R. K. S., KESAVARDHANA, S. & KANNEGANTI, T. D. 2019. ZBP1 and TAK1: Master Regulators of NLRP3 Inflammasome/Pyroptosis, Apoptosis, and Necroptosis (PAN-optosis). *Front Cell Infect Microbiol,* 9**,** 406.

MANI, S. A., GUO, W., LIAO, M. J., EATON, E. N., AYYANAN, A., ZHOU, A. Y., BROOKS, M., REINHARD, F., ZHANG, C. C., SHIPITSIN, M., CAMPBELL, L. L., POLYAK, K., BRISKEN, C., YANG, J. & WEINBERG, R. A. 2008. The epithelial-mesenchymal transition generates cells with properties of stem cells. *Cell,* 133**,** 704-15.

MAREEL, M., OLIVEIRA, M. J. & MADANI, I. 2009. Cancer invasion and metastasis: interacting ecosystems. *Virchows Arch,* 454**,** 599-622.

MARONI, P., BENDINELLI, P., FERRARETTO, A. & LOMBARDI, G. 2021. Interleukin 11 (IL-11): Role(s) in Breast Cancer Bone Metastases. *Biomedicines,* 9.

MARONI, P., BENDINELLI, P., RESNATI, M., MATTEUCCI, E., MILAN, E. & DESIDERIO, M. A. 2016. The Autophagic Process Occurs in Human Bone Metastasis and Implicates Molecular Mechanisms Differently Affected by Rab5a in the Early and Late Stages. *Int J Mol Sci,* 17**,** 443.

MARQUES, S., BORGES, A. C., SILVA, A. C., FREITAS, S., CORDENONSI, M. & BELO, J. A. 2004. The activity of the Nodal antagonist Cerl-2 in the mouse node is required for correct L/R body axis. *Genes Dev,* 18**,** 2342-7.

MARTINEZ, J. & ZHANG, X. H. 2013. BMP/Coco antagonism as a deterministic factor of metastasis dormancy in lung. *Breast Cancer Res,* 15**,** 302.

MASUDA, H., ZHANG, D., BARTHOLOMEUSZ, C., DOIHARA, H., HORTOBAGYI, G. N. & UENO, N. T. 2012. Role of epidermal growth factor receptor in breast cancer. *Breast Cancer Res Treat,* 136**,** 331-45.

MATSUDA, K., MARUYAMA, H., GUO, F., KLEEFF, J., ITAKURA, J., MATSUMOTO, Y., LANDER, A. D. & KORC, M. 2001. Glypican-1 is overexpressed in human breast cancer and modulates the mitogenic effects of multiple heparin-binding growth factors in breast cancer cells. *Cancer Res,* 61**,** 5562-9.

MATSUMOTO, Y., OTSUKA, F., TAKANO-NARAZAKI, M., KATSUYAMA, T., NAKAMURA, E., TSUKAMOTO, N., INAGAKI, K., SADA, K. E. & MAKINO, H. 2013. Estrogen facilitates osteoblast differentiation by upregulating bone morphogenetic protein-4 signaling. *Steroids,* 78**,** 513-20.

MAURIZI, A. & RUCCI, N. 2018. The Osteoclast in Bone Metastasis: Player and Target. *Cancers (Basel),* 10.

MAZERBOURG, S. & HSUEH, A. J. 2006. Genomic analyses facilitate identification of receptors and signalling pathways for growth differentiation factor 9 and related orphan bone morphogenetic protein/growth differentiation factor ligands. *Hum Reprod Update,* 12**,** 373-83.

MAZERBOURG, S., SANGKUHL, K., LUO, C. W., SUDO, S., KLEIN, C. & HSUEH, A. J. 2005. Identification of receptors and signaling pathways for orphan bone morphogenetic protein/growth differentiation factor ligands based on genomic analyses. *J Biol Chem,* 280**,** 32122-32.

MCPHERRON, A. C., LAWLER, A. M. & LEE, S. J. 1997. Regulation of skeletal muscle mass in mice by a new TGF-beta superfamily member. *Nature,* 387**,** 83-90.

MCPHERRON, A. C., LAWLER, A. M. & LEE, S. J. 1999. Regulation of anterior/posterior patterning of the axial skeleton by growth/differentiation factor 11. *Nat Genet,* 22**,** 260-4.

MCPHERRON, A. C. & LEE, S. J. 1993. GDF-3 and GDF-9: two new members of the transforming growth factor-beta superfamily containing a novel pattern of cysteines. *J Biol Chem,* 268**,** 3444-9.

MCSHERRY, E. A., DONATELLO, S., HOPKINS, A. M. & MCDONNELL, S. 2007. Molecular basis of invasion in breast cancer. *Cell Mol Life Sci,* 64**,** 3201-18.

MEGO, M., MANI, S. A. & CRISTOFANILLI, M. 2010. Molecular mechanisms of metastasis in breast cancer--clinical applications. *Nat Rev Clin Oncol,* 7**,** 693-701.

MERINO, R., RODRIGUEZ-LEON, J., MACIAS, D., GANAN, Y., ECONOMIDES, A. N. & HURLE, J. M. 1999. The BMP antagonist Gremlin regulates outgrowth, chondrogenesis and programmed cell death in the developing limb. *Development,* 126**,** 5515-22.

MILLET, C., YAMASHITA, M., HELLER, M., YU, L. R., VEENSTRA, T. D. & ZHANG, Y. E. 2009. A negative feedback control of transforming growth

factor-beta signaling by glycogen synthase kinase 3-mediated Smad3 linker phosphorylation at Ser-204. *J Biol Chem,* 284**,** 19808-16.

MILLS, M., LIVERINGHOUSE, C., LEE, F., NANDA, R. H., AHMED, K. A., WASHINGTON, I. R., THAPA, R., FRIDLEY, B. L., BLUMENCRANZ, P., EXTERMANN, M., LOFTUS, L., BALDUCCI, L. & DIAZ, R. 2021. The prevalence of luminal B subtype is higher in older postmenopausal women with ER+/HER2- breast cancer and is associated with inferior outcomes. *J Geriatr Oncol,* 12**,** 219-226.

MINAMI, Y. 2015. Overview: Cancer Stem Cell and Tumor Environment. *Oncology,* 89 Suppl 1**,** 22-4.

MITCHELL, D., POBRE, E. G., MULIVOR, A. W., GRINBERG, A. V., CASTONGUAY, R., MONNELL, T. E., SOLBAN, N., UCRAN, J. A., PEARSALL, R. S., UNDERWOOD, K. W., SEEHRA, J. & KUMAR, R. 2010. ALK1-Fc inhibits multiple mediators of angiogenesis and suppresses tumor growth. *Mol Cancer Ther,* 9**,** 379-88.

MOCK, K., PRECA, B. T., BRUMMER, T., BRABLETZ, S., STEMMLER, M. P. & BRABLETZ, T. 2015. The EMT-activator ZEB1 induces bone metastasis associated genes including BMP-inhibitors. *Oncotarget,* 6**,** 14399-412.

MONTESANO, R., SARKOZI, R. & SCHRAMEK, H. 2008. Bone morphogenetic protein-4 strongly potentiates growth factor-induced proliferation of mammary epithelial cells. *Biochem Biophys Res Commun,* 374**,** 164-8.

MOORE, R. K., OTSUKA, F. & SHIMASAKI, S. 2003. Molecular basis of bone morphogenetic protein-15 signaling in granulosa cells. *J Biol Chem,* 278**,** 304-10.

MORAN, M. S., SCHNITT, S. J., GIULIANO, A. E., HARRIS, J. R., KHAN, S. A., HORTON, J., KLIMBERG, S., CHAVEZ-MACGREGOR, M., FREEDMAN, G., HOUSSAMI, N., JOHNSON, P. L. & MORROW, M. 2014. Society of Surgical Oncology-American Society for Radiation Oncology consensus guideline on margins for breast-conserving surgery with whole-breast irradiation in stages I and II invasive breast cancer. *Int J Radiat Oncol Biol Phys,* 88**,** 553-64.

MOREAU, J. E., ANDERSON, K., MAUNEY, J. R., NGUYEN, T., KAPLAN, D. L. & ROSENBLATT, M. 2007. Tissue-engineered bone serves as a target for metastasis of human breast cancer in a mouse model. *Cancer Res,* 67**,** 10304-8.

MOREL, D., JEFFERY, D., ASPESLAGH, S., ALMOUZNI, G. & POSTEL-VINAY, S. 2020. Combining epigenetic drugs with other therapies for solid tumours - past lessons and future promise. *Nat Rev Clin Oncol,* 17**,** 91-107.

MORRELL, N. W., YANG, X., UPTON, P. D., JOURDAN, K. B., MORGAN, N., SHEARES, K. K. & TREMBATH, R. C. 2001. Altered growth responses of pulmonary artery smooth muscle cells from patients with primary pulmonary

hypertension to transforming growth factor-beta(1) and bone morphogenetic proteins. *Circulation,* 104**,** 790-5.

MOUSTAKAS, A., SOUCHELNYTSKYI, S. & HELDIN, C. H. 2001. Smad regulation in TGF-beta signal transduction. *J Cell Sci,* 114**,** 4359-69.

MULDER, K. M. 2000. Role of Ras and Mapks in TGFbeta signaling. *Cytokine Growth Factor Rev,* 11**,** 23-35.

MULLER, A., HOMEY, B., SOTO, H., GE, N., CATRON, D., BUCHANAN, M. E., MCCLANAHAN, T., MURPHY, E., YUAN, W., WAGNER, S. N., BARRERA, J. L., MOHAR, A., VERASTEGUI, E. & ZLOTNIK, A. 2001. Involvement of chemokine receptors in breast cancer metastasis. *Nature,* 410**,** 50-6.

MURAKAMI, G., WATABE, T., TAKAOKA, K., MIYAZONO, K. & IMAMURA, T. 2003. Cooperative inhibition of bone morphogenetic protein signaling by Smurf1 and inhibitory Smads. *Mol Biol Cell,* 14**,** 2809-17.

MURAOKA-COOK, R. S., SHIN, I., YI, J. Y., EASTERLY, E., BARCELLOS-HOFF, M. H., YINGLING, J. M., ZENT, R. & ARTEAGA, C. L. 2006. Activated type I TGFbeta receptor kinase enhances the survival of mammary epithelial cells and accelerates tumor progression. *Oncogene,* 25**,** 3408-23.

MURAOKA, R. S., KOH, Y., ROEBUCK, L. R., SANDERS, M. E., BRANTLEY-SIEDERS, D., GORSKA, A. E., MOSES, H. L. & ARTEAGA, C. L. 2003. Increased malignancy of Neu-induced mammary tumors overexpressing active transforming growth factor beta1. *Mol Cell Biol,* 23**,** 8691-703.

NABER, H. P., WIERCINSKA, E., PARDALI, E., VAN LAAR, T., NIRMALA, E., SUNDQVIST, A., VAN DAM, H., VAN DER HORST, G., VAN DER PLUIJM, G., HECKMANN, B., DANEN, E. H. & TEN DIJKE, P. 2012. BMP-7 inhibits TGF-beta-induced invasion of breast cancer cells through inhibition of integrin beta(3) expression. *Cell Oncol (Dordr),* 35**,** 19-28.

NAGY, V. & PENNINGER, J. M. 2015. The RANKL-RANK Story. *Gerontology,* 61**,** 534-42.

NAKAHARA, T., TOMINAGA, K., KOSEKI, T., YAMAMOTO, M., YAMATO, K., FUKUDA, J. & NISHIHARA, T. 2003. Growth/differentiation factor-5 induces growth arrest and apoptosis in mouse B lineage cells with modulation by Smad. *Cell Signal,* 15**,** 181-7.

NAKAYAMA, N., HAN, C. Y., CAM, L., LEE, J. I., PRETORIUS, J., FISHER, S., ROSENFELD, R., SCULLY, S., NISHINAKAMURA, R., DURYEA, D., VAN, G., BOLON, B., YOKOTA, T. & ZHANG, K. 2004. A novel chordin-like BMP inhibitor, CHL2, expressed preferentially in chondrocytes of developing cartilage and osteoarthritic joint cartilage. *Development,* 131**,** 229-40.

NECKMANN, U., WOLOWCZYK, C., HALL, M., ALMAAS, E., REN, J., ZHAO, S., JOHANNESSEN, B., SKOTHEIM, R. I., BJORKOY, G., TEN DIJKE, P. & HOLIEN, T. 2019. GREM1 is associated with metastasis and predicts poor prognosis in ER-negative breast cancer patients. *Cell Commun Signal,* 17**,** 140.

NELSON, D. J., CLARK, B., MUNYARD, K., WILLIAMS, V., GROTH, D., GILL, J., PRESTON, H. & CHAN, A. 2017. A review of the importance of immune responses in luminal B breast cancer. *Oncoimmunology,* 6**,** e1282590.

NEUHAUS, H., ROSEN, V. & THIES, R. S. 1999. Heart specific expression of mouse BMP-10 a novel member of the TGF-beta superfamily. *Mech Dev,* 80**,** 181-4.

NEUMAN, H. B., MORROGH, M., GONEN, M., VAN ZEE, K. J., MORROW, M. & KING, T. A. 2010. Stage IV breast cancer in the era of targeted therapy: does surgery of the primary tumor matter? *Cancer,* 116**,** 1226-33.

NICKEL, J. & MUELLER, T. D. 2019. Specification of BMP Signaling. *Cells,* 8.

NIELSEN, T. O., HSU, F. D., JENSEN, K., CHEANG, M., KARACA, G., HU, Z., HERNANDEZ-BOUSSARD, T., LIVASY, C., COWAN, D., DRESSLER, L., AKSLEN, L. A., RAGAZ, J., GOWN, A. M., GILKS, C. B., VAN DE RIJN, M. & PEROU, C. M. 2004. Immunohistochemical and clinical characterization of the basal-like subtype of invasive breast carcinoma. *Clin Cancer Res,* 10**,** 5367-74.

NISHITOH, H., ICHIJO, H., KIMURA, M., MATSUMOTO, T., MAKISHIMA, F., YAMAGUCHI, A., YAMASHITA, H., ENOMOTO, S. & MIYAZONO, K. 1996. Identification of type I and type II serine/threonine kinase receptors for growth/differentiation factor-5. *J Biol Chem,* 271**,** 21345-52.

NOHNO, T., ISHIKAWA, T., SAITO, T., HOSOKAWA, K., NOJI, S., WOLSING, D. H. & ROSENBAUM, J. S. 1995. Identification of a human type II receptor for bone morphogenetic protein-4 that forms differential heteromeric complexes with bone morphogenetic protein type I receptors. *J Biol Chem,* 270**,** 22522-6.

OCHIYA, T. 2016. Novel therapeutic strategies targeting liver cancer stem cells. *Chin Clin Oncol,* 5**,** 59.

OHSHIBA, T., MIYAURA, C. & ITO, A. 2003. Role of prostaglandin E produced by osteoblasts in osteolysis due to bone metastasis. *Biochem Biophys Res Commun,* 300**,** 957-64.

ONG, D. B., COLLEY, S. M., NORMAN, M. R., KITAZAWA, S. & TOBIAS, J. H. 2004. Transcriptional regulation of a BMP-6 promoter by estrogen receptor alpha. *J Bone Miner Res,* 19**,** 447-54.

ONICHTCHOUK, D., CHEN, Y. G., DOSCH, R., GAWANTKA, V., DELIUS, H., MASSAGUE, J. & NIEHRS, C. 1999. Silencing of TGF-beta signalling by the pseudoreceptor BAMBI. *Nature,* 401**,** 480-5.

OSKARSSON, T., BATLLE, E. & MASSAGUE, J. 2014. Metastatic stem cells: sources, niches, and vital pathways. *Cell Stem Cell,* 14**,** 306-21.

OTSUKA, F., MOORE, R. K., IEMURA, S., UENO, N. & SHIMASAKI, S. 2001. Follistatin inhibits the function of the oocyte-derived factor BMP-15. *Biochem Biophys Res Commun,* 289**,** 961-6.

OWENS, P., POLIKOWSKY, H., PICKUP, M. W., GORSKA, A. E., JOVANOVIC, B., SHAW, A. K., NOVITSKIY, S. V., HONG, C. C. & MOSES, H. L. 2013. Bone Morphogenetic Proteins stimulate mammary fibroblasts to promote mammary carcinoma cell invasion. *PLoS One,* 8**,** e67533.

OZKAYNAK, E., RUEGER, D. C., DRIER, E. A., CORBETT, C., RIDGE, R. J., SAMPATH, T. K. & OPPERMANN, H. 1990. OP-1 cDNA encodes an osteogenic protein in the TGF-beta family. *Embo J,* 9**,** 2085-93.

OZKAYNAK, E., SCHNEGELSBERG, P. N., JIN, D. F., CLIFFORD, G. M., WARREN, F. D., DRIER, E. A. & OPPERMANN, H. 1992. Osteogenic protein-2. A new member of the transforming growth factor-beta superfamily expressed early in embryogenesis. *J Biol Chem,* 267**,** 25220-7.

PARFITT, A. M. 2002. Targeted and nontargeted bone remodeling: relationship to basic multicellular unit origination and progression. *Bone,* 30**,** 5-7.

PARISH, C. R., JAKOBSEN, K. B. & COOMBE, D. R. 1992. A basement-membrane permeability assay which correlates with the metastatic potential of tumour cells. *Int J Cancer,* 52**,** 378-83.

PARK, K. S., DUBON, M. J. & GUMBINER, B. M. 2015. N-cadherin mediates the migration of MCF-10A cells undergoing bone morphogenetic protein 4-mediated epithelial mesenchymal transition. *Tumour Biol,* 36**,** 3549-56.

PARKER, B. & SUKUMAR, S. 2003. Distant metastasis in breast cancer: molecular mechanisms and therapeutic targets. *Cancer Biol Ther,* 2**,** 14-21.

PATHI, S. P., KOWALCZEWSKI, C., TADIPATRI, R. & FISCHBACH, C. 2010. A novel 3-D mineralized tumor model to study breast cancer bone metastasis. *PLoS One,* 5**,** e8849.

PAUL, A. & PAUL, S. 2014. The breast cancer susceptibility genes (BRCA) in breast and ovarian cancers. *Front Biosci (Landmark Ed),* 19**,** 605-18.

PECHEUR, I., PEYRUCHAUD, O., SERRE, C. M., GUGLIELMI, J., VOLAND, C., BOURRE, F., MARGUE, C., COHEN-SOLAL, M., BUFFET, A., KIEFFER, N. & CLEZARDIN, P. 2002. Integrin alpha(v)beta3 expression confers on tumor cells a greater propensity to metastasize to bone. *FASEB J,* 16**,** 1266-8.

PELLEGRINELLI, V., PEIRCE, V. J., HOWARD, L., VIRTUE, S., TUREI, D., SENZACQUA, M., FRONTINI, A., DALLEY, J. W., HORTON, A. R., BIDAULT, G., SEVERI, I., WHITTLE, A., RAHMOUNI, K., SAEZ-

RODRIGUEZ, J., CINTI, S., DAVIES, A. M. & VIDAL-PUIG, A. 2018. Adipocyte-secreted BMP8b mediates adrenergic-induced remodeling of the neuro-vascular network in adipose tissue. *Nat Commun,* 9**,** 4974.

PERA, M. F., ANDRADE, J., HOUSSAMI, S., REUBINOFF, B., TROUNSON, A., STANLEY, E. G., WARD-VAN OOSTWAARD, D. & MUMMERY, C. 2004. Regulation of human embryonic stem cell differentiation by BMP-2 and its antagonist noggin. *J Cell Sci,* 117**,** 1269-80.

PEROU, C. M., SORLIE, T., EISEN, M. B., VAN DE RIJN, M., JEFFREY, S. S., REES, C. A., POLLACK, J. R., ROSS, D. T., JOHNSEN, H., AKSLEN, L. A., FLUGE, O., PERGAMENSCHIKOV, A., WILLIAMS, C., ZHU, S. X., LONNING, P. E., BORRESEN-DALE, A. L., BROWN, P. O. & BOTSTEIN, D. 2000. Molecular portraits of human breast tumours. *Nature,* 406**,** 747-52.

PI, W., GUO, X., SU, L. & XU, W. 2012. BMP-2 up-regulates PTEN expression and induces apoptosis of pulmonary artery smooth muscle cells under hypoxia. *PLoS One,* 7**,** e35283.

PICCOLO, S., AGIUS, E., LEYNS, L., BHATTACHARYYA, S., GRUNZ, H., BOUWMEESTER, T. & DE ROBERTIS, E. M. 1999. The head inducer Cerberus is a multifunctional antagonist of Nodal, BMP and Wnt signals. *Nature,* 397**,** 707-10.

PICCOLO, S., SASAI, Y., LU, B. & DE ROBERTIS, E. M. 1996. Dorsoventral patterning in Xenopus: inhibition of ventral signals by direct binding of chordin to BMP-4. *Cell,* 86**,** 589-98.

PIERRE, A., PISSELET, C., MONGET, P., MONNIAUX, D. & FABRE, S. 2005. Testing the antagonistic effect of follistatin on BMP family members in ovine granulosa cells. *Reprod Nutr Dev,* 45**,** 419-25.

PORE, M., MEIJER, C., DE BOCK, G. H., BOERSMA-VAN EK, W., TERSTAPPEN, L. W., GROEN, H. J., TIMENS, W., KRUYT, F. A. & HILTERMANN, T. J. 2016. Cancer Stem Cells, Epithelial to Mesenchymal Markers, and Circulating Tumor Cells in Small Cell Lung Cancer. *Clin Lung Cancer,* 17**,** 535-542.

POULIOT, F., BLAIS, A. & LABRIE, C. 2003. Overexpression of a dominant negative type II bone morphogenetic protein receptor inhibits the growth of human breast cancer cells. *Cancer Res,* 63**,** 277-81.

PRICE, T. T., BURNESS, M. L., SIVAN, A., WARNER, M. J., CHENG, R., LEE, C. H., OLIVERE, L., COMATAS, K., MAGNANI, J., KIM LYERLY, H., CHENG, Q., MCCALL, C. M. & SIPKINS, D. A. 2016. Dormant breast cancer micrometastases reside in specific bone marrow niches that regulate their transit to and from bone. *Sci Transl Med,* 8**,** 340ra73.

PROVENZANO, E., ULANER, G. A. & CHIN, S. F. 2018. Molecular Classification of Breast Cancer. *PET Clin,* 13**,** 325-338.

PSAILA, B., KAPLAN, R. N., PORT, E. R. & LYDEN, D. 2006. Priming the 'soil' for breast cancer metastasis: the pre-metastatic niche. *Breast Dis,* 26**,** 65-74.

PUGH, C. W. & RATCLIFFE, P. J. 2003. Regulation of angiogenesis by hypoxia: role of the HIF system. *Nat Med,* 9**,** 677-84.

RAIDA, M., CLEMENT, J. H., LEEK, R. D., AMERI, K., BICKNELL, R., NIEDERWIESER, D. & HARRIS, A. L. 2005. Bone morphogenetic protein 2 (BMP-2) and induction of tumor angiogenesis. *J Cancer Res Clin Oncol,* 131**,** 741-50.

RAKHA, E. A., EL-SAYED, M. E., GREEN, A. R., LEE, A. H., ROBERTSON, J. F. & ELLIS, I. O. 2007a. Prognostic markers in triple-negative breast cancer. *Cancer,* 109**,** 25-32.

RAKHA, E. A., TAN, D. S., FOULKES, W. D., ELLIS, I. O., TUTT, A., NIELSEN, T. O. & REIS-FILHO, J. S. 2007b. Are triple-negative tumours and basal-like breast cancer synonymous? *Breast Cancer Res,* 9**,** 404; author reply 405.

RAMOSHEBI, L. N. & RIPAMONTI, U. 2000. Osteogenic protein-1, a bone morphogenetic protein, induces angiogenesis in the chick chorioallantoic membrane and synergizes with basic fibroblast growth factor and transforming growth factor-beta1. *Anat Rec,* 259**,** 97-107.

RAZAVI, P., CHANG, M. T., XU, G., BANDLAMUDI, C., ROSS, D. S., VASAN, N., CAI, Y., BIELSKI, C. M., DONOGHUE, M. T. A., JONSSON, P., PENSON, A., SHEN, R., PAREJA, F., KUNDRA, R., MIDDHA, S., CHENG, M. L., ZEHIR, A., KANDOTH, C., PATEL, R., HUBERMAN, K., SMYTH, L. M., JHAVERI, K., MODI, S., TRAINA, T. A., DANG, C., ZHANG, W., WEIGELT, B., LI, B. T., LADANYI, M., HYMAN, D. M., SCHULTZ, N., ROBSON, M. E., HUDIS, C., BROGI, E., VIALE, A., NORTON, L., DICKLER, M. N., BERGER, M. F., IACOBUZIO-DONAHUE, C. A., CHANDARLAPATY, S., SCALTRITI, M., REIS-FILHO, J. S., SOLIT, D. B., TAYLOR, B. S. & BASELGA, J. 2018. The Genomic Landscape of Endocrine-Resistant Advanced Breast Cancers. *Cancer Cell,* 34**,** 427-438 e6.

RE'EM-KALMA, Y., LAMB, T. & FRANK, D. 1995. Competition between noggin and bone morphogenetic protein 4 activities may regulate dorsalization during Xenopus development. *Proc Natl Acad Sci U S A,* 92**,** 12141-5.

REBBAPRAGADA, A., BENCHABANE, H., WRANA, J. L., CELESTE, A. J. & ATTISANO, L. 2003. Myostatin signals through a transforming growth factor beta-like signaling pathway to block adipogenesis. *Mol Cell Biol,* 23**,** 7230-42.

REN, W., LIU, Y., WAN, S., FEI, C., WANG, W., CHEN, Y., ZHANG, Z., WANG, T., WANG, J., ZHOU, L., WENG, Y., HE, T. & ZHANG, Y. 2014a. BMP9 inhibits proliferation and metastasis of HER2-positive SK-BR-3 breast cancer cells through ERK1/2 and PI3K/AKT pathways. *PLoS One,* 9**,** e96816.

REN, W., SUN, X., WANG, K., FENG, H., LIU, Y., FEI, C., WAN, S., WANG, W., LUO, J., SHI, Q., TANG, M., ZUO, G., WENG, Y., HE, T. & ZHANG, Y. 2014b. BMP9 inhibits the bone metastasis of breast cancer cells by downregulating CCN2 (connective tissue growth factor, CTGF) expression. *Mol Biol Rep,* 41**,** 1373-83.

RETSKY, M. & DEMICHELI, R. 2014. Multimodal hazard rate for relapse in breast cancer: quality of data and calibration of computer simulation. *Cancers (Basel),* 6**,** 2343-55.

REUFSTECK, C., LIFSHITZ-SHOVALI, R., ZEPP, M., BAUERLE, T., KUBLER, D., GOLOMB, G. & BERGER, M. R. 2012. Silencing of skeletal metastasis-associated genes impairs migration of breast cancer cells and reduces osteolytic bone lesions. *Clin Exp Metastasis,* 29**,** 441-56.

RIBEIRO, N., SOUSA, S. R., BREKKEN, R. A. & MONTEIRO, F. J. 2014. Role of SPARC in bone remodeling and cancer-related bone metastasis. *J Cell Biochem,* 115**,** 17-26.

RICARD, N., CIAIS, D., LEVET, S., SUBILEAU, M., MALLET, C., ZIMMERS, T. A., LEE, S. J., BIDART, M., FEIGE, J. J. & BAILLY, S. 2012. BMP9 and BMP10 are critical for postnatal retinal vascular remodeling. *Blood,* 119**,** 6162-71.

RICARTE, F. R., LE HENAFF, C., KOLUPAEVA, V. G., GARDELLA, T. J. & PARTRIDGE, N. C. 2018. Parathyroid hormone(1-34) and its analogs differentially modulate osteoblastic Rankl expression via PKA/SIK2/SIK3 and PP1/PP2A-CRTC3 signaling. *J Biol Chem,* 293**,** 20200-20213.

RIEUNIER, G., WU, X., MACAULAY, V. M., LEE, A. V., WEYER-CZERNILOFSKY, U. & BOGENRIEDER, T. 2019. Bad to the Bone: The Role of the Insulin-Like Growth Factor Axis in Osseous Metastasis. *Clin Cancer Res,* 25**,** 3479-3485.

ROJAS, K. & STUCKEY, A. 2016. Breast Cancer Epidemiology and Risk Factors. *Clin Obstet Gynecol,* 59**,** 651-672.

ROMAGNOLI, M., BELGUISE, K., YU, Z., WANG, X., LANDESMAN-BOLLAG, E., SELDIN, D. C., CHALBOS, D., BARILLE-NION, S., JEZEQUEL, P., SELDIN, M. L. & SONENSHEIN, G. E. 2012. Epithelial-to-mesenchymal transition induced by TGF-beta1 is mediated by Blimp-1-dependent repression of BMP-5. *Cancer Res,* 72**,** 6268-78.

ROODMAN, G. D. 2004. Mechanisms of bone metastasis. *N Engl J Med,* 350**,** 1655-64.

ROSE, A. A. & SIEGEL, P. M. 2010. Emerging therapeutic targets in breast cancer bone metastasis. *Future Oncol,* 6**,** 55-74.

ROSENZWEIG, B. L., IMAMURA, T., OKADOME, T., COX, G. N., YAMASHITA, H., TEN DIJKE, P., HELDIN, C. H. & MIYAZONO, K. 1995. Cloning and characterization of a human type II receptor for bone morphogenetic proteins. *Proc Natl Acad Sci U S A,* 92**,** 7632-6.

ROSS, J. J., SHIMMI, O., VILMOS, P., PETRYK, A., KIM, H., GAUDENZ, K., HERMANSON, S., EKKER, S. C., O'CONNOR, M. B. & MARSH, J. L. 2001. Twisted gastrulation is a conserved extracellular BMP antagonist. *Nature,* 410**,** 479-83.

ROSS, K. R., COREY, D. A., DUNN, J. M. & KELLEY, T. J. 2007. SMAD3 expression is regulated by mitogen-activated protein kinase kinase-1 in epithelial and smooth muscle cells. *Cell Signal,* 19**,** 923-31.

ROTHHAMMER, T., POSER, I., SONCIN, F., BATAILLE, F., MOSER, M. & BOSSERHOFF, A. K. 2005. Bone morphogenic proteins are overexpressed in malignant melanoma and promote cell invasion and migration. *Cancer Res,* 65**,** 448-56.

ROUZIER, R., PEROU, C. M., SYMMANS, W. F., IBRAHIM, N., CRISTOFANILLI, M., ANDERSON, K., HESS, K. R., STEC, J., AYERS, M., WAGNER, P., MORANDI, P., FAN, C., RABIUL, I., ROSS, J. S., HORTOBAGYI, G. N. & PUSZTAI, L. 2005. Breast cancer molecular subtypes respond differently to preoperative chemotherapy. *Clin Cancer Res,* 11**,** 5678-85.

ROYCE, M. E. & OSMAN, D. 2015. Everolimus in the Treatment of Metastatic Breast Cancer. *Breast Cancer (Auckl),* 9**,** 73-9.

RUCCI, N. & TETI, A. 2010. Osteomimicry: how tumor cells try to deceive the bone. *Front Biosci (Schol Ed),* 2**,** 907-15.

SAHA, D., DATTA, P. K. & BEAUCHAMP, R. D. 2001. Oncogenic ras represses transforming growth factor-beta /Smad signaling by degrading tumor suppressor Smad4. *J Biol Chem,* 276**,** 29531-7.

SAKAI, H., FURIHATA, M., MATSUDA, C., TAKAHASHI, M., MIYAZAKI, H., KONAKAHARA, T., IMAMURA, T. & OKADA, T. 2012. Augmented autocrine bone morphogenic protein (BMP) 7 signaling increases the metastatic potential of mouse breast cancer cells. *Clin Exp Metastasis,* 29**,** 327-38.

SAKUTA, H., SUZUKI, R., TAKAHASHI, H., KATO, A., SHINTANI, T., IEMURA, S., YAMAMOTO, T. S., UENO, N. & NODA, M. 2001. Ventroptin: a BMP-4 antagonist expressed in a double-gradient pattern in the retina. *Science,* 293**,** 111-5.

SAMAD, T. A., REBBAPRAGADA, A., BELL, E., ZHANG, Y., SIDIS, Y., JEONG, S. J., CAMPAGNA, J. A., PERUSINI, S., FABRIZIO, D. A., SCHNEYER, A. L., LIN, H. Y., BRIVANLOU, A. H., ATTISANO, L. & WOOLF, C. J. 2005. DRAGON, a bone morphogenetic protein co-receptor. *J Biol Chem,* 280**,** 14122-9.

SAMMAR, M., STRICKER, S., SCHWABE, G. C., SIEBER, C., HARTUNG, A., HANKE, M., OISHI, I., POHL, J., MINAMI, Y., SEBALD, W., MUNDLOS, S. & KNAUS, P. 2004. Modulation of GDF5/BRI-b signalling through interaction with the tyrosine kinase receptor Ror2. *Genes Cells,* 9**,** 1227-38.

SANDERS, A. J., YE, L., LI, J., MASON, M. D. & JIANG, W. G. 2014. Tumour angiogenesis and repulsive guidance molecule b: a role in HGF- and BMP-7-mediated angiogenesis. *Int J Oncol,* 45**,** 1304-12.

SAPKOTA, G., ALARCON, C., SPAGNOLI, F. M., BRIVANLOU, A. H. & MASSAGUE, J. 2007. Balancing BMP signaling through integrated inputs into the Smad1 linker. *Mol Cell,* 25**,** 441-54.

SASAL, Y., LU, B., STEINBELSSER, H. & DE ROBERTIS, E. M. 1995. Regulation of neural induction by the Chd and Bmp-4 antagonistic patterning signals in Xenopus. *Nature,* 378**,** 419.

SATHIAKUMAR, N., DELZELL, E., MORRISEY, M. A., FALKSON, C., YONG, M., CHIA, V., BLACKBURN, J., ARORA, T., BRILL, I. & KILGORE, M. L. 2012. Mortality following bone metastasis and skeletal-related events among women with breast cancer: a population-based analysis of U.S. Medicare beneficiaries, 1999-2006. *Breast Cancer Res Treat,* 131**,** 231-8.

SAVAGE, K., LEUNG, S., TODD, S. K., BROWN, L. A., JONES, R. L., ROBERTSON, D., JAMES, M., PARRY, S., RODRIGUES PINILLA, S. M., HUNTSMAN, D. & REIS-FILHO, J. S. 2008. Distribution and significance of caveolin 2 expression in normal breast and invasive breast cancer: an immunofluorescence and immunohistochemical analysis. *Breast Cancer Res Treat,* 110**,** 245-56.

SCHARPFENECKER, M., VAN DINTHER, M., LIU, Z., VAN BEZOOIJEN, R. L., ZHAO, Q., PUKAC, L., LOWIK, C. W. & TEN DIJKE, P. 2007. BMP-9 signals via ALK1 and inhibits bFGF-induced endothelial cell proliferation and VEGF-stimulated angiogenesis. *J Cell Sci,* 120**,** 964-72.

SCHERBERICH, A., TUCKER, R. P., DEGEN, M., BROWN-LUEDI, M., ANDRES, A. C. & CHIQUET-EHRISMANN, R. 2005. Tenascin-W is found in malignant mammary tumors, promotes alpha8 integrin-dependent motility and requires p38MAPK activity for BMP-2 and TNF-alpha induced expression in vitro. *Oncogene,* 24**,** 1525-32.

SCHOEBERL, B., PACE, E. A., FITZGERALD, J. B., HARMS, B. D., XU, L., NIE, L., LINGGI, B., KALRA, A., PARAGAS, V., BUKHALID, R., GRANTCHAROVA, V., KOHLI, N., WEST, K. A., LESZCZYNIECKA, M., FELDHAUS, M. J., KUDLA, A. J. & NIELSEN, U. B. 2009. Therapeutically targeting ErbB3: a key node in ligand-induced activation of the ErbB receptor-PI3K axis. *Sci Signal,* 2**,** ra31.

SCHOLZE, A. R., FOO, L. C., MULINYAWE, S. & BARRES, B. A. 2014. BMP signaling in astrocytes downregulates EGFR to modulate survival and maturation. *PLoS One,* 9**,** e110668.

SCHWALBE, M., SANGER, J., EGGERS, R., NAUMANN, A., SCHMIDT, A., HOFFKEN, K. & CLEMENT, J. H. 2003. Differential expression and regulation of bone morphogenetic protein 7 in breast cancer. *Int J Oncol,* 23**,** 89-95.

SCHWAPPACHER, R., WEISKE, J., HEINING, E., EZERSKI, V., MAROM, B., HENIS, Y. I., HUBER, O. & KNAUS, P. 2009. Novel crosstalk to BMP signalling: cGMP-dependent kinase I modulates BMP receptor and Smad activity. *EMBO J,* 28**,** 1537-50.

SCULLY, O. J., BAY, B. H., YIP, G. & YU, Y. 2012. Breast cancer metastasis. *Cancer Genomics Proteomics,* 9**,** 311-20.

SEGAL, R., EVANS, W., JOHNSON, D., SMITH, J., COLLETTA, S., GAYTON, J., WOODARD, S., WELLS, G. & REID, R. 2001. Structured exercise improves physical functioning in women with stages I and II breast cancer: results of a randomized controlled trial. *J Clin Oncol,* 19**,** 657-65.

SERRAO, A., JENKINS, L. M., CHUMANEVICH, A. A., HORST, B., LIANG, J., GATZA, M. L., LEE, N. Y., RONINSON, I. B., BROUDE, E. V. & MYTHREYE, K. 2018. Mediator kinase CDK8/CDK19 drives YAP1-dependent BMP4-induced EMT in cancer. *Oncogene,* 37**,** 4792-4808.

SETON-ROGERS, S. E., LU, Y., HINES, L. M., KOUNDINYA, M., LABAER, J., MUTHUSWAMY, S. K. & BRUGGE, J. S. 2004. Cooperation of the ErbB2 receptor and transforming growth factor beta in induction of migration and invasion in mammary epithelial cells. *Proc Natl Acad Sci U S A,* 101**,** 1257-62.

SHAHBA, S., JAFARI SHAKIB, R., JAMSHIDI, A., VOJDANIAN, M., AKHTARI, M., ASLANI, S., POURSANI, S., NIKOKAR, I. & MAHMOUDI, M. 2018. Association study of copy number variation in BMP8A gene with the risk of ankylosing spondylitis in Iranian population. *J Cell Biochem*.

SHARMA, R., GOGOI, G., SAIKIA, S., SHARMA, A., KALITA, D. J., SARMA, A., LIMAYE, A. M., GAUR, M. K., BHATTACHARYYA, J. & JAGANATHAN, B. G. 2022. BMP4 enhances anoikis resistance and chemoresistance of breast cancer cells through canonical BMP signaling. *J Cell Commun Signal,* 16**,** 191-205.

SHARMA, S., XING, F., LIU, Y., WU, K., SAID, N., POCHAMPALLY, R., SHIOZAWA, Y., LIN, H. K., BALAJI, K. C. & WATABE, K. 2016. Secreted Protein Acidic and Rich in Cysteine (SPARC) Mediates Metastatic Dormancy of Prostate Cancer in Bone. *J Biol Chem,* 291**,** 19351-63.

SHI, C., IURA, A., TERAJIMA, M., LIU, F., LYONS, K., PAN, H., ZHANG, H., YAMAUCHI, M., MISHINA, Y. & SUN, H. 2016. Deletion of BMP receptor

type IB decreased bone mass in association with compromised osteoblastic differentiation of bone marrow mesenchymal progenitors. *Sci Rep,* 6**,** 24256.

SHIOZAWA, Y., PEDERSEN, E. A., HAVENS, A. M., JUNG, Y., MISHRA, A., JOSEPH, J., KIM, J. K., PATEL, L. R., YING, C., ZIEGLER, A. M., PIENTA, M. J., SONG, J., WANG, J., LOBERG, R. D., KREBSBACH, P. H., PIENTA, K. J. & TAICHMAN, R. S. 2011. Human prostate cancer metastases target the hematopoietic stem cell niche to establish footholds in mouse bone marrow. *J Clin Invest,* 121**,** 1298-312.

SI, J., WANG, C., ZHANG, D., WANG, B. & ZHOU, Y. 2020. Osteopontin in Bone Metabolism and Bone Diseases. *Med Sci Monit,* 26**,** e919159.

SIEGEL, P. M. & MASSAGUE, J. 2003. Cytostatic and apoptotic actions of TGF-beta in homeostasis and cancer. *Nat Rev Cancer,* 3**,** 807-21.

SIGISMUND, S., AVANZATO, D. & LANZETTI, L. 2018. Emerging functions of the EGFR in cancer. *Mol Oncol,* 12**,** 3-20.

SINGH, V., SINGH, L. C., VASUDEVAN, M., CHATTOPADHYAY, I., BORTHAKAR, B. B., RAI, A. K., PHUKAN, R. K., SHARMA, J., MAHANTA, J., KATAKI, A. C., KAPUR, S. & SAXENA, S. 2015. Esophageal Cancer Epigenomics and Integrome Analysis of Genome-Wide Methylation and Expression in High Risk Northeast Indian Population. *OMICS,* 19**,** 688-99.

SMITTENAAR, C. R., PETERSEN, K. A., STEWART, K. & MOITT, N. 2016. Cancer incidence and mortality projections in the UK until 2035. *Br J Cancer,* 115**,** 1147-1155.

SORITSA, D., TEDER, H., ROOSIPUU, R., TAMM, H., LAISK-PODAR, T., SOPLEPMANN, P., ALTRAJA, A., SALUMETS, A. & PETERS, M. 2018. Whole exome sequencing of benign pulmonary metastasizing leiomyoma reveals mutation in the BMP8B gene. *BMC Med Genet,* 19**,** 20.

SORLIE, T., TIBSHIRANI, R., PARKER, J., HASTIE, T., MARRON, J. S., NOBEL, A., DENG, S., JOHNSEN, H., PESICH, R., GEISLER, S., DEMETER, J., PEROU, C. M., LONNING, P. E., BROWN, P. O., BORRESEN-DALE, A. L. & BOTSTEIN, D. 2003. Repeated observation of breast tumor subtypes in independent gene expression data sets. *Proc Natl Acad Sci U S A,* 100**,** 8418-23.

SOSA, M. S., AVIVAR-VALDERAS, A., BRAGADO, P., WEN, H. C. & AGUIRRE-GHISO, J. A. 2011. ERK1/2 and p38alpha/beta signaling in tumor cell quiescence: opportunities to control dormant residual disease. *Clin Cancer Res,* 17**,** 5850-7.

SOSA, M. S., BRAGADO, P. & AGUIRRE-GHISO, J. A. 2014. Mechanisms of disseminated cancer cell dormancy: an awakening field. *Nat Rev Cancer,* 14**,** 611-22.

SOSA, M. S., PARIKH, F., MAIA, A. G., ESTRADA, Y., BOSCH, A., BRAGADO, P., EKPIN, E., GEORGE, A., ZHENG, Y., LAM, H. M., MORRISSEY, C., CHUNG, C. Y., FARIAS, E. F., BERNSTEIN, E. & AGUIRRE-GHISO, J. A. 2015. NR2F1 controls tumour cell dormancy via SOX9- and RARbeta-driven quiescence programmes. *Nat Commun,* 6**,** 6170.

SPENCER, J. A., FERRARO, F., ROUSSAKIS, E., KLEIN, A., WU, J., RUNNELS, J. M., ZAHER, W., MORTENSEN, L. J., ALT, C., TURCOTTE, R., YUSUF, R., COTE, D., VINOGRADOV, S. A., SCADDEN, D. T. & LIN, C. P. 2014. Direct measurement of local oxygen concentration in the bone marrow of live animals. *Nature,* 508**,** 269-73.

STEGER, G. G. & BARTSCH, R. 2011. Denosumab for the treatment of bone metastases in breast cancer: evidence and opinion. *Ther Adv Med Oncol,* 3**,** 233-43.

STRAUSBERG, R. L., FEINGOLD, E. A., GROUSE, L. H., DERGE, J. G., KLAUSNER, R. D., COLLINS, F. S., WAGNER, L., SHENMEN, C. M., SCHULER, G. D., ALTSCHUL, S. F., ZEEBERG, B., BUETOW, K. H., SCHAEFER, C. F., BHAT, N. K., HOPKINS, R. F., JORDAN, H., MOORE, T., MAX, S. I., WANG, J., HSIEH, F., DIATCHENKO, L., MARUSINA, K., FARMER, A. A., RUBIN, G. M., HONG, L., STAPLETON, M., SOARES, M. B., BONALDO, M. F., CASAVANT, T. L., SCHEETZ, T. E., BROWNSTEIN, M. J., USDIN, T. B., TOSHIYUKI, S., CARNINCI, P., PRANGE, C., RAHA, S. S., LOQUELLANO, N. A., PETERS, G. J., ABRAMSON, R. D., MULLAHY, S. J., BOSAK, S. A., MCEWAN, P. J., MCKERNAN, K. J., MALEK, J. A., GUNARATNE, P. H., RICHARDS, S., WORLEY, K. C., HALE, S., GARCIA, A. M., GAY, L. J., HULYK, S. W., VILLALON, D. K., MUZNY, D. M., SODERGREN, E. J., LU, X., GIBBS, R. A., FAHEY, J., HELTON, E., KETTEMAN, M., MADAN, A., RODRIGUES, S., SANCHEZ, A., WHITING, M., YOUNG, A. C., SHEVCHENKO, Y., BOUFFARD, G. G., BLAKESLEY, R. W., TOUCHMAN, J. W., GREEN, E. D., DICKSON, M. C., RODRIGUEZ, A. C., GRIMWOOD, J., SCHMUTZ, J., MYERS, R. M., BUTTERFIELD, Y. S., KRZYWINSKI, M. I., SKALSKA, U., SMAILUS, D. E., SCHNERCH, A., SCHEIN, J. E., JONES, S. J. & MARRA, M. A. 2002. Generation and initial analysis of more than 15,000 full-length human and mouse cDNA sequences. *Proc Natl Acad Sci U S A,* 99**,** 16899-903.

STROSCHEIN, S. L., WANG, W., ZHOU, S., ZHOU, Q. & LUO, K. 1999. Negative feedback regulation of TGF-beta signaling by the SnoN oncoprotein. *Science,* 286**,** 771-4.

SUDO, S., AVSIAN-KRETCHMER, O., WANG, L. S. & HSUEH, A. J. 2004. Protein related to DAN and cerberus is a bone morphogenetic protein antagonist that participates in ovarian paracrine regulation. *J Biol Chem,* 279**,** 23134-41.

SUN, Z., CAI, S., ZABKIEWICZ, C., LIU, C. & YE, L. 2020. Bone morphogenetic proteins mediate crosstalk between cancer cells and the tumour microenvironment at primary tumours and metastases (Review). *Int J Oncol,* 56**,** 1335-1351.

SUNG, H., FERLAY, J., SIEGEL, R. L., LAVERSANNE, M., SOERJOMATARAM, I., JEMAL, A. & BRAY, F. 2021. Global Cancer Statistics 2020: GLOBOCAN Estimates of Incidence and Mortality Worldwide for 36 Cancers in 185 Countries. *CA Cancer J Clin,* 71**,** 209-249.

SUZUKI, A., KANEKO, E., MAEDA, J. & UENO, N. 1997. Mesoderm induction by BMP-4 and -7 heterodimers. *Biochem Biophys Res Commun,* 232**,** 153-6.

TAHARA, R. K., BREWER, T. M., THERIAULT, R. L. & UENO, N. T. 2019. Bone Metastasis of Breast Cancer. *Adv Exp Med Biol,* 1152**,** 105-129.

TAKAHASHI, M., OTSUKA, F., MIYOSHI, T., OTANI, H., GOTO, J., YAMASHITA, M., OGURA, T., MAKINO, H. & DOIHARA, H. 2008. Bone morphogenetic protein 6 (BMP6) and BMP7 inhibit estrogen-induced proliferation of breast cancer cells by suppressing p38 mitogen-activated protein kinase activation. *J Endocrinol,* 199**,** 445-55.

TALMADGE, J. E. & FIDLER, I. J. 2010. AACR centennial series: the biology of cancer metastasis: historical perspective. *Cancer Res,* 70**,** 5649-69.

TAMURA, D., HIRAGA, T., MYOUI, A., YOSHIKAWA, H. & YONEDA, T. 2008. Cadherin-11-mediated interactions with bone marrow stromal/osteoblastic cells support selective colonization of breast cancer cells in bone. *Int J Oncol,* 33**,** 17-24.

TAN, C. C., LI, G. X., TAN, L. D., DU, X., LI, X. Q., HE, R., WANG, Q. S. & FENG, Y. M. 2016. Breast cancer cells obtain an osteomimetic feature via epithelial-mesenchymal transition that have undergone BMP2/RUNX2 signaling pathway induction. *Oncotarget,* 7**,** 79688-79705.

TARRAGONA, M., PAVLOVIC, M., ARNAL-ESTAPE, A., UROSEVIC, J., MORALES, M., GUIU, M., PLANET, E., GONZALEZ-SUAREZ, E. & GOMIS, R. R. 2012. Identification of NOG as a specific breast cancer bone metastasis-supporting gene. *J Biol Chem,* 287**,** 21346-55.

TASCA, A., ASTLEFORD, K., BLIXT, N. C., JENSEN, E. D., GOPALAKRISHNAN, R. & MANSKY, K. C. 2018. SMAD1/5 signaling in osteoclasts regulates bone formation via coupling factors. *PLoS One,* 13**,** e0203404.

TATSUMI, S., ISHII, K., AMIZUKA, N., LI, M., KOBAYASHI, T., KOHNO, K., ITO, M., TAKESHITA, S. & IKEDA, K. 2007. Targeted ablation of osteocytes induces osteoporosis with defective mechanotransduction. *Cell Metab,* 5**,** 464-75.

TEN DIJKE, P., YAMASHITA, H., SAMPATH, T. K., REDDI, A. H., ESTEVEZ, M., RIDDLE, D. L., ICHIJO, H., HELDIN, C. H. & MIYAZONO, K. 1994. Identification of type I receptors for osteogenic protein-1 and bone morphogenetic protein-4. *J Biol Chem,* 269**,** 16985-8.

TEO, J. L. & KAHN, M. 2010. The Wnt signaling pathway in cellular proliferation and differentiation: A tale of two coactivators. *Adv Drug Deliv Rev,* 62**,** 1149-55.

THERIAULT, R. L. & THERIAULT, R. L. 2012. Biology of bone metastases. *Cancer Control,* 19**,** 92-101.

THOMAS, D. A. & MASSAGUE, J. 2005. TGF-beta directly targets cytotoxic T cell functions during tumor evasion of immune surveillance. *Cancer Cell,* 8**,** 369-80.

TIAN, Q., HE, X. C., HOOD, L. & LI, L. 2005. Bridging the BMP and Wnt pathways by PI3 kinase/Akt and 14-3-3zeta. *Cell Cycle,* 4**,** 215-6.

TSAI, S. Y., HUANG, Y. L., YANG, W. H. & TANG, C. H. 2012. Hepatocyte growth factor-induced BMP-2 expression is mediated by c-Met receptor, FAK, JNK, Runx2, and p300 pathways in human osteoblasts. *Int Immunopharmacol,* 13**,** 156-62.

TSANG, J. Y. S. & TSE, G. M. 2020. Molecular Classification of Breast Cancer. *Adv Anat Pathol,* 27**,** 27-35.

TSUCHIDA, K., ARAI, K. Y., KURAMOTO, Y., YAMAKAWA, N., HASEGAWA, Y. & SUGINO, H. 2000. Identification and characterization of a novel follistatin-like protein as a binding protein for the TGF-beta family. *J Biol Chem,* 275**,** 40788-96.

UEDA, Y., WANG, S., DUMONT, N., YI, J. Y., KOH, Y. & ARTEAGA, C. L. 2004. Overexpression of HER2 (erbB2) in human breast epithelial cells unmasks transforming growth factor beta-induced cell motility. *J Biol Chem,* 279**,** 24505-13.

URIST, M. R. 1965. Bone: formation by autoinduction. *Science,* 150**,** 893-9.

VACCA, M., LESLIE, J., VIRTUE, S., LAM, B. Y. H., GOVAERE, O., TINIAKOS, D., SNOW, S., DAVIES, S., PETKEVICIUS, K., TONG, Z., PEIRCE, V., NIELSEN, M. J., AMENT, Z., LI, W., KOSTRZEWSKI, T., LEEMING, D. J., RATZIU, V., ALLISON, M. E. D., ANSTEE, Q. M., GRIFFIN, J. L., OAKLEY, F. & VIDAL-PUIG, A. 2020. Bone morphogenetic protein 8B promotes the progression of non-alcoholic steatohepatitis. *Nat Metab,* 2**,** 514-531.

VALDERRAMA-CARVAJAL, H., COCOLAKIS, E., LACERTE, A., LEE, E. H., KRYSTAL, G., ALI, S. & LEBRUN, J. J. 2002. Activin/TGF-beta induce apoptosis through Smad-dependent expression of the lipid phosphatase SHIP. *Nat Cell Biol,* 4**,** 963-9.

VAN CALSTER, B., VANDEN BEMPT, I., DRIJKONINGEN, M., POCHET, N., CHENG, J., VAN HUFFEL, S., HENDRICKX, W., DECOCK, J., HUANG, H. J., LEUNEN, K., AMANT, F., BERTELOOT, P., PARIDAENS, R., WILDIERS, H., VAN LIMBERGEN, E., WELTENS, C., TIMMERMAN, D., VAN GORP, T., SMEETS, A., VAN DEN BOGAERT, W., VERGOTE, I.,

CHRISTIAENS, M. R. & NEVEN, P. 2009. Axillary lymph node status of operable breast cancers by combined steroid receptor and HER-2 status: triple positive tumours are more likely lymph node positive. *Breast Cancer Res Treat,* 113**,** 181-7.

VAN DEN WIJNGAARD, A., MULDER, W. R., DIJKEMA, R., BOERSMA, C. J., MOSSELMAN, S., VAN ZOELEN, E. J. & OLIJVE, W. 2000. Antiestrogens specifically up-regulate bone morphogenetic protein-4 promoter activity in human osteoblastic cells. *Mol Endocrinol,* 14**,** 623-33.

VAN POZNAK, C. & SAUTER, N. P. 2005. Clinical management of osteoporosis in women with a history of breast carcinoma. *Cancer,* 104**,** 443-56.

VARGA, A. C. & WRANA, J. L. 2005. The disparate role of BMP in stem cell biology. *Oncogene,* 24**,** 5713-21.

VENTURA, J. J., KENNEDY, N. J., FLAVELL, R. A. & DAVIS, R. J. 2004. JNK regulates autocrine expression of TGF-beta1. *Mol Cell,* 15**,** 269-78.

VERA-RAMIREZ, L., VODNALA, S. K., NINI, R., HUNTER, K. W. & GREEN, J. E. 2018. Autophagy promotes the survival of dormant breast cancer cells and metastatic tumour recurrence. *Nat Commun,* 9**,** 1944.

VERMEULEN, Z., SEGERS, V. F. & DE KEULENAER, G. W. 2016. ErbB2 signaling at the crossing between heart failure and cancer. *Basic Res Cardiol,* 111**,** 60.

VIGNAIS, M. L. 2000. [Ski and SnoN: antagonistic proteins of TGFbeta signaling]. *Bull Cancer,* 87**,** 135-7.

VINCENT, T., NEVE, E. P., JOHNSON, J. R., KUKALEV, A., ROJO, F., ALBANELL, J., PIETRAS, K., VIRTANEN, I., PHILIPSON, L., LEOPOLD, P. L., CRYSTAL, R. G., DE HERREROS, A. G., MOUSTAKAS, A., PETTERSSON, R. F. & FUXE, J. 2009. A SNAIL1-SMAD3/4 transcriptional repressor complex promotes TGF-beta mediated epithelial-mesenchymal transition. *Nat Cell Biol,* 11**,** 943-50.

VODUC, K. D., CHEANG, M. C., TYLDESLEY, S., GELMON, K., NIELSEN, T. O. & KENNECKE, H. 2010. Breast cancer subtypes and the risk of local and regional relapse. *J Clin Oncol,* 28**,** 1684-91.

VOORZANGER-ROUSSELOT, N., GOEHRIG, D., JOURNE, F., DORIATH, V., BODY, J. J., CLEZARDIN, P. & GARNERO, P. 2007. Increased Dickkopf-1 expression in breast cancer bone metastases. *Br J Cancer,* 97**,** 964-70.

WALSH, D. W., GODSON, C., BRAZIL, D. P. & MARTIN, F. 2010. Extracellular BMP-antagonist regulation in development and disease: tied up in knots. *Trends Cell Biol,* 20**,** 244-56.

WANG, C., HU, F., GUO, S., MI, D., SHEN, W., ZHANG, J., QIAO, Y., ZHU, T. & YANG, S. 2011a. BMP-6 inhibits MMP-9 expression by regulating heme

oxygenase-1 in MCF-7 breast cancer cells. *J Cancer Res Clin Oncol,* 137**,** 985-95.

WANG, D., HUANG, P., ZHU, B., SUN, L., HUANG, Q. & WANG, J. 2012. Induction of estrogen receptor alpha-36 expression by bone morphogenetic protein 2 in breast cancer cell lines. *Mol Med Rep,* 6**,** 591-6.

WANG, K., FENG, H., REN, W., SUN, X., LUO, J., TANG, M., ZHOU, L., WENG, Y., HE, T. C. & ZHANG, Y. 2011b. BMP9 inhibits the proliferation and invasiveness of breast cancer cells MDA-MB-231. *J Cancer Res Clin Oncol,* 137**,** 1687-96.

WANG, L. P., DONG, J. Z., XIONG, L. J., SHI, K. Q., ZOU, Z. L., ZHANG, S. N., CAO, S. T., LIN, Z. & CHEN, Y. P. 2014. BMP-7 attenuates liver fibrosis via regulation of epidermal growth factor receptor. *Int J Clin Exp Pathol,* 7**,** 3537-47.

WANG, S. E., SHIN, I., WU, F. Y., FRIEDMAN, D. B. & ARTEAGA, C. L. 2006. HER2/Neu (ErbB2) signaling to Rac1-Pak1 is temporally and spatially modulated by transforming growth factor beta. *Cancer Res,* 66**,** 9591-600.

WANG, S. E., XIANG, B., ZENT, R., QUARANTA, V., POZZI, A. & ARTEAGA, C. L. 2009. Transforming growth factor beta induces clustering of HER2 and integrins by activating Src-focal adhesion kinase and receptor association to the cytoskeleton. *Cancer Res,* 69**,** 475-82.

WANG, W., WENG, Y., REN, W., ZHANG, Z., WANG, T., WANG, J., JIANG, Y., CHEN, Y., ZHOU, L., HE, T. & ZHANG, Y. 2015. Biological roles of human bone morphogenetic protein 9 in the bone microenvironment of human breast cancer MDA-MB-231 cells. *Am J Transl Res,* 7**,** 1660-74.

WANG, Y., HU, J., WANG, Y., YE, W., ZHANG, X., JU, H., XU, D., LIU, L., YE, D., ZHANG, L., ZHU, D., DENG, J., ZHANG, Z. & LIU, S. 2018. EGFR activation induced Snail-dependent EMT and myc-dependent PD-L1 in human salivary adenoid cystic carcinoma cells. *Cell Cycle,* 17**,** 1457-1470.

WANG, Y., XIE, Y. & OUPICKY, D. 2016. Potential of CXCR4/CXCL12 Chemokine Axis in Cancer Drug Delivery. *Curr Pharmacol Rep,* 2**,** 1-10.

WEIDLE, U. H., BIRZELE, F., KOLLMORGEN, G. & RUGER, R. 2016. Molecular Mechanisms of Bone Metastasis. *Cancer Genomics Proteomics,* 13**,** 1-12.

WENDT, M. K., TAYLOR, M. A., SCHIEMANN, B. J. & SCHIEMANN, W. P. 2011. Down-regulation of epithelial cadherin is required to initiate metastatic outgrowth of breast cancer. *Mol Biol Cell,* 22**,** 2423-35.

WENG, X., ZHANG, H., YE, J., KAN, M., LIU, F., WANG, T., DENG, J., TAN, Y., HE, L. & LIU, Y. 2015. Hypermethylated Epidermal growth factor receptor (EGFR) promoter is associated with gastric cancer. *Sci Rep,* 5**,** 10154.

WHISSELL, G., MONTAGNI, E., MARTINELLI, P., HERNANDO-MOMBLONA, X., SEVILLANO, M., JUNG, P., CORTINA, C., CALON, A., ABULI, A., CASTELLS, A., CASTELLVI-BEL, S., NACHT, A. S., SANCHO, E., STEPHAN-OTTO ATTOLINI, C., VICENT, G. P., REAL, F. X. & BATLLE, E. 2014. The transcription factor GATA6 enables self-renewal of colon adenoma stem cells by repressing BMP gene expression. *Nat Cell Biol,* 16**,** 695-707.

WHITTLE, A. J., CAROBBIO, S., MARTINS, L., SLAWIK, M., HONDARES, E., VAZQUEZ, M. J., MORGAN, D., CSIKASZ, R. I., GALLEGO, R., RODRIGUEZ-CUENCA, S., DALE, M., VIRTUE, S., VILLARROYA, F., CANNON, B., RAHMOUNI, K., LOPEZ, M. & VIDAL-PUIG, A. 2012. BMP8B increases brown adipose tissue thermogenesis through both central and peripheral actions. *Cell,* 149**,** 871-85.

WICKS, S. J., HAROS, K., MAILLARD, M., SONG, L., COHEN, R. E., DIJKE, P. T. & CHANTRY, A. 2005. The deubiquitinating enzyme UCH37 interacts with Smads and regulates TGF-beta signalling. *Oncogene,* 24**,** 8080-4.

WILKES, M. C., MITCHELL, H., PENHEITER, S. G., DORE, J. J., SUZUKI, K., EDENS, M., SHARMA, D. K., PAGANO, R. E. & LEOF, E. B. 2005. Transforming growth factor-beta activation of phosphatidylinositol 3-kinase is independent of Smad2 and Smad3 and regulates fibroblast responses via p21-activated kinase-2. *Cancer Res,* 65**,** 10431-40.

WISNIESKI, F., LEAL, M. F., CALCAGNO, D. Q., SANTOS, L. C., GIGEK, C. O., CHEN, E. S., ARTIGIANI, R., DEMACHKI, S., ASSUMPCAO, P. P., LOURENCO, L. G., BURBANO, R. R. & SMITH, M. C. 2017. BMP8B Is a Tumor Suppressor Gene Regulated by Histone Acetylation in Gastric Cancer. *J Cell Biochem,* 118**,** 869-877.

WOLTJE, K., JABS, M. & FISCHER, A. 2015. Serum induces transcription of Hey1 and Hey2 genes by Alk1 but not Notch signaling in endothelial cells. *PLoS One,* 10**,** e0120547.

WOZNEY, J. M., ROSEN, V., BYRNE, M., CELESTE, A. J., MOUTSATSOS, I. & WANG, E. A. 1990. Growth factors influencing bone development. *J Cell Sci Suppl,* 13**,** 149-56.

WOZNEY, J. M., ROSEN, V., CELESTE, A. J., MITSOCK, L. M., WHITTERS, M. J., KRIZ, R. W., HEWICK, R. M. & WANG, E. A. 1988. Novel regulators of bone formation: molecular clones and activities. *Science,* 242**,** 1528-34.

WU, F. J., LIN, T. Y., SUNG, L. Y., CHANG, W. F., WU, P. C. & LUO, C. W. 2017. BMP8A sustains spermatogenesis by activating both SMAD1/5/8 and SMAD2/3 in spermatogonia. *Sci Signal,* 10.

WU, F. J. & LUO, C. W. 2017. Discovery of spermatogenic activators: a lesson from bone morphogenetic protein 8. *Oncotarget,* 8**,** 84641-84642.

WU, F. J., WANG, Y. W. & LUO, C. W. 2020. Human BMP8A suppresses luteinization of rat granulosa cells via the SMAD1/5/8 pathway. *Reproduction,* 159**,** 315-324.

XIE, Y., AVELLO, M., SCHIRLE, M., MCWHINNIE, E., FENG, Y., BRIC-FURLONG, E., WILSON, C., NATHANS, R., ZHANG, J., KIRSCHNER, M. W., HUANG, S. M. & CONG, F. 2013. Deubiquitinase FAM/USP9X interacts with the E3 ubiquitin ligase SMURF1 protein and protects it from ligase activity-dependent self-degradation. *J Biol Chem,* 288**,** 2976-85.

XIONG, J. & O'BRIEN, C. A. 2012. Osteocyte RANKL: new insights into the control of bone remodeling. *J Bone Miner Res,* 27**,** 499-505.

XU, G., CHHANGAWALA, S., COCCO, E., RAZAVI, P., CAI, Y., OTTO, J. E., FERRANDO, L., SELENICA, P., LADEWIG, E., CHAN, C., DA CRUZ PAULA, A., WITKIN, M., CHENG, Y., PARK, J., SERNA-TAMAYO, C., ZHAO, H., WU, F., SALLAKU, M., QU, X., ZHAO, A., COLLINGS, C. K., D'AVINO, A. R., JHAVERI, K., KOCHE, R., LEVINE, R. L., REIS-FILHO, J. S., KADOCH, C., SCALTRITI, M., LESLIE, C. S., BASELGA, J. & TOSKA, E. 2020. ARID1A determines luminal identity and therapeutic response in estrogen-receptor-positive breast cancer. *Nat Genet,* 52**,** 198-207.

XU, J., KIMBALL, T. R., LORENZ, J. N., BROWN, D. A., BAUSKIN, A. R., KLEVITSKY, R., HEWETT, T. E., BREIT, S. N. & MOLKENTIN, J. D. 2006. GDF15/MIC-1 functions as a protective and antihypertrophic factor released from the myocardium in association with SMAD protein activation. *Circ Res,* 98**,** 342-50.

YAHIRO, Y., MAEDA, S., MORIKAWA, M., KOINUMA, D., JOKOJI, G., IJUIN, T., KOMIYA, S., KAGEYAMA, R., MIYAZONO, K. & TANIGUCHI, N. 2020. BMP-induced Atoh8 attenuates osteoclastogenesis by suppressing Runx2 transcriptional activity and reducing the Rankl/Opg expression ratio in osteoblasts. *Bone Res,* 8**,** 32.

YAMAJI, N., CELESTE, A. J., THIES, R. S., SONG, J. J., BERNIER, S. M., GOLTZMAN, D., LYONS, K. M., NOVE, J., ROSEN, V. & WOZNEY, J. M. 1994. A mammalian serine/threonine kinase receptor specifically binds BMP-2 and BMP-4. *Biochem Biophys Res Commun,* 205**,** 1944-51.

YAMASHITA, H., OGIYA, A., SHIEN, T., HORIMOTO, Y., MASUDA, N., INAO, T., OSAKO, T., TAKAHASHI, M., ENDO, Y., HOSODA, M., ISHIDA, N., HORII, R., YAMAZAKI, K., MIYOSHI, Y., YASOJIMA, H., TOMIOKA, N. & COLLABORATIVE STUDY GROUP OF SCIENTIFIC RESEARCH OF THE JAPANESE BREAST CANCER, S. 2016. Clinicopathological factors predicting early and late distant recurrence in estrogen receptor-positive, HER2-negative breast cancer. *Breast Cancer,* 23**,** 830-843.

YAN, H., ZHU, S., SONG, C., LIU, N. & KANG, J. 2012. Bone morphogenetic protein (BMP) signaling regulates mitotic checkpoint protein levels in human breast cancer cells. *Cell Signal,* 24**,** 961-8.

YANG, L., BAI, Y., ZHANG, C., DU, J., CHENG, Y., WANG, Q., ZHANG, B. & YANG, Y. 2021. Overexpression of BMP9 promotes ovarian cancer progression via Notch1 signaling. *Neoplasma,* 68**,** 1190-1200.

YANG, M., LIU, P. & HUANG, P. 2016. Cancer stem cells, metabolism, and therapeutic significance. *Tumour Biol,* 37**,** 5735-42.

YANG, S., DU, J., WANG, Z., YUAN, W., QIAO, Y., ZHANG, M., ZHANG, J., GAO, S., YIN, J., SUN, B. & ZHU, T. 2007. BMP-6 promotes E-cadherin expression through repressing deltaEF1 in breast cancer cells. *BMC Cancer,* 7**,** 211.

YE, L., BOKOBZA, S., LI, J., MOAZZAM, M., CHEN, J., MANSEL, R. E. & JIANG, W. G. 2010. Bone morphogenetic protein-10 (BMP-10) inhibits aggressiveness of breast cancer cells and correlates with poor prognosis in breast cancer. *Cancer Sci,* 101**,** 2137-44.

YE, L., BOKOBZA, S. M. & JIANG, W. G. 2009a. Bone morphogenetic proteins in development and progression of breast cancer and therapeutic potential (review). *Int J Mol Med,* 24**,** 591-7.

YE, L. & JIANG, W. G. 2016. Bone morphogenetic proteins in tumour associated angiogenesis and implication in cancer therapies. *Cancer Lett,* 380**,** 586-597.

YE, L., KYNASTON, H. & JIANG, W. G. 2009b. Bone morphogenetic protein-10 suppresses the growth and aggressiveness of prostate cancer cells through a Smad independent pathway. *J Urol,* 181**,** 2749-59.

YE, L., LEWIS-RUSSELL, J. M., DAVIES, G., SANDERS, A. J., KYNASTON, H. & JIANG, W. G. 2007a. Hepatocyte growth factor up-regulates the expression of the bone morphogenetic protein (BMP) receptors, BMPR-IB and BMPR-II, in human prostate cancer cells. *Int J Oncol,* 30**,** 521-9.

YE, L., LEWIS-RUSSELL, J. M., KYANASTON, H. G. & JIANG, W. G. 2007b. Bone morphogenetic proteins and their receptor signaling in prostate cancer. *Histol Histopathol,* 22**,** 1129-47.

YE, L., LEWIS-RUSSELL, J. M., SANDERS, A. J., KYNASTON, H. & JIANG, W. G. 2008. HGF/SF up-regulates the expression of bone morphogenetic protein 7 in prostate cancer cells. *Urol Oncol,* 26**,** 190-7.

YE, L., MASON, M. D. & JIANG, W. G. 2011a. Bone morphogenetic protein and bone metastasis, implication and therapeutic potential. *Front Biosci (Landmark Ed),* 16**,** 865-97.

YE, L., MASON, M. D. & JIANG, W. G. 2011b. Bone morphogenetic protein and bone metastasis, implication and therapeutic potential. *Front Biosci (Landmark Ed),* 16**,** 865-97.

YI, J. Y., SHIN, I. & ARTEAGA, C. L. 2005. Type I transforming growth factor beta receptor binds to and activates phosphatidylinositol 3-kinase. *J Biol Chem,* 280**,** 10870-6.

YING, X., SUN, Y. & HE, P. 2015. Bone Morphogenetic Protein-7 Inhibits EMT-Associated Genes in Breast Cancer. *Cell Physiol Biochem,* 37**,** 1271-8.

YOKOUCHI, Y., VOGAN, K. J., PEARSE, R. V., 2ND & TABIN, C. J. 1999. Antagonistic signaling by Caronte, a novel Cerberus-related gene, establishes left-right asymmetric gene expression. *Cell,* 98**,** 573-83.

YOKOYAMA-KOBAYASHI, M., SAEKI, M., SEKINE, S. & KATO, S. 1997. Human cDNA encoding a novel TGF-beta superfamily protein highly expressed in placenta. *J Biochem (Tokyo),* 122**,** 622-6.

YONEDA, T. & HIRAGA, T. 2005. Crosstalk between cancer cells and bone microenvironment in bone metastasis. *Biochem Biophys Res Commun,* 328**,** 679-87.

YOSHIDA, G. J. & SAYA, H. 2016. Therapeutic strategies targeting cancer stem cells. *Cancer Sci,* 107**,** 5-11.

YOSHIDA, Y., TANAKA, S., UMEMORI, H., MINOWA, O., USUI, M., IKEMATSU, N., HOSODA, E., IMAMURA, T., KUNO, J., YAMASHITA, T., MIYAZONO, K., NODA, M., NODA, T. & YAMAMOTO, T. 2000. Negative regulation of BMP/Smad signaling by Tob in osteoblasts. *Cell,* 103**,** 1085-97.

YOSHIMATSU, Y., LEE, Y. G., AKATSU, Y., TAGUCHI, L., SUZUKI, H. I., CUNHA, S. I., MARUYAMA, K., SUZUKI, Y., YAMAZAKI, T., KATSURA, A., OH, S. P., ZIMMERS, T. A., LEE, S. J., PIETRAS, K., KOH, G. Y., MIYAZONO, K. & WATABE, T. 2013. Bone morphogenetic protein-9 inhibits lymphatic vessel formation via activin receptor-like kinase 1 during development and cancer progression. *Proc Natl Acad Sci U S A,* 110**,** 18940-5.

YU, Y. P., CAI, L. C., WANG, X. Y., CHENG, S. Y., ZHANG, D. M., JIAN, W. G., WANG, T. D., YANG, J. K., YANG, K. B. & ZHANG, C. 2020. BMP8A promotes survival and drug resistance via Nrf2/TRIM24 signaling pathway in clear cell renal cell carcinoma. *Cancer Sci,* 111**,** 1555-1566.

YUAN, F. L., XU, M. H., LI, X., XINLONG, H., FANG, W. & DONG, J. 2016. The Roles of Acidosis in Osteoclast Biology. *Front Physiol,* 7**,** 222.

YUE, J. & MULDER, K. M. 2000. Requirement of Ras/MAPK pathway activation by transforming growth factor beta for transforming growth factor beta 1 production in a smad-dependent pathway. *J Biol Chem,* 275**,** 35656.

YUNUS, J., SALMAN, M., LINTIN, G. B. R., MUCHTAR, M., SARI, D. C. R., ARFIAN, N. & ROMI, M. M. 2020. Chlorogenic acid attenuates kidney fibrosis via antifibrotic action of BMP-7 and HGF. *Med J Malaysia,* 75**,** 5-9.

ZABKIEWICZ, C., RESAUL, J., HARGEST, R., JIANG, W. G. & YE, L. 2017. Bone morphogenetic proteins, breast cancer, and bone metastases: striking the right balance. *Endocr Relat Cancer,* 24**,** R349-R366.

ZEKRI, A. R., HAFEZ, M. M., BAHNASSY, A. A., HASSAN, Z. K., MANSOUR, T., KAMAL, M. M. & KHALED, H. M. 2008. Genetic profile of Egyptian hepatocellular-carcinoma associated with hepatitis C virus Genotype 4 by 15 K cDNA microarray: preliminary study. *BMC Res Notes,* 1**,** 106.

ZHAN, L., XIANG, B. & MUTHUSWAMY, S. K. 2006. Controlled activation of ErbB1/ErbB2 heterodimers promote invasion of three-dimensional organized epithelia in an ErbB1-dependent manner: implications for progression of ErbB2-overexpressing tumors. *Cancer Res,* 66**,** 5201-8.

ZHANG, J., HE, X. C., TONG, W. G., JOHNSON, T., WIEDEMANN, L. M., MISHINA, Y., FENG, J. Q. & LI, L. 2006. Bone morphogenetic protein signaling inhibits hair follicle anagen induction by restricting epithelial stem/progenitor cell activation and expansion. *Stem Cells,* 24**,** 2826-39.

ZHANG, J. F., LI, G., CHAN, C. Y., MENG, C. L., LIN, M. C., CHEN, Y. C., HE, M. L., LEUNG, P. C. & KUNG, H. F. 2010. Flavonoids of Herba Epimedii regulate osteogenesis of human mesenchymal stem cells through BMP and Wnt/beta-catenin signaling pathway. *Mol Cell Endocrinol,* 314**,** 70-4.

ZHANG, L., LUGA, V., ARMITAGE, S. K., MUSIOL, M., WON, A., YIP, C. M., PLOTNIKOV, S. V. & WRANA, J. L. 2016a. A lateral signalling pathway coordinates shape volatility during cell migration. *Nat Commun,* 7**,** 11714.

ZHANG, L., YE, Y., LONG, X., XIAO, P., REN, X. & YU, J. 2016b. BMP signaling and its paradoxical effects in tumorigenesis and dissemination. *Oncotarget,* 7**,** 78206-78218.

ZHANG, M., WANG, Q., YUAN, W., YANG, S., WANG, X., YAN, J. D., DU, J., YIN, J., GAO, S. Y., SUN, B. C. & ZHU, T. H. 2007. Epigenetic regulation of bone morphogenetic protein-6 gene expression in breast cancer cells. *J Steroid Biochem Mol Biol,* 105**,** 91-7.

ZHANG, Q., LIANG, F., KE, Y., HUO, Y., LI, M., LI, Y. & YUE, J. 2015. Overexpression of neogenin inhibits cell proliferation and induces apoptosis in human MDA-MB-231 breast carcinoma cells. *Oncol Rep,* 34**,** 258-64.

ZHANG, W. Z., LAN, T., NIE, C. H., GUAN, N. N. & GAO, Z. X. 2018. Characterization and spatiotemporal expression analysis of nine bone morphogenetic protein family genes during intermuscular bone development in blunt snout bream. *Gene,* 642**,** 116-124.

ZHANG, X. H., GIULIANO, M., TRIVEDI, M. V., SCHIFF, R. & OSBORNE, C. K. 2013. Metastasis dormancy in estrogen receptor-positive breast cancer. *Clin Cancer Res,* 19**,** 6389-97.

ZHANG, Y., WU, X., ZHU, K., LIU, S., YANG, Y., YUAN, D., WANG, T., HE, Y., DUN, Y., WU, J., ZHANG, C. & ZHAO, H. 2022. Icariin attenuates perfluorooctane sulfonate-induced testicular toxicity by alleviating Sertoli cell injury and downregulating the p38MAPK/MMP9 pathway. *Food Funct,* 13**,** 3674-3689.

ZHAO, G. Q. & HOGAN, B. L. 1996. Evidence that mouse Bmp8a (Op2) and Bmp8b are duplicated genes that play a role in spermatogenesis and placental development. *Mech Dev,* 57**,** 159-68.

ZHAO, G. X., PAN, H., OUYANG, D. Y. & HE, X. H. 2015. The critical molecular interconnections in regulating apoptosis and autophagy. *Ann Med,* 47**,** 305-15.

ZHEN, R., YANG, J., WANG, Y., LI, Y., CHEN, B., SONG, Y., MA, G. & YANG, B. 2018. Hepatocyte growth factor improves bone regeneration via the bone morphogenetic protein2mediated NFkappaB signaling pathway. *Mol Med Rep,* 17**,** 6045-6053.

ZHENG, Z. Y., ANURAG, M., LEI, J. T., CAO, J., SINGH, P., PENG, J., KENNEDY, H., NGUYEN, N. C., CHEN, Y., LAVERE, P., LI, J., DU, X. H., CAKAR, B., SONG, W., KIM, B. J., SHI, J., SEKER, S., CHAN, D. W., ZHAO, G. Q., CHEN, X., BANKS, K. C., LANMAN, R. B., SHAFAEE, M. N., ZHANG, X. H., VASAIKAR, S., ZHANG, B., HILSENBECK, S. G., LI, W., FOULDS, C. E., ELLIS, M. J. & CHANG, E. C. 2020. Neurofibromin Is an Estrogen Receptor-alpha Transcriptional Co-repressor in Breast Cancer. *Cancer Cell,* 37**,** 387-402 e7.

ZHU, W., KIM, J., CHENG, C., RAWLINS, B. A., BOACHIE-ADJEI, O., CRYSTAL, R. G. & HIDAKA, C. 2006. Noggin regulation of bone morphogenetic protein (BMP) 2/7 heterodimer activity in vitro. *Bone,* 39**,** 61-71.

ZUZARTE-LUIS, V., MONTERO, J. A., RODRIGUEZ-LEON, J., MERINO, R., RODRIGUEZ-REY, J. C. & HURLE, J. M. 2004. A new role for BMP5 during limb development acting through the synergic activation of Smad and MAPK pathways. *Dev Biol,* 272**,** 39-52.

Supplements

Supplementary file 1

VectorBuilder www.vectorbuilder.com

Vector Summary

Vector ID	VB180207-1092dmp
Vector Name	pLV[Exp]-mCherry:T2A:Hygro-EFS>hBMP8A[NM_181809.3]
Date Created (Pacific Time)	2018-02-06
Size	10053 bp
Vector Type	Lentivirus gene expression vector (3rd generation)
Inserted Promoter	EFS
Inserted ORF	hBMP8A[NM_181809.3]
Inserted Marker	mCherry:T2A:Hygro
Plasmid Copy Number	High
Antibiotic Resistance	Ampicillin
Cloning Host	Stbl3 (or alternative strain)

Vector Map

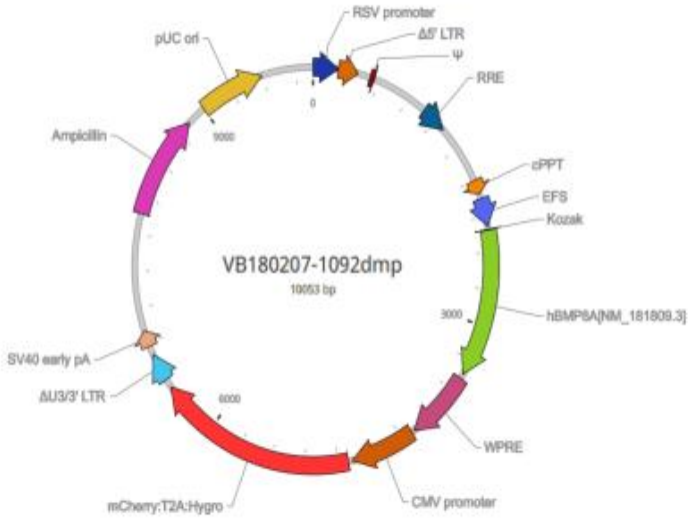

Vector Components

Name	Position	Size (bp)	Type	Description	Application notes
RSV promoter	1-229	229	Promoter	Rous sarcoma virus enhancer/promoter	Strong promoter; drives transcription of viral RNA in packaging cells.
Δ5' LTR	230-410	181	LTR	Truncated HIV-1 5' long terminal repeat	Allows transcription of viral RNA and its packaging into virus.
Ψ	521-565	45	Miscellaneous	HIV-1 packaging signal	Allows packaging of viral RNA into virus.
RRE	1075-1308	234	Miscellaneous	HIV-1 Rev response element	Rev protein binding site that allows Rev-dependent nuclear export of viral RNA during viral packaging.
cPPT	1803-1920	118	Miscellaneous	Central polypurine tract	Facilitates the nuclear import of HIV-1 cDNA through a central DNA flap.

Name	Position	Size (bp)	Type	Description	Application notes
EFS	1959-2190	232	Promoter	Human eukaryotic translation elongation factor 1 α1 short form	Strong promoter.
Kozak	2215-2220	6	Miscellaneous	Kozak translation initiation sequence	Facilitates translation initiation of ATG start codon downstream of the Kozak sequence.
hBMP8A[NM_181809.3]	2221-3429	1209	ORF	*None*	*None*
WPRE	3468-4065	598	Miscellaneous	Woodchuck hepatitis virus posttranscriptional regulatory element	Enhances viral RNA stability in packaging cells, leading to higher titer of packaged virus.
CMV promoter	4087-4674	588	Promoter	Human cytomegalovirus immediate early enhancer/promoter	Strong promoter; may have variable strength in some cell types.
mCherry:T2A:Hygro	4706-6502	1797	ORF	mCherry and Hygro linked by T2A	Allows cells to be visualized by red fluorescence and resistant to hygromycin B.
ΔU3/3' LTR	6573-6807	235	LTR	Truncated HIV-1 3' long terminal repeat	Allows packaging of viral RNA into virus; self-inactivates the 5' LTR by a copying mechanism during viral genome integration; contains polyadenylation signal for transcription termination.
SV40 early pA	6880-7014	135	PolyA_signal	Simian virus 40 early polyadenylation signal	Allows transcription termination and polyadenylation of mRNA transcribed by Pol II RNA polymerase.
Ampicillin	7968-8828	861	ORF	Ampicillin resistance gene	Allows E. coli to be resistant to ampicillin.
pUC ori	8999-9587	589	Rep_origin	pUC origin of replication	Facilitates plasmid replication in E. coli; regulates high-copy plasmid number (500-700).

Note: Components added by user are listed in bold red text.

Vector Sequence

```
   1 AATGTAGTCT TATGCAATAC TCTTGTAGTC TTGCAACATG GTAACGATGA GTTAGCAACA TGCCTTACAA GGAGAGAAAA AGCACCGTGC ATGCCGATTG
 101 GTGGAAGTAA GGTGGTACGA TCGTGCCTTA TTAGGAAGGC AACAGACGGG TCTGACATGG ATTGGACGAA CCACTGAATT GCCGCATTGC AGAGATATTG
 201 TATTTAAGTG CCTAGCTCGA TACATAAACG GGTCTCTCTG GTTAGACCAG ATCTGAGCCT GGGAGCTCTC TGGCTAACTA GGGAACCCAC TGCTTAAGCC
 301 TCAATAAAGC TTGCCTTGAG TGCTTCAAGT AGTGTGTGCC CGTCTGTTGT GTGACTCTGG TAACTAGAGA TCCCTCAGAC CCTTTTAGTC AGTGTGGAAA
 401 ATCTCTAGCA GTGGCGCCCG AACAGGGACT TGAAAGCGAA AGGGAAACCA GAGGAGCTCT CTCGACGCAG GACTCGGCTT GCTGAAGCGC GCACGGCAAG
 501 AGGCGAGGGG CGGCGACTGG TGAGTACGCC AAAAATTTTG ACTAGCGGAG GCTAGAAGGA GAGAGATGGG TGCGAGAGCG TCAGTATTAA GCGGGGGAGA
 601 ATTAGATCGC GATGGGAAAA AATTCGGTTA AGGCCAGGGG GAAAGAAAAA ATATAAATTA AAACATATAG TATGGGCAAG CAGGGAGCTA GAACGATTCG
 701 CAGTTAATCC TGGCCTGTTA GAAACATCAG AAGGCTGTAG ACAAATACTG GGACAGCTAC AACCATCCCT TCAGACAGGA TCAGAAGAAC TTAGATCATT
 801 ATATAATACA GTAGCAACCC TCTATTGTGT GCATCAAAGG ATAGAGATAA AAGACACCAA GGAAGCTTTA GACAAGATAG AGGAAGAGCA AAACAAAAGT
 901 AAGACCACCG CACAGCAAGC GGCCGCTGAT CTTCAGACCT GGAGGAGGAG ATATGAGGGA CAATTGGAGA AGTGAATTAT ATAAATATAA AGTAGTAAAA
1001 ATTGAACCAT TAGGAGTAGC ACCCACCAAG GCAAAGAGAA GAGTGGTGCA GAGAGAAAAA AGAGCAGTGG GAATAGGAGC TTTGTTCCTT GGGTTCTTGG
1101 GAGCAGCAGG AAGCACTATG GGCGCAGCGT CAATGACGCT GACGGTACAG GCCAGACAAT TATTGTCTGG TATAGTGCAG CAGCAGAACA ATTTGCTGAG
1201 GGCTATTGAG GCGCAACAGC ATCTGTTGCA ACTCACAGTC TGGGGCATCA AGCAGCTCCA GGCAAGAATC CTGGCTGTGG AAAGATACCT AAAGGATCAA
1301 CAGCTCCTGG GGATTTGGGG TTGCTCTGGA AAACTCATTT GCACCACTGC TGTGCCTTGG AATGCTAGTT GGAGTAATAA ATCTCTGGAA CAGATTTGGA
1401 ATCACACGAC CTGGATGGAG TGGGACAGAG AAATTAACAA TTACACAAGC TTAATACACT CCTTAATTGA AGAATCGCAA AACCAGCAAG AAAAGAATGA
1501 ACAAGAATTA TTGGAATTAG ATAAATGGGC AAGTTTGTGG AATTGGTTTA ACATAACAAA TTGGCTGTGG TATATAAAAT TATTCATAAT GATAGTAGGA
1601 GGCTTGGTAG GTTTAAGAAT AGTTTTTGCT GTACTTTCTA TAGTGAATAG AGTTAGGCAG GGATATTCAC CATTATCGTT TCAGACCCAC CTCCCAACCC
1701 CGAGGGGACC CGACAGGCCC GAAGGAATAG AAGAAGAAGG TGGAGAGAGA GACAGAGACA GATCCATTCG ATTAGTGAAC GGATCTCGAC GGTATCGCTA
1801 GCTTTTAAAA GAAAAGGGGG GATTGGGGGG TACAGTGCAG GGGAAAGAAT AGTAGACATA ATAGCAACAG ACATACAAAC TAAAGAATTA CAAAAACAAA
1901 TTACAAAAAT TCAAAATTTT ACTAGTGATT ATCGGATCAA CTTTGTATAG AAAAGTTGGG CTCCGGTGCC CGTCAGTGGG CAGAGCGCAC ATCGCCCACA
```

```
2001 GTCCCCGAGA AGTTGGGGGG AGGGGTCGGC AATTGATCCG GTGCCTAGAG AAGGTGGCGC GGGGTAAACT GGGAAAGTGA TGTCGTGTAC TGGCTCCGCC
2101 TTTTTCCCGA GGGTGGGGGA GAACCGTATA TAAGTGCAGT AGTCGCCGTG AACGTTCTTT TTCGCAACGG GTTTGCCGCC AGAACACAGG CAAGTTTGTA
2201 CAAAAAAGCA GGCTGCCACC ATGGCCGCGC GCCCCGGACC GCTCTGGCTT CTGGGCCTGA CGTTGTGCGC GCTGGGCGGG GGCGGCCCCG GCCTGCGACC
2301 CCCGCCCGGC TGTCCCCAGC GACGTCTGGG CGCGCGCGAG CGCCGGGACG TGCAGCGCGA GATCCTGGCG GTGCTCGGGC TACCCGGGCG GCCCCGGCCC
2401 CGCGCGCCAC CCGCCGCCTC CCGGCTGCCC GCGTCCGCGC CGCTCTTCAT GCTGGACCTG TACCACGCCA TGGCTGGCGA CGACGACGAG GACGGCGCGC
2501 CCGCGGAGCA GCGCCTGGGC CGCGCCGACC TGGTCATGAG CTTCGTCAAC ATGGTGGAGC GAGACCGTGC CCTGGGCCAC CAGGAGCCCC ATTGGAAGGA
2601 GTTCCGCTTT GACCTGACCC AGATCCCGGC TGGGGAGGCG GTCACAGCTG CGGAGTTCCG GATTTACAAG GTGCCCAGCA TCCACCTGCT CAACAGGACC
2701 CTCCACGTCA GCATGTTCCA GGTGGTCCAG GAGCAGTCCA ACAGGGAGTC TGACTTGTTC TTTTTGGATC TTCAGACGCT CCGAGCTGGA GACGAGGGCT
2801 GGCTGGTGCT GGATGTCACA GCAGCCAGTG ACTGCTGGTT GCTGAAGCGT CACAAGGACC TGGGACTCCG CCTCTATGTG GAGACTGAGG ACGGGCACAG
2901 CGTGGATCCT GGCCTGGCCG GCCTGCTGGG TCAACGGGCC CCACGCTCCC AACAGCCTTT CGTGGTCACT TTCTTCAGGG CCAGTCCGAG TCCCATCCGC
3001 ACCCCTCGGG CAGTGAGGCC ACTGAGGAGG AGGCAACCGA AGAAAAGCAA CGAGCTGCCG CAGGCCAACC GACTCCCAGG GATCTTTGAT GACGTCCGCG
3101 GCTCCCACGG CCGGCAGGTC TGCCGTCGGC ACGAGCTCTA CGTCAGCTTC CAGGACCTTG GCTGGCTGGA CTGGGTCATC GCCCCCCAAG GCTACTCAGC
3201 CTATTACTGT GAGGGGGAGT GCTCCTTCCC GCTGGACTCC TGCATGAACG CCACCAACCA CGCCATCCTG CAGTCCCTGG TGCACCTGAT GAAGCCAAAC
3301 GCAGTCCCCA AGGCGTGCTG TGCACCCACC AAGCTGAGCG CCACCTCTGT GCTCTACTAT GACAGCAGCA ACAACGTCAT CCTGCGCAAG CACCGCAACA
3401 TGGTGGTCAA GGCCTGCGGC TGCCACTGAA CCCAGCTTTC TTGTACAAAG TGGTGATAAT CGAATTCCGA TAATCAACCT CTGGATTACA AAATTTGTGA
3501 AAGATTGACT GGTATTCTTA ACTATGTTGC TCCTTTTACG CTATGTGGAT ACGCTGCTTT AATGCCTTTG TATCATGCTA TTGCTTCCCG TATGGCTTTC
3601 ATTTTCTCCT CCTTGTATAA ATCCTGGTTG CTGTCTCTTT ATGAGGAGTT GTGGCCCGTT GTCAGGCAAC GTGGCGTGGT GTGCACTGTG TTTGCTGACG
3701 CAACCCCCAC TGGTTGGGGC ATTGCCACCA CCTGTCAGCT CCTTTCCGGG ACTTTCGCTT TCCCCCTCCC TATTGCCACG GCGGAACTCA TCGCCGCCTG
3801 CCTTGCCCGC TGCTGGACAG GGGCTCGGCT GTTGGGCACT GACAATTCCG TGGTGTTGTC GGGGAAGCTG ACGTCCTTTC CATGGCTGCT CGCCTGTGTT
3901 GCCACCTGGA TTCTGCGCGG GACGTCCTTC TGCTACGTCC CTTCGGCCCT CAATCCAGCG GACCTTCCTT CCCGCGGCCT GCTGCCGGCT CTGCGGCCTC
4001 TTCCGCGTCT TCGCCTTCGC CCTCAGACGA GTCGGATCTC CCTTTGGGCC GCCTCCCCGC ATCGGGAATT CCCGCGGTTC GAACGCGTTG ACATTGATTA
4101 TTGACTAGTT ATTAATAGTA ATCAATTACG GGGTCATTAG TTCATAGCCC ATATATGGAG TTCCGCGTTA CATAACTTAC GGTAAATGGC CCGCCTGGCT
4201 GACCGCCCAA CGACCCCGCC CCATTGACGT CAATAATGAC GTATGTTCCC ATAGTAACGC CAATAGGGAC TTTCCATTGA CGTCAATGGG TGGAGTATTT
4301 ACGGTAAACT GCCCACTTGG CAGTACATCA AGTGTATCAT ATGCCAAGTA CGCCCCCTAT TGACGTCAAT GACGGTAAAT GGCCCGCCTG GCATTATGCC
4401 CAGTACATGA CCTTATGGGA CTTTCCTACT TGGCAGTACA TCTACGTATT AGTCATCGCT ATTACCATGG TGATGCGGTT TTGGCAGTAC ATCAATGGGC
4501 GTGGATAGCG GTTTGACTCA CGGGGATTTC CAAGTCTCCA CCCCATTGAC GTCAATGGGA GTTTGTTTTG GCACCAAAAT CAACGGGACT TTCCAAAATG
4601 TCGTAACAAC TCCGCCCCAT TGACGCAAAT GGGCGGTAGG CGTGTACGGT GGGAGGTCTA TATAAGCAGA GCTCTCTGGC TAACTAGAGA ACCCACTGCG
4701 CCACCATGGT GAGCAAGGGC GAGGAGGATA ACATGGCCAT CATCAAGGAG TTCATGCGCT TCAAGGTGCA CATGGAGGGC TCCGTGAACG GCCACGAGTT
4801 CGAGATCGAG GGCGAGGGCG AGGGCCGCCC CTACGAGGGC ACCCAGACCG CCAAGCTGAA GGTGACCAAG GGTGGCCCCC TGCCCTTCGC CTGGGACATC
4901 CTGTCCCCTC AGTTCATGTA CGGCTCCAAG GCCTACGTGA AGCACCCCGC CGACATCCCC GACTACTTGA AGCTGTCCTT CCCCGAGGGC TTCAAGTGGG
5001 AGCGCGTGAT GAACTTCGAG GACGGCGGCG TGGTGACCGT GACCCAGGAC TCCTCCCTGC AGGACGGCGA GTTCATCTAC AAGGTGAAGC TGCGCGGCAC
5101 CAACTTCCCC TCCGACGGCC CCGTAATGCA GAAGAAGACC ATGGGCTGGG AGGCCTCCTC CGAGCGGATG TACCCCGAGG ACGGCGCCCT GAAGGGCGAG
5201 ATCAAGCAGA GGCTGAAGCT GAAGGACGGC GGCCACTACG ACGCTGAGGT CAAGACCACC TACAAGGCCA AGAAGCCCGT GCAGCTGCCC GGCGCCTACA
5301 ACGTCAACAT CAAGTTGGAC ATCACCTCCC ACAACGAGGA CTACACCATC GTGGAACAGT ACGAACGCGC CGAGGGCCGC CACTCCACCG GCGGCATGGA
5401 CGAGCTGTAC AAGGGCTCCG GAGAGGGCAG GGGAAGTCTT CTAACATGCG GGGACGTGGA GGAAAATCCC GGCCCCATGA AAAAGCCTGA ACTCACCGCG
5501 ACGTCTGTCG AGAAGTTTCT GATCGAAAAG TTCGACAGCG TCTCCGACCT GATGCAGCTC TCGGAGGGCG AAGAATCTCG TGCTTTCAGC TTCGATGTAG
5601 GAGGGCGTGG ATATGTCCTG CGGGTAAATA GCTGCGCCGA TGGTTTCTAC AAAGATCGTT ATGTTTATCG GCACTTTGCA TCGGCCGCGC TCCCGATTCC
5701 GGAAGTGCTT GACATTGGGG AATTTAGCGA GAGCCTGACC TATTGCATCT CCCGCCGTGC ACAGGGTGTC ACGTTGCAAG ACCTGCCTGA AACCGAACTG
5801 CCCGCTGTTC TGCAGCCGGT CGCGGAGGCC ATGGATGCGA TCGCTGCGGC CGATCTTAGC CAGACGAGCG GGTTCGGCCC ATTCGGACCG CAAGGAATCG
5901 GTCAATACAC TACATGGCGT GATTTCATAT GCGCGATTGC TGATCCCCAT GTGTATCACT GGCAAACTGT GATGGACGAC ACCGTCAGTG CGTCCGTCGC
6001 GCAGGCTCTC GATGAGCTGA TGCTTTGGGC CGAGGACTGC CCCGAAGTCC GGCACCTCGT GCACGCGGAT TTCGGCTCCA ACAATGTCCT GACGGACAAT
6101 GGCCGCATAA CAGCGGTCAT TGACTGGAGC GAGGCGATGT TCGGGGATTC CCAATACGAG GTCGCCAACA TCTTCTTCTG GAGGCCGTGG TTGGCTTGTA
6201 TGGAGCAGCA GACGCGCTAC TTCGAGCGGA GGCATCCGGA GCTTGCAGGA TCGCCGCGGC TCCGGGCGTA TATGCTCCGC ATTGGTCTTG ACCAACTCTA
6301 TCAGAGCTTG GTTGACGGCA ATTTCGATGA TGCAGCTTGG GCGCAGGGTC GATGCGACGC AATCGTCCGA TCCGGAGCCG GGACTGTCGG GCGTACACAA
6401 ATCGCCCGCA GAAGCGCGGC CGTCTGGACC GATGGCTGTG TAGAAGTACT CGCCGATAGT GGAAACCGAC GCCCCAGCAC TCGTCCGAGG GCAAAGGAAT
6501 AGGGTACCTT TAAGACCAAT GACTTACAAG GCAGCTGTAG ATCTTAGCCA CTTTTTAAAA GAAAAGGGGG GACTGGAAGG GCTAATTCAC TCCCAACGAA
6601 GACAAGATCT GCTTTTTGCT TGTACTGGGT CTCTCTGGTT AGACCAGATC TGAGCCTGGG AGCTCTCTGG CTAACTAGGG AACCCACTGC TTAAGCCTCA
6701 ATAAAGCTTG CCTTGAGTGC TTCAAGTAGT GTGTGCCCGT CTGTTGTGTG ACTCTGGTAA CTAGAGATCC CTCAGACCCT TTTAGTCAGT GTGGAAAATC
6801 TCTAGCAGTA GTAGTTCATG TCATCTTATT ATTCAGTATT TATAACTTGC AAAGAAATGA ATATCAGAGA GTGAGAGGAA CTTGTTTATT GCAGCTTATA
6901 ATGGTTACAA ATAAAGCAAT AGCATCACAA ATTTCACAAA TAAAGCATTT TTTTCACTGC ATTCTAGTTG TGGTTTGTCC AAACTCATCA ATGTATCTTA
7001 TCATGTCTGG CTCTAGCTAT CCCGCCCCTA ACTCCGCCCA TCCCGCCCCT AACTCCGCCC AGTTCCGCCC ATTCTCCGCC CCATGGCTGA CTAATTTTTT
7101 TTATTTATGC AGAGGCCGAG GCCGCCTCGG CCTCTGAGCT ATTCCAGAAG TAGTGAGGAG GCTTTTTTGG AGGCCTAGGG ACGTACCCAA TTCGCCCTAT
7201 AGTGAGTCGT ATTACGCGCG CTCACTGGCC GTCGTTTTAC AACGTCGTGA CTGGGAAAAC CCTGGCGTTA CCCAACTTAA TCGCCTTGCA GCACATCCCC
7301 CTTTCGCCAG CTGGCGTAAT AGCGAAGAGG CCCGCACCGA TCGCCCTTCC CAACAGTTGC GCAGCCTGAA TGGCGAATGG CGCGCGCCCT GTAGCGGCGC
7401 ATTAAGCGCG GCGGGTGTGG TGGTTACGCG CAGCGTGACC GCTACACTTG CCAGCGCCCT AGCGCCCGCT CCTTTCGCTT TCTTCCCTTC CTTTCTCGCC
```

```
7501  ACGTTCGCCG GCTTTCCCCG TCAAGCTCTA AATCGGGGGC TCCCTTTAGG GTTCCGATTT AGTGCTTTAC GGCACCTCGA CCCCAAAAAA CTTGATTAGG
7601  GTGATGGTTC ACGTAGTGGG CCATCGCCCT GATAGACGGT TTTTCGCCCT TTGACGTTGG AGTCCACGTT CTTTAATAGT GGACTCTTGT TCCAAACTGG
7701  AACAACACTC AACCCTATCT CGGTCTATTC TTTTGATTTA TAAGGGATTT TGCCGATTTC GGCCTATTGG TTAAAAAATG AGCTGATTTA ACAAAAATTT
7801  AACGCGAATT TTAACAAAAT ATTAACGCTT ACAATTTAGG TGGCACTTTT CGGGGAAATG TGCGCGGAAC CCCTATTTGT TTATTTTCTT AAATACATTC
7901  AAATATGTAT CCGCTCATGA GACAATAACC CTGATAAATG CTTCAATAAT ATTGAAAAAG GAAGAGTATG AGTATTCAAC ATTTCCGTGT CGCCCTTATT
8001  CCCTTTTTTG CGGCATTTTG CCTTCCTGTT TTTGCTCACC CAGAAACGCT GGTGAAAGTA AAAGATGCTG AAGATCAGTT GGGTGCACGA GTGGGTTACA
8101  TCGAACTGGA TCTCAACAGC GGTAAGATCC TTGAGAGTTT TCGCCCCGAA GAACGTTTTC CAATGATGAG CACTTTTAAA GTTCTGCTAT GTGGCGCGGT
8201  ATTATCCCGT ATTGACGCCG GGCAAGAGCA ACTCGGTCGC CGCATACACT ATTCTCAGAA TGACTTGGTT GAGTACTCAC CAGTCACAGA AAAGCATCTT
8301  ACGGATGGCA TGACAGTAAG AGAATTATGC AGTGCTGCCA TAACCATGAG TGATAACACT GCGGCCAACT TACTTCTGAC AACGATCGGA GGACCGAAGG
8401  AGCTAACCGC TTTTTTGCAC AACATGGGGG ATCATGTAAC TCGCCTTGAT CGTTGGGAAC CGGAGCTGAA TGAAGCCATA CCAAACGACG AGCGTGACAC
8501  CACGATGCCT GTAGCAATGG CAACAACGTT GCGCAAACTA TTAACTGGCG AACTACTTAC TCTAGCTTCC CGGCAACAAT TAATAGACTG GATGGAGGCG
8601  GATAAAGTTG CAGGACCACT TCTGCGCTCG GCCCTTCCGG CTGGCTGGTT TATTGCTGAT AAATCTGGAG CCGGTGAGCG TGGGTCTCGC GGTATCATTG
8701  CAGCACTGGG GCCAGATGGT AAGCCCTCCC GTATCGTAGT TATCTACACG ACGGGGAGTC AGGCAACTAT GGATGAACGA AATAGACAGA TCGCTGAGAT
8801  AGGTGCCTCA CTGATTAAGC ATTGGTAACT GTCAGACCAA GTTTACTCAT ATATACTTTA GATTGATTTA AAACTTCATT TTTAATTTAA AAGGATCTAG
8901  GTGAAGATCC TTTTTGATAA TCTCATGACC AAAATCCCTT AACGTGAGTT TTCGTTCCAC TGAGCGTCAG ACCCCGTAGA AAAGATCAAA GGATCTTCTT
9001  GAGATCCTTT TTTTCTGCGC GTAATCTGCT GCTTGCAAAC AAAAAAACCA CCGCTACCAG CGGTGGTTTG TTTGCCGGAT CAAGAGCTAC CAACTCTTTT
9101  TCCGAAGGTA ACTGGCTTCA GCAGAGCGCA GATACCAAAT ACTGTTCTTC TAGTGTAGCC GTAGTTAGGC CACCACTTCA AGAACTCTGT AGCACCGCCT
9201  ACATACCTCG CTCTGCTAAT CCTGTTACCA GTGGCTGCTG CCAGTGGCGA TAAGTCGTGT CTTACCGGGT TGGACTCAAG ACGATAGTTA CCGGATAAGG
9301  CGCAGCGGTC GGGCTGAACG GGGGGTTCGT GCACACAGCC CAGCTTGGAG CGAACGACCT ACACCGAACT GAGATACCTA CAGCGTGAGC TATGAGAAAG
9401  CGCCACGCTT CCCGAAGAGA GAAAGGCGGA CAGGTATCCG GTAAGCGGCA GGGTCGGAAC AGGAGAGCGC ACGAGGGAGC TTCCAGGGGG AAACGCCTGG
9501  TATCTTTATA GTCCTGTCGG GTTTCGCCAC CTCTGACTTG AGCGTCGATT TTTGTGATGC TCGTCAGGGG GGCGGAGCCT ATGGAAAAAC GCCAGCAACG
9601  CGGCCTTTTT ACGGTTCCTG GCCTTTTGCT GGCCTTTTGC TCACATGTTC TTTCCTGCGT TATCCCCTGA TTCTGTGGAT AACCGTATTA CCGCCTTTGA
9701  GTGAGCTGAT ACCGCTCGCC GCAGCCGAAC GACCGAGCGC AGCGAGTCAG TGAGCGAGGA AGCGGAAGAG CGCCCAATAC GCAAACCGCC TCTCCCCGCG
9801  CGTTGGCCGA TTCATTAATG CAGCTGGCAC GACAGGTTTC CCGACTGGAA AGCGGGCAGT GAGCGCAACG CAATTAATGT GAGTTAGCTC ACTCATTAGG
9901  CACCCCAGGC TTTACACTTT ATGCTTCCGG CTCGTATGTT GTGTGGAATT GTGAGCGGAT AACAATTTCA CACAGGAAAC AGCTATGACC ATGATTACGC
10001 CAAGCGCGCA ATTAACCCTC ACTAAAGGGA ACAAAAGCTG GAGCTGCAAG CTT
```

Validation by Restriction Enzyme Digestion

Cutters	Locations	Fragments (bp)
NheI	1798	10053
AscI	2496	10053
XmaI	2384	10053
ApaLI	3281, 3321, 3682, 4767, 5758, 6060, 8084, 9330	40, 361, 1085, 991, 302, 2024, 1246, 4004
AvrII	7175	10053
ApaLI+XmaI	2384, 3281, 3321, 3682, 4767, 5758, 6060, 8084, 9330	897, 40, 361, 1085, 991, 302, 2024, 1246, 3107
ApaLI+AscI	2496, 3281, 3321, 3682, 4767, 5758, 6060, 8084, 9330	785, 40, 361, 1085, 991, 302, 2024, 1246, 3219
ApaLI+NheI	1798, 3281, 3321, 3682, 4767, 5758, 6060, 8084, 9330	1483, 40, 361, 1085, 991, 302, 2024, 1246, 2521
ApaLI+AvrII	3281, 3321, 3682, 4767, 5758, 6060, 7175, 8084, 9330	40, 361, 1085, 991, 302, 1115, 909, 1246, 4004

Supplementary file 2

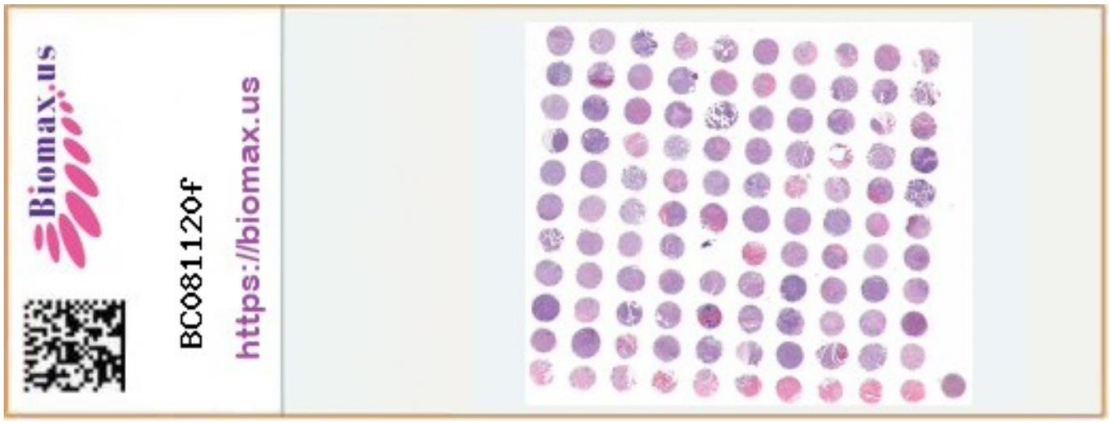

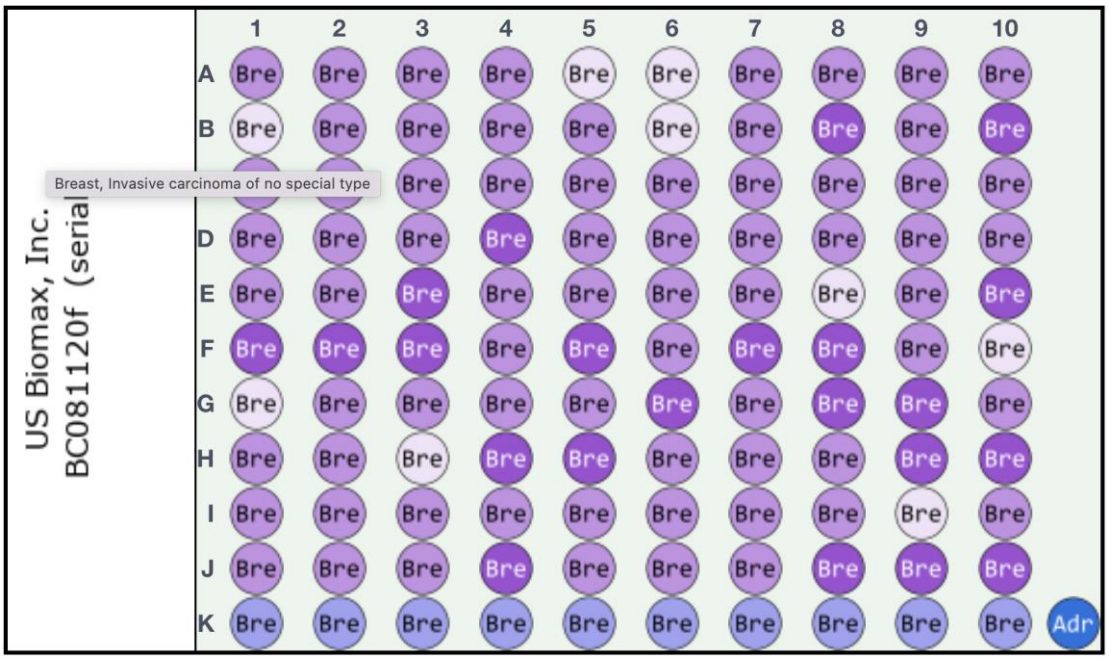

Specification Sheet (Sortable), tissue IDs are available in exported Excel files.

Pos.	No.	Age	Sex	Organ/Anatomic Site	Pathology diagnosis	TNM	Grade	Stage	Type	ER	PR	HER2	Image
A1	1	40	F	Breast	Invasive carcinoma of no special type	T2N0M0	2	IIA	Malignant	+	-	3+	
A2	2	45	F	Breast	Invasive carcinoma of no special type	T2N0M0	2	IIA	Malignant	++	+++	0	
A3	3	46	F	Breast	Invasive carcinoma of no special type	T2N0M0	2	IIA	Malignant	+++	++	0	
A4	4	69	F	Breast	Invasive carcinoma of no special type	T2N1M0	2	IIB	Malignant	*	*	*	
A5	5	45	F	Breast	Invasive carcinoma of no special type	T1N0M0	2	IA	Malignant	++	++	0	
A6	6	44	F	Breast	Invasive carcinoma of no special type	T1N0M0	2	IA	Malignant	+++	+++	0	
A7	7	45	F	Breast	Invasive carcinoma of no special type	T2N1M0	2	IIB	Malignant	++	-	3+	
A8	8	53	F	Breast	Invasive carcinoma of no special type	T2N0M0	2	IIA	Malignant	-	-	0	
A9	9	46	F	Breast	Invasive carcinoma of no special type	T2N0M0	2	IIA	Malignant	+++	+++	0	
A10	10	41	F	Breast	Invasive carcinoma of no special type	T2N0M0	2	IIA	Malignant	+	-	0	
B1	11	43	F	Breast	Invasive carcinoma of no special type	T1N1M0	3	IB	Malignant	-	-	0	
B2	12	45	F	Breast	Invasive carcinoma of no special type	T2N1M0	2	IIB	Malignant	+++	++	3+	
B3	13	37	F	Breast	Invasive carcinoma of no special type	T2N0M0	2	IIA	Malignant	+++	+++	0	
B4	14	63	F	Breast	Invasive carcinoma of no special type	T2N0M0	1--2	IIA	Malignant	+++	+++	0	
B5	15	65	F	Breast	Invasive carcinoma of no special type	T2N0M0	1--2	IIA	Malignant	+++	-	0	
B6	16	43	F	Breast	Invasive carcinoma of no special type	T1N1M0	2	IB	Malignant	+++	+	0	
B7	17	44	F	Breast	Invasive carcinoma of no special type	T2N0M0	2	IIA	Malignant	-	-	3+	
B8	18	34	F	Breast	Invasive carcinoma of no special type	T4N0M0	2	IIIB	Malignant	++	-	0	

Pos.	No.	Age	Sex	Organ/Anatomic Site	Pathology diagnosis	TNM	Grade	Stage	Type	ER	PR	HER2	Image
B9	19	48	F	Breast	Invasive carcinoma of no special type	T2N0M0	3	IIA	Malignant	+++	++	1+	
B10	20	62	F	Breast	Invasive carcinoma of no special type	T3N1M0	2	IIIA	Malignant	+++	-	0	
C1	21	44	F	Breast	Invasive carcinoma of no special type	T2N1M0	2	IIB	Malignant	-	-	3+	
C2	22	67	F	Breast	Invasive carcinoma of no special type	T2N0M0	2	IIA	Malignant	+++	++	0	
C3	23	55	F	Breast	Invasive carcinoma of no special type	T2N0M0	2	IIA	Malignant	+++	+++	0	
C4	24	57	F	Breast	Invasive carcinoma of no special type	T2N0M0	2	IIA	Malignant	+++	+++	3+	
C5	25	63	F	Breast	Invasive carcinoma of no special type	T2N0M0	2	IIA	Malignant	+++	-	0	
C6	26	39	F	Breast	Invasive carcinoma of no special type	T2N1M0	2	IIB	Malignant	+++	-	3+	
C7	27	42	F	Breast	Invasive carcinoma of no special type	T2N0M0	2	IIA	Malignant	+++	+++	0	
C8	28	40	F	Breast	Invasive carcinoma of no special type	T2N0M0	2	IIA	Malignant	+++	+++	0	
C9	29	42	F	Breast	Invasive carcinoma of no special type	T2N0M0	2	IIA	Malignant	+	+	0	
C10	30	32	F	Breast	Invasive carcinoma of no special type	T2N0M0	2	IIA	Malignant	-	-	0	
D1	31	52	F	Breast	Invasive carcinoma of no special type	T3N0M0	2	IIB	Malignant	+++	+++	0	
D2	32	48	F	Breast	Invasive carcinoma of no special type	T2N0M0	2	IIA	Malignant	+++	+++	0	
D3	33	54	F	Breast	Invasive carcinoma of no special type (sparse)	T2N1M0	2	IIB	Malignant	+	-	0	
D4	34	47	F	Breast	Invasive carcinoma of no special type	T3N2M0	2	IIIA	Malignant	-	-	0	
D5	35	46	F	Breast	Invasive carcinoma of no special type	T3N0M0	2	IIB	Malignant	+++	++	3+	
D6	36	68	F	Breast	Invasive carcinoma of no special type	T2N0M0	2	IIA	Malignant	+++	+++	0	

Pos.	No.	Age	Sex	Organ/Anatomic Site	Pathology diagnosis	TNM	Grade	Stage	Type	ER	PR	HER2	Image
D7	37	53	F	Breast	Invasive carcinoma of no special type	T2N0M0	2	IIA	Malignant	-	-	0	
D8	38	58	F	Breast	Invasive carcinoma of no special type	T2N1M0	2	IIB	Malignant	++	+	0	
D9	39	42	F	Breast	Invasive carcinoma of no special type	T3N0M0	2	IIB	Malignant	-	-	3+	
D10	40	34	F	Breast	Invasive carcinoma of no special type	T3N0M0	2	IIB	Malignant	+++	+	3+	
E1	41	47	F	Breast	Invasive carcinoma of no special type	T3N0M0	2	IIB	Malignant	+++	+++	0	
E2	42	42	F	Breast	Invasive carcinoma of no special type	T3N0M0	2	IIB	Malignant	-	-	3+	
E3	43	48	F	Breast	Invasive carcinoma of no special type	T4N2M0	2	IIIB	Malignant	++	++	0	
E4	44	32	F	Breast	Invasive carcinoma of no special type	T2N1M0	2	IIB	Malignant	++	+	0	
E5	45	52	F	Breast	Invasive carcinoma of no special type	T2N1M0	2	IIB	Malignant	-	-	0	
E6	46	37	F	Breast	Invasive carcinoma of no special type	T2N1M0	3	IIB	Malignant	-	-	0	
E7	47	74	F	Breast	Invasive carcinoma of no special type	T2N0M0	3	IIA	Malignant	*	*	*	
E8	48	46	F	Breast	Invasive carcinoma of no special type (sparse)	T1N0M0	2	IA	Malignant	+	-	0	
E9	49	48	F	Breast	Invasive carcinoma of no special type	T2N1M0	2	IIB	Malignant	++	+++	0	
E10	50	51	F	Breast	Invasive carcinoma of no special type	T3N1M0	3	IIIA	Malignant	-	-	3+	
F1	51	52	F	Breast	Invasive carcinoma of no special type	T2N2M0	2	IIIA	Malignant	+++	+	2+	
F2	52	51	F	Breast	Invasive carcinoma of no special type	T2N2M0	2	IIIA	Malignant	-	-	0	
F3	53	46	F	Breast	Invasive carcinoma of no special type	T4N2M0	2	IIIB	Malignant	+++	-	0	
F4	54	49	F	Breast	Invasive carcinoma of no special type	T2N0M0	2	IIA	Malignant	+++	+++	0	

Pos.	No.	Age	Sex	Organ/Anatomic Site	Pathology diagnosis	TNM	Grade	Stage	Type	ER	PR	HER2	Image
F5	55	46	F	Breast	Invasive carcinoma of no special type	T4N0M0	2	IIIB	Malignant	+++	+++	0	
F6	56	69	F	Breast	Invasive carcinoma of no special type	T3N0M0	2	IIB	Malignant	+++	-	0	
F7	57	45	F	Breast	Invasive carcinoma of no special type	T4N1M0	2	IIIB	Malignant	++	+	0	
F8	58	50	F	Breast	Invasive carcinoma of no special type	T4N1M0	3	IIIB	Malignant	-	-	0	
F9	59	49	F	Breast	Invasive carcinoma of no special type	T2N0M0	3	IIA	Malignant	*	*	*	
F10	60	40	F	Breast	Invasive carcinoma of no special type	T1N0M0	2	IA	Malignant	++	+	3+	
G1	61	60	F	Breast	Invasive carcinoma of no special type	T1N0M0	2	IA	Malignant	++	+	0	
G2	62	49	F	Breast	Invasive carcinoma of no special type	T2N0M0	2	IIA	Malignant	-	-	0	
G3	63	50	F	Breast	Invasive carcinoma of no special type	T2N1M0	2	IIB	Malignant	+++	+	0	
G4	64	64	F	Breast	Invasive carcinoma of no special type	T2N0M0	2	IIA	Malignant	-	-	3+	
G5	65	59	F	Breast	Invasive carcinoma of no special type	T2N0M0	3	IIA	Malignant	-	-	0	
G6	66	38	F	Breast	Invasive carcinoma of no special type	T3N1M0	2	IIIA	Malignant	*	*	*	
G7	67	56	F	Breast	Invasive carcinoma of no special type	T2N1M0	2	IIB	Malignant	-	-	0	
G8	68	45	F	Breast	Invasive carcinoma of no special type	T4N2M0	2	IIIB	Malignant	+++	+++	0	
G9	69	58	F	Breast	Invasive carcinoma of no special type	T3N1M0	2	IIIA	Malignant	++	-	0	
G10	70	29	F	Breast	Invasive carcinoma of no special type	T2N0M0	2	IIA	Malignant	-	-	3+	
H1	71	47	F	Breast	Invasive carcinoma of no special type	T2N1M0	2	IIB	Malignant	++	+	0	
H2	72	55	F	Breast	Invasive carcinoma of no special type	T2N0M0	2	IIA	Malignant	++	-	3+	
H3	73	45	F	Breast	Invasive carcinoma of no special type	T1N0M0	2	IA	Malignant	-	-	0	

Pos.	No.	Age	Sex	Organ/Anatomic Site	Pathology diagnosis	TNM	Grade	Stage	Type	ER	PR	HER2	Image
H4	74	55	F	Breast	Invasive carcinoma of no special type	T3N2M0	2	IIIA	Malignant	+++	+++	0	
H5	75	54	F	Breast	Invasive carcinoma of no special type	T2N2M0	2	IIIA	Malignant	+	-	3+	
H6	76	40	F	Breast	Invasive carcinoma of no special type	T2N0M0	3	IIA	Malignant	++	+	0	
H7	77	53	F	Breast	Invasive carcinoma of no special type	T2N0M0	3	IIA	Malignant	-	-	0	
H8	78	46	F	Breast	Invasive carcinoma of no special type (breast tissue)	T2N0M0	*	IIA	Malignant	-	-	0	
H9	79	52	F	Breast	Invasive carcinoma of no special type	T4N2M0	3	IIIB	Malignant	-	-	3+	
H10	80	48	F	Breast	Invasive carcinoma of no special type	T4N0M0	2--3	IIIB	Malignant	+++	+++	0	
I1	81	27	F	Breast	Invasive carcinoma of no special type	T2N1M0	3	IIB	Malignant	+++	-	3+	
I2	82	70	F	Breast	Invasive carcinoma of no special type	T2N0M0	2--3	IIA	Malignant	-	-	0	
I3	83	42	F	Breast	Invasive carcinoma of no special type	T2N1M0	3	IIB	Malignant	-	-	0	
I4	84	31	F	Breast	Invasive carcinoma of no special type	T2N0M0	3	IIA	Malignant	-	-	3+	
I5	85	47	F	Breast	Invasive carcinoma of no special type	T2N0M0	3	IIA	Malignant	+++	+	0	
I6	86	34	F	Breast	Invasive carcinoma of no special type	T2N0M0	3	IIA	Malignant	-	-	0	
I7	87	56	F	Breast	Invasive carcinoma of no special type	T2N0M0	3	IIA	Malignant	+++	-	0	
I8	88	37	F	Breast	Invasive carcinoma of no special type	T2N1M0	3	IIB	Malignant	-	-	2+	
I9	89	43	F	Breast	Invasive carcinoma of no special type	T1N0M0	3	IA	Malignant	+++	+	0	
I10	90	45	F	Breast	Invasive carcinoma of no special type	T2N0M0	3	IIA	Malignant	-	-	0	
J1	91	48	F	Breast	Invasive carcinoma of no special type	T2N1M0	3	IIB	Malignant	+++	-	0	

Pos.	No.	Age	Sex	Organ/Anatomic Site	Pathology diagnosis	TNM	Grade	Stage	Type	ER	PR	HER2	Image
J2	92	38	F	Breast	Invasive carcinoma of no special type	T2N0M0	3	IIA	Malignant	-	-	0	
J3	93	47	F	Breast	Invasive carcinoma of no special type	T2N0M0	3	IIA	Malignant	-	-	2+	
J4	94	51	F	Breast	Invasive carcinoma of no special type	T3N1M0	3	IIIA	Malignant	-	-	3+	
J5	95	52	F	Breast	Invasive carcinoma of no special type	T3N0M0	3	IIB	Malignant	-	-	3+	
J6	96	43	F	Breast	Invasive carcinoma of no special type	T2N1M0	3	IIB	Malignant	*	*	*	
J7	97	68	F	Breast	Invasive carcinoma of no special type	T2N0M0	3	IIA	Malignant	+++	+	0	
J8	98	30	F	Breast	Invasive carcinoma of no special type	T2N2M0	3	IIIA	Malignant	-	-	3+	
J9	99	46	F	Breast	Invasive carcinoma of no special type	T4N0M0	3	IIIB	Malignant	-	-	0	
J10	100	45	F	Breast	Invasive carcinoma of no special type	T3N1M0	3	IIIA	Malignant	++	+	3+	
K1	101	43	F	Breast	Adjacent normal breast tissue (fibrofatty tissue)	-	*	-	NAT	+	+	0	
K2	102	48	F	Breast	Adjacent normal breast tissue	-	-	-	NAT	+	+	0	
K3	103	40	F	Breast	Adjacent normal breast tissue	-	-	-	NAT	+	+	0	
K4	104	41	F	Breast	Adjacent normal breast tissue (adenosis)	-	-	-	NAT	+	+	0	
K5	105	38	F	Breast	Adjacent normal breast tissue	-	*	-	NAT	+	+	0	
K6	106	29	F	Breast	Adjacent normal breast tissue (adenosis)	-	-	-	NAT	+	+	0	
K7	107	41	F	Breast	Adjacent normal breast tissue	-	*	-	NAT	*	*	*	

Pos.	No.	Age	Sex	Organ/Anatomic Site	Pathology diagnosis	TNM	Grade	Stage	Type	ER	PR	HER2	Image
					(fibrofatty tissue)								
K8	108	42	F	Breast	Adjacent normal breast tissue (adenosis)	-	*	-	NAT	+	+	0	
K9	109	35	F	Breast	Adjacent normal breast tissue (adenosis)	-	-	-	NAT	*	*	*	
K10	110	43	F	Breast	Adjacent normal breast tissue (adenosis)	-	-	-	NAT	*	*	*	
-	0	42	M	Adrenal gland	Pheochromocytoma (tissue marker)		-		Malignant				